

The effect of diet on the susceptibility to helminth infection

A thesis submitted to the University of Manchester for the degree of Doctor
of Philosophy in the Faculty of Biology, Medicine and Health

2019

Evelyn Funjika

**School of Biological Sciences
Division of Infection, Immunity and Respiratory Medicine**

Table of Contents

List of figures.....	8
List of tables.....	11
List of equations.....	11
List of abbreviations.....	12
Abstract.....	15
Declaration.....	16
Copyright Statement.....	16
Acknowledgement.....	17
Dedication.....	17
Chapter 1 : Introduction.....	18
1.1 Introduction.....	19
1.1.1 Global burden of obesity.....	19
1.1.2 The burden of infectious diseases.....	20
1.1.3 Dual burden of disease: Zambia as a case study.....	21
1.2 Soil transmitted helminth (STH) infections.....	25
1.2.1 <i>Trichuris muris</i> as a model to study host immune responses to STH.....	25
1.2.2 The life cycle of <i>T. muris</i>	26
1.3 Defining the immune response to <i>T. muris</i> infection.....	27
1.3.1 The gastrointestinal barrier as a first line defence.....	27
1.3.2 The cytokine mediated immune response to <i>T. muris</i> infection.....	30
1.3.3 ILC2 cells in <i>T. muris</i> infection.....	35
1.3.4 The role of antibody responses in <i>T. muris</i> immunity.....	36
1.3.5 Dose-dependent immunity to <i>T. muris</i>	36
1.3.6 The role of genetics in immunity to <i>T. muris</i>	37
1.4 Helminths and metabolic homeostasis in obesity.....	38
1.5 The use of mouse models to learn more about high fat diet (HFD) induced obesity.....	41
1.5.1 The role of leptin in obesity.....	41
1.5.2 HFD and the immune response.....	42
1.5.3 HFD and epithelial cell proliferation.....	43
1.5.4 Hyperglycaemia and intestinal barrier dysregulation.....	44
1.6 HFD and the mucus barrier.....	45
1.7 The intestinal microbiota and its biological importance.....	47
1.7.1 HFD and the intestinal microbiota.....	48
1.7.2 Helminth infections and the intestinal microbiota.....	49
1.8 HFD and the progression of helminth infections.....	50

1.9 Project aim and objectives.....	51
Chapter 2 : Materials and methods	52
2.1 Animals.....	53
2.2 Diet modifications	53
2.3 <i>T. muris</i> infection of mice	55
2.3.1 <i>T. muris</i> propagation in the lab.....	55
2.3.2 Preparation of <i>T. muris</i> excretory secretory product (E/S).....	57
2.3.3 <i>T. muris</i> infection of mice	57
2.4 Worm counts	58
2.5 Faecal egg count	58
2.6 Blood glucose measurement	58
2.7 Histology	59
2.7.1 Tissue collection and processing	59
2.7.2 Tissue sectioning	59
2.7.3 Tissue staining	60
2.7.4 Image acquisition	63
2.7.5 Quantification of histological staining	63
2.8 Serum collection	63
2.9 Serum antibody ELISA	64
2.10 Serum leptin assay	64
2.11 Extraction of immune cells.....	64
2.11.1 Mesenteric lymph nodes	65
2.11.2 Lamina propria	65
2.11.3 Mesenteric fat.....	66
2.12 Cell re-stimulation assay	66
2.13 CD3/CD28 activation assay	67
2.14 Cytometric bead array (CBA)	67
2.15 Flow cytometry	68
2.15.1 Flow cytometry staining and data acquisition	68
2.15.2 Flow cytometry gating strategy	68
2.16 RNA extraction	73
2.17 cDNA synthesis and qPCR	73
2.18 Analysis of faecal DNA by denaturing gradient gel electrophoresis (DGGE)	74
2.19 Statistics	75
Chapter 3 : Results I	77
3.1 Introduction	78

3.2 Results.....	80
3.2.1 The effect of a low dose of <i>T. muris</i> infection on host body weight in normal chow mice	81
I. Comparison of body weight changes between naïve and <i>T. muris</i> infected normal chow mice.....	81
II. Comparison of epididymal and subcutaneous fat pads between naïve and <i>T. muris</i> infected normal chow mice	84
III. Comparison of food intake between naïve and trickle dose infected normal chow mice	86
IV. Comparison of serum leptin levels and adipocyte area between naïve and <i>T. muris</i> infected normal chow mice	87
V. Comparison of macrophages, eosinophils and dendritic cells in mesenteric fat between naïve and <i>T. muris</i> infected normal chow mice	90
3.2.2 The effect of low dose <i>T. muris</i> infection on the pancreas, liver and lung.....	93
I. Comparison of blood glucose levels and area of pancreatic islet of Langerhans between naïve and <i>T. muris</i> infected normal chow mice.....	93
II. Assessment of liver function in <i>T. muris</i> infected normal chow mice	96
III. Comparison of PAS/AB stained sections of lung tissue from naïve and low dose <i>T. muris</i> infected normal chow mice	96
3.2.3 The effect of a low dose <i>T. muris</i> infection on body weight in mice fed a high fat diet.....	100
I. Comparison of body weight changes between naïve and <i>T. muris</i> infected HFDIO mice	100
II. Comparison of epididymal and subcutaneous fat pads between naïve and <i>T. muris</i> infected HFDIO mice	103
III. Comparison of food intake between naïve and trickle dose infected HFDIO mice	103
IV. Comparison of serum leptin levels and adipocyte area between naïve and <i>T. muris</i> infected HFDIO mice	106
V. Comparison of macrophages, eosinophils and dendritic cells in mesenteric fat between naïve and <i>T. muris</i> infected mice	107
3.2.4 The effect of low dose <i>T. muris</i> on the pancreas, liver and lung in HFDIO mice	111
I. Comparison of blood glucose levels and area of pancreatic islet of Langerhans between naïve and <i>T. muris</i> infected HFDIO mice.....	111
II. Assessment of liver function in <i>T. muris</i> infected HFDIO mice	114
III. Comparison of PAS/AB stained sections of lung tissue from HFDIO mice.....	114
3.3 Discussion.....	118
3.3.1 A low dose of <i>T. muris</i> infection did not have an effect on body weight	118
3.3.2 Serum <i>leptin</i> levels were increased in infected HFDIO mice but not in normal mice after single and trickle low dose of <i>T. muris</i> infection.....	119
3.3.3 A low dose of <i>T. muris</i> infection did not have a significant effect on blood glucose levels or pancreas pathology	120

3.3.4 A low dose of <i>T. muris</i> did not result in liver pathology or improve symptoms of fatty liver disease.....	121
3.3.5 A low dose of <i>T. muris</i> infection did not increase lung PAS/AB staining in normal and HFDIO mice	122
3.4 Conclusion.....	122
Chapter 4 : Results II	124
4.1 Introduction	125
4.2 Results.....	127
4.2.1 How does HFDIO affect the outcome of a single low dose of <i>T. muris</i> infection?	127
I. Worm burden of single dose <i>T. muris</i> infected mice.....	127
II. Serum antibody responses of single dose <i>T. muris</i> infected mice.....	129
III. Cytokine responses of re-stimulated immune cells collected from single dose <i>T. muris</i> infected mice.....	131
4.2.2 How does short-term HFD feeding affect the outcome of a single low dose of <i>T. muris</i> infection?.....	131
I. Worm burden of single dose <i>T. muris</i> infected 3-week pre-fed mice	133
II. Serum antibody responses of single dose <i>T. muris</i> infected mice after 3 weeks of HFD feeding	133
III. Cytokine responses of re-stimulated immune cells collected from single dose <i>T. muris</i> infected mice after 3 weeks of HFD feeding.....	133
4.2.3 How does HFDIO affect the outcome of a low dose trickle infection with <i>T. muris</i> ?.....	137
I. Worm burden of trickle dose <i>T. muris</i> infected mice after 12 weeks of HFD feeding	137
II. Serum antibody responses of trickle dose <i>T. muris</i> infected mice after 12 weeks of HFD feeding	137
III. Cytokine responses of re-stimulated immune cells collected from trickle dose <i>T. muris</i> infected mice after 12 weeks of HFD feeding.....	140
4.2.4 How does HFD feeding affect the outcome of pre-infected <i>T. muris</i> mice?	142
I. Worm burden of <i>T. muris</i> infected mice started on a HFD at either day 13 or day 32 post infection.	142
II. Serum antibody responses of post-fed <i>T. muris</i> infected mice	143
III. Cytokine responses of re-stimulated immune cells collected from post-fed <i>T. muris</i> infected mice.....	143
4.3 Discussion.....	147
4.3.1 HFD induces early worm expulsion during chronic <i>T. muris</i> infection	147
4.3.2 HFD changes the worm specific antibody profile after a low dose <i>T. muris</i> infection ..	148
4.3.3 HFD enhances a Th2 immune response.....	149
4.3.4 HFD dampened the Th1 immune response	150
4.3.5 HFD feeding does not induce resistance in <i>T. muris</i> infected mice started on a HFD at either day 13 or day 32 post infection.....	151

4.4 Conclusion.....	152
Chapter 5 : Results III	154
5.1 Introduction	155
5.2 Results.....	157
5.2.1 The effect of HFDIO on the establishment of <i>T. muris</i>	157
5.2.2 Faecal microbial population at day 21 post infection in normal chow and HFDIO mice	161
5.2.3 The effect of HFDIO on T-cell responses in <i>T. muris</i> infected mice	161
I. Cytokine production of CD3/CD28 activated T-cells from the mesenteric lymph nodes	163
II. CD4 ⁺ IFN- γ ⁺ T-cell population in the mesenteric lymph nodes and lamina propria at day 21 post infection	166
III. CD4 ⁺ FoxP3 ⁺ T-cells (Tregs) and CD4 ⁺ Tbet ⁺ T-cells in the mesenteric lymph nodes at day 21 post infection	169
5.2.4 TSLP gene expression in the caecum at day 21 post infection	171
5.2.5 Goblet cell responses and crypt depth measurements in the caecum	172
5.2.6 RELM β gene expression in the caecum at day 21 post infection	175
5.2.7 The outcome of a low dose <i>T. muris</i> infection in normal chow and HFDIO C57BL/6 RAG ^{-/-} mice.....	176
I. Body weight and blood glucose levels of C57BL/6 RAG ^{-/-} mice	176
II. Outcome of infection in normal chow and HFDIO RAG ^{-/-} mice.....	176
III. Caecal goblet cell responses and crypt depth measures in <i>T. muris</i> infected normal chow and HFDIO RAG ^{-/-} mice	179
5.2.8 Tuft cell responses at day 21 post infection in normal chow and HFDIO C57BL/6 mice	180
5.2.9 Correlation between worm burden and weight of <i>T. muris</i> infected mice	183
5.3 Summary	187
5.3.1 HFD induced changes to the intestinal microbiota did not affect the ability of <i>T. muris</i> to establish in the host.....	187
5.3.2 HFD did not cause a significant shift in the faecal microbial population of <i>T. muris</i> infected mice at day 21 post infection	188
5.3.2 HFD influences T-cell specific responses which alters the balance of Th1/Th2 responses	189
5.3.3 HFDIO alters CD4 T-cell responses which are important in driving mechanisms of resistance against <i>T. muris</i> infection.....	191
5.3.4 Resistance to a low dose of <i>T. muris</i> in HFDIO mice is also observed in the absence of the adaptive immune response	193
5.3.5 HFD had no effect on the number of intestinal tuft cells	194
5.3.6 There was no clear correlation between worm burden and mouse weight	194
5.4 Conclusion.....	195

Chapter 6 : General Discussion	196
6.1 HFD induced obesity induces early expulsion of <i>T. muris</i> worms.....	198
6.2 HFD induced obesity skews T-cells towards a Th2 immune response	200
6.3 Innate immune responses contribute to enhanced protection against <i>T. muris</i> in HFDIO mice	203
6.4 Single and trickle low dose <i>T. muris</i> infections do not cause significant pathology in normal chow mice	205
6.5 Single and trickle low dose <i>T. muris</i> infection did not reverse the pathology of HFD induced obesity.....	206
6.6 HFDIO induced shift in faecal microbial population has no effect on establishment of <i>T. muris</i> infection.	208
6.7 There was no difference in faecal microbial population between normal chow and HFDIO <i>T. muris</i> infected mice at day 21 post infection.....	209
6.8 What could be driving the HFD induced resistance against a low dose <i>T. muris</i> infection?	210
6.9 Conclusions	211
Chapter 7 : References.....	213

Word count: 49, 304

List of figures

Chapter 1

Figure 1-1: Prevalence of STH infections in Zambia.....	24
Figure 1-2: The life cycle of <i>T. muris</i>	26
Figure 1-3: Th1 and Th2 immune responses.....	32
Figure 1-4: The role of Th2 immunity in thermogenic regulation.	40
Figure 1-5: HFD and the intestinal barrier	46

Chapter 2

Figure 2-1: Flow cytometry gating for IFN- γ ⁺ CD4 ⁺ T-cells and IL-13 ⁺ CD4 ⁺ T cells.	70
Figure 2-2: Flow cytometry gating for CD4 ⁺ FoxP3 ⁺ T-cells and CD4 ⁺ Tbet ⁺ T-cells.	71
Figure 2-3: Flow cytometry gating strategy for macrophages, eosinophils and dendritic cells.	72
Figure 2-4: Sample of DNA gels for microbial composition analysis by DGGE	76

Chapter 3

Figure 3-1: Experimental design.	80
Figure 3-2: Weight change in single dose <i>T. muris</i> infected mice.	82
Figure 3-3: Weight change in trickle dose <i>T. muris</i> infected mice.....	83
Figure 3-4: Comparison of epididymal and subcutaneous fat pads between naïve and <i>T. muris</i> infected mice on normal chow.	85
Figure 3-5: Comparison of food consumption between naïve and trickle dose infected mice.....	86
Figure 3-6: Comparison of serum leptin between naïve and <i>T. muris</i> infected mice.....	88
Figure 3-7: Comparison of adipocyte area between naïve and infected mice.	89
Figure 3-8: Flow gating strategy for macrophages, eosinophils and dendritic cells in naïve and <i>T. muris</i> infected mice.....	91
Figure 3-9: Comparison of macrophages, eosinophils and dendritic cell populations in mesenteric fat from naïve and <i>T. muris</i> infected mice.	92
Figure 3-10: Comparison of blood glucose between naïve and <i>T. muris</i> infected mice.....	94
Figure 3-11: Comparison of the islet of Langerhans area between naïve and infected mice.	95
Figure 3-12: Serum liver function tests in naïve and single dose infected mice.	97
Figure 3-13: Serum liver function tests in naïve and trickle dose infected mice.....	98
Figure 3-14: Comparison of PAS/AB stained lung sections from naïve and <i>T. muris</i> infected mice.....	99
Figure 3-15: Weight change in single low dose <i>T. muris</i> infected HFDIO mice.	101
Figure 3-16: Weight change in trickle low dose <i>T. muris</i> infected HFDIO mice.....	102
Figure 3-17: Comparison of epididymal and subcutaneous fat pads in single low dose and trickle infected HFDIO mice.	104
Figure 3-18: Comparison of food consumption between naïve and trickle dose infected HFDIO mice.....	105
Figure 3-19: Comparison of serum leptin between naïve and <i>T. muris</i> infected HFDIO mice.	106
Figure 3-20: Comparison of adipocyte area between naïve and infected HFDIO mice.....	108
Figure 3-21: Flow gating strategy for macrophages, eosinophils and dendritic cells in naïve and <i>T. muris</i> infected HFDIO mice.	109
Figure 3-22: Comparison of macrophages, eosinophils and dendritic cell populations in mesenteric fat from naïve and <i>T. muris</i> infected HFDIO mice.....	110

Figure 3-23: Comparison of blood glucose between naïve and <i>T. muris</i> infected HFDIO mice.	112
Figure 3-24: Comparison of the islet of Langerhans area between naïve and infected HFDIO mice.	113
Figure 3-25: Serum liver function tests in single dose infected HFDIO mice.....	115
Figure 3-26: Serum liver function tests in naïve and trickle dose infected HFDIO mice.	116
Figure 3-27: Comparison of PAS/AB stained lung sections from naïve and <i>T. muris</i> infected HFDIO mice.....	117

Chapter 4

Figure 4-1: Worm burden of single low dose mice pre-fed for 12 weeks.	128
Figure 4-2: Parasite specific IgG1 and IgG2a/c antibody ELISA of single dose infected mice after 12 weeks of feeding.	130
Figure 4-3: Re-stimulation of mesenteric lymph node derived cells from single low dose infected mice after 12 weeks of pre-feeding.	132
Figure 4-4: Worm burden of single low dose mice pre-fed for 3 weeks.	134
Figure 4-5: IgG1 and IgG2a/c antibody ELISA of single dose infected mice after 3 weeks of pre-feeding.	135
Figure 4-6: Re-stimulation of mesenteric lymph node derived cells from single low dose infected mice after 3 weeks of pre-feeding.	136
Figure 4-7: Worm burden and faecal egg count of mice given a trickle low dose of <i>T. muris</i> after 12 weeks of feeding.	138
Figure 4-8: Parasite specific IgG1 and IgG2a/c antibody ELISA of trickle low dose infected mice after 12 weeks of pre-feeding.....	139
Figure 4-9: Re-stimulation of mesenteric lymph node derived cells from mice given trickle low dose infection after 12 weeks of feeding.	141
Figure 4-10: Experimental design.	142
Figure 4-11: Weight gain and worm burden of mice started on a HFD after <i>T. muris</i> infection.	144
Figure 4-12: <i>T. muris</i> specific antibody responses of mice started on a HFD after <i>T. muris</i> infection.	145
Figure 4-13: Re-stimulation of mesenteric lymph node derived cells from post-fed mice given a single low dose infection.	146

Chapter 5

Figure 5-1: DGGE analysis of faecal microbiota after 12 weeks of feeding.	159
Figure 5-2: Worm burdens at day 13 post infection in normal chow and HFDIO mice.....	160
Figure 5-3: DGGE analysis of faecal microbiota at day 21 post infection.	162
Figure 5-4: Comparison of Th2 associated cytokine production of cells re-stimulated with <i>T. muris</i> E/S or activated via CD3/CD28 stimulation.	164
Figure 5-5: Comparison of proinflammatory cytokine production of cells re-stimulated with <i>T. muris</i> E/S or activated via CD3/CD28 stimulation.....	165
Figure 5-6: Analysis of Interferon- γ producing CD4 ⁺ T cells in the mesenteric lymph nodes.....	167
Figure 5-7: Analysis of Interferon- γ producing CD4 ⁺ T cells in the lamina propria.....	168
Figure 5-8: Analysis of CD4 ⁺ FoxP3 ⁺ Tregs and CD4 ⁺ Tbet ⁺ T-cells in the mesenteric lymph nodes.	170
Figure 5-9: Comparison of TSLP expression in the caecum of between naïve and single dose infected mice.	171
Figure 5-10: PAS/AB and Muc2 stained caecum sections from naïve and <i>T. muris</i> infected mice at day 21 post infection.	173

Figure 5-11: PAS/AB and Muc2 stained caecum sections from naïve and <i>T. muris</i> infected mice at day 42 post infection.	174
Figure 5-12: Comparison of RELM β expression in the caecum of between naïve and single dose infected mice.	175
Figure 5-13: Body weight, fat pad weight and blood glucose measurements of C56BL/6 RAG ^{-/-} mice infected with a single low dose of <i>T. muris</i>	177
Figure 5-14: Outcome of a single low dose of <i>T. muris</i> infection in C57BL/6 RAG ^{-/-} mice.	178
Figure 5-15: Comparison of PAS/AB stained caecum sections from normal chow and HFDIO C57BL/6 RAG ^{-/-} mice.	179
Figure 5-16: Representative images of tuft cell staining in the jejunum, caecum and colon.....	181
Figure 5-17: Comparison of the number of tuft cells in normal chow and HFDIO mice.	182
Figure 5-18: Regression analysis between the number of <i>T. muris</i> worms and mouse weight at day 21 post infection.	184
Figure 5-19: Regression analysis between the number of <i>T. muris</i> worms and mouse weight at day 42 post infection.	185
Figure 5-20: Regression analysis between the number of <i>T. muris</i> worms and mouse weight at day 42 post infection for normal chow and HFDIO C57BL/6 RAG ^{-/-} mice.....	186

Chapter 6

Figure 6-1: Understanding mechanism behind the enhanced resistance in HFD mice.....	212
---	-----

List of tables

Table 2.1: Composition of mouse normal chow and high fat diet.....	54
Table 2.2: Treatment groups based on feeding and infection periods.....	56
Table 2.3: Tissue processing protocol for Carnoy's fixed tissue	60
Table 2.4: Standard tissue processing for NBF fixed tissue	61
Table 2.5: List of antibodies used for flow cytometry	69
Table 2.6: qPCR primer sequences	74

List of equations

Equation 2.1: Determination of faecal egg load per sample	58
Equation 3.1: Equation for calculating the percent weight gain in mice from the time of infection until the day of sacrifice.....	81

List of abbreviations

ACK	Ammonium-chloride-potassium
AIDS	Acquired immunodeficiency syndrome
ALP	Alanine phosphatase
ALT	Alanine transaminase
ANOVA	Analysis of variance
BMI	Body mass index
BSA	Bovine serum albumin
CaCl ₂	Calcium chloride
CBA	Cytometric bead array
cDNA	Complimentary DNA
CEABAC10	mice expressing human CEACAMs
CEACAMs	Carcinoembryonic antigen-related cell adhesion molecule 6
CO ₂	Carbon dioxide
Con A	Concavalin A
CXCL10	C-X-C motif chemokine 10
CXCL11	C-X-C motif chemokine 11
DGGE	Denaturing gradient gel electrophoresis
dH ₂ O	Distilled water
DIO	Diet induced obesity
DNA	Deoxyribonucleic acid
dNTPs	Deoxyribonucleotide triphosphate
DPBS	Dulbecco's phosphate buffered saline
DTT	Dithiothreitol
E/S	Excretory/secretory
EDTA	Ethylenediaminetetraacetic acid
ELISA	Enzyme linked immunosorbent assay
FBS	Fetal bovine serum
FXR	Farnesoid X receptor
H&E	Haematoxylin and eosin
HBSS	Hank's balanced salt solution

HFD	High fat diet
HFDIO	High fat diet induced obesity (obese)
HIV	Human immune virus
IDO	Indolamine 2.3-dioxygenase
ILC	Innate lymphoid cells
IMS	Industrial methylated spirit
INF- γ	Interferon gamma
KO	Knock out
LFT	Liver function test
LNFP III	<i>Schistosoma mansoni</i> immunomodulatory glycan lacto-N-fucopentaose III
MHC	major histocompatibility complex
MMPtype2	multi-potent progenitor type 2
Na ₂ CO ₃	Sodium carbonate
NaCl	Sodium chloride
NAFLD	Non-alcoholic fatty liver disease
NaHCO ₃	Sodium bicarbonate
NaHPO ₄	Sodium hydrogen phosphate
NBF	Neutral buffered formalin
NCD	Non-communicable disease
ND	Not detected
NF- κ B	NF-kappa B
NMDS	Non-parametric multidimensional scaling
NTD	Neglected tropical disease
PAS	Periodic acid-Schiff
PAS	Periodic acid-Schiff
PBMCs	Peripheral blood mononuclear cells
PBS	Phosphate buffered saline
PCR	Polymerase chain reaction
PGC-1 α	Peroxisome proliferator-activated receptor gamma coactivator 1-alpha
PHA	Phytohemagglutinin
PMA	Phorbol 12-myristate 13-acetate
qPCR	Quantitative polymerase chain reaction

RAG	Recombination activating gene
RELM β	Resistin-like molecule beta
RNA	Ribonuclei acid
rRNA	ribosomal ribonuclei acid
rTNF- α	recombinant tumour necrosis factor alpha
SA-POD	Streptavidin bound peroxidase
SCFAs	Short chain fatty acids
SCID	Severely combined immunodeficient mice
SEA	<i>Schistosoma mansoni</i> soluble egg antigen
SEM	Standard error of the mean
STAT6	Signal transducer and activator of transcription 6
STH	Soil transmitted helminths
T-bet	T-box expressed in T-cells
TNCB	Trinitrochlorobenzene
TNFR	Tumour necrosis factor receptor
TNF- α	Tumour necrosis factor alpha
TSLP	Thymic stromal lymphopietin
TSLPR	Thymic stromal lymphopietin receptor
UCP1	Uncoupling protein 1
WFP	World food programme
WHO	World Health Organisation

Abstract

Gastrointestinal (GI) nematode infections comprising *Necator*, *Ancylostoma*, *Ascaris* as well as *Trichuris* affect around a quarter of the world's population and the associated morbidity brings huge socio-economic loss. Increased rural-urban migration in developing countries has led to the adoption of new diets with increased consumption of sugary and fatty foods. Therefore, people face the dual burden of GI nematode infection and that of diet-related illnesses. In this thesis, the well-described murine model of GI nematode infection, *Trichuris muris*, was used to investigate the effect of high fat diet (HFD) on immune-regulated protection. C57BL/6 mice were fed either normal chow (12% energy from fat) or HFD (60% energy from fat) for 12 weeks. The mice were then infected with a low dose of *T. muris* eggs, known to produce a chronic, Th1 cytokine mediated response during standard chow nutrition. To mimic natural infection, mice were also given 7 to 9 weekly repeated trickle low doses of *T. muris* eggs. The mice were sacrificed either 21 or 42 days (single dose group) post infection or 2 weeks after the final infection (trickle dose group). The *T. muris* infected normal chow mice remained asymptomatic, while hyperglycaemia, elevated serum leptin and non-alcoholic fatty liver disease induced by a HFD were not reversed by a single or trickle low dose *T. muris* infection. Strikingly, single or trickle low dose *T. muris* infected HFD induced obese (HFDIO) mice had significantly lower worm burdens, higher serum levels of parasite specific IgG1 and reduced levels of parasite specific IgG2a/c in comparison to the normal chow fed controls. However, mice already infected with a single low dose *T. muris* infection retained a chronic infection when started on a HFD at either day 13 or day 32 post infection. Therefore, HFD induces changes in the naïve host that drive resistance against *T. muris* in the pre-fed HFD mice. Furthermore, immune cells from the mesenteric lymph node of HFDIO mice showed a trend towards increased production of helminth expelling Th2 cytokines and there was a significant reduction in CD4⁺Interferon gamma⁺ T-cells in comparison to cells collected from normal chow mice. Finally, work showed that RAG^{-/-} HFDIO mice had significantly reduced worm burden in comparison to RAG^{-/-} normal chow mice at day 42 post infection suggesting that innate immunity plays a role in enhancing resistance in HFDIO mice. Overall these findings suggest that dietary fat enhances resistance to chronic *T. muris* infection. However, more work is needed to define the mechanisms involved and how they can be translationally targeted to boost immune responses in infected communities.

Declaration

No portion of the work referred to in the thesis has been submitted in support of an application for another degree or qualification of this or any other university or other institute of learning.

Copyright Statement

The author of this thesis (including any appendices and/or schedules to this thesis) owns certain copyright or related rights in it (the "Copyright") and s/he has given The University of Manchester certain rights to use such Copyright, including for administrative purposes.

Copies of this thesis, either in full or in extracts and whether in hard or electronic copy, may be made only in accordance with the Copyright, Designs and Patents Act 1988 (as amended) and regulations issued under it or, where appropriate, in accordance with the University's Presentation of Theses Policy. You are required to submit your thesis electronically (Page 11 of 25) with licensing agreements which the University has from time to time. This page must form part of any such copies made.

The ownership of certain Copyright, patents, designs, trademarks and other intellectual property (the "Intellectual Property") and any reproductions of copyright works in the thesis, for example graphs and tables ("Reproductions"), which may be described in this thesis, may not be owned by the author and may be owned by third parties. Such Intellectual Property and Reproductions cannot and must not be made available for use without the prior written permission of the owner(s) of the relevant Intellectual Property and/or Reproductions.

Further information on the conditions under which disclosure, publication and commercialisation of this thesis, the Copyright and any Intellectual Property and/or Reproductions described in it may take place is available in the University IP Policy (see <http://documents.manchester.ac.uk/DocuInfo.aspx?DocID=2442> 0), in any relevant Thesis restriction declarations deposited in the University Library, The University Library's regulations (see <http://www.library.manchester.ac.uk/about/regulations/>) and in The University's policy on Presentation of Theses.

Acknowledgement

I want to thank my supervisors for all their help and support throughout my PhD. I shall always be grateful to you all for guiding me throughout my research and it is because of your support I have been able to complete the work that I set out to do.

Dave: thank you for your invaluable feedback and for ensuring that I do not lose track of my objectives. Richard: thank you for always pushing me and encouraging me throughout my studies. John: thank you for helping me plan my experiments and taking time to train me in the lab.

I would also like to say thank you to past and present member of both the Thornton and Grencis groups. Caroline, Eamon, Alison, Jayde, Laura, Kelly, Seona and Simon. All the practical tips and advice that you gave me have helped me to improve my research skills. Becca, Cat, Stef and Abdulelah thank you for helping me to learn my way around the lab and having time to help me with my long experiments. Thank you Alba for helping me complete the tuft cell staining.

I want to say thank you to Adefunke, Christine and all the friends I made in Manchester who kept me company over the past few years.

I want to thank my mother for taking time to stay with me and making sure I always had help. My son, Tumelo, you have been with me every day of my journey and you are the source of my energy each morning. A big thank you to my husband, you have supported my work from the start and your sacrifice has motivated me to complete my studies. Thank you to the rest of my family for always being there for me.

Lastly, I want to thank my sponsors, the Commonwealth Scholarship Commission for funding my research and have provided me with this life changing opportunity.

Dedication

I want to dedicate this work to my late father, Lieutenant General Wilford Joseph Funjika, and my late sister, Mrs Pumulo Chinoya Kalenguesa.

Chapter 1 : Introduction

1.1 Introduction

Good nutrition is important for providing the energy we need to carry out daily activities as well as providing essential elements important for normal growth and development. Agricultural and industrial advancement has led to the mass production of food to feed an ever-increasing world population. However, many people in developing countries still fail to obtain adequate nutritious diets and it is becoming very clear that more work needs to be done to improve methods of food delivery to ensure that even the poor can benefit from increased global food production (Gould, 2017; Hugo, 1983; Peng and Berry, 2018). Malnutrition is normally associated with a lack of a well-balanced diet so that there are not enough calories to meet the body's demand and one effect of this is stunted growth in children. The global nutrition index highlights two additional forms of malnutrition: micronutrient deficiency and obesity (Rosenbloom et al., 2008). Micronutrient deficiency, also referred to as hidden hunger, is the failure to provide the required amount of vitamins and minerals which play a vital role in a variety of metabolic pathways. Obesity is due to over nutrition or excess energy intake which results in increased body weight (Rosenbloom et al., 2008). A balanced diet would therefore provide not only the right type of food but also in sufficient amounts to avoid both under and over nutrition. It is becoming increasingly evident that host nutritional status interacts with the immune system and this has implications host susceptibility to infection (Cressler et al., 2014).

1.1.1 Global burden of obesity

According to the World health Organisation (WHO), 1.9 billion people over the age of 18 years were overweight in 2016 and of these, 39 % were obese. They also report that, 18 % of children and adolescents were obese. WHO suggests that the main factors that have led to such high levels of global obesity are reduced physical activity due to modern lifestyles and the increased consumption of energy dense foods.

As early as 1994, Popkin pointed out the crisis that lower income countries would face due to nutritional transition (Popkin, 1994). Developing countries have seen high rates of rural urban migration. Furthermore, people in urban areas have much busier lifestyles and therefore they tend to buy processed foods which require less preparation time

(Popkin, 2012). However, most of the affordable food contains high levels of refined sugars and fat but less fibre. As a result, there is an increase in obesity and other diet related diseases in developing countries (James, 2004; Monteiro et al., 2004; Popkin, 2012). Providing proper care and medical costs of these non-communicable diseases (NCDs) are a challenge to the families of affected individuals as well as the rest of the community.

A major cause of concern is the co-existence of under nutrition and obesity in the same population and households. A number of studies have reported the dual existence of child under nutrition and adult obesity in the same house (Deleuze Ntandou Bouzitou et al., 2005; Freire et al., 2018). Infants and young children are exposed to foods with low nutritional value thereby affecting their growth and development. In order to address this, the global community adopted 17 goals for sustainable development to improve people's lives by 2030. One priority for the world food programme (WFP) has been to address the second goal which is zero hunger – pledges to end hunger, achieve food security, improve nutrition and promote sustainable agriculture. The world food programme hopes to achieve this by making nutrition a priority, starting with the first 1000 days of a child's life (WFP, 2017). While considerable focus has been aimed at reducing malnutrition due to undernourishment, there is a clear need for more action against obesity (Peng and Berry, 2018).

1.1.2 The burden of infectious diseases

Another challenge for people living in developing countries has been the fight against food and waterborne parasitic infections. These are normally prevalent in densely populated areas where people have a low income and do not have access to safe water. The scarcity and contamination of water distribution systems makes it harder to provide safe water (Moe and Rheingans, 2006). One main source of contamination is waste sewage, due to a lack of proper sanitation infrastructure. A study in Uganda showed that 15 % of people in a particular area used public pit latrines and 75 % of people used shared toilets (Katukiza et al., 2010). However a major disadvantage of shared facilities is that without any proper management these shared facilities tend to become dirty thereby

facilitating the spread of infectious diseases (Kwiringira et al., 2014). Furthermore, the lack of proper sewerage systems means there is an increased chance of waste water contaminating the water in boreholes and other water bodies. As a result, disease outbreaks still occur especially in the rainy season when excess rain water mixes with waste water (Chidavaenzi et al., 2000; Kostyla et al., 2015). Therefore, bacterial and parasitic nematode infections are still endemic in developing countries.

Over recent years there has been more awareness of soil-transmitted helminth (STH) infections which are regarded as neglected tropical diseases (NTDs). Pullan and co-workers estimated that by 2010, at least 1.45 billion people worldwide were infected with one species of intestinal STH (Pullan et al., 2014). Governments worked together with international organisations such as WHO to implement mass deworming campaigns to help control the spread of STH infections (WHO, 2012). A study in Kenya reported that school deworming programmes led to improved health and school attendance (Miguel and Kremer, 2003). However there is a need to carefully analyse the data collected from such studies as there are many confounding factors that may affect the findings (Jullien et al., 2016). There has been some doubt about the long-term effectiveness and sustainability of school deworming programmes. Community based integrated programs may provide long term benefits by combining deworming with improvements to water, sanitation and hygiene (Clarke et al., 2018). In addition emerging economies such as India have also directed more effort to improve their own pharmaceutical markets in order to provide medicine for the treatment of NTDs that are more affordable and sustainable (Holt et al., 2012).

1.1.3 Dual burden of disease: Zambia as a case study

Zambia is a sub-Saharan country located in southern Africa. It has a population of just over 17 million and at least 44% of the population live in urban areas or in surrounding peri-urban areas. According to a living condition monitoring survey conducted by the Central statistical office in Zambia and published in November 2016, within Lusaka province 18.1 % of people migrating had moved from rural to urban areas. The reasons

for migrating ranged from employment or business opportunity, marriage and education as well as other personal reasons.

I. The prevalence of obesity in Zambia

Most people migrating to urban areas adopt new lifestyles and this has led to the increased prevalence of NCDs including obesity. A number of studies have highlighted the increasing prevalence of obesity in Zambia. A survey conducted in 2012 by Rudatsikira and colleagues reported that 14.2 % of participants from selected regions in Zambia were obese. They suggested that obesity could be due to peoples' reluctance to exercise and also as a culturally accepted symbol of wealth especially for women (Rudatsikira et al., 2012). In another study conducted over a period of 14 years in selected African countries, it was reported that obesity in Zambian women had increased from 4 % in 1991 to 9 % in 2014 (Amugsi et al., 2017). More recently a survey of NCD risk factors completed in September 2017 indicated that 24 % of adults were obese with 19 % of them reporting increased blood pressure (Daniel, 2018). Despite the reported increase in obesity and its associated diseases there is still a lot of work that needs to be done to support affected individuals. This was highlighted in a study which investigated the management of hypertension in both urban and rural areas. The study reported a lack of medication in health centres and poor patient follow up (Yan et al., 2017). This could be because health centres are already overwhelmed with caring for malaria and HIV/AIDS patients.

II. The prevalence of STH infections in Zambia

The management of soil and waterborne diseases is a big challenge in Zambia and seasonal outbreaks of infectious diseases still occur; as was evident with the recent cholera outbreak in the capital city Lusaka which lasted until early 2018 (Sinyange et al., 2018). In order to control the spread of the disease, the government set up mass cleaning efforts around the city especially in the markets and in residence areas having high populations as they tend to have poor sanitation facilities (Sinyange et al., 2018).

Furthermore, the lack of clean water supply systems means that most people rely on communal water tanks or streams. The combination of poor sanitation and no running water greatly increases the risk of STH infection. Figure 1.1 shows the combined prevalence of STH infections in Zambia based on data collected from different studies. The areas around the capital city are shown to have high prevalence of infection which could be due to the fact that this is the most densely populated region of the country. Stool collected from volunteers living in an area of Lusaka was found to contain eggs from different types of helminths. However, most infected individuals did not show any symptoms of infection (Kelly et al., 2009). The lack of symptoms would mean no medical treatment would be sought, and therefore, the infected individuals unknowingly host the parasites allowing for them to secrete their eggs into the environment which would continue transmission.

The Ministry of health has worked together with WHO to introduce mandatory deworming in school children and ensure the availability of anti-helminthic drugs health centres. However, the lack of sanitary facilities and poor hygiene mean the risk of infection still remains high. A study carried out by Siwila and co-workers in 2015 reported that STH infection in school children was positively associated with poor hygiene in schools (Siwila et al., 2015). Furthermore, they also reported that STH infection was more common in children who had uneducated mothers. Low education levels could mean people are less likely to ensure proper treatment of water before it is used for drinking and cooking (Siwila et al., 2015).

Taken together, Zambia is a clear case of the dual occurrence of STH infection and obesity due to combined multifactorial effects including increasing rural-urban migration, poor lifestyle choices, poverty and illiteracy. These are a huge drain on the society because the affected individuals fail to fully contribute to the socioeconomic growth of the community which leads to a continuous cycle of poverty.

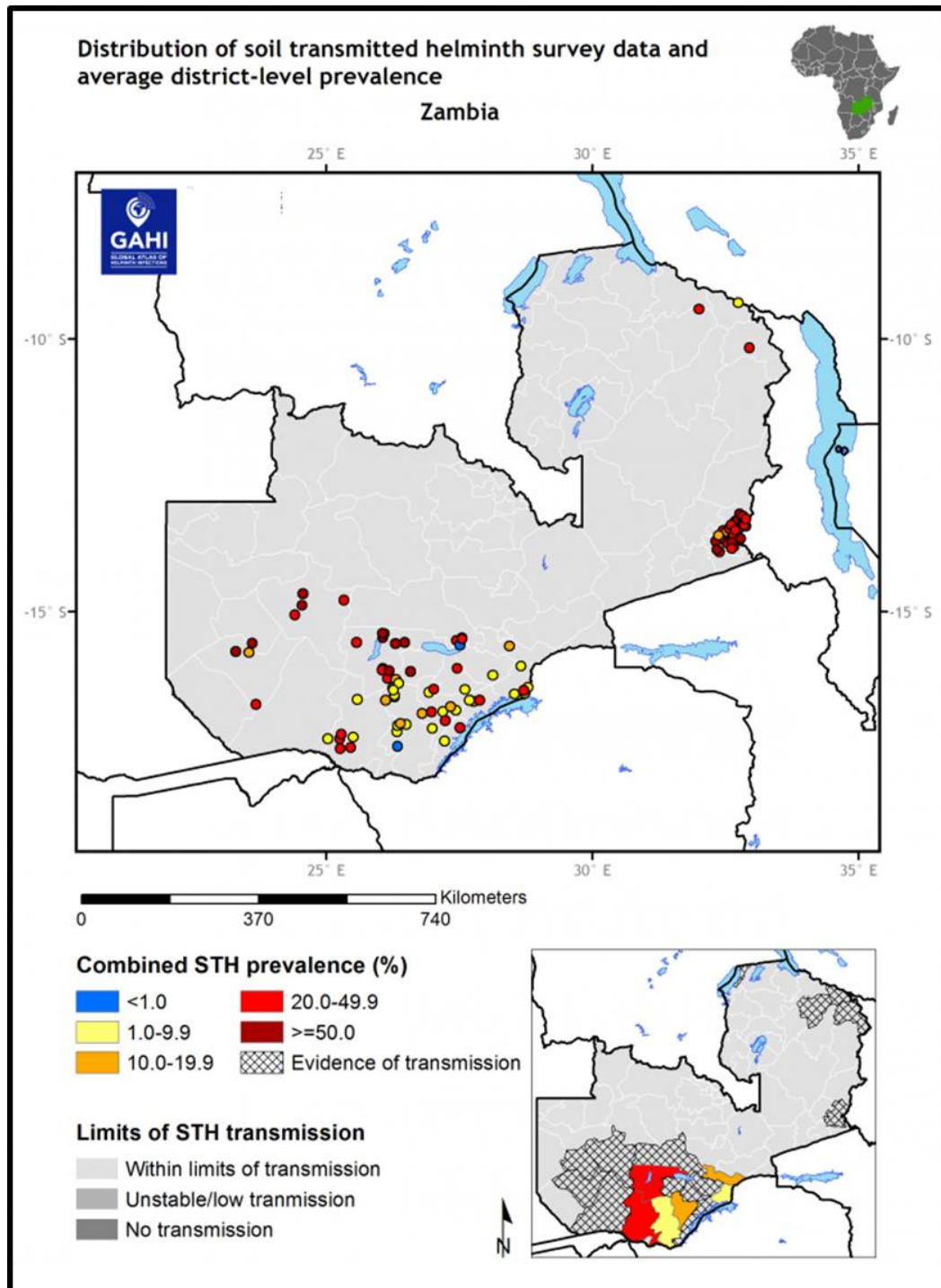


Figure 1-1: Prevalence of STH infections in Zambia.

The prevalence of combined infection with different STH species based on surveys conducted around the country. The insert shows the limits of STH transmission calculated as an average of surveys conducted. Grey shaded areas indicate absence of survey data. Copyright: licenced to the global atlas of worm infections (www.thismywormword.org) under a creative commons attribution-non-commercial 4.0 international licence (<http://creativecommons.org/licenses/by-nc/4.0>)

1.2 Soil transmitted helminth (STH) infections

Helminths are multicellular eukaryotic worms and they include three major groups: cestodes (tapeworms), nematodes (roundworms) and trematodes (flukes). The most ubiquitous are the intestinal nematodes which are comprised of the roundworm (*Ascaris lumbricoides*), the whipworm (*Trichuris trichiura*) and the hookworms (*Necator americanus* and *Ancylostoma duodenale*) (Bethony et al., 2006). STH infections affect at least a quarter of the world's population. In humans these infections are normally not fatal but most of them result in chronic infection, and they can persist in communities if their life cycles are not interrupted. Helminths also compete with the host for nutrients leading to nutritional deficiencies (Bethony et al., 2006). Symptoms of infection include diarrhoea, abdominal pains and intestinal bleeding which may eventually result in anaemia (Stephenson et al., 2000). In addition, chronic helminth infection has also been associated with increased anxiety-like activity in mice (Bercik et al., 2010). However, no clear evidence has been provided to show that helminth infections in humans result in altered behaviour or cognitive functioning (Taylor-Robinson et al., 2015).

1.2.1 *Trichuris muris* as a model to study host immune responses to STH

The naturally occurring infection of mice by *T. muris* has been widely used as a laboratory model of helminth infection. *T. muris* infects the same site as the human whipworm *T. trichiura* and they share antibody cross reactivity (Roach et al., 1988). Advanced genomic analysis has also enabled the comparison of the *T. muris* and *T. trichiura* genomes. Foch and colleagues reported that 9650 genes were predicted in *T. trichiura* whereas 11004 genes were predicted in *T. muris*. Furthermore more than 5800 genes from both species belonged to the same gene family and 5,060 proteins had at least 79 % similarity in their amino acid sequences (Foth et al., 2014). Hence *T. muris* provides a good model to study the immune response to *T. trichiura*, allowing researchers to carry out controlled experiments to gain better understanding of the mechanisms involved in the generation of immunity.

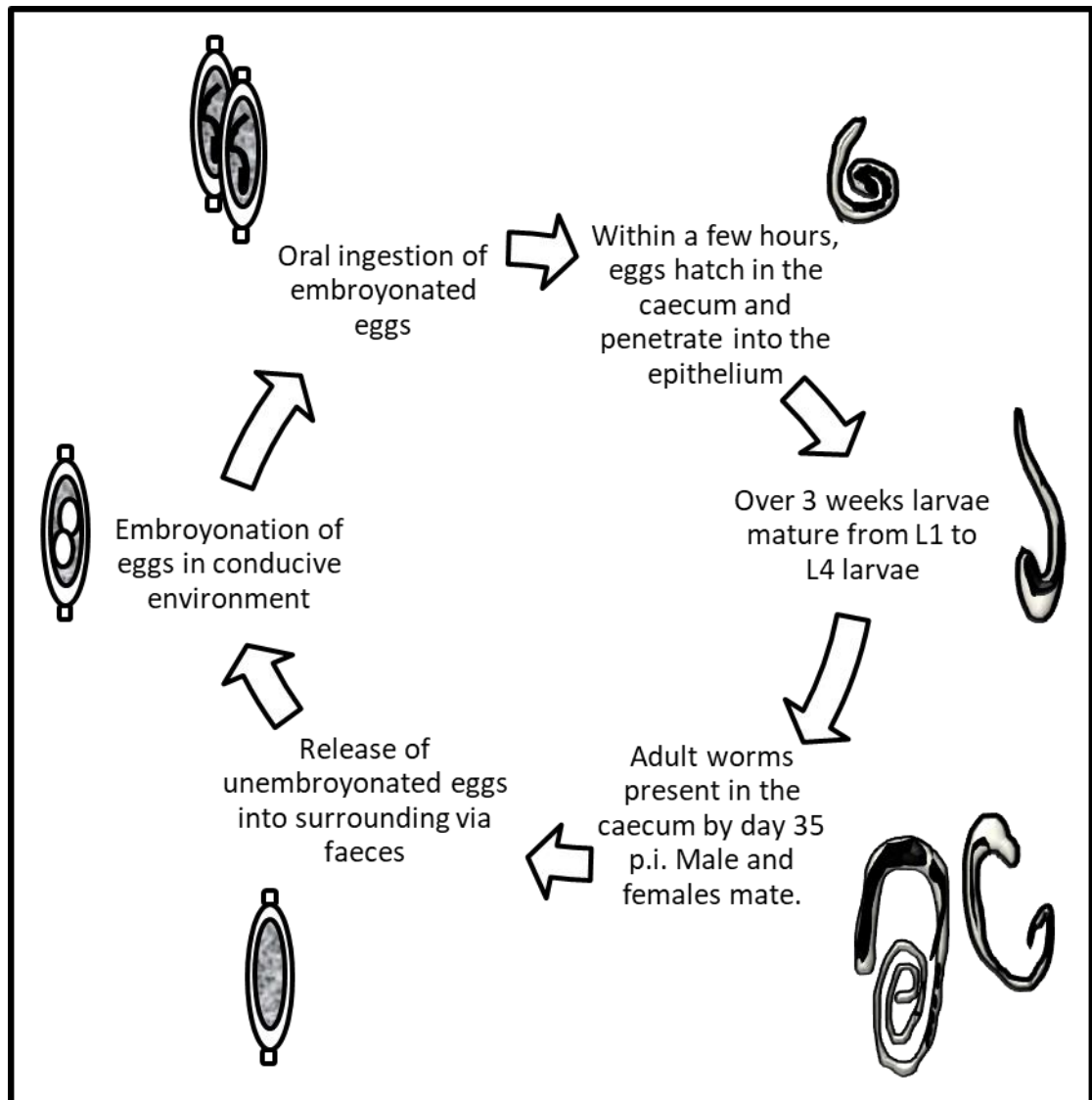
1.2.2 The life cycle of *T. muris*

Figure 1-2: The life cycle of *T. muris*.

Embryonated eggs are ingested by the host. In the caecum the eggs hatch into L1 larvae which then penetrate the host epithelium. The larvae moult through L1 to L4 larval stages. L4 larvae develop into adult worms and after mating the females secrete unembryonated eggs. The eggs mix with the faeces and are released into the environment for embryonation after which they can continue the cycle of infection once ingested.

Once ingested by mice, *T. muris* eggs move to the caecum. After interaction with microbes present in the caecum, the eggs hatch into the first larval stage referred to as L1 larvae (Hayes et al., 2010). The L1 larvae penetrate the epithelial layer of the caecum and proximal colon where they reside. The L1 larvae further moult through the L2, L3 and L4 stages at days 9-11, 17 and 22 post-infection respectively (Cliffe and Grecis, 2004). The presence of the parasite in the epithelium leads to the creation of tunnels as the parasite grows due to the disruption of neighbouring cells (Tilney et al., 2005). After 32 days from the time of infection, adults mature from the L4 larvae and their posterior ends protrude into the lumen of the intestine, whereas the anterior end remains burrowed into the epithelium (Tilney et al., 2005). After mating, the females start to produce unembryonated eggs which are released into the environment by the host mixed with the faeces. Once the eggs are in a suitably warm and moist environment, they become embryonated over a period of 2 months. After this time they become infective once ingested by mice to complete the cycle as shown in figure 1.2 (Cliffe and Grecis, 2004).

1.3 Defining the immune response to *T. muris* infection

Over the past years, a considerable amount of research has focused on understanding the various components of the immune response to STH infection. Both the innate and adaptive immune systems have been shown to play critical roles in the host protection against *T. muris*. Resistance to infection is normally characterised by the ability of the host to generate an immune response that leads to early expulsion of the parasite. On the other hand, susceptibility to infection is characterised by the inability of the host to expel worms thereby leading to the development of a chronic infection (Bancroft et al., 1994b).

1.3.1 The gastrointestinal barrier as a first line defence

The gastrointestinal system is a complex and coordinated system that plays an important role not only in the absorption of food but also in the protection against pathogens. It acts as a selective barrier allowing the passage of dietary molecules while hindering the access of harmful pathogens. One main feature of the gastrointestinal tract that forms

the protective barrier is the mucus gel that covers the underlying epithelial cells (Birchenough et al., 2015).

The supporting framework of the mucus gel is formed by mucins, which are large glycoproteins produced by goblet cells located within the epithelium. The main mucin gene expressed in the intestinal tract is *MUC2* which belongs to the class of secreted polymeric gel forming mucins together with *MUC5AC*, *MUC5B* and *MUC6* (Sheehan and Thornton, 2000). Mucins have a protein backbone to which multiple oligosaccharide chains are attached. The N- and C-termini of the mucin polypeptide have features similar to the von Willebrand factor and are important for the formation of intermolecular disulphide bonds to form the mucin polymers (Gum et al., 1994; Perez-Vilar and Hill, 1999). The internal region of the polypeptide, known as the mucin domain, is rich in the amino acids threonine and serine which provide free hydroxyl groups that are used for the formation of O-glycosidic bonds which anchor the extended oligosaccharide chains (Thornton et al., 2008). The main types of monosaccharides found in mucin oligosaccharides are N-acetylgalactosamine, N-acetylglucosamine, galactose, fucose, and sialic acids. The overall monosaccharide composition will determine if the mucins are neutral or acidic (Sheehan et al., 1996; Thornton et al., 2008). The composition of the oligosaccharide chains gives mucins their characteristic properties. Furthermore, modification by glycosyltransferases and sulphotransferases which add sialic acid and sulphate groups respectively allows further classification of acidic mucins into sialomucins or sulphomucins (Bergstrom and Xia, 2013).

The pre-formed mucin polymers are stored in condensed form inside secretory granules within the goblet cells and upon their release into the extracellular matrix, the aqueous nature of the environment causes the mucins to expand leading the formation of the mucus gel (Thornton et al., 2008). In the large intestine, the mucus gel forms two distinct layers (Johansson et al., 2008). There is a loose outer mucin-rich layer that can be easily aspirated off, which allows for anything trapped in the mucus to be washed away and expelled. The second, inner layer which is firmly associated with the underlying epithelium consists of more densely packed mucins and forms a 'sterile zone' (Johansson et al., 2008; McGuckin et al., 2011). Both layers are underpinned by the *MUC2* mucin.

I. The role of mucins in *T. muris* immunity

A number of studies have shown that infections with *T. muris* results in changes to the mucus barrier. Resistance and susceptibility to *T. muris* each result in distinctive changes to mucin production and glycosylation. Upon infection with *T. muris*, mice showed an increase in the number of Muc2-containing goblet cells and this led to increased mucus production (Hasnain et al., 2011b). Furthermore, Muc2 deficient mice showed a delay in expulsion of *T. muris* worms (Hasnain et al., 2010). Surprisingly, as part of the protection against the worms mice produce the Muc5ac mucin which is not found in the intestine of naïve mice. Further work showed that Muc5ac deficient mice are unable to expel *T. muris* worms indicating that Muc5ac plays an important role in the expulsion process (Hasnain et al., 2010). *In vitro* incubation of Muc5ac with live *T. muris* worms reduced the energy status of the worms suggesting that Muc5ac was affecting their sensory abilities which made it easier for the host to expel the parasite (Hasnain et al., 2011a).

The physical properties of the mucins also change during infection which comes about due to a change in glycosylation. In mice that are resistant, infection with *T. muris* leads to an increase in the level of N-acetylgalactosamine on the mucins (Hasnain et al., 2011b). Furthermore, worm expulsion is associated with increased levels of sulphated mucins. On the other hand, chronic infections in susceptible mice is associated with increased sialylation of mucins which is believed to make the mucins easier to degrade (Hasnain et al., 2017). In addition, *T. muris* secretes serine proteases which target the N-terminal domain of Muc2 thereby degrading the mucin polymers (Drake et al., 1994; Hasnain et al., 2012). This leads to a disruption in the mucus barrier as Muc2 is a major component of the mucus gel. Mice that are resistant to *T. muris* secrete serpins which are protease inhibitors and Muc5ac which is resistant to degradation consequently the mucus barrier is kept intact (Hasnain et al., 2012).

Overall the changes to the mucus barrier results in the formation of a thicker, less permeable barrier which has direct anti-worm activity, is more resistant to degradation thus providing protection against *T. muris* infection.

II. The role of anti-microbial proteins in *T. muris* immunity

The mucus gel also contains antimicrobial peptides which contribute to the protection against *T. muris*. The production of the goblet cell derived resistin-like molecule β (RELM β) is increased upon infection with *T. muris* in resistant mice (Artis et al., 2004). RELM β is believed to directly affect the chemosensory apparatus of the parasites leading to impaired chemotaxis (Artis et al., 2004). However, RELM β is not critical for the resistance to *T. muris* as RELM β deficient mice are still resistant to infection. In addition, the mice displayed a reduction in inflammation associated with reduced production of IFN- γ and TNF- α (Nair et al., 2008).

Angiogenin4 (Ang4) is an antimicrobial protein believed to be toxic to gut dwelling parasites (Hooper et al., 2003). Differential expression is also observed upon *T. muris* infection, with resistant mice increasing their production of Ang4 which is produced by goblet cells in the large intestine (D'Elia et al., 2009b). Another change observed during chronic *T. muris* infection is the up-regulation of indolamine 2.3-dioxygenase (IDO) (Datta et al., 2005). IDO is an enzyme involved in the metabolism of tryptophan via the kynurenine pathway. IDO is believed to play a role in suppressing effector T-cell function and decreases the rate of cell proliferation resulting in reduced epithelial turnover (Bell and Else, 2011).

1.3.2 The cytokine mediated immune response to *T. muris* infection

Upon infection, a complex interplay of immune signalling, activation and regulation occur. T-cells have been shown to be very important in the immune response to *T. muris* infection and nude mice which are congenitally athymic fail to expel worms. However, the transfer of T-cells enriched from infected mice enabled nude mice to expel worms (Yoichi, 1991). In particular, it is the CD4⁺ T cells that play a critical role in the immune response to *T. muris* infection. The transfer of CD4⁺ T-cells from resistant mice to susceptible severely combined immunocompromised (SCID) mice led to worm expulsion (Else and Grecis, 1996). Depending on the signals they receive, the CD4⁺ T-cells can be polarised to

produce either regulatory or pro-inflammatory cytokines. These cytokines play an important role of driving the immune response to infection as shown in figure 1.3.

I. Th2 immune response to *T. muris* infection

The ability to expel parasites early in infection is a feature of host resistance and is attributed to the ability of the host to mount a Th2 immune response against the invading parasite. The Th2 response is characterised by the production of the cytokines IL-4, IL-13 and IL-9 (Else et al., 1992). The combined effect of these cytokines brings about changes that result in the embedded parasites being dislodged and pushed out of the intestinal tract. Early in infection, resistant mice show increased levels IL-33 which is linked to the increased production of thymic stromal lymphopoietin (TSLP) that is important for priming Th2 responses (Humphreys et al., 2008). TSLP neutralisation or deletion of its receptor, TSLPR, resulted in the development of chronic infections in normally resistant mice and this was accompanied by increased production of inflammatory cytokines (Taylor et al., 2009).

Resistance has also been associated with an increase in the number dendritic cells moving to the epithelium of the large intestine (Cruickshank et al., 2009). Moreover, dendritic cells have also been hypothesised to work together with basophils to favour the maturation of Th2 CD4⁺ T-cells (Kim et al., 2010). However both dendritic cells and basophils have been shown to be dispensable in the development of Th2 immune responses (Kim et al., 2010; Perrigoue et al., 2009) Therefore, more research is required to fully delineate the roles of different cell populations in the development of the protective immune response to *T. muris*.

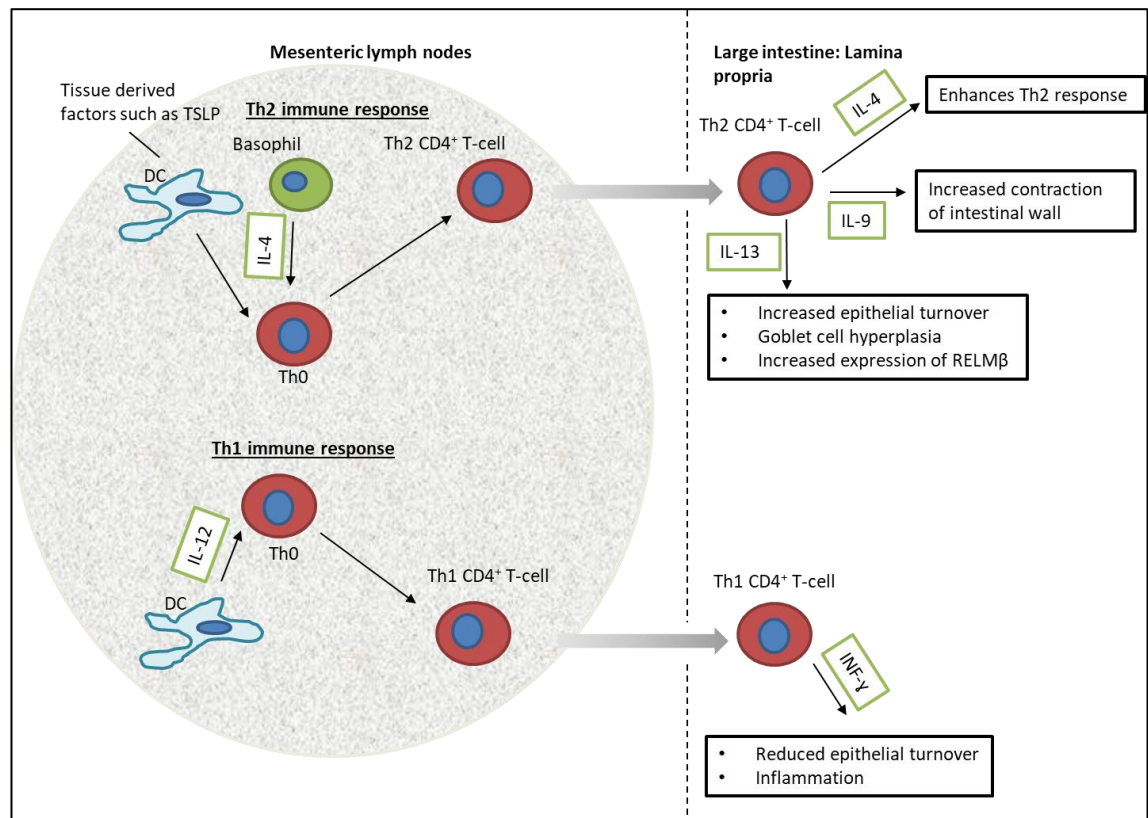


Figure 1-3: Th1 and Th2 immune responses.

T. muris infection leads to the generation of a Th1 immune response in susceptible mice and a Th2 immune response in resistant mice. Dendritic cells play a role in priming the T helper cell response. In resistant mice, CD4⁺ T-cells are stimulated to produce IL-4, IL-9 and IL-13 whereas in susceptible mice, CD4⁺ T-cells predominantly produce IFN- γ . The Th2 cytokines cause an increase in mucus production, epithelial turnover and contraction of muscles in the intestinal wall leading to worm expulsion. On the other hand Th1 cytokine responses lead to increased inflammation and reduced epithelial turnover resulting in the failure to expel worms.

Th2 CD4⁺ T-cells produce IL-4 and IL-13 which are very important in the response to *T. muris* in resistant mice. IL-4 acts on Th0 CD4⁺ T-cells to promote production of Th2 CD4⁺ T-cells. IL4 KO mice are incapable of generating Th2-type immune responses and develop chronic infection (Bancroft et al., 1998). Another important Th2 cytokine that is critical in the immunity against *T. muris* is IL-13. Even though IL-13 KO mice could produce low levels of Th2 cytokines early in infection, the mice could not generate a strong Th2 immune response resulting in the failure to expel worms (Bancroft et al., 1998). Further work showed that administration of recombinant IL-13 to male IL-4 KO BALB/c resulted in a reduction in worm burden (Bancroft et al., 2000). This work highlighted the important role of IL-13 in developing mechanisms that are essential for resistance to *T. muris*. IL-13 increases the production of mucus by increasing the differentiation goblet cells via Signal transducer and activator of transcription 6 (STAT6) signalling (Hasnain et al., 2011b; Khan et al., 2001). In addition, IL-13 increases intestinal muscle contractility and stimulates production of the antimicrobial peptide, RELM β (Hasnain et al., 2011b).

Another mechanism that has been shown to play an important role in worm expulsion is epithelial turnover (Cliffe et al., 2005). Epithelial turnover is the movement of cells from the bottom of the crypt known as the proliferation zone to the top of the crypt known as the shedding zone forming what is referred to as an epithelial escalator. IL-13 increases the rate of epithelial turnover which is believed to facilitate dislodging of the parasite from the epithelium (Cliffe et al., 2005).

Expulsion of the parasite requires the contraction of muscles in the intestine wall. This is associated with IL-9 and the administration of IL-9 to susceptible mice led to faster expulsion (Faulkner et al., 1998). In a study conducted by Khan and colleagues it was observed that neutralising IL-9, by inducing the production of antibodies against IL-9 using treatment with IL-9-OVA complex, led to reduced smooth muscle contractility (Khan et al., 2003). Muscle contraction is believed to be important in worm expulsion as it helps with generating the movements necessary for the expulsion process. The peak of IL-9 production occurs around the time of parasite expulsion.

Th2 immune responses also lead to the generation of IL-5. IL-5 works together with C-X-C motif chemokine 11 (CXCL11) to recruit eosinophils resulting in eosinophilia. Furthermore, the eosinophils from resistant mice were shown to produce IL-4 suggesting

that they may contribute to the development of Th2 immune responses (Dixon et al., 2006; Svensson et al., 2011). However, eosinophils are not a crucial element in the resistance to helminth infection since the absence of eosinophils does not impair worm expulsion (Betts and Else, 1999).

Therefore, different factors are involved in the generation of a successful Th2 immune response. However, regulation of the immune response is also important and IL-10 is an important regulator of immune responses in during *T. muris* infection. IL-10 deficient mice are susceptible to infections and show increased morbidity highlighting the importance of IL-10 as an anti-inflammatory cytokine (Schopf et al., 2002a). Tumor necrosis factor alpha (TNF- α) is also involved in the regulation of host immune responses. C57BL/6 mice treated with anti-TNF- α antibody and then infected with a high dose of *T. muris* failed to expel worms by day 21 post infection. In addition, TNFR deficient mice were susceptible to *T. muris* infection and produced very low levels of Th2 cytokines (Artis et al., 1999a). However further work showed that administration of recombinant TNF- α (rTNF- α) delayed worm expulsion in C57BL/6 and AKR mice (Hayes et al., 2007). rTNF- α treatment was shown to enhance the production of Th2 cytokines in highly resistant BALB/c mice. On the other hand C57BL/6 treated mice produced elevated levels of both Th1 and Th2 cytokines whereas AKR mice which are susceptible to a high dose of *T. muris* infection produced elevated levels of Th1 cytokines (Hayes et al., 2007). Therefore, this suggests that the role of TNF- α is to enhance the established immune response.

II. Th1 immune response

Susceptible mice are unable to successfully mount a Th2 response, instead they generate a Th1 immune response characterised by the production of the pro-inflammatory cytokine IFN- γ by Th1 CD4⁺ T-cells. The mice fail to expel the parasite and develop a chronic infection (Bancroft et al., 1994b). Artis and co-workers showed that susceptible mice also had elongated crypts due to hyper-proliferation of the epithelial layer which they suggested may be associated with elevated levels of IFN- γ (Artis et al., 1999b). Apart from controlling proliferation, IFN- γ and IFN- γ induced protein 10 (CXCL10) were shown to down regulate epithelial cell turnover which is believed to be a major mechanism

involved in parasite expulsion (Cliffe et al., 2005). IFN- γ production during chronic infection was shown to be associated with an increase in apoptosis which controls the number of cells within the crypt (Cliffe et al., 2007). Therefore, during chronic *T. muris* infection, the balance between proliferation and apoptosis is offset resulting in reduced epithelial turnover and crypt elongation.

IL-12 is a regulatory cytokine associated with increased Th1 immune responses. Administration of IL-12 to resistant mice led to the development of Th1 immune responses which could be reversed by treatment with IFN- γ antibody (Bancroft et al., 1997). In addition, impairing Th2 immune responses by neutralising TSLP or knocking out its receptor to generate TSLPR KO mice led to an increase in expression of the IL-12/23p40 subunit upon infection with *T. muris*. This was associated with increased production of IFN- γ and IL-17A implying that the Th1 immune responses were enhanced (Taylor et al., 2009).

1.3.3 ILC2 cells in *T. muris* infection

Increased IL-13 production has also been observed in other helminth infections including *Nippostrongylus brasiliensis* in response to IL-25 produced by tuft cells (Gerbe et al., 2016; Gerbe et al., 2011). IL-25 is important for maintaining/generating the population of group 2 innate lymphoid cells (ILC2). Upon infection with *N. brasiliensis*, an increase in tuft cells results in increased IL-25 production and this activates ILC2 cells to produce IL-13 (von Moltke et al., 2016). Therefore, ILC2 cells play a role in promoting Th2 immune responses. Previously it was shown that IL-25 deficient mice are susceptible to *T. muris* infection and produce less Th2 cytokines. However, the transfer of multi-potent progenitor type 2 (MMP^{type2}) cells improved worm expulsion (Saenz et al., 2010). MMP^{type2} promote Th2 immune responses and lineage markers have differentiated MMP^{type2} from ILC2 (Saenz et al., 2013). Interestingly, recent work has shown that during *T. muris* infection there is no increase in the number of ILCs and that they are not critical for resistance (Glover, 2017). Therefore, more research is necessary to understand the role IL-25 and ILC2s may play during *T. muris* infection.

1.3.4 The role of antibody responses in *T. muris* immunity

The type of dominant antibody response observed in infected mice correlates with the type of immune response. Therefore, *T. muris* specific antibody serum levels are normally used as markers for resistance or chronicity. Resistance is associated with production of IgG1, whereas chronicity is associated with increased IgG2a production (Koyama et al., 1999). B cell deficient mice (μ MT mice) are susceptible to *T. muris* infection which can be rescued by transferring either B-Cells or IgG from resistant mice (Blackwell and Else, 2001). However, further work in the μ MT mice showed that blocking of IL-12 to inhibit Th1 responses led to antibody independent worm expulsion implying that B cells are not crucial for resistance (Blackwell and Else, 2001). This is more evident in the ability of SCID mice to expel worm by the transfer of T-cells alone which are vital for the expulsion of *T. muris* (Else and Grencis, 1996).

1.3.5 Dose-dependent immunity to *T. muris*

In BALB/K mice, a high infection dose of approximately 400 eggs generates a strong Th2 immune response, whereas when given as a low dose of less than 40 eggs, the mice develop chronic infections (Bancroft et al., 1994b). This clearly shows that the infective dose can cause a shift in the immune response. Researchers have taken advantage of this dose-dependent effect to investigate acute and chronic immune responses to *T. muris*. However, in nature there is a high possibility of repeated exposure infection. To make the mouse model more reflective of natural infections, repeated low dose infections are given to mice on a weekly basis in what is termed as trickle infection (Wakelin, 1973). Early investigations into trickle infections showed that mice given daily low dose infections of approximately 5 to 10 eggs over two weeks developed protective immunity (Wakelin, 1973). Bancroft and colleagues reported that during the course of a trickle infection, C57BL/6 mice had a build-up of worm burden which was not observed in BALB/K mice which are more resistant to *T. muris* infection (Bancroft et al., 2001). Further work showed that there appears to be a threshold level of infection above which expulsion is induced in the C57BL/6 mice as the immunity starts to build up (Glover, 2017). This form of acquired immunity is a very important aspect of immunity to helminth

infections for people at high risk of repeated infection due to repeated daily exposure (Bancroft et al., 2001).

1.3.6 The role of genetics in immunity to *T. muris*

The outcome of *T. muris* infection has been shown to differ based on the mouse strain. Studies have shown that mice with the same background gene, but a different allele of the major histocompatibility complex (MHC), differ in their response to *T. muris*. Mice that have an H-2^K haplotype were shown to be more susceptible to infection than mice having other haplotypes such as H-2^b or H-2^q (Else and Wakelin, 1988). In addition, mice with the same MHC gene but different background also have different responses to *T. muris* infection. BALB/K mice and AKR mice both have the H-2^K haplotype, however, BALB/K are resistant to infection and expel worms as early as 14 days post-infection. On the other hand, AKR mice fail to expel and develop chronic infection (Else et al., 1992). This indicates that other non H-2 linked genetic factors strongly influence the type of immune response generated upon infection. For example, BALB/c mice which are more resistant to infection develop stronger Th2 immune responses with increased number of CD4⁺ T-cells at day 21 post infection in comparison to the AKR mice (Little et al., 2005).

Another genetic factor affecting the outcome of infection is gender. Female IL-4 deficient BALB/c mice are resistant to *T. muris* infection, whereas their male counterparts develop chronic infection. This difference in the immune response is believed to be due to sex hormones with dihydrotestosterone favouring Th1 immune responses in males, while 17- β estradiol favours Th2 immune responses in the females (Hepworth et al., 2010). Resistance was enhanced in castrated mice or when IL-13 was administered to the male mice (Bancroft et al., 2000; Hepworth et al., 2010). This highlights the importance of sex hormones in the development of immune responses.

Furthermore, the outcome of infection depends on the *T. muris* isolate used. The three isolates of *T. muris* used in the laboratory are the E (Edinburgh), J (Japan) and S (Sobreda) isolates (Bellaby et al., 1996; Koyama and Ito, 1996). Infection with the E and J isolates resulted in Th2 immune responses. On the other hand, the S isolate resulted in Th1 immune responses in mice that were resistant to the E and J isolates (Bellaby et al., 1996).

In C57BL/6 mice susceptibility to the S isolate was shown to be due to increased numbers of T regulatory cells (Tregs) in the gut providing evidence that Tregs promote the development of chronic infections (D'Elia et al., 2009a).

1.4 Helminths and metabolic homeostasis in obesity

Helminth infections lead to a variety of symptoms depending on the load of infection including bleeding which can lead to anaemia (Stephenson et al., 2000). Increasing awareness of helminth infections has led to global efforts to reduce the risk of infection such as encouraging good hygiene and sanitation practises. In addition, deworming of school children and commercial availability of anti-helminthic drugs are also helping to reduce the transmission. Apart from the undesirable symptoms, the helminth driven immune responses can also provide some benefits to the host such as preventing the adverse effects of inflammatory diseases by enhancing the production of regulatory cytokines (Wegener Parfrey et al., 2017). Epidemiological studies have shown that there is an inverse relationship between helminth infections and the occurrence of some non-communicable diseases such as type II diabetes (Wiria et al., 2014). In a review by Guigas and Molofsky, the authors suggest that anti-helminthic drugs also target benign helminths which do not cause adverse symptoms in the host and that there is no clear understanding of how eradication of these helminths may affect the metabolic health of people around the world (Guigas and Molofsky, 2015).

Obesity is associated with impaired ILC2 function in adipose tissue. The loss of ILC2 function has recently been associated with increased levels of TNF- α which was shown to increase the expression of the inhibitory receptor PD-1 on ILC2s (Oldenhove et al., 2018). ILC2s play a role in regulating calorific usage in white adipose tissue (Brestoff et al., 2015). ILC2s produce IL-5 and this recruits eosinophils (figure 1.4) which then recruit alternatively activated macrophages (M2 macrophages) through IL-4 signalling to the white adipose tissue (Hams et al., 2013; Lee et al., 2015).

Helminths are strong drivers of Th2 immune responses associated with an increase in the number of ILC2s as is observed in *N. brasiliensis* infection (von Moltke et al., 2016). Mice infected with *Heligmosomoides polygyrus* also develop strong Th2 immune responses and

this was associated with an increase in the number of anti-inflammatory M2 macrophages in gonadal fat of obese C57BL/6 mice (Su et al., 2018). When naïve high fat diet (HFD) pre-fed obese mice were given M2 cells from *H. polygyrus* infected mice a number of changes were observed including reduced blood glucose and cholesterol as well as altered gene expression of leptin and TNF- α in the subcutaneous fat (Su et al., 2018). Similar observations have also been seen in obese mice infected with *Schistosoma mansoni* and *N. brasiliensis* (Hussaarts et al., 2015; Yang et al., 2013)

Helminth infections result in increased production of uncoupling protein 1 (UCP1) (Su et al., 2018). The increased production of UCP1 is due to the infiltration of M2 macrophages. M2 macrophages induce the production of UCP1 by producing thyroxine hydroxylase which is a limiting enzyme in catecholamine synthesis (Qiu et al., 2014). However, ILC2 cells can also directly induce UCP1 synthesis in white adipose tissue by secreting the opioid met enkephalin (Brestoff et al., 2015). UCP1 uncouples oxidative phosphorylation, leading to the generation of heat and this reduces weight gain by increasing metabolism in white adipose tissue (Hams et al., 2013). Therefore uncoupling of oxidative phosphorylation which has been known to be a way in which the body increases heat production upon exposure to cold has now been shown to be involved in improving metabolic health in obesity (Lee et al., 2015; Qiu et al., 2014).

Apart from their role in metabolic homeostasis, a new role for eosinophils has recently been reported. A study by Withers and colleagues has showed that eosinophils released catecholamines that are important for the activation of β 3-adrenoreceptors expressed on adipocytes. As a result, adipocytes release nitric oxide and adiponectin which are important for maintaining the anti-contractile properties of perivascular adipose tissue and vascular tissue (Withers et al., 2017). Therefore by increasing the number of eosinophils, helminth infections not only improve metabolic health but they may also improve vascular health.

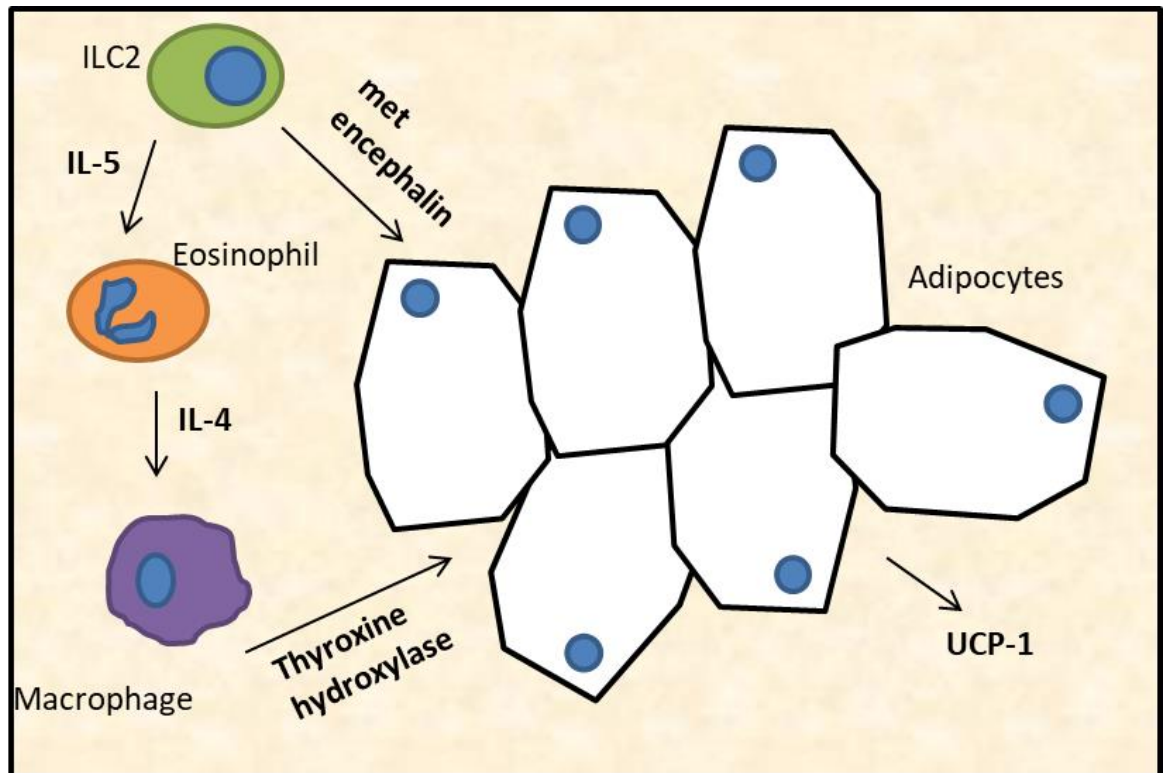


Figure 1-4: The role of Th2 immunity in thermogenic regulation.

ILC2 cells are involved in Th2 immune responses. In white fat, ILC2 cells recruit eosinophils via IL-5 signalling. The eosinophils recruit alternative activated macrophages which produce the enzyme thyroxine hydroxylase which promotes the production of UCP1. ILC2 cells also secrete met-enkephalin which acts directly on white adipose tissue to induce the production of UCP1, this results in an increase in heat generation by uncoupling of oxidation phosphorylation.

1.5 The use of mouse models to learn more about high fat diet (HFD) induced obesity

Obesity is an increasing challenge of modern society affecting people from both developed and developing countries. A great deal is known about the medical outcomes of obesity such as increased risk of diabetes and stroke. Researchers have used a variety of mouse models to investigate the mechanisms involved in the development of obesity and how they lead to the development of disease.

The development of diet-induced obesity (DIO) is strain dependent with C57BL/6 mice prone to DIO, whereas some other mouse strains such as BALB/c mice are more resistant (Surwit et al., 1995). C57BL/6 mice that are fed on western type diets or high fat diets show increased weight and hyperglycaemia, therefore providing a good model of human obesity and diabetes II (Rebuffé-Scrive et al., 1993). Thus, a number of researchers have used C57BL/6 mice to gain insight into the development and progression of DIO. Genetically altered mice which are prone to obesity have also been used to learn about the mechanisms involved in the development of DIO (Koch et al., 2010; Koch et al., 2013; Lindstrom, 2007). Together these studies have provided more insight into the regulation of different pathways at the onset of obesity which are discussed below.

1.5.1 The role of leptin in obesity

Food intake and energy expenditure are known to be regulated by the hormone leptin. In obesity, the level of circulating leptin increases, however its ability to regulate both food intake and increase energy expenditure reduces (Schwartz et al., 1996). This insensitivity to leptin is believed to be a main factor in the development of obesity (Friedman and Halaas, 1998). The loss of function of the gene responsible for leptin production predisposes mice to obesity as is the case for $lep^{ob/ob}$ mice which are grossly overweight and develop severe insulin resistance (Ingalls et al., 1950; Lindstrom, 2007). When $Lep^{ob/ob}$ mice are given chronic intracerebroventricular infusion of leptin, there is an improvement in glucose metabolism and reduction in body weight (Koch et al., 2010). Interestingly, when the $Lep^{ob/ob}$ mice were then fed on a HFD after leptin infusion, the presence of leptin could not reverse the obesity characteristics (Koch et al., 2013). This suggests that the HFD caused the mice to become insensitive to the administered leptin.

1.5.2 HFD and the immune response

Obesity has been linked to changes in the immune response to various stimulants. Splenocytes from DIO mice stimulated with phytohemagglutinin (PHA) produced higher levels of IL-4 and IFN- γ in comparison to splenocytes from mice fed on a control diet (Sato Mito et al., 2009). Co-culture of splenocytes with PHA and leptin led to reduced IL-4 production but had no effect on IFN- γ in DIO mice. However, control mice had increased IL-4 and IFN- γ suggesting that obesity may be associated with enhanced proinflammatory responses (Sato Mito et al., 2009).

Altered immune responses have also been reported in obese C57BL/6 mice in response to treatment with the chemically reactive hapten trinitrochlorobenzene (TNCB). Chemically reactive haptens are used in contact hypersensitivity (CH) reactions which study cell mediated immune responses (Friedmann, 1989). An initial application of TNCB solution to clipped areas of the skin results in immunization against TNCB. The mice can then be further challenged by a second application of TNCB on the ears after a selected number of days following the initial application. The response to TNCB treatment can be assessed in a number of ways such as measuring ear swelling at different time points post application and by measuring cytokine response from immune cells extracted from the lymph nodes. CH is believed to be mediated by CD4⁺ T-cells and has suggested to be driven by type 1 immune responses (Gautam et al., 1991). However, work by Dieli and colleagues showed that IL4-KO mice had impaired CH responses to TNCB suggesting that IL-4 may be playing an important role in the development of the reaction to TNCB (Dieli et al., 1999). Investigations carried out in obese mice showed that obese mice treated with TNCB showed reduced production of IFN- γ and IL-4 production by cervical lymph node cells in the neck in comparison to the control mice (Katagiri et al., 2007). In a separate study, T-cells collected from the spleen of ovalbumin immunised HFD mice had impaired antigen dependent proliferation compared to cells collected from standard diet mice. In addition, the T-cells from the HFD immunized mice showed enhanced production of the Th2 cytokine IL-4 in comparison to the standard diet mice (Verwaerde et al., 2006). These studies suggest that HFD causes a change in cytokine profiles of immune cells which play a critical role in the development of immune responses.

The mechanisms behind the altered immune responses in obesity are not yet fully understood. In addition to the role in regulating food intake and glucose metabolism, leptin has been showed to affect the composition of T-cells in the thymus of obese mice (Howard et al., 1999). *In vitro* studies have shown that leptin can modulate T-cell function and enhance the production of pro-inflammatory cytokines (Lord et al., 2002). Therefore, leptin may play a role in altering the immune responses in obese mice although more conclusive evidence is still required.

Another factor believed to be associated with the altered immune responses in obesity is the effect of HFD on transcription regulators. Obesity is associated with increased acetylation of transcriptional regulators. In a study conducted by Kim and co-workers, it was observed that over time, that HFD feeding in C57BL/6J male mice was associated with increased acetylation of the nuclear receptor, FXR, which plays a key role in regulating fatty acid and glucose metabolism as well as regulating anti-inflammatory responses (Kim et al., 2014). The increased acetylation of FXR was associated with increased expression of mRNA for proinflammatory genes such as IL6, IL1 and TNF- α . Furthermore, they show that increased acetylation of FXR in mice fed on a HFD was associated with a reduction in SUMOylation of FXR. SUMOylation of FXR is believed to repress NF-kB target inflammatory genes hence reduced SUMOylation would increase the expression of inflammatory genes in obese mice. Therefore changes in acetylation/SUMOylation of nuclear receptors associated with obesity may provide an explanation for altered immune responses associated with obesity (Kim et al., 2014).

1.5.3 HFD and epithelial cell proliferation

The ability to renew the cells of the epithelium is very important in maintaining the integrity of the epithelial barrier. Intestinal epithelial stem cells located in the intestinal crypts give rise to progenitor cells which can then mature into the different types of epithelial cell such as goblet cells, enterocytes or Paneth cells (Cheng and Leblond, 1974). Obesity has been shown to result in hyper-proliferation of intestinal epithelial cells (Dailey, 2014; Mah et al., 2014). The restriction of calorie intake shows that hyperphagia in obese mice led to increased proliferation of intestinal epithelial stem cells through

altered beta catenin signalling which is important for maintaining cell proliferation and homeostasis (Mao et al., 2013).

A recent study by Zhou and colleagues investigated the changes to the size and function of intestinal epithelial stem cells from HFD-fed obese mice and compared them to those of control diet fed mice, and to HFD fed mice with restricted calorie intake to keep them lean as the control mice. They found that only intestinal epithelial stem cells collected from HFD-fed obese mice formed larger enterospheres and *in vivo* they showed that the HFD obese mice had increased crypt depth as well as villus height in the jejunum (Zhou et al., 2018). Interestingly, the restricted HFD fed mice had features similar to the control diet fed mice. This work highlights the fact that HFD induced changes result from obesity due to hyperphagia and not just as a result of consuming a HFD (Zhou et al., 2018). Therefore, it is possible that it the oversupply of nutrients in obesity induces the changes to the intestinal epithelium.

1.5.4 Hyperglycaemia and intestinal barrier dysregulation

Similar to humans, mice on a HFD exhibited elevated levels of serum triglycerides as well as increased intolerance to hormones such as insulin and leptin, which are involved in glucose metabolism and regulation of food intake respectively (Lam et al., 2012). Elevated blood glucose due to insulin insensitivity is one the features associated with HFD. In a study by Ikemoto and colleagues, separate groups of C57BL/6J mice were each fed high fat diet containing dietary oil derived from different sources such as soybean, palm, lard or fish oil. Irrespective of the source of dietary oil, all the mice fed on a HFD had showed changes in glucose tolerance by 3 weeks of feeding (Ikemoto et al., 1996).

Another feature of obesity is low grade inflammation due to the increased systemic circulation of microbial molecules sometimes referred to as metabolic syndrome. HFD reduces the expression of the tight junction proteins which are required to maintain the integrity of the epithelium (Benoit et al., 2015). This loss of epithelial integrity is associated with enhanced permeability of the intestinal barrier and this is believed to be the cause of the increased translocation of the microbial molecules including bacterial lipopolysaccharide into the systemic circulation. This results in the development of low-

grade inflammation in the host (Cani et al., 2008; Lam et al., 2012). Using a range of mouse models of obesity, Christoph and colleagues have shown that hyperglycaemia is in fact a key factor that drives intestinal barrier permeability. They suggest that hyperglycaemia leads to metabolic and transcriptional alterations that lead to the reprogramming of epithelial cells eventually resulting in the dysregulation of the epithelial barrier (Thaiss et al., 2018).

1.6 HFD and the mucus barrier

A number of researchers have investigated the effects of HFD feeding on mucin glycosylation, changes in which would alter the properties of the mucus gel. Feeding C57BL/6 mice a western diet led to increased acidity of colonic mucins with an increase in sialo/sulphomucin ratio, as well as increased binding of soybean lectin (SBA) which has an affinity for N-acetyl-galactosamine (Yang et al., 1996). Similarly mice fed on a HFD for 25 weeks also show an increase in the number of colonic goblet cell mucins, as well as increased sialo/sulphomucin ratios (Mastrodonato et al., 2014). In addition, Martinez-medina and colleagues reported that HFD feeding of CEABAC10 mice, which are prone to Crohn's disease, led to a reduction in the thickness of the mucus barrier. This would potentially makes it easier for pathogenic bacteria to penetrate the mucus lining and induce low grade inflammation (Martinez-Medina et al., 2014). Therefore, compromising the mucus barrier would make the host more susceptible to pathogenic infection. Paradoxically, Hartmann and co-workers have shown that absence of the mucus barrier may offer benefits to the host. Muc2 deficient mice, which do not have a mucus barrier, had increased production of IL-22 and reduced inflammation in comparison to wild type control mice after 16 weeks of HFD feeding (Hartmann et al., 2016). Furthermore, the HFD fed Muc2 deficient mice also showed improved glucose tolerance and insulin responsiveness. These findings may indicate that the absence of the mucus layer may improve overall glucose homeostasis (Hartmann et al., 2016).

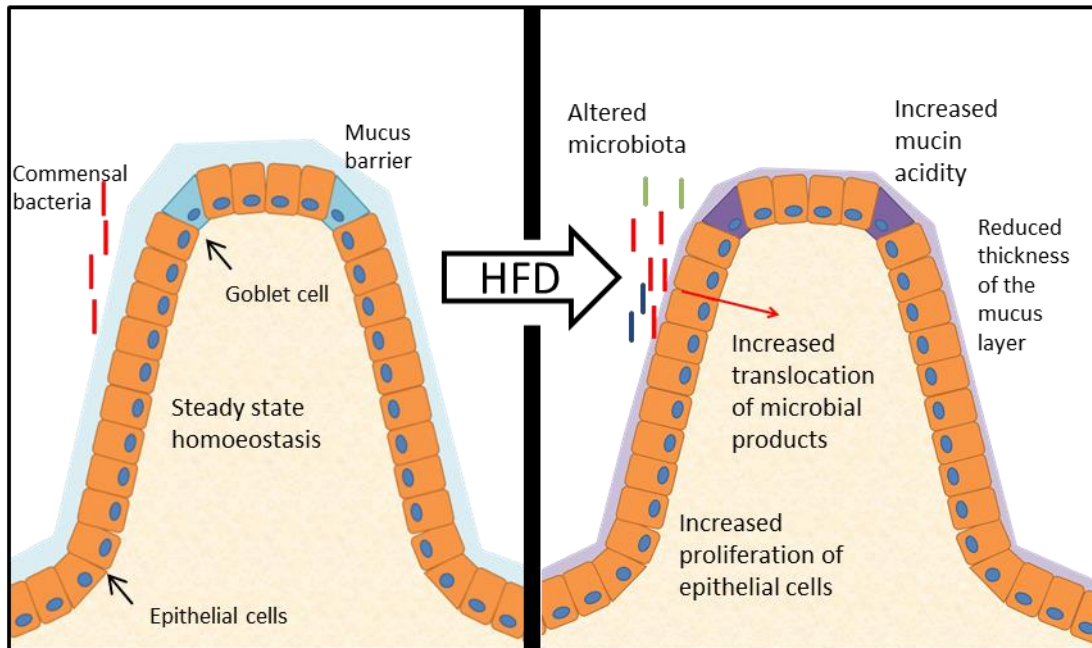


Figure 1-5: HFD and the intestinal barrier

The intestinal barrier is composed of the mucus layer that is located directly above of the epithelial cells. HFD induces changes to the properties of the mucus barrier and induces proliferation of epithelial cells. HFD alters the composition of the intestinal microbiota and increases the permeability of the intestine barrier leading to increased translocation of bacterial products.

Taken together, these studies show that there is a complex relationship between HFD and the intestinal barrier as shown in figure 1.5. These changes may increase host susceptibility to infection while also enhancing protective mucosal immunity which would be of benefit to the host.

1.7 The intestinal microbiota and its biological importance

The intestine is home to trillions of bacteria. The conditions in the intestine provide a suitable environment for the growth of these bacteria (Smith, 1965; Whitman et al., 1998). The presence of these commensal bacteria helps to hinder colonisation by pathogenic organisms (Sekirov et al., 2008). The bacteria also produce enzymes that can harvest energy from complex dietary molecules, thereby making these foods available to the host. Short chain fatty acids (SCFAs) such as acetate, propionate and butyrate are by products of bacterial fermentation (Rémésy et al., 1992). These SCFAs are taken up by the epithelial and into host circulation where they have a range of functions including regulating hormone control and immune responses (Park et al., 2007).

The connection between the intestinal microbiota and other tissues or organs is a major area of interest. For example, the intestinal microbiota has been linked to neurological disorders and heart disease (Bogiatzi et al., 2018; Cox and Weiner, 2018; Spychala et al., 2018). In addition, the microbiota has been linked to circadian biology of the host, with microbiota influenced by the time of day, as well as eating patterns (Kaczmarek et al., 2017). This emerging field has directed attention to the importance of gut microbiota and how the uncontrolled use of antibiotics may be affecting our health. Antibiotics not only target the pathogenic microbes but they also affect the commensal bacteria. This results in an altered host microbiota (Sekirov et al., 2008). Recent studies have also linked changes in the gut microbiota to diseases such as inflammatory bowel disease and the development of obesity (Cani et al., 2008; Guslandi, 2011). One way of correcting dysbiosis has been through the use of probiotics which contain specifically formulated live cultures of bacteria that have been shown to have health benefits (Lee et al., 2018).

1.7.1 HFD and the intestinal microbiota

The exact composition of the microbiota differs between individuals. However, the majority of the mammalian intestinal microbiota falls in the phyla *Bacteroidetes*, *Firmicutes* and *Actinobacteria* (Musso et al., 2011). There has been great interest in how a HFD changes the composition of the intestinal microbiota. A study in 12 unrelated obese men and women showed an overall reduction in *Bacteroidetes*. When the participants were switched to a low calorie diet, the degree of weight loss was proportional to the increase in *Bacteroidetes* (Ley et al., 2006). Similar to humans, mice on a HFD show changes in the composition of intestinal microflora with an increase of bacteria belonging to the phyla *Firmicutes* and a reduction in *Bacteroidetes* (Benoit et al., 2015; Kim et al., 2012; Thi Loan Anh et al., 2015). Specific changes at the genus level are also associated with HFD, with HFD fed mice having reduced *Ruminococcaceae*, *Parabacteriodes*, *Christensenellaceae* and *Lactobacillus* (Zhou et al., 2017).

The microbiota of the different compartments of the gastrointestinal tract shows variations in response to HFD. In the ileum there is an increase in total microbial content with particular increase in *Firmicutes*, *Proteobacteria* and *Verrucomicrobia* (Tomas et al., 2016). In the distal colon, HFD causes an increase in bacteria belonging to the class *Mollicutes* and switching mice to low calorie diet, which did not induce weight gain, reversed the changes in the microbiota (Turnbaugh et al., 2008). HFD also resulted in reduced microbial diversity causing an enrichment of bacteria that utilise simple sugars such as fructose and mannose which are abundant in high fat rich food (Turnbaugh et al., 2006b). In addition, HFD also increased the number of bacteria able to import and metabolise host glycans such as GalNAc which are part of the host mucus (Turnbaugh et al., 2006b).

One bacterium that has been a subject of increasing interest is *Akkermansia muciniphila*. *A. muciniphila* is a Gram-negative strict anaerobe that belongs to the phylum *Verrucomicrobia*. It thrives in the outer mucus layer as it is capable of utilising host mucins as a source of food (Derrien et al., 2004). The bacterial products of *A. muciniphila* are believed to stimulate the growth of other commensal bacteria in the mucus which reduces colonisation by invading pathogens (Derrien et al., 2004). Mice fed on a HFD show a reduction in *A. muciniphila* and oral administration of *A. muciniphila* reverses

HFD induced obesity (Everard et al., 2013). Furthermore, *A. muciniphilia* has been shown to improve the intestinal barrier function and immunological homeostasis by inducing the production of IL-10 (Ottman et al., 2017). This provides evidence of a link between host microbiota and obesity. This is also observed in germ-free mice which do not develop the features of diet induced obesity when fed on a HFD (Backhed et al., 2007). The resistance to obesity in germ-free mice is dependent on the type of dietary intervention. Germ-free mice fed on a cholesterol-rich, lard base did not develop diet induced obesity, whereas mice fed on a palm oil based diet developed obesity (Kübeck et al., 2016).

1.7.2 Helminth infections and the intestinal microbiota

Gastrointestinal parasites occupy the same niche as the intestinal microbiota. Therefore, there is a high chance of associations developing between the parasites and the intestinal microflora. Altering the intestinal microbiota directly affects the hatching of *T. muris* (Hayes et al., 2010). During the course of *T. muris* infection, microbiome changes in mice have been observed with a reduction in the diversity of bacterial communities. At early stages there is an increase in *Bifidobacterium* by day 13 and increased *Lactobacillus* at day 20 post-infection (Holm et al., 2015). By day 27 to 35, there is an overall change in bacterial composition with an increase in *Firmicutes* and reduction in *Bacteroidetes* in faecal samples (Holm et al., 2015). A separate study by Houlden and colleagues also reported a shift in microbiota between day 14 and 28 in *T. muris* infected mice. Infected mice had reduced diversity as well as abundance of *Bacteroidetes*. Furthermore, when mice were treated with mebendazole to clear the parasite, the microbiota in the infected treated mice started to recover and resemble that of naïve mice by day 91 (Houlden et al., 2015).

Changes in the microbiota have also been reported following infection by the thread worm *Strongyloides venezuelensis* in mice that had been fed on either normal diet or HFD (Pace et al., 2018). Similar to infected mice on a control diet, infected HFD mice showed an increase in *Firmicutes* with a reduction in *Bacteroidetes*. In addition, both control diet and HFD fed mice showed an increase in *Lactobacillus* spp upon infection (Pace et al., 2018). *Lactobacillus* is a prebiotic which is believed to increase the uptake of butyrate in

intestinal epithelial cells. Butyrate promotes hormone secretion and reduces inflammation. HFD fed mice given a prebiotic treatment showed improved glucose tolerance and glucose utilisation compared to untreated HFD fed mice (Pace et al., 2018). HFD is associated with a reduction in *Lactobacillus* spp which can be reversed by supplementing with sodium butyrate (Zhou et al., 2017). Interestingly, the HFD mice supplemented with sodium butyrate also had lower body weight, reduced serum glucose and improved liver steatohepatitis in comparison to mice fed on a HFD alone ((Zhou et al., 2017).

Therefore, these studies show that there seems to be an association between gastrointestinal helminths and the host microbiota which can be explored for therapeutic purposes.

1.8 HFD and the progression of helminth infections

HFD is associated with increased production of leptin and pro-inflammatory cytokines by adipose tissue adipocytes, such as TNF- α and IL-6, which have been implicated with the development of metabolic syndrome and increased risk of metabolic disease (Hotamisligil et al., 1993; Pradhan et al., 2001; Trembleau et al., 2003). Furthermore, the increased inflammation induced by HFD is associated with reduced levels of anti-inflammatory Tregs in the adipose tissue which play a role in modulating inflammation (Deiuliis et al., 2011; Pettersson et al., 2012). Changes in the cytokine environment of HFD mice may influence the development of the immune response to parasitic infection. Previous researchers have attempted to evaluate the effect of HFD on the progression and outcome of helminth infections. An early study by Sudati and colleagues using the intestinal fluke, *Echinostoma caproni*, reported that fewer worms were recovered from HFD fed mice in comparison to control mice. They also showed a reduction in worm dry weight and uterine egg counts (Sudati et al., 1996). In contrast, HFD fed mice infected with *Schistosoma mansoni* showed an increase in tissue egg density as well as increased faecal egg counts in comparison to normal chow fed mice (Alencar et al., 2009; Neves et al., 2007). A follow up study showed that the HFD *S. mansoni* infected mice had different stages of granulomas, whereas the normal chow infected mice only had exudative

granulomas. They also reported that diet and infection caused changes in the morphology of the duodenum and jejunum which are the principal site affected by *S. mansoni* (De Barros Alencar et al., 2012). These findings present evidence that long term HFD feeding has an effect on the outcome of parasitic helminth infections. However, the influence of HFD on the immune response to parasitic helminth infection still remains unclear.

1.9 Project aim and objectives

The increase in the occurrence of obesity globally has resulted in increased dual morbidity of obesity and helminth infection. Currently there is no data on what effect HFD induced changes may have on the outcome of *T. muris* infection. HFD is proposed to induce changes in the mucosal barrier, increase epithelial turnover and alter the development of Th1/Th2 immune responses. These are key elements in the immunity against *T. muris*.

Drawing upon these two strands of research, the overall aim of the work presented here is to use the well-defined model of *T. muris* infection in C57BL/6 mice to investigate the influence of HFD on the progression of chronic helminth infection.

The main objectives of my research are to:

- I. Investigate what effects chronic *T. muris* infection may have on the pathology of HFD induced obesity.
- II. Investigate if HFD consumption may alter the outcome of chronic *T. muris* infection in mice.
- III. Investigate the mechanism involved in the altered immune response to *T. muris* infection in HFD fed mice.

Chapter 2 : Materials and methods

All routinely used solvents, chemicals and media were laboratory reagent grade reagents acquired from Sigma-Aldrich or Thermo Fisher Scientific unless indicated.

2.1 Animals

Male C57BL/6 mice (ENVIGO, UK) and C57BL/6 RAG^{-/-} mice (housed at the University of Lancaster) were kept in individually ventilated cages on a 12 hour light or dark cycle at 22 ± 1 °C and 65 % humidity. All procedures were carried out on 6 to 8 week old littermates after 1 week of acclimatisation and in accordance with the Home Office Science Act (1986). All experiments carried out the University of Manchester were conducted under the project licence 70/8127 and experiments carried out at the University of Lancaster were carried out under the project licence 70/8521. All experiments conformed to the University of Manchester Animal Welfare and Ethical Review Body (AWERB) and ARRIVE guidelines. All animals were humanely killed by CO₂ inhalation followed by terminal exsanguination.

2.2 Diet modifications

After the 1-week acclimatisation period, the mice were fed with either normal chow (12 % Kcal from fat, Research Diets Inc, USA, D16011009) or HFD (60 % Kcal from fat, Research Diets Inc. USA, D12492) for varying periods of time before or after infection. The compositions of each diet are shown in Table 2.1. The mice had free access to water and food unless otherwise indicated. The dietary treatments were maintained throughout the experimental period once started. The mice were weighed once a week to monitor weight change.

Table 2.1: Composition of mouse normal chow and high fat diet

	Normal chow		HFD	
	g %	kcal %	g %	kcal %
Protein	19.4	20	26.2	20
Carbohydrate	66.1	68	26.3	20
Fat	5.2	12	34.9	60
Total		100		100
Kcal/g	3.89		5.24	
Ingredient	g	kcal	g	kcal
Casein	200	800	200	800
L-Cystine	3	12	3	12
Corn starch	511.2	2045	0	0
Maltodextrin 10	100	400	125	500
Sucrose	68.8	275	68.8	275
Cellulose	50	0	50	0
Soybean oil	25	225	25	225
Lard	29	261	245	2205
Mineral mix S10026	10	0	10	0
Dicalcium phosphate	13	0	13	0
calcium carbonate	5.5	0	5.5	0
Potassium citrate, 1 H ₂ O	16.5	0	16.5	0
Vitamin mix V10001	10	40	10	40
Choline bitartrate	2	0	2	0
FD&C Red dye #40	0.05	0	0	0
FD&C Blue dye #1	0	0	0.05	0
Total	1044	4058	773.9	4057

In chapter 3 the pathology of *T. muris* infection was studied using the mouse groups in table 2.2. For each group control mice were fed on normal chow and a separate group of mice were fed on a HFD. In addition to groups A to D described in table (with repeat experiments of group A and B), the worm burden and immunological response described in Chapter 4 were also investigated for groups E to H. In chapter 5, the results described were obtained using the mouse groups I to K. Each group had age matched naïve mice as controls with the exception of groups G, H and K.

2.3 *T. muris* infection of mice

2.3.1 *T. muris* propagation in the lab

All mice were infected with the Edinburgh (E) strain of *T. muris* which was propagated in the laboratory according to previously described methods (Wakelin, 1967) using SCID mice. SCID mice were infected with approximately 400 embryonated *T. muris* eggs and the mice were sacrificed between 35 to 42 days post infection (p.i) in order to collect adult worms from the caecum. The caecum was cut open longitudinally and washed in warm RPMI media (500 ml RPMI 1640 media containing 500 U/ml penicillin, 500 µg/ml streptomycin). Worms were pulled out gently using forceps and transferred into a 6 well plate. The worms were incubated in RPMI media at 37 °C in a wet chamber for 4 hours after which the worms were split into two wells containing fresh media and further incubated overnight. The next day, the media collected after the 4 hour and overnight incubations were centrifuged at 2000 x g for 15 minutes. The supernatant was taken for preparation of *T. muris* excretory/secretory product (see section 2.3.2). The egg pellet was re-suspended in 40 ml of deionised water and then filter sterilised using a 100 µm sieve. The egg suspension was transferred to a cell culture flask and stored in the dark for 8 weeks to allow for embryonation. The egg suspension was then stored at 4 °C ready to be used for infection. In order to check infectivity of the prepared batch of eggs, mice were given a high dose infection of 200 embryonated eggs by oral gavage and the number of recovered worms on around 11 to 13 days post infection was used to calculate percentage infectivity.

Table 2.2: Treatment groups based on feeding and infection periods

Group	Time on diet before infection	Experimental endpoint	Mouse strain
Chapter 3			
A	12 weeks	Day 21 post infection	C57BL/6
B	12 weeks	Day 42 post infection	C57BL/6
C	12 weeks	Week 9 (after 7 weeks of trickle infection)	C57BL/6
D	12 weeks	Week 11 (after 9 weeks of trickle infection)	C57BL/6
Chapter 4			
A-2	12 weeks [‡]	Day 21 post infection	C57BL/6
B-2	12 weeks [‡]	Day 42 post infection	C57BL/6
E	3 weeks	Day 21 post infection	C57BL/6
F	3 weeks	Day 42 post infection	C57BL/6
G	-	Day 31 post infection (started on diet at day 13 post infection)	C57BL/6
H	-	Day 52 post infection (started on diet at day 32 post infection)	C57BL/6
Chapter 5			
I	12 weeks	Day 13 post infection	C57BL/6
J	12 weeks [*]	Day 21 post infection	C57BL/6
K	12 weeks	Day 42 post infection	C57BL/6 RAG ^{-/-}

The data shown was collected from 2 independent experiments([‡]) or 3 independent experiments (^{*})

2.3.2 Preparation of *T. muris* excretory secretory product (E/S)

The media supernatant collected from section 2.3.1 was filter sterilised before concentrating using an Amicon Ultra 15 centrifugal filter unit (Merck Millipore, UFC903024) by centrifugation at $3000 \times g$ for 15 minutes at 4 °C. The E/S was then dialysed against PBS using Slide-A-Lyzer™ 3.5K molecular weight cut off dialysis cassettes, (Thermo Fisher Scientific, 66330) at 4 °C. The concentration of the E/S in mg/ μ l was measured using the NanoDrop 1000 spectrophotometer (Labtech International) and aliquoted before storing at -20 °C.

2.3.3 *T. muris* infection of mice

5 ml of egg suspension was placed in a 50 ml tube and centrifuged at $2600 \times g$ for 15 minutes (with medium acceleration and deceleration 4) using a Beckman Coulter Allegra™ 21 centrifuge. The pelleted eggs were resuspended in 5 ml of deionised water.

For low dose infections, 70 μ l of the egg suspension was put on a clean slide. Using a pipette approximately 20 to 30 embryonated eggs were individually picked and transferred to an Eppendorf tube. The egg suspension was topped up with deionised water to the 200 μ l mark. Mice were then orally infected with 200 μ l of the egg suspension using a 1 ml syringe and a blunt metal gavage needle. For trickle infection, mice were given repeated low dose infection once every week for the specified period of time.

For high dose infections, the resuspended egg solution was concentrated or diluted taking into account the percentage infectivity to achieve the required number of eggs per 50 μ l. Mice were infected with 200 μ l of egg suspension by oral gavage to infect mice with approximately 200 eggs.

2.4 Worm counts

Fresh or frozen whole caecum and proximal colon were placed into a petri dish containing tap water. For larval stages, the tissue was scrapped using curved tweezers to release the larvae which were then counted under a Leica M275 light microscope. For adult worms, the worms were gently pulled out from the epithelium and placed in water. Only the posterior ends were counted to avoid repetition.

2.5 Faecal egg count

Faecal pellets were collected from mice and weighed before the addition of 1 ml of distilled water (dH₂O). After 1 hour at room temperature the pellets were solubilised by vigorous vortexing for at least 30 seconds. 1 to 2 ml of highly saturated solution (4 M sodium chloride) was added to the samples. 450 µl of the suspension was placed into a McMaster counting chamber (VWR) and the number of eggs within the defined grid lines was counted under a Leica M275 light microscope. The number of eggs per gram of faeces for each sample was then determined using the equation 2.1.

$$\text{Mean eggs per chamber} \times \frac{\text{Volume of dH}_2\text{O} + \text{Grams of faeces} + \text{Volume NaCl}}{(\text{Grams of faeces} \times 0.15)}$$

Equation 2.1: Determination of faecal egg load per sample

2.6 Blood glucose measurement

Glucose was measured from freshly drawn blood using an Accu-Chek® Aviva blood glucose meter (Roche, 06988563016) from either non-fasted or overnight fasted mice. A prick was made on the tail using a 23G x 1'' – Nr. 16 needle (BD Microlance™ 3, 300800) and a drop of blood was collected onto a new Accu-Chek® Aviva test strip (Roche,

06453970). The strip was then inserted into the glucose meter in order to obtain a value for the blood glucose in mg/dL.

2.7 Histology

2.7.1 Tissue collection and processing

A 1 cm segment of the caecum and proximal colon were collected immediately post-mortem from mice and fixed overnight in Carnoy's solution (64 % methanol, 27 % chloroform, 9 % acetic acid). The single right lobe of the lung was also collected and was inflated with Carnoy's solution. The inflated lung was stored in Carnoy's solution overnight. All the Carnoy's fixed tissues were washed in absolute methanol for 30 minutes and stored in absolute ethanol until further processing. Tissue processing was carried out as shown in table 2.3 using the Leica ASP300 tissue processor. Once complete, the processed tissue was then embedded in paraffin (pfm medical UK Ltd, 9000).

Freshly collected segment of the jejunum, liver (upper right lobe), pancreas and mesenteric fat were fixed by placing in freshly made 10 % neutral buffered formalin (NBF, (37 - 41 % formaldehyde), EINECS, 231-791-2) in Dulbecco's phosphate buffered saline (DPBS). The samples were left at room temperature in fixative for at least 48 hours and then washed in PBS for 30 minutes before transferring to 75% ethanol for storage until processing. Tissue processing was carried out as shown in table 2.4.

2.7.2 Tissue sectioning

Five-micron thick tissue sections were obtained using an HM 325 Microm microtome. Sections were floated in a warm water bath and then collected on gelatin-coated slides (Deltalab, D100004). The slides were coated by immersing in gelatin (0.1 % gelatin, 0.0 1 % chromium (III) potassium sulphate dodecahydrate, and thymol crystals in dH₂O) and then air-dried overnight.

Sections used for haematoxylin and Eosin staining were collected on gelatin-free slides. The slides were left to dry overnight in an oven set at 40 °C.

2.7.3 Tissue staining

For paraffin embedded tissue the sections were first dewaxed by immersing twice in citroclear (TCS Biosciences, HC5005) for 5 minutes. The sections were then rehydrated down an ethanol gradient (100 %, 90 %, 70 % and 50 %) and finally placed in dH₂O.

Table 2.3: Tissue processing protocol for Carnoy's fixed tissue

Solution	Time (minutes)	Temperature (°C)
Absolute Ethanol	45	ambient
Xylene	15	40
Xylene	30	40
Xylene	60	40
Paraffin wax	15	61
Paraffin wax	30	61
Paraffin wax	60	61

Table 2.4: Standard tissue processing for NBF fixed tissue

Solution	Time (minutes)	Temperature (°C)
70% IMS	20	ambient
70% IMS	30	ambient
90% IMS	45	ambient
90% IMS	60	ambient
Absolute Ethanol	30	ambient
Absolute Ethanol	45	ambient
Absolute Ethanol	60	ambient
Xylene	20	40
Xylene	30	40
Xylene	40	40
Paraffin wax	70	61
Paraffin wax	70	61
Paraffin wax	70	61

I. Periodic acid-Schiff's and Alcian blue (PAS/AB) stain

Tissue sections were washed in dH₂O before staining with AB at pH 2.5 (1 % AB in 3 % acetic acid) for 5 minutes. Slides were washed in dH₂O before treatment with 1 % orthoperiodic acid (VWR chemicals, 294604D) for 5 minutes and after a brief rinse in water the sections were placed in Schiff's fuchsin-sulphite reagent (Sigma-Aldrich, S5133) for 15 minutes. The slides were washed under running tap water for 10 minutes before counter staining with Mayer's haematoxylin (Sigma-Aldrich, MHS32) for 30 seconds. The slides were then placed in warm water for 5 minutes and then dehydrated in an increasing ethanol gradient (50 %, 70 %, 90 % and 100 %). The slides were cleared in

citroclear twice for 5 minutes each, before mounting in DPX (Thermo Fisher Scientific, D/5319/05).

II. Haematoxylin and eosin (H&E) stain

Tissue sections were washed in dH₂O and then placed in Harris haematoxylin (Sigma-Aldrich, HHS32) for 5 minutes. After rinsing in dH₂O the sections were placed in acid alcohol (1 % HCL in 70 % ethanol) for 10 seconds before placing under running warm water for 3 to 5 minutes. The sections were counterstained in 0.5 % w/v Eosin Y alcoholic solution (Sigma-Aldrich HT110116) for 1 minute (except mesenteric fat sections which were kept for 5 minutes) and after rinsing, the sections were dehydrated in an increasing ethanol gradient. The slides were then cleared in citroclear twice before mounting in DPX.

III. Staining for immunofluorescence microscopy

Standard immunofluorescence staining methods were performed using commercially available antibodies. Briefly after clearing and dehydrating, the tissue sections were washed in PBS before blocking for 1 hour using 5 % goat serum in PBS at 4 °C. After washing, the tissue sections were incubated overnight in primary antibody: anti-Muc2 (1:200, Santa Cruz, H-300, Sc-15334) or anti-DCAMKL1 (1:500, Abcam, Ab31704) at 4 °C and then washed in PBS the next day. Sections were then incubated with secondary antibody (donkey anti-rabbit conjugated-Alexa548, 1:800, Thermo Fisher Scientific, A21207) for 1 hour at room temperature. After washing in PBS, slides were counterstained with DAPI for 5 minutes and washed in PBS followed by water. The slides were left to air dry before mounting in mowiol (2.5 % DABCO in 0.1 M Tris HCl, pH 8.5, 10 % mowiol, 25 % glycerol).

2.7.4 Image acquisition

I. Brightfield microscopy

Axioskop upright microscope (AxioCam colour CCD camera through Axiovision software).

Nikon eclipse Ci upright microscope (Nikon DS-Fi3 colour camera through NIS-Element software).

II. Fluorescent microscopy

Olympus BX51 upright microscope (Coolsnap ES camera (Photometrics) through MetaVue software).

All images were captured using either 10x or 20x objectives. The images were then processed and analysed using ImageJ software (<http://rsb.info.nih.gov/ij>).

2.7.5 Quantification of histological staining

The number of goblet cells was obtained by counting the number of both PAS⁺ (purple-pink) and AB⁺ (blue) cells in 20 – 30 randomly selected longitudinally sectioned crypts. The depth of 30 randomly selected longitudinally sectioned crypts was measured and recorded as average depth per crypt. The number of tuft cells was analysed by comparing the number of DCAMKL1⁺ cells per 10 randomly selected adjacent crypts. The area of 10 - 15 islets of Langerhans and adipocytes was measured using ImageJ software. The intensity of PAS/AB staining was measured on 16-bit images using image J software.

2.8 Serum collection

Blood was collected into 1.5 ml Eppendorf tubes from mice at autopsy and left to settle at room temperature for at least an hour. The samples were then centrifuged for 10 minutes at 13,000 x g. The serum was carefully collected, and aliquots were stored at -20 °C.

2.9 Serum antibody ELISA

The amount of *T. muris* specific IgG1 and IgG2a/c was determined by ELISA as previously described (Blackwell N.M, Else K.J 2001). Briefly 96 well immunoGrade plates (BrandTech Scientific, Inc) were coated overnight at 4°C with *T. muris* derived E/S at 5 µg/ ml in carbonate buffer at pH 9.6 (0.0.15 M Na₂CO₃, 0.035 M NaHCO₃). The next day the plates were washed 3 times with wash buffer (0.5 % Tween 20 in PBS) using a SKATRON SkanWASHER 400 (Molecular Devices). Blocking of non-specific binding was done by adding 3% BSA in PBS to the wells for 1 hour before washing off. For each mouse a 1:20 dilution of serum was added to the top well and the serum was serially diluted down the plate in a 1:2 ratio. The serum was incubated for 90 minutes at room temperature. After washing either Biotin Rat anti-mouse IgG1 (Bio-Rad Laboratories, MCA336B) at 1:1000 or Biotin Rat anti-mouse IgG2a/c (BD Biosciences, 553446) at 1:2000 was added to the plates for 1 hour at room temperature. The plates were washed before the addition of streptavidin bound peroxidase (SA-POD, Roche Diagnostics, 11098153001) diluted at 1:1000 and incubated for 1 hour at room temperature. After washing off unbound SA-POD, colour was developed by adding 10% ABTS solution (10 % w/v ABTS in citrate buffer (0.4 M NaHPO₄, 0.03 M citric acid)), 90 % 0.03 M citrate buffer, 0.01 % 1 µl H₂O₂). After 5 to 10 minutes the absorbance was read at 490 nm with reference at 590 nm using a VersaMax microplate reader (Molecular Devices).

2.10 Serum leptin assay

The amount of leptin in serum was measured using the mouse leptin ELISA kit (Abcam, ab100718) according to the manufacturer's instructions.

2.11 Extraction of immune cells

All media and other components used to make culture or digestion media were obtained from Sigma-Aldrich unless otherwise indicated.

2.11.1 Mesenteric lymph nodes

Mesenteric lymph nodes were collected into wash media (RPMI 1640 media containing 1 % Penicillin-streptomycin solution, 1 % L-glutamine, 2 % FBS) and kept on ice. The lymph nodes were disaggregated through a 100 µm sieve into a petri dish. The cell suspension was transferred into a 15 ml centrifuge tube and centrifuged at 500 × g for 5 minutes. The pellet was washed in 10 ml of wash media and centrifuged at 500 × g for 5 minutes. The pellet was re-suspended in 1 ml of complete media (RPMI 1640 media containing 1 % Penicillin-streptomycin solution, 1 % L-glutamine, 10 % FBS). To obtain the number of live cells, a 1:2000 dilution of each sample was prepared by diluting 5 µl of each sample into 10 µl of CASY ton (OMNIlife science™,5651808) solution before running on the CASY®1 counter (Schärfe System).

2.11.2 Lamina propria

Immediately after collection, caecum-proximal colon segments were placed into Hank's balanced salt solution (HBSS) and kept on ice until all samples were collected. The tissue was cut open and washed in HBSS 5 to 6 times before placing into 25 ml of digestion media I (RPMI 1640 media containing 3 % FBS, 20 mM Hepes solution, 0.04 mM DTT (Melford Laboratories, D11000-25), 5mM EDTA) and after vigorous shaking the tissue was digested for 20 minutes at 37°C in a shaking incubator. The digested tissue was poured onto a 100 µm sieve and then washed three times with 2mM EDTA/RPMI 1640 media. The tissue was then further digested by adding digestion media II (RPMI 1640 media containing 0.48 mg/ml Collagenase II, Thermo Fisher Scientific, 17101015; 0.48 mg/ml Dispase, Sigma Aldrich D4818, 9.4 % FBS) for 20 minutes at 37°C in a shaking incubator. The samples were centrifuged at 500 × g for 5 minutes and the pellet was re-suspended in 1 ml of complete media (prepared as described in section 2.11.1) before proceeding to count the number of live cells as described in section 2.11.1.

2.11.3 Mesenteric fat

Mesenteric fat was digested according to a previously described protocol (Orr, 2013) with a few modifications. The mesenteric fat was collected in 0.5% FBS in PBS on ice. Once all samples were collected the fat was placed into fat digestion media (DPBS containing 4 mg/ml Collagenase type II, Sigma Aldrich C6885, 10 mM CaCl₂ and 0.5 % BSA). The fat was incubated for 30 minutes at 37°C in a shaking incubator and then 10 ml of 0.5 % BSA in DPBS was added to each sample. Using a 10 ml serological pipette, each sample was triturated numerous times before pouring the cell suspension through a 100 µm sieve. The cell suspension was centrifuged at 500 × g for 10 minutes and the pellet was resuspended in 3 ml of ACK (ammonium-chloride-potassium) lysing solution to lyse the red blood cells. The samples were then washed by adding 10 ml of complete media (prepared as described in section 2.11.1) and the centrifuged at 500 × g for 5 minutes. The pellet was resuspended in 1 ml of complete media before proceeding to count the number of live cells as described in section 2.11.1.

2.12 Cell re-stimulation assay

The cell suspensions collected from the mesenteric lymph were adjusted to a concentration of 5 ×10⁶ cells/ml. For each sample 200 µl of the cell suspension was plated out into 3 wells in a sterile 96 well round bottomed plate. The first well was used as a media control with no stimulation, to the second well 2.5 mg/ml of Con A was added and to the third well 50 µg/ml of *T. muris* derived E/S. The cells were incubated at 37°C for 40 hours (100% humidity and 5 % CO₂). The plates were then centrifuged at 500 x g for 5 minutes and the supernatant was transferred to a sterile 96 well flat bottom plate. The supernatants were stored short term at -20 °C or long term at -80 °C until analysis for cytokine composition using the cytometric bead array.

Some of the extracted cells were re-suspended in 500 µl of complete media. The cells were stimulated with 1X PMA/ ionomycin stimulation cocktail (2 µl/ml) (eBioscience 4970) and 1X brefeldin A (3 µg/ml) (eBioscience 4506) to inhibit transport out of the Golgi

apparatus which allows the cytokines to accumulate in the cell. The cells were then incubated at 37°C overnight (100% humidity and 5 % CO₂) after which the cells were collected and immediately stained for flow cytometry analysis.

2.13 CD3/CD28 activation assay

A 96 well plate was precoated with 200 µl of anti-CD3 antibody (3 µg/ml) and stored overnight at 4°C. The next day the wells were washed twice using 100 µl of DPBS. 200 µl of the cell suspension (5 ×10⁶ cells/ml) collected from the mesenteric lymph node were added to each well. 5µg/ml of anti-CD28 was then added to each well. The cells were incubated at 37°C for 40 hours (100% humidity and 5 % CO₂). The plates were then centrifuged at 500 x g for 5 minutes and the supernatant was transferred to a sterile 96 well flat bottom plate. The supernatants were stored short term at -20 °C or long term at -80 °C until analysis for cytokine composition using the cytometric bead array.

2.14 Cytometric bead array (CBA)

The frozen supernatants were analysed for cytokines of interest using the BD Biosciences cytometric bead array according to the manufacturer's instructions with only a few modifications. The analysed cytokines were IL-5, IL-6, IL-9, IL-10, IL-13, IL-17a, TNF-α and INF-γ. Standards were simultaneously prepared and analysed. 12.5 µl of each sample and standards was transferred to a 96 well round bottom plate. To each standard and sample, 12.5 µl of capture bead mix containing the capture beads for each cytokine of interest was added. After incubating for 90 minutes at room temperature, 12.5 µl of the detection bead mix was added to each well and incubated for 1 hour in the dark at room temperature. 140 µl of wash buffer was then added to each well before spinning down the plates at 1500 x g for 5 minutes. The supernatant was carefully tipped off and the pellet was resuspended in 70 µl of wash buffer. The samples were then run on the MACSQuant® analyser (Miltenyi Biotec) and the data were analysed using the BD FACSDiva™ software.

2.15 Flow cytometry

2.15.1 Flow cytometry staining and data acquisition

The Foxp3/Transcription factor staining buffer set was used for permeabilisation (eBioscience, 5523). A set of single stain controls for each antibody used, were simultaneously prepared alongside the samples for comparison. The stimulated cell suspensions were centrifuged at $500 \times g$ and resuspended in $200 \mu\text{l}$ of 1x permeabilisation buffer. The cells were pelleted by centrifuging at $400 \times g$ for 5 minutes. $200 \mu\text{l}$ of the Foxp3/Transcription factor staining buffer was added and left for 30 minutes at 4°C . After washing in 1x permeabilisation buffer, non-specific binding was blocked by adding $2.5 \mu\text{g/ml}$ of CD16/CD32 Fc block (eBioscience) for 20 minutes at 4°C . $50 \mu\text{l}$ of cell surface markers and intracellular cytokine antibody cocktail was added ($1.5 \mu\text{g/ml}$ for surface makers and $3 \mu\text{g/ml}$ for intracellular cytokines) to the samples and incubated for 30 minutes at 4°C . The details of the antibodies used are shown in table 2.5. The samples were washed in 1x permeabilisation buffer and re-suspended in $250 \mu\text{l}$ of FACS buffer before analysing on the CytoFlex-BeckMann Coulter flow cytometer. The data were analysed using FlowJo_V10 software.

2.15.2 Flow cytometry gating strategy

Representative plots for the gating strategy used for analysis are shown in figures 2.1, 2.2. and 2.3.

Table 2.5: List of antibodies used for flow cytometry

Marker	Fluorochrome	Clone	Supplier
CD45	B525	30-F11	Thermo Fisher Scientific
CD3	AF700	eBio50042	Thermo Fisher Scientific
CD4	Pe-Cy7	GK1.5	Thermo Fisher Scientific
CD8	APC-Cy7	53-6.7	Thermo Fisher Scientific
IFN- γ	FITC	XMG1.2	Thermo Fisher Scientific
IL-13	e450	eBio134	Thermo Fisher Scientific
CD45	Amcyan	30-F11	Thermo Fisher Scientific
CD4	B450	GK1.5	Thermo Fisher Scientific
CD3	AF700	eBio50042	Thermo Fisher Scientific
Foxp3	FITC	FJK-16s	Thermo Fisher Scientific
T-bet	Pe-Cy7	eBio4B10	Thermo Fisher Scientific
CD45	Amcyan	30-F11	Thermo Fisher Scientific
CD11b	APC	M1/70	Thermo Fisher Scientific
F4/80	APC-Cy7	BM8	Thermo Fisher Scientific
CD11c	Pe-Cy7	N418	Thermo Fisher Scientific
SiglecF	PE	E50-2440	BD Bioscience

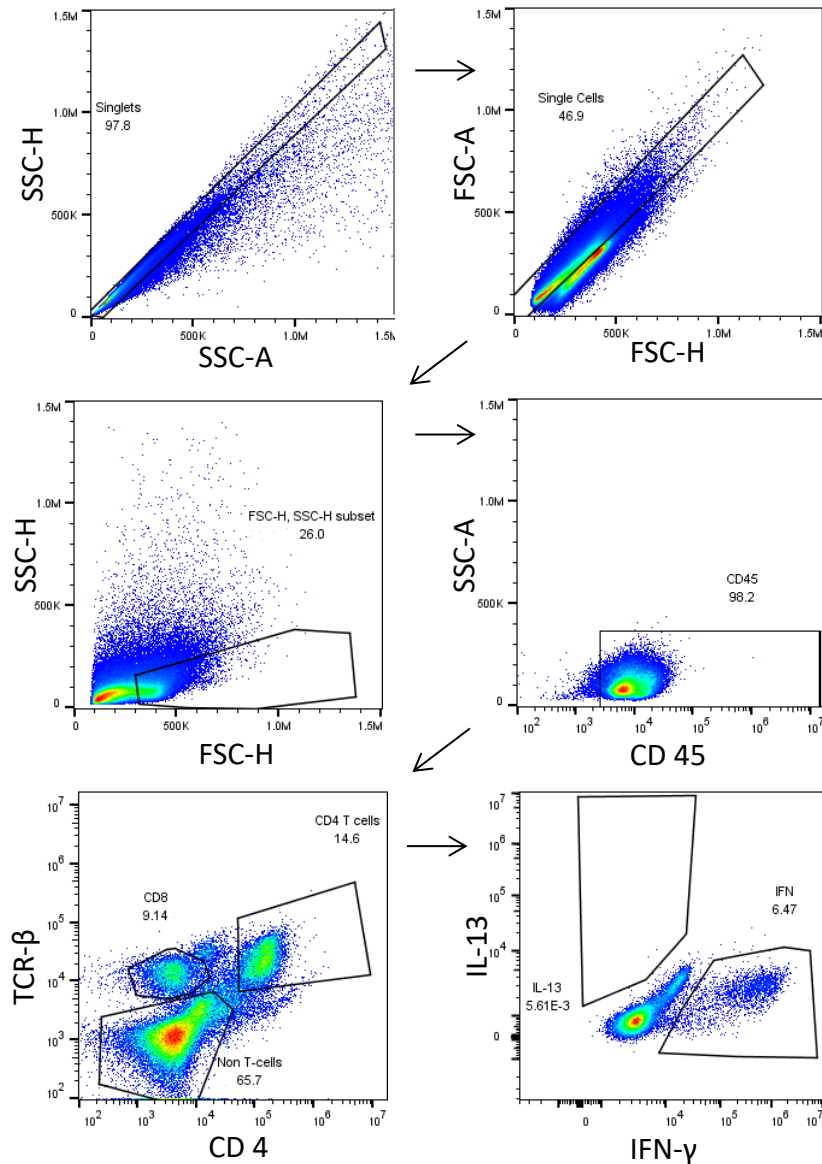


Figure 2-1: Flow cytometry gating for IFN- γ ⁺CD4⁺ T-cells and IL-13⁺CD4⁺ T cells.

C57BL/6 mice were fed on normal chow or HFD for 12 weeks. The mice were given a single low dose *T. muris* infection. At day 21 post infection cells were collected from the mesenteric lymph nodes and lamina propria. The number of CD4⁺IFN γ ⁺ T-cells and CD4⁺IL-13⁺T-cells was determined by flow analysis.

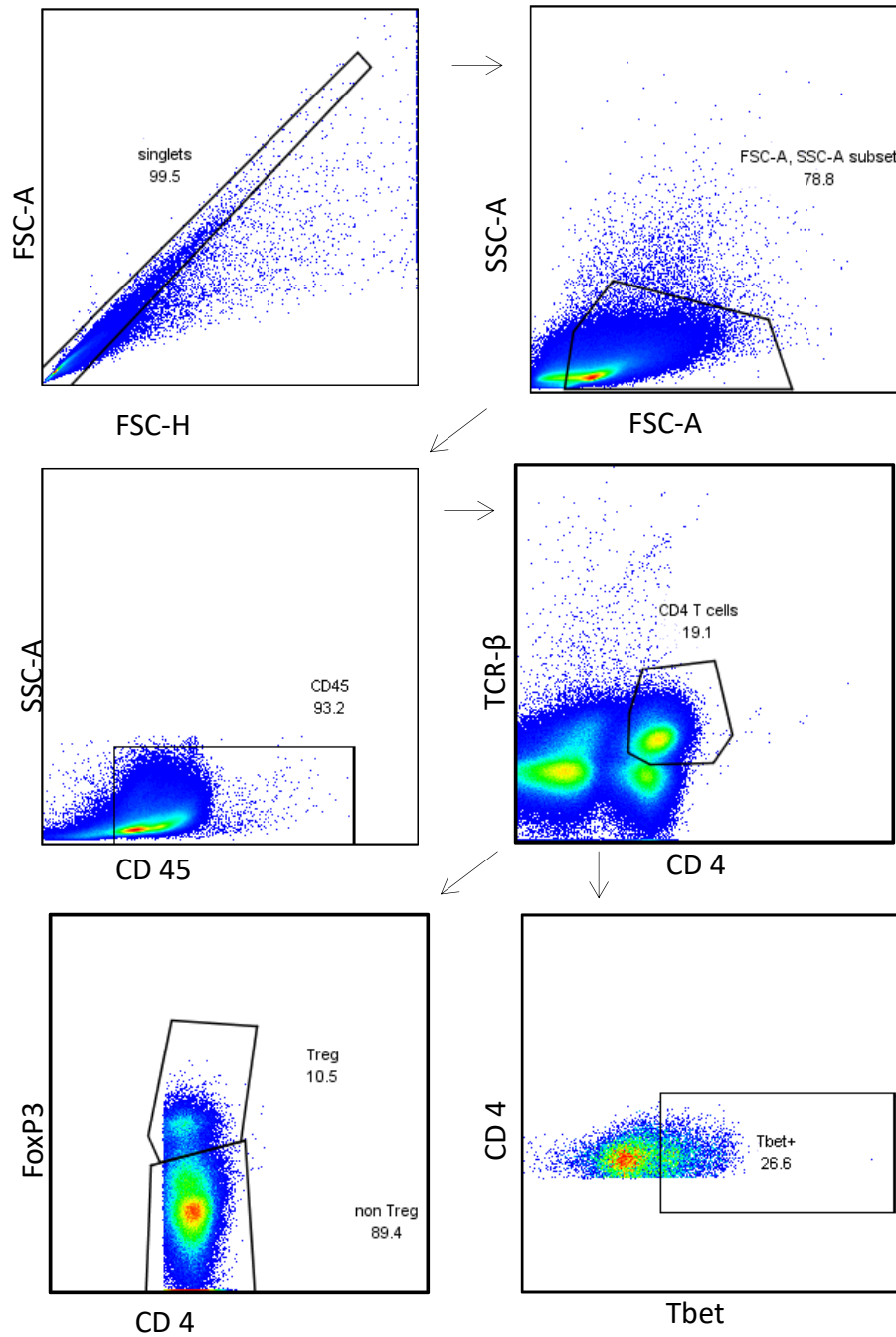


Figure 2-2: Flow cytometry gating for CD4⁺FoxP3⁺ T-cells and CD4⁺Tbet⁺ T-cells.

C57BL/6 mice were fed on normal chow or HFD for 12 weeks. The mice were given a single low dose *T. muris* infection. At day 21 post infection immune cells were collected from the mesenteric lymph nodes. The number of CD4⁺FoxP3⁺ T-cells and CD4⁺Tbet⁺ T-cells was determined by flow analysis.

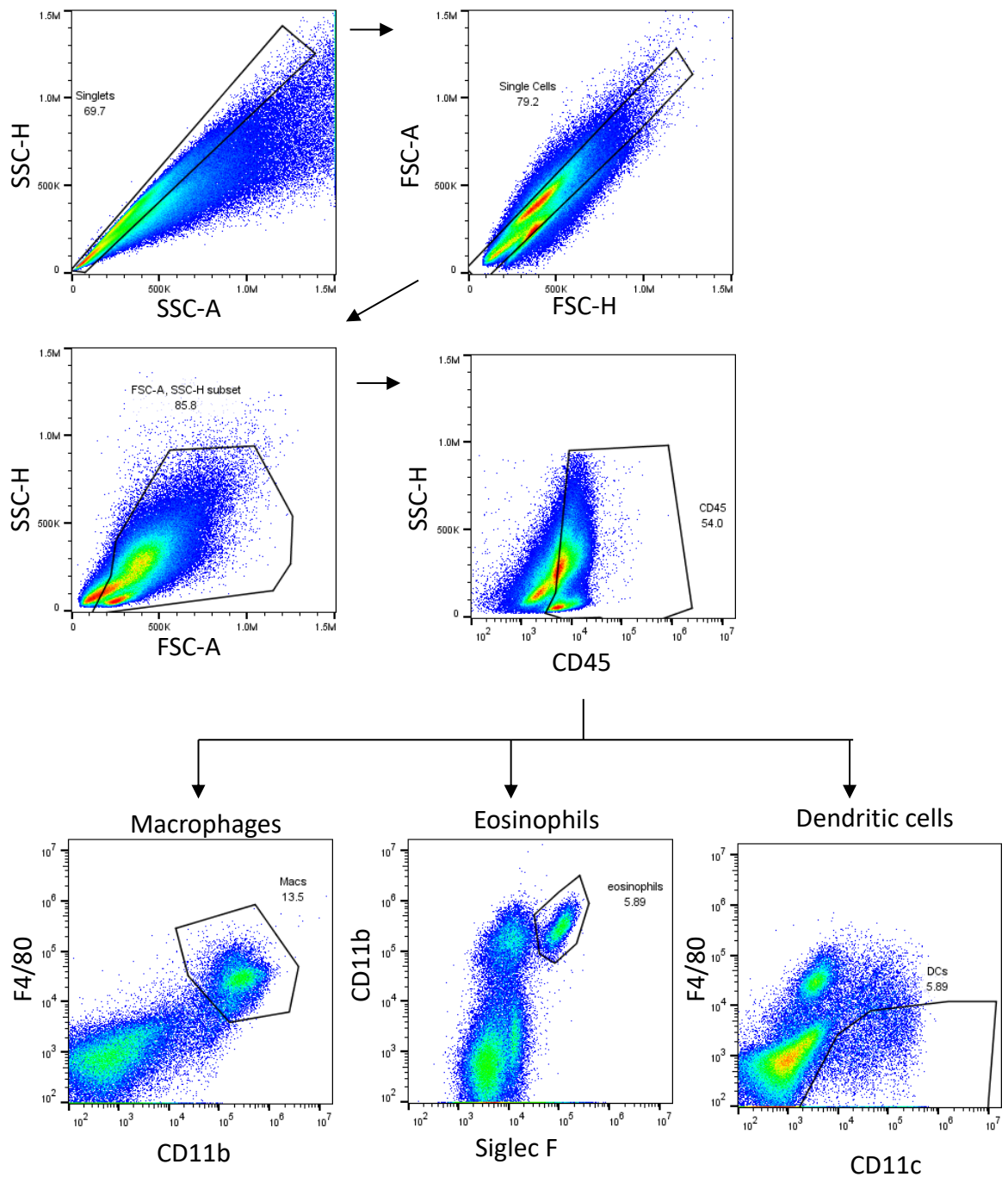


Figure 2-3: Flow cytometry gating strategy for macrophages, eosinophils and dendritic cells.

C57BL/6 mice were fed on normal chow or HFD for 12 weeks. The mice were given a single low dose *T. muris* infection. At day 21 post infection, mesenteric fat was collected, and enzymatic digestion was used to extract immune cells. The number of macrophages (F4/80⁺CD11b⁺), eosinophils (CD11b⁺SiglecF⁺) and dendritic cells (CD11c⁺F4/80⁺) was determined by flow analysis.

2.16 RNA extraction

Freshly collected tissue was snap frozen on dry ice and stored at -80°C until processing. Frozen samples were placed into 1 ml of TRIzol[®] reagent (Thermo Fisher Scientific, 15596026). Samples were homogenised at 4.0 m/s for 30 seconds using the Fastprep[®]-24 tissue homogenizer (MP Biomedicals). The homogenisation process was repeated 4 times with a 5-minute incubation period on ice after each 30 second run. The samples were allowed to equilibrate to room temperature for 10 minutes before adding 200 μl of chloroform and after shaking, the samples were left to stand for 5 minutes. The samples were then centrifuged at $12,000 \times g$ for 15 minutes at 4°C . The aqueous top layer was collected and 200 μl of isopropanol was added to the samples to precipitate the RNA. After incubating at -20°C for 1 hour, the samples were centrifuged at $12,000 \times g$ for 10 minutes and the pellets were washed in 70 % ethanol. The samples were centrifuged at $7500 \times g$ for 5 minutes and after discarding the supernatant, the residual ethanol was removed. The pellet was left to air dry for approximately 10 minutes before resuspension in 30 μl of RNase/DNase free water (Ambion, AM9930) and quantified using the ND-1000 spectrophotometer (Labtech International).

2.17 cDNA synthesis and qPCR

The GoScript[™] reverse transcription kit (Promega, A5001) was used for cDNA synthesis according to manufacturer's instructions. The samples were mixed and then placed in a BioRAD T100[™] thermocycler (Bio-Rad Laboratories). The conditions were: annealing at 25°C for 5 minutes, extension at 42°C for 1 hour and reverse transcriptase inactivation at 70°C for 15 minutes. The cDNA was stored at -20°C . Samples for qPCR were prepared using the SensiFAST[™] SYBR[®] Hi-ROX kit (Bioline, BIO-92005). The samples were placed in a StepOne Plus qPCR machine with the following cycle conditions: hold at 90°C for 2 minutes followed by 40 cycles at 95°C for 5 seconds, 60°C for 30 seconds and 72°C for 20 seconds. For the melt curve analysis, the conditions were: 95°C for 15 seconds, 60°C for 1 minute and 95°C for 15 seconds. Relative gene expression of the target genes was

normalised to the expression of β -actin and calculated using the $2^{-\Delta\Delta CT}$ values. The primer sequences are shown in table 2.6.

Table 2.6: qPCR primer sequences

Target	Forward primer 5' > 3'	Reverse primer 5' > 3'
β -actin	TCTTGGGTATGGAATGTGGCA	ACAGCACTGTGTTGGCATAGAGGT
TSLP	AGCAAGCCAGTCTGTC TCGTGAAA	TGTGCCAATTCCTGAGTA CCGTCA
RELM- β	GCTCTTCCCTTTCCTT CTCAA	AACACAGTGTAGGCTTCA TGCTGTA

2.18 Analysis of faecal DNA by denaturing gradient gel electrophoresis (DGGE)

Stool samples were collected from mice and DNA was extracted the QIAamp Fast DNA Stool Mini kit from QIAGEN according to manufacturer's instructions. The DNA was eluted in 100 μ l of buffer ATE and quantified using the ND-1000 spectrophotometer (Labtech International).

The V3 region of 16 bacterial rRNA was amplified using the 341F_GC primer 5' > 3': CGCCCGCCGCGCGGCGGGCGGGGCGGGGGCACGGGGGGCCTACGGGAGGCAGCAG and 518R primer 5' > 3': ATTACCGCGGCTGCTGG. 2.5 ng/ μ l of DNA was added to a master mix containing 1 x buffer, 2 mM forward primer and 2 mM reverse primer 0.5 mM dNTPs, 2 U Taq DNA polymerase (Roche Diagnostics), 0.5 μ l BSA (1:100, New England Biolabs, B9000S) and made up to 50 μ l with dH₂O. The samples were mixed and then placed in a BioRAD T100™ thermocycler (Bio-Rad Laboratories). The conditions were; hold at 90°C for 2 minutes followed by 40 cycles at 95°C for 5 seconds, 60°C for 30 seconds and 72°C for 20 seconds. 5 μ l of PCR product was run on a 2 % agarose gel in 1 x Novex™ TBE running buffer (Thermo Fisher LC6675) at 120 V for 1 hour to check the size of the amplicon expected to be around 250 bp. A sample image of the agarose gel showing the

PCR amplicon is shown in figure 2.4 A. The remainder of the amplified DNA was purified using the MinElute PCR Purification kit from (QIAGEN, 28104) according to manufacturer's instructions and eluted in 40 μ l of elution buffer. The DNA was quantified using the ND-1000 spectrophotometer (Labtech International) and stored at -20°C . 150 ng of the amplified DNA was analysed by denaturing gradient gel electrophoresis (DGGE) on an acrylamide gel with 30 % to 70 % gradient. The gel was run for 16 hours at 60°C (63 V) using the Bio-Rad DCode™ Universal Mutation Detection System and stained with the SYBR Gold Nucleic Acid Gel Stain (Thermo Fisher Scientific, S11494) for 30 minutes. The stain was washed off using deionised water and then visualised using a bench top UV transilluminator, BioDoc-It Imaging System (UVP). A Sample image of the DGGE gel showing the separated bands of DNA is shown in figure 2.4 B. Each lane in the gel represents DNA sample extracted from the faecal pellets collected from an individual mouse and each band represents DNA amplified from a bacterial species. Gel bands were detected using Phoretix 1D software to produce a binary matrix to enable comparison between samples. RStudio software version 3.3.2 was used for non-parametric multidimensional scaling (NMDS) analysis using the generated binary matrix. This generates a 2-dimensional plot which shows the Euclidian distance between samples and colour coded clusters were used to identify samples belonging to the same group. Statistical analysis of the NMDS plots was carried out using permutation ANOVA.

2.19 Statistics

All results are expressed as the mean \pm standard deviation with each experimental group having 3 to 6 mice. Statistical analysis was carried out using GraphPad Prism version 7. Comparison between two groups was assessed using the Mann-Whitney U post-test. Unless otherwise stated comparison between more than 2 groups was assessed using one-way ANOVA followed by Kruskal-Wallis post-test. Linear regression and correlation analysis were performed using STATA version 14. Throughout the document statistical significance was considered when $p < 0.05$ (*), $p < 0.01$ (**) or $p < 0.001$ (***)

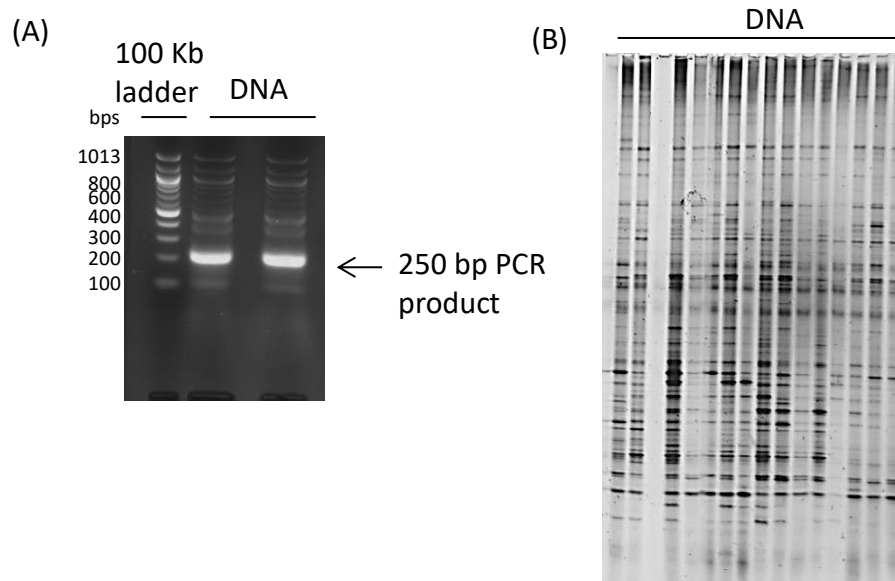


Figure 2-4: Sample of DNA gels for microbial composition analysis by DGGE

C57BL/6 mice were fed on normal chow or HFD for 12 weeks and were then given either a high or single low dose of *T. muris* infection. DNA was extracted from faecal pellets collected from mice at different time points and analysed by denaturing gradient gel electrophoresis. (A) Sample image of an agarose gel image showing the amplified DNA. (B) Sample image of DGGE gel used for microbial analysis.

Chapter 3 : Results I

The effect of low dose *T. muris* infection on host pathology in normal and HFD diet induced obese mice

3.1 Introduction

According to the world health organisation, STH infections are some of the most common infections worldwide. The majority of infected individuals live in developing countries due to a lack of sanitary infrastructure. The clinical symptoms of infections vary depending on the parasite and the site of infection (Jourdan et al., 2018). *T. trichiuria* parasites reside in the intestine and anchor into the intestinal epithelium with their anterior end. This results in the formation of petechial lesions due to minor bleeding. Affected individuals sometimes complain of abdominal pain and may also result in anaemia depending on the severity of infection (Jourdan et al., 2018).

In addition to this helminths are able to modulate the host's immune responses so as to dampen down the generation of protective host immunity resulting in chronic infections (Doetze et al., 2000; Worthington et al., 2013a). Studies have reported that the immune tolerance resulting from helminth infections results in reduced cases of autoimmune disease and allergy for people living in endemic areas (Correale and Farez, 2011; Greenwood, 1968).

Furthermore, studies have also related helminth infections to improved metabolic health (Mohamed et al., 2017; Shen et al., 2015). This has led to more research into the use of helminths as therapy for obesity and associated metabolic diseases. Studies in obese mice have shown that infection with *N. brasiliensis* or *H. polygyrus* resulted in reduced body weight and improved regulation of blood glucose (Su et al., 2018; Yang et al., 2013). Further work showed that increased browning of white adipose tissue resulted in an increased rate of metabolism resulting in weight loss (Su et al., 2018). However, these studies have used models of infection, where the development of strong Th2 immune responses and parasite expulsion follow a single high dose infection.

In order to investigate the effect of chronic STH infection on body weight and HFD induced pathology, we infected C57BL/6 mice with a low dose of *T. muris* eggs that results in a Th1 immune response (Bancroft et al., 1994a; Bancroft et al., 2001). Previous studies have shown that chronic *T. muris* infection results in gut inflammation and pathology that is similar to that observed in Crohn's disease (Foth et al., 2014; Hayes et al., 2017; Levison et al., 2010). However, although the intestine is the site of infection the

present experiments were designed to investigate if chronic *T. muris* infection would also induce pathology in distant tissues. In addition, the effect a chronic *T. muris* infection had on the pathology of obesity in mice was investigated with a focus on the adipose tissue, liver and lung which play important roles in maintaining physiological homeostasis.

The main objectives of the work in this chapter were:

- I. To investigate the effect of single and trickle low dose *T. muris* infections on the body weight
- II. To investigate the effect of single and trickle low dose *T. muris* infections on the pancreas, liver and lung
- III. To investigate the effect of single and trickle low dose *T. muris* infections on the body weight of HFDIO mice
- IV. To investigate the effect of single and trickle low dose *T. muris* infections on the pancreas, liver and lung of HFDIO mice

3.2 Results

The results presented in this chapter were collected from mice in groups A, B, C and D which are described in table 2.2 and are shown in figure 3.1. Seven-week old male C57BL/6 mice were fed on normal chow or HFD for 12 weeks to induce obesity and were maintained on their respective diet throughout the experimental period. To investigate the effect of infection, mice were given either a single or a trickle low dose of *T. muris* infection. Mice given single low dose infections were sacrificed at day 21 or day 42 post infection. Another set of mice were given low dose infections once every week for 7 or 9 weeks (trickle infection) and were sacrificed 2 weeks after the last infection.

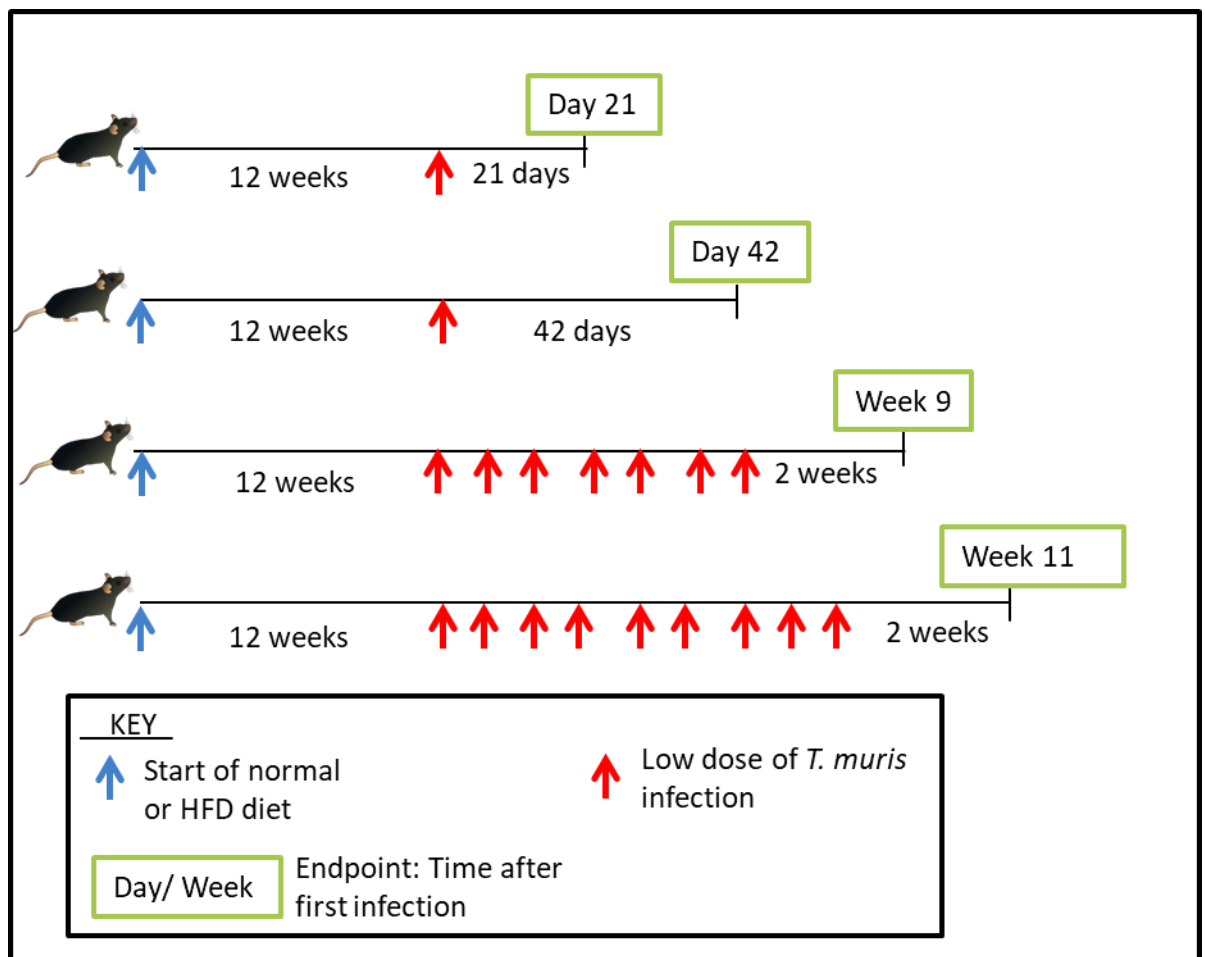


Figure 3-1: Experimental design.

Mice received either normal diet or HFD. After 12 weeks of feeding, mice were given a single low dose infection and observed for 21 or 42 days. Another group of mice were given trickle low dose infections over a period of 7 to 9 weeks and then observed for 2 weeks after the last infection. Mice were sacrificed at the end of the specified observation periods.

3.2.1 The effect of a low dose of *T. muris* infection on host body weight in normal chow mice

I. Comparison of body weight changes between naïve and *T. muris* infected normal chow mice

The body weights of naïve and single low dose infected mice were recorded weekly during the study period. The mice steadily gained weight during the course of the experiment as shown in figure 3.2 A and B. After a single low dose infection with *T. muris* the weights of the mice at day 21 and day 42 post infection were compared. The percentage weight gain from the time of infection at week 12 until the time of sacrifice was also compared. This was calculated as shown in equation 3.1.

$$\text{Percentage weight gain} = \frac{(\text{final weight} - \text{weight at time of infection})}{\text{weight at time of infection}} \times 100$$

Equation 3.1: Equation for calculating the percent weight gain in mice from the time of infection until the day of sacrifice.

At day 21, there was no significant difference in the mean final weight and percentage weight gain between the naïve and infected mice (figure 3.2 C and D). Similarly, at day 42 post infection, there was no significant difference in the mean final weight and percentage weight gain between the naïve and infected mice (figure 3.2 E and F). The weight gain in mice after 7 or 9 weeks of low dose trickle infections was compared. During the course of the trickle infections the infected mice did not gain as much weight as the naïve counterparts (figure 3.3 A and B). After 7 weeks of trickle infection, there was a significant reduction in the final body weight of the weight of the infected mice in comparison to the naïve mice (figure 3.3 C). However, there was no significant difference in the mean percentage weight gain between the naïve and infected mice (figure 3.3 D).

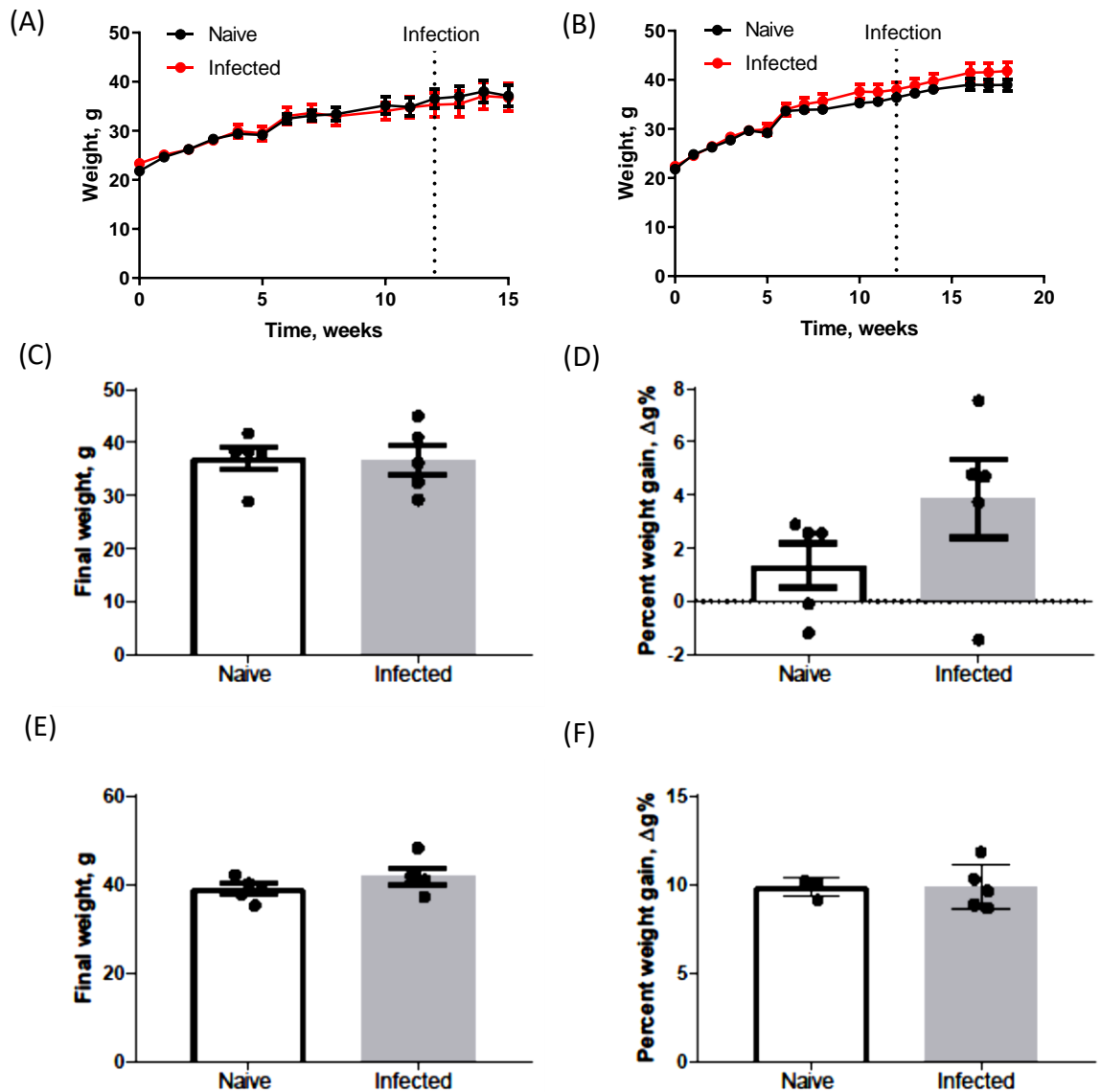


Figure 3-2: Weight change in single dose *T. muris* infected mice.

C57BL/6 mice were fed on normal chow for 12 weeks and then given a single low dose infection of *T. muris*. The weights of the mice were recorded weekly throughout the experiment. (A) Weekly weight record of mice until day 21 post infection. (B) Weekly weight record of mice until day 42 post infection. (C) Final weight of the mice at day 21 post infection. (D) Percentage weight gain of the mice from the time of infection until 21 days post infection. (E) Final weight of the mice at day 42 post infection. (F) Percentage weight gain of the mice from the time of infection until day 42 post infection. N = 5, results show mean \pm SEM.

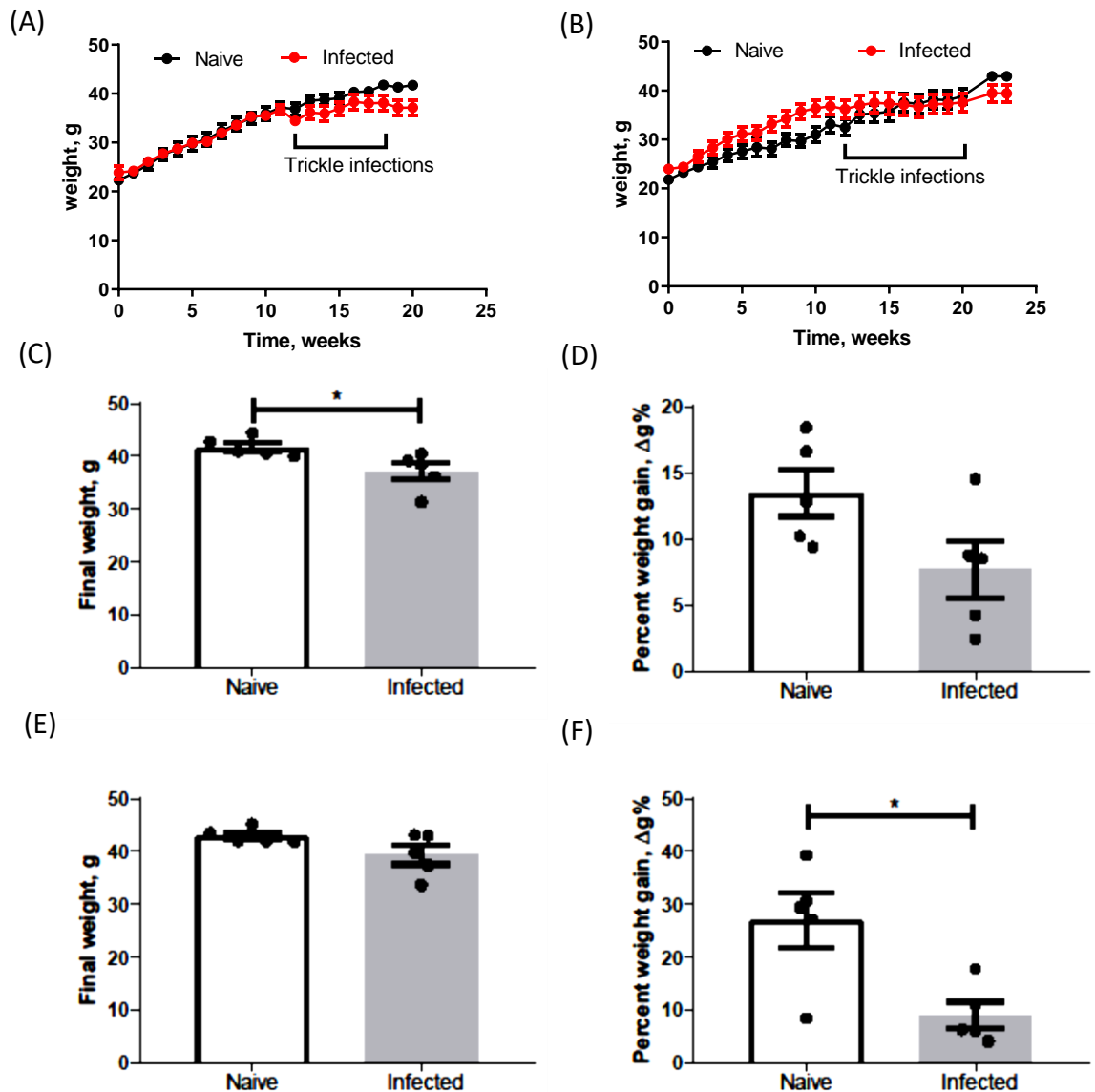


Figure 3-3: Weight change in trickle dose *T. muris* infected mice.

C57BL/6 mice were fed on normal chow for 12 weeks and then given a trickle *T. muris* infection for 7 or 9 weeks and then observed for 2 weeks before sacrifice. The weights of the mice were recorded weekly throughout the experiment. (A) Weekly weight record of 7 week trickle infected mice. (B) Weekly weight record of 9 week trickle infected mice. (C) Final weight of the 7 week trickle infected mice. (D) Percentage weight gain of the 7 week trickle infected mice. (E) Final weight of the 9 week trickle infected mice. (F) Percentage weight gain of the 9 week trickle infected mice. N = 5, results show mean \pm SEM.

After 9 weeks of trickle infection there was no difference in the final weight of the infected mice as compared to the naïve mice (figure 3.3 E). However, the percentage weight gain in 9 week trickle infected mice was significantly less as compared to the naïve mice (figure 3.3 F).

II. Comparison of epididymal and subcutaneous fat pads between naïve and *T. muris* infected normal chow mice

The majority of the body's triglycerides are stored in the white adipose tissue depots. The two main fat depots are the visceral and subcutaneous fat pads (Mann et al., 2014). As a measure of visceral fat, the weight of the gonadal fat pads was compared. Gonadal fat pads are in close proximity with the epididymis in males and are also referred to as epididymal fat pads.

After a single low infection with *T. muris* there was no difference between the mean weight of epididymal fat pads between the naïve and infected mice at day 21 and day 42 post infection (figure 3.4 A and B). There was no significant difference in the mean weight of the epididymal fat pads in the 7 week and 9 week trickle infected mice as compared to the naïve mice (figure 3.4 C and D). The weight of the subcutaneous fat pads after a single low dose infection with *T. muris* at day 42 post infection was also measured and there was no difference in the mean weight between the naïve and infected mice (figure 3.4 E). After 9 weeks of trickle infection there was a trend towards reduced weight of the subcutaneous fat pads in the infected mice as compared to the naïve mice although this was not significant (figure 3.4 F).

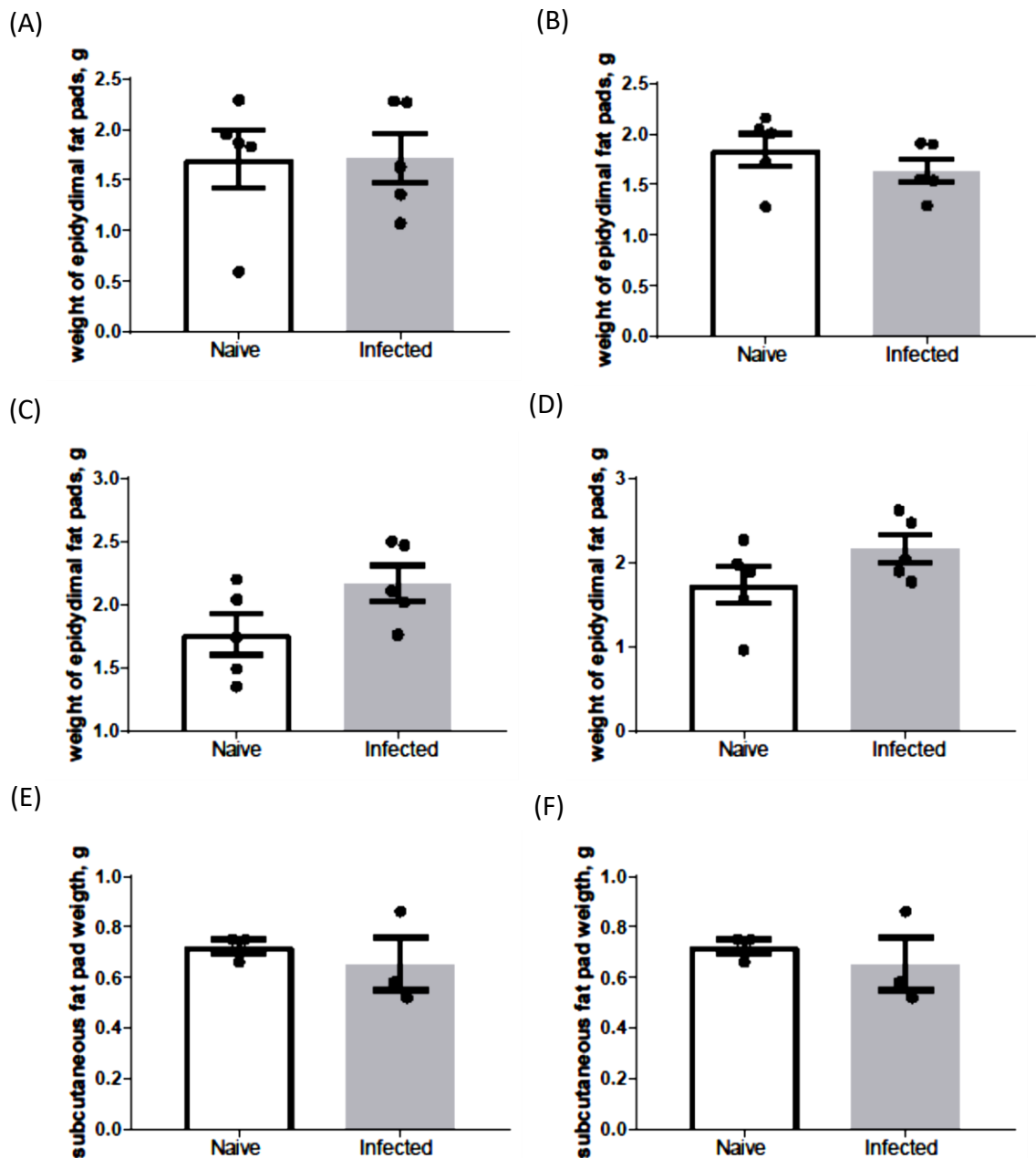


Figure 3-4: Comparison of epididymal and subcutaneous fat pads between naïve and *T. muris* infected mice on normal chow.

C57BL/6 mice were fed on normal chow for 12 weeks and then given either a single low dose or trickle *T. muris* infection. At the time of sacrifice the epididymal and subcutaneous fat pads were collected and weighed. (A) Weight of epididymal fat pads of single low dose infected mice at day 21 post infection. (B) Weight of epididymal fat pads of single low dose infected mice at day 42 post infection. (C) Weight of epididymal fat pads of 7 week trickle infected mice at week 9. (D) Weight of epididymal fat pads of 9 week trickle infected mice at week 11. (E) Weight of subcutaneous fat pads of single dose infected mice at day 42 post infection. (F) Weight of subcutaneous fat pads of 9 week trickle infected mice at week 11. N = 3 to 5, results show mean \pm SEM.

III. Comparison of food intake between naïve and trickle dose infected normal chow mice

To compare the food intake between naïve and infected mice, the food intake during the 2 weeks of observation after the 9 weeks of trickle infection was measured. The infected mice consumed less food per day in comparison to the naïve mice (figure 3.5 A). The mean amount of Kilocalories consumed per day over the two weeks of observation by the infected mice was less than that of the naïve mice (figure 3.5 B).

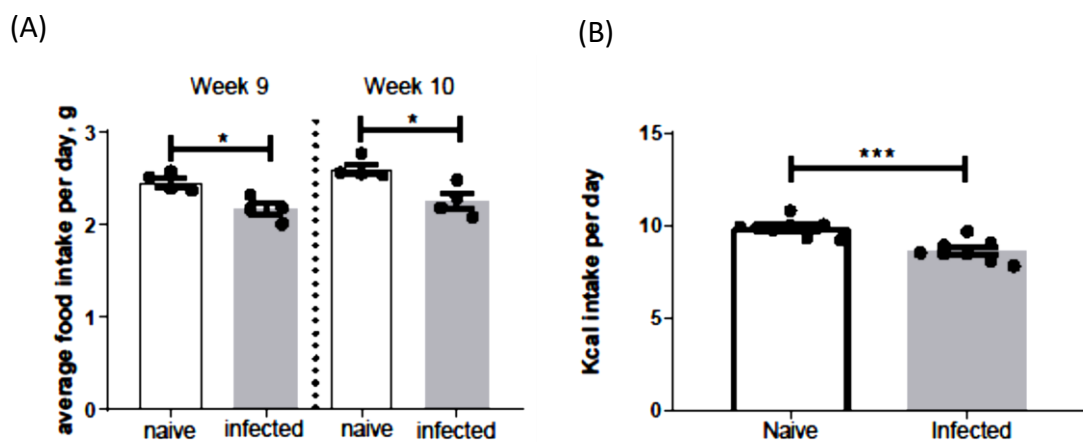


Figure 3-5: Comparison of food consumption between naïve and trickle dose infected mice.

C57BL/6 mice were fed on normal chow for 12 weeks and then given trickle *T. muris* infections for 9 weeks. The mice were observed for 2 weeks after the last dose of infection. The amount of food consumed was recorded daily. (A) Average daily food intake per mouse during week 9. (B) Average daily food intake per mouse during week 10. N = 5 to 10, results show mean \pm SEM. **Kcal content: Normal chow = 3.89 Kcal/g; HFD = 5.24 Kcal/g.**

IV. Comparison of serum leptin levels and adipocyte area between naïve and *T. muris* infected normal chow mice

Adipocytes release leptin which plays a role in regulating food intake (Friedman and Halaas, 1998; Halaas et al., 1995). Leptin production is strongly associated with adipocyte size (Zhang et al., 2002). Therefore, the concentration of leptin in serum as well as adipocyte area between naïve and infected mice was measured with a focus on mesenteric fat adipocytes due to their close proximity with the site of *T. muris* infection.

Serum leptin levels were compared 21 days after a single low dose *T. muris* infection and two weeks after 7 weeks of trickle infections. At day 21 in the single low dose infected mice there was no difference in the mean level of serum leptin between the naïve and infected mice (figure 3.6 A). Similarly, there was no difference in the mean level of serum leptin in the 7 week trickle infected mice in comparison to the naïve mice (figure 3.6 B).

Representative images of sections collected from mesenteric fat are shown in figure 3.7 A and B. At day 21 and day 42 there was no difference in the mean area of the adipocytes between naïve and infected mice (figure 3.7 C). Similarly, no difference was observed in the mean adipocyte area in the 7 and 9 week trickle infected mice in comparison to the naïve mice (figure 3.7 D).

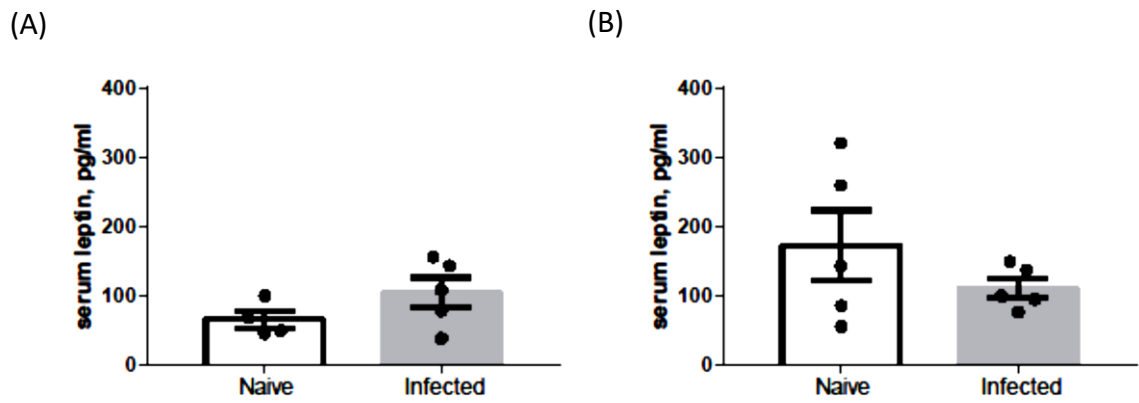


Figure 3-6: Comparison of serum leptin between naïve and *T. muris* infected mice.

C57BL/6 mice were fed on normal chow for 12 weeks and then given either a single low dose or trickle *T. muris* infection. At the time of sacrifice blood was collected from the mice and centrifuged at 13000 x g to collect serum. Serum leptin was measured using a commercially available kit from Abcam. (A) Serum leptin levels of single dose infected mice at day 21 post infection. (B) Serum leptin levels of 7 week trickle infected mice at week 9. N = 5, results show mean \pm SEM.

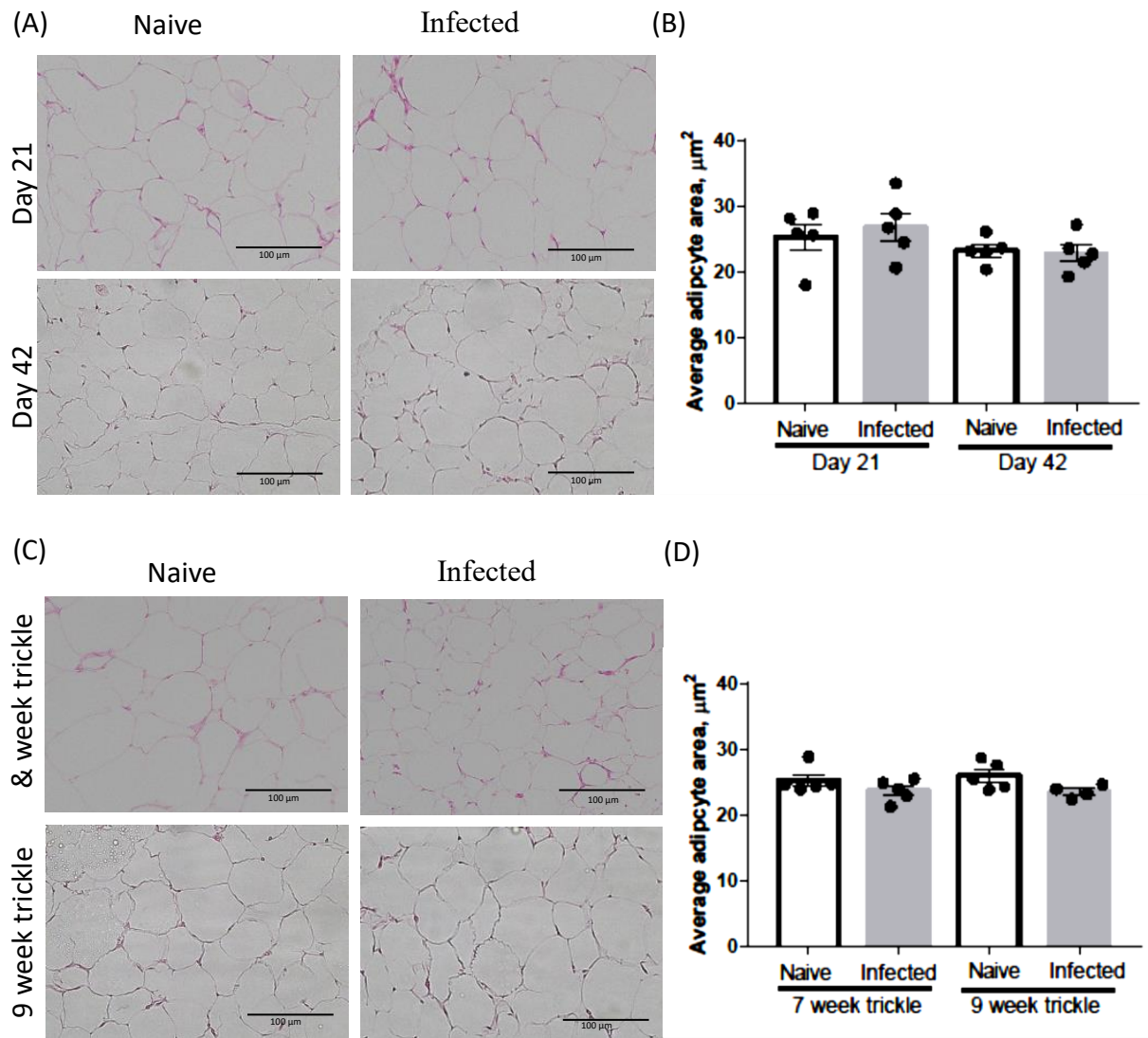


Figure 3-7: Comparison of adipocyte area between naïve and infected mice.

C57BL/6 mice were fed on normal chow for 12 weeks and then given either a single or trickle low dose *T. muris* infection. At the time of sacrifice the mesenteric fat was collected and fixed in NBF before embedding in wax. (A) Representative images of H&E stained sections of the mesenteric fat at day 21 and day 42 post infection in single dose infected mice and naïve mice. (B) Average area of adipocytes at day 21 and day 42 post infection in single dose infected mice and naïve mice. (C) Representative images of H&E stained sections of the mesenteric fat after 7 and 9 weeks of trickle infection. (D) Average area of adipocytes in 7 and 9 week trickle mice. x20 magnification, Bars = 100 μm . N = 4 to 5, results show mean \pm SEM.

V. Comparison of macrophages, eosinophils and dendritic cells in mesenteric fat between naïve and *T. muris* infected normal chow mice

Adipose tissue immune cells play an important role in maintaining metabolic homeostasis in white adipose tissue (Lee et al., 2015; Su et al., 2018; Withers et al., 2017). To investigate the effect of a low dose *T. muris* infection on the immune cell population, cells extracted from digested mesenteric fat collected from naïve and infected was analysed by flow cytometry. The population of macrophages, eosinophils and dendritic cells was compared between naïve and *T. muris* infected mice.

Representative plots showing the gating on macrophages, eosinophils and dendritic cells are shown in figure 3.8. There was no significant difference in the mean percentage macrophages, eosinophils and dendritic cells between naïve and infected mice (figure 3.9 A, C and E). There was considerable variation in the number of macrophages, eosinophils and dendritic cells. There was a trend towards increased number of macrophages, eosinophils and dendritic cells in the infected mice in comparison to the naïve mice however the differences in the mean number of cells were not significant (figure 3.9 B, D and F).

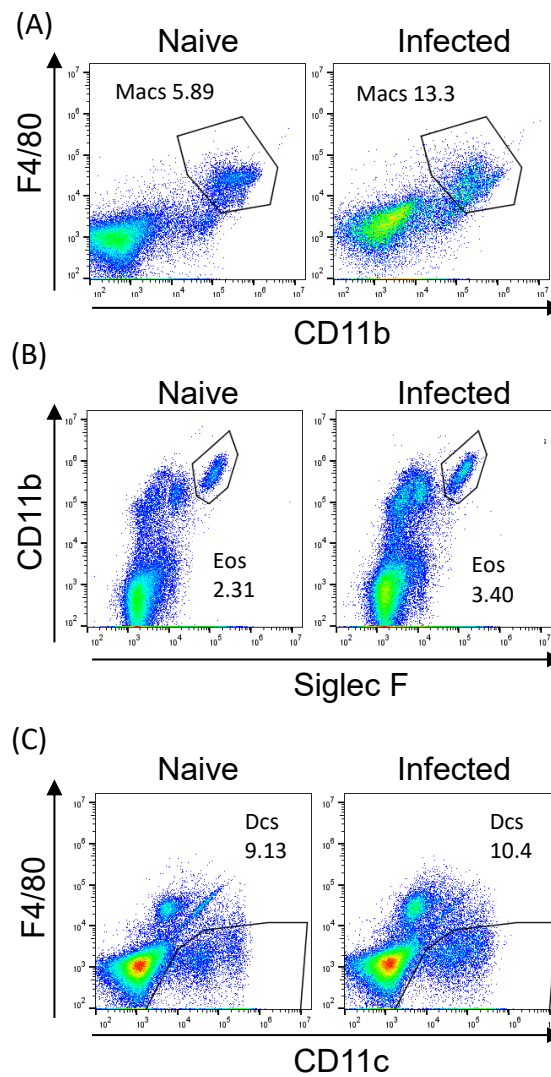


Figure 3-8: Flow gating strategy for macrophages, eosinophils and dendritic cells in naive and *T. muris* infected mice.

C57BL/6 mice were fed on normal chow for 12 weeks and then given a single low dose *T. muris* infection. Mesenteric fat was collected at day 21 post infection and digested enzymatically in order to extract immune cells. The collected cells were analysed by flow cytometry. Representative plots show the gating on: (A) F4/80⁺CD11b⁺ macrophages; (B) SiglecF⁺CD11b⁺ eosinophils; (C) CD11c⁺F4/80⁻ dendritic cells. Macrophages (Macs), Eosinophils (Eos), Dendritic cells (Dcs).

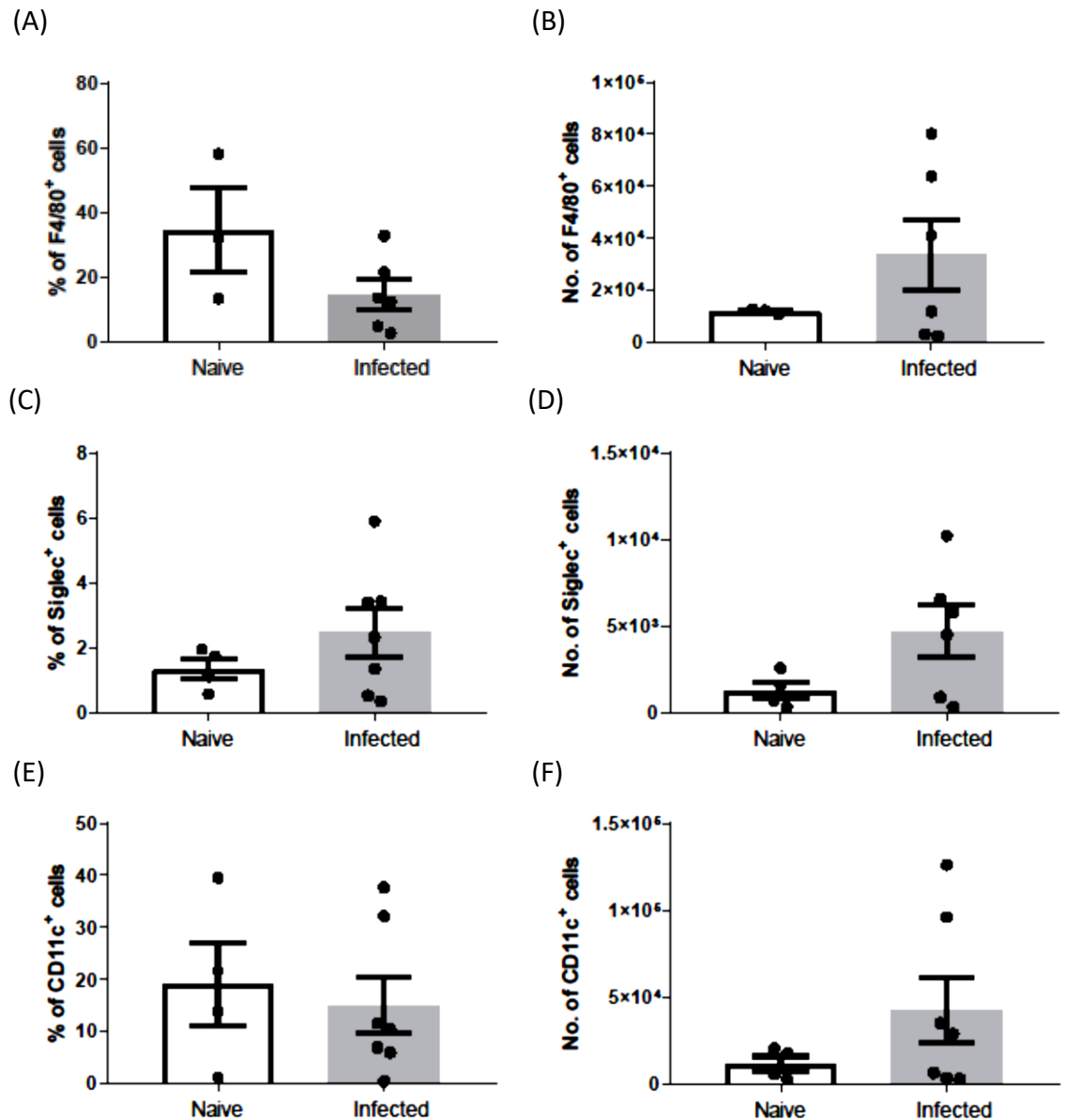


Figure 3-9: Comparison of macrophages, eosinophils and dendritic cell populations in mesenteric fat from naive and *T. muris* infected mice.

C57BL/6 mice were fed on normal chow for 12 weeks and then given a single low dose *T. muris* infection. Mesenteric fat was collected at day 21 post infection and digested enzymatically in order to extract immune cells. The collected cells were analysed by flow cytometry. (A) Percentage of F4/80⁺CD11b⁺ macrophages. (B) Number of F4/80⁺CD11b⁺ macrophages. (C) Percentage of SiglecF⁺CD11b⁺ eosinophils. (D) Number of SiglecF⁺CD11b⁺ eosinophils. (E) Percentage of CD11c⁺CD11b⁻ dendritic cells. (F) Number of CD11c⁺CD11b⁻ dendritic cells. N = 3 to 7, results show mean \pm SEM.

3.2.2 The effect of low dose *T. muris* infection on the pancreas, liver and lung

I. Comparison of blood glucose levels and area of pancreatic islet of Langerhans between naïve and *T. muris* infected normal chow mice

Pro-inflammatory cytokines have been implicated in the development of autoimmune diabetes as well as type 2 diabetes in humans and in mice (Hotamisligil et al., 1993; Pradhan et al., 2001; Trembleau et al., 2003). Chronic *T. muris* infection is associated with production of pro-inflammatory cytokines (Else and Grecis, 1991). The effect of chronic *T. muris* infection on blood glucose and size of the pancreatic islets of Langerhans, which are both altered in diabetes, were measured (Hummel et al., 1972; Pettersson et al., 2012).

Blood glucose levels between naïve and *T. muris* infected (single and trickle low dose infections) non-fasted mice was measured at different time points. At day 30 post infection after a single low dose infection there was a significant reduction in the mean concentration of glucose in the blood from infected mice as compared to blood collected from naïve mice. However, at day 37 no significant difference in the mean concentration of blood glucose between the naïve and infected mice was observed (figure 3.10 A). Blood glucose for the 9 week trickle infected mice was measured at week 10. There was no difference in the mean blood glucose levels between the naïve and infected mice (figure 3.10 B).

The mean size of the pancreatic islets of Langerhans between naïve and infected mice was measured. Representative images of pancreas tissue collected from single and trickle low dose infected mice are shown in figure 3.11 A and B. After a single low infection with *T. muris* there was no difference in the mean area of the islet of Langerhans between naïve and single dose infected mice at day 21 and day 42 post infection (figure 3.11 C). There was no difference in the mean area of the islet of Langerhans between naïve and infected mice after 7 and 9 weeks of trickle infection (figure 3.11 D).

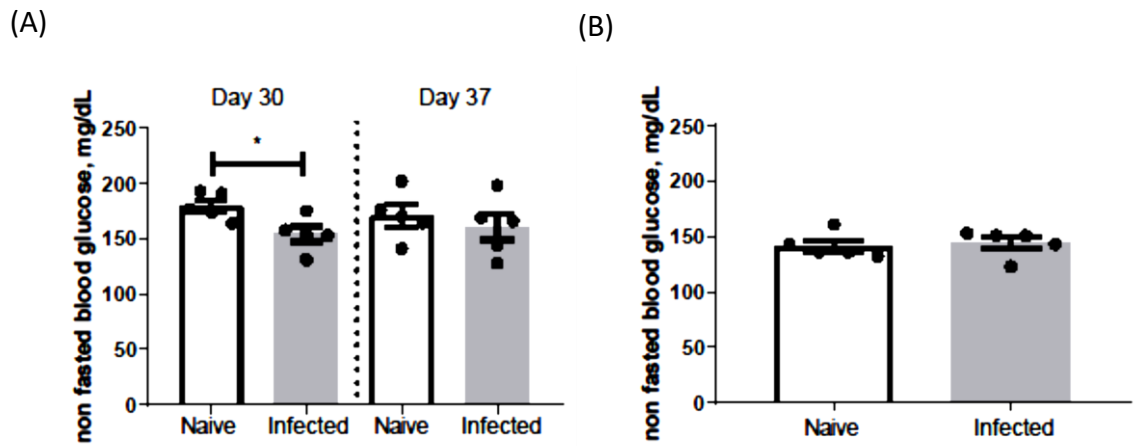


Figure 3-10: Comparison of blood glucose between naïve and *T. muris* infected mice.

C57BL/6 mice were fed on normal chow for 12 weeks and then given either a single low dose or trickle *T. muris* infection. A drop of blood was collected from the tail of non-fasted mice and blood glucose was measured using an Accu-chek Aviva glucometer. (A) Blood glucose levels in mg/dL measured at day 30 and day 37 post infection after a single low dose infection (B) Blood glucose levels in mg/dL measured in week 10 after 9 weeks of trickle infections. N = 5, results show mean \pm SEM.

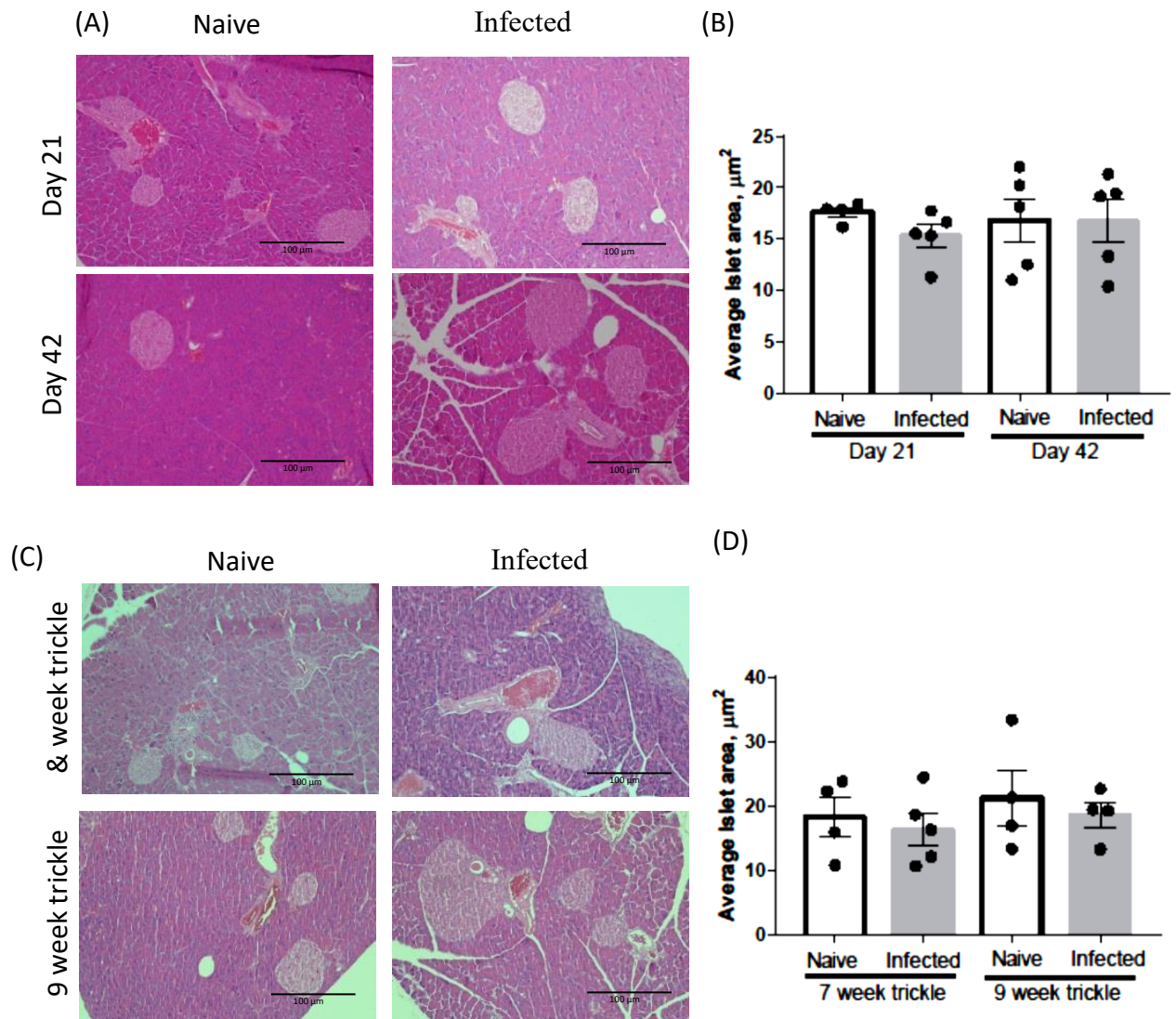


Figure 3-11: Comparison of the islet of Langerhans area between naive and infected mice.

C57BL/6 mice were fed on normal chow for 12 weeks and then given either a single low dose or trickle *T. muris* infection. At the time of sacrifice the pancreas was collected and fixed in NBF before embedding in wax. (A) Representative images of H&E stained sections of the pancreas at day 21 and day 42 post infection in single dose infected mice and naive mice. (B) Average area of islets at day 21 and day 42 post infection in single dose infected mice and naive mice. (C) Representative images of H&E stained sections of the pancreas at after 7 and 9 weeks of trickle infection and in naive mice. (D) Average area of islets in 7 and 9 week trickle mice and naive mice. x20 magnification, bars = 100 μm . N = 4 to 5, results show mean \pm SEM.

II. Assessment of liver function in *T. muris* infected normal chow mice

Liver disease is caused by a variety of factors including alcohol, obesity, viral infection and parasitic infections. Chronic liver disease is associated with progressive destruction of liver tissue resulting in fibrosis and cirrhosis which affect the functional ability of the liver (Liu et al., 2012).

At day 21 after a single low infection with *T. muris* the appearance of freshly collected liver as well as H&E stained liver sections from infected mice was similar to that of naïve mice (figure 3.12 A). Furthermore, a range of tests for different parameters in the serum associated with liver function were measured (Gowda et al., 2009). At day 21 and day 42 after a single low dose infection there was no difference in total serum albumin, alanine phosphatase (ALP), alanine transaminase (ALT) and total protein (figure 3.12 B and C). Liver function tests were also performed on serum collected from mice after 7 weeks of trickle infection. There was no difference in serum albumin, ALP, ALT, and total protein between the naïve and infected mice (figure 3.13).

III. Comparison of PAS/AB stained sections of lung tissue from naïve and low dose *T. muris* infected normal chow mice

Previous work has shown that a low dose of *T. muris* alters cytokine production in the lung (Chenery et al., 2016). To investigate if low dose *T. muris* infection would also have an effect on the production of mucus in the lung tissue sections were co-stained using periodic acid Schiff (PAS) reagent and alcian blue (AB). Representative images of PAS/AB stained sections are shown in figure 3.14 A and C. No increase in PAS/AB staining was observed between naïve and infected mice after 21 and 42 days of a single low dose infection (figure 3.14 B). Furthermore, no difference in PAS/AB staining was observed in the 7 and 9 week trickle mice compared to naïve mice (figure 3.14 D).

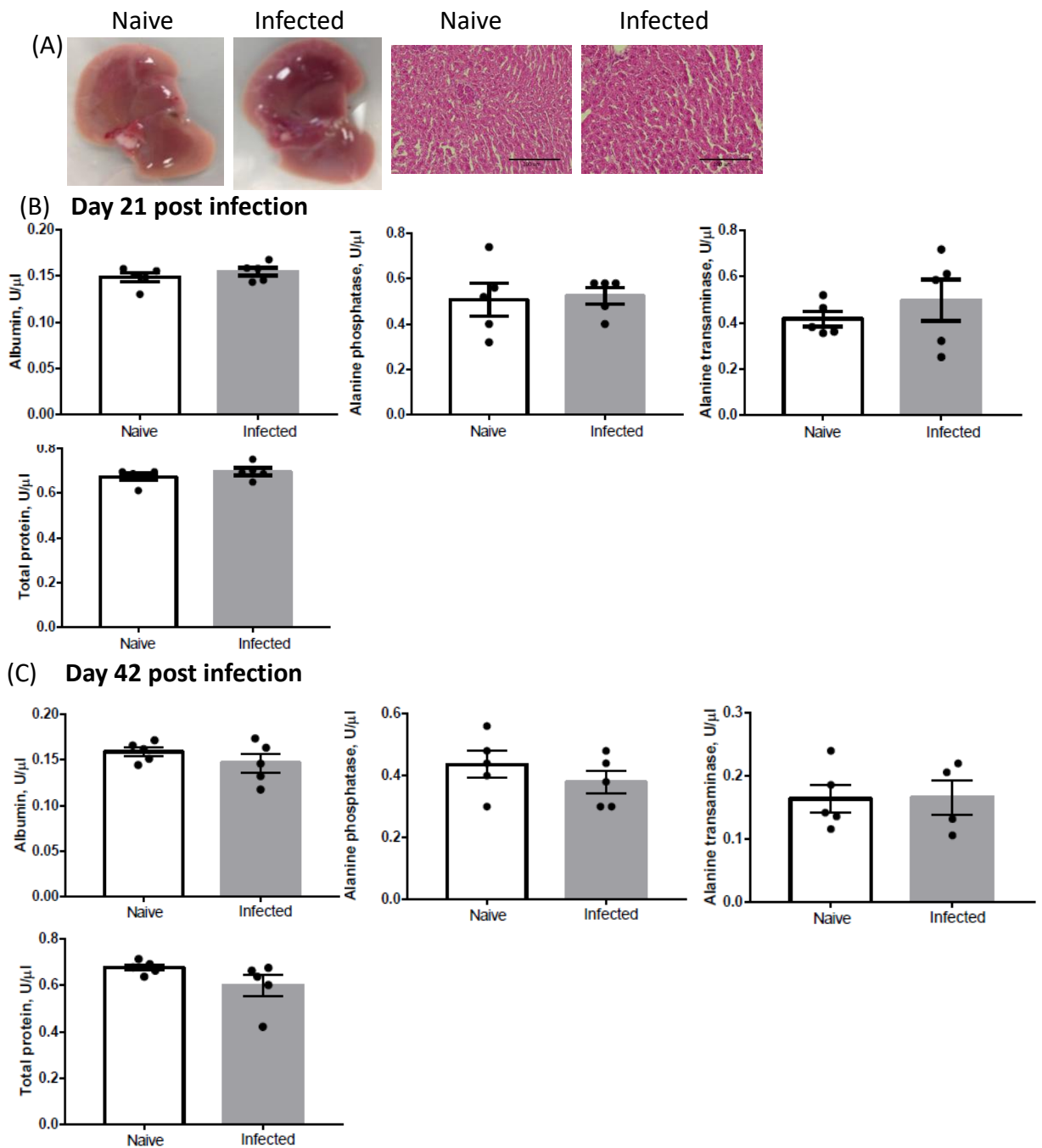


Figure 3-12: Serum liver function tests in naïve and single dose infected mice.

C57BL/6 mice were fed on normal chow for 12 weeks and then given a single low dose infection of *T. muris*. Blood was collected from mice at day 21 post infection and centrifuged at 13000 x g to collect serum used for the liver function tests. Liver function tests compared levels of serum albumin, alanine phosphatase, alanine transaminase and total protein between naïve and infected mice. (A) Representative images of fresh liver and H&E stained liver sections from mice at 21 days post infection. (B) Results of liver function tests performed on serum collected at day 21 post infection. (C) Results of liver function tests performed on serum collected at day 42 post infection. x20 magnification, bars = 100 µm. N = 5, results show mean ± SEM.

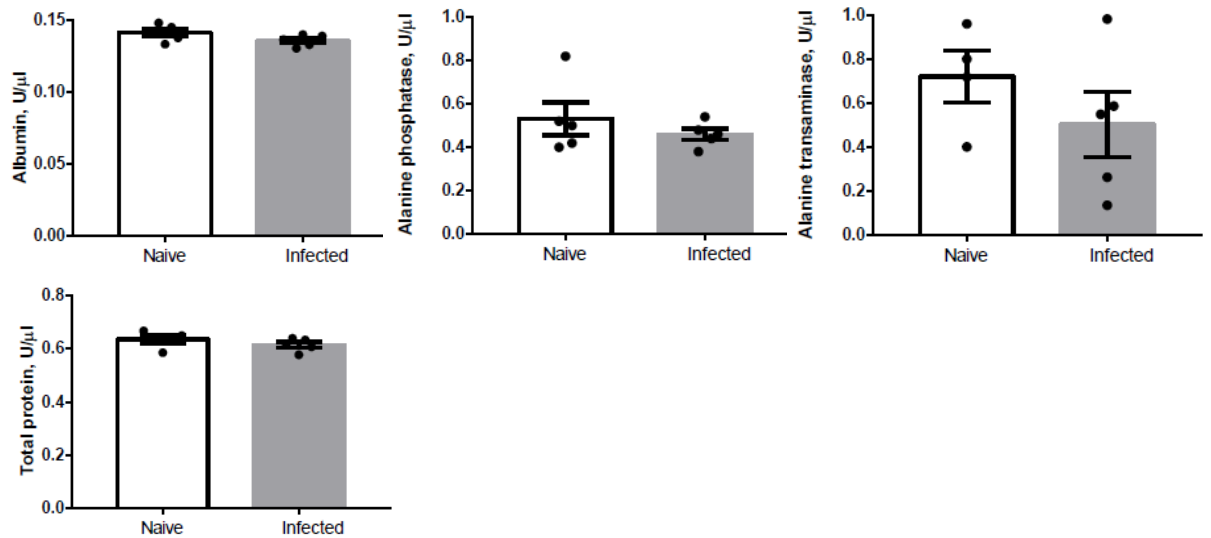


Figure 3-13: Serum liver function tests in naïve and trickle dose infected mice.

C57BL/6 mice were fed on normal chow for 12 weeks and then given a trickle low dose infection of *T. muris* for 7 weeks. Blood was collected from mice in week 9 and centrifuged at 13000 x g to collect serum used for the liver function tests. Liver function tests compared levels of serum albumin, alanine phosphatase, alanine transaminase and total protein between naïve and infected mice. N = 5, results show mean ± SEM.

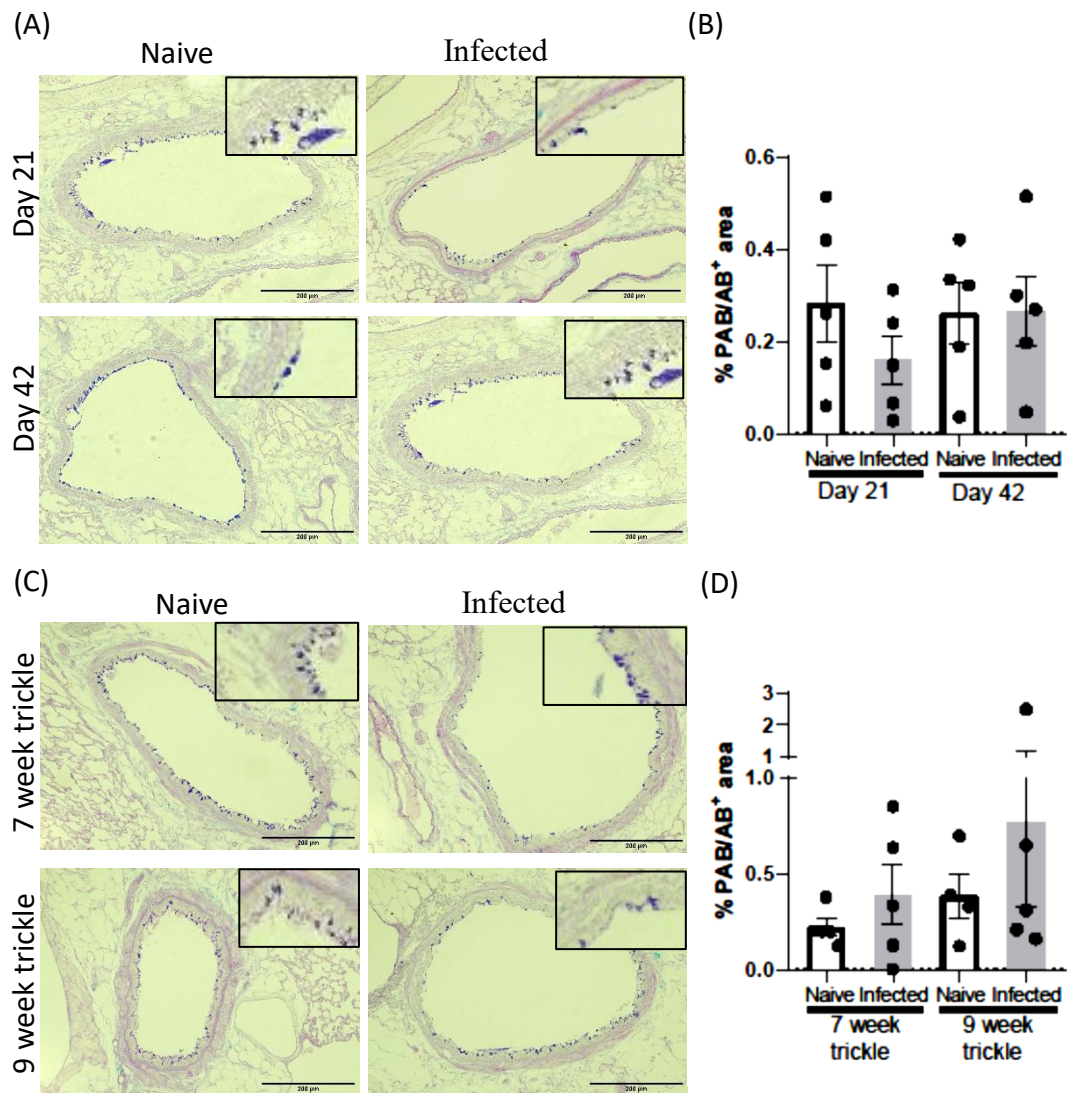


Figure 3-14: Comparison of PAS/AB stained lung sections from naïve and *T. muris* infected mice.

C57BL/6 mice were fed on normal chow for 12 weeks and then given either a single low dose or trickle *T. muris* infection. At the time of sacrifice the single left lung lobe was fixed in Carnoy's reagent before embedding in wax. (A) Representative images of PAS/AB stained lung sections at day 21 and day 42 post infection in single dose infected mice and naïve mice. (B) Mean percentage of total area per field of view that is PAS/AB⁺ at day 21 and day 42 post infection (C) Representative images of PAS/AB stained lung sections from 7 and 9 week trickle mice and naïve mice. (D) Mean percentage of total area per field of view that is PAS/AB⁺ from 7 and 9 week trickle mice. x10 magnification, bars, 200 µm. Insert shows x500 magnification of the lung section. N = 5, results show mean ± SEM.

3.2.3 The effect of a low dose *T. muris* infection on body weight in mice fed a high fat diet

I. Comparison of body weight changes between naïve and *T. muris* infected HFDIO mice

Mice were placed on a HFD for 12 weeks in order to induce obesity. The mice were then given a single low dose *T. muris* infection and observed for either 21 or 42 days post infection. In the first 10 to 12 weeks of feeding there was a sharp increase in body weight after which the weight of the mice stabilised (figure 3.15 A and B). As expected, the HFD fed mice gained more weight in comparison to the normal chow fed mice by day 21 post infection (figure 3.15 C). Overall the final weight of the HFDIO mice was increased in comparison to the naïve normal chow mice. However the normal chow mice showed a trend towards a higher increase in percentage weight gain in comparison to the HFDIO mice from the time of infection to the day of sacrifice (figure 3.15 D to G).

After 21 days of infection, there was no difference in weight and percentage weight gain after infection between the naïve and infected HFDIO mice (figure 3.15 D and E). At day 42, there was no difference in the final weight of the HFDIO mice and in the percentage weight gain from the time of infection (figure 3.15 F and G).

Mice were also given low dose *T. muris* trickle infection. The weight of the mice were recorded weekly before and during the course of trickle infection (figure 3.16 A and B). At the end of the 7 week trickle infection experiment there was no difference in the weight of the naïve and infected mice. There was no difference in the percentage weight gain between naïve and infected HFDIO mice (figure 3.16 C and D). After 9 weeks of trickle infection the infected HFDIO mice had a significant reduction in the mean body weight as compared to the naïve HFDIO mice, although the percentage weight change between the two groups was not significant (figure 3.16 E and F).

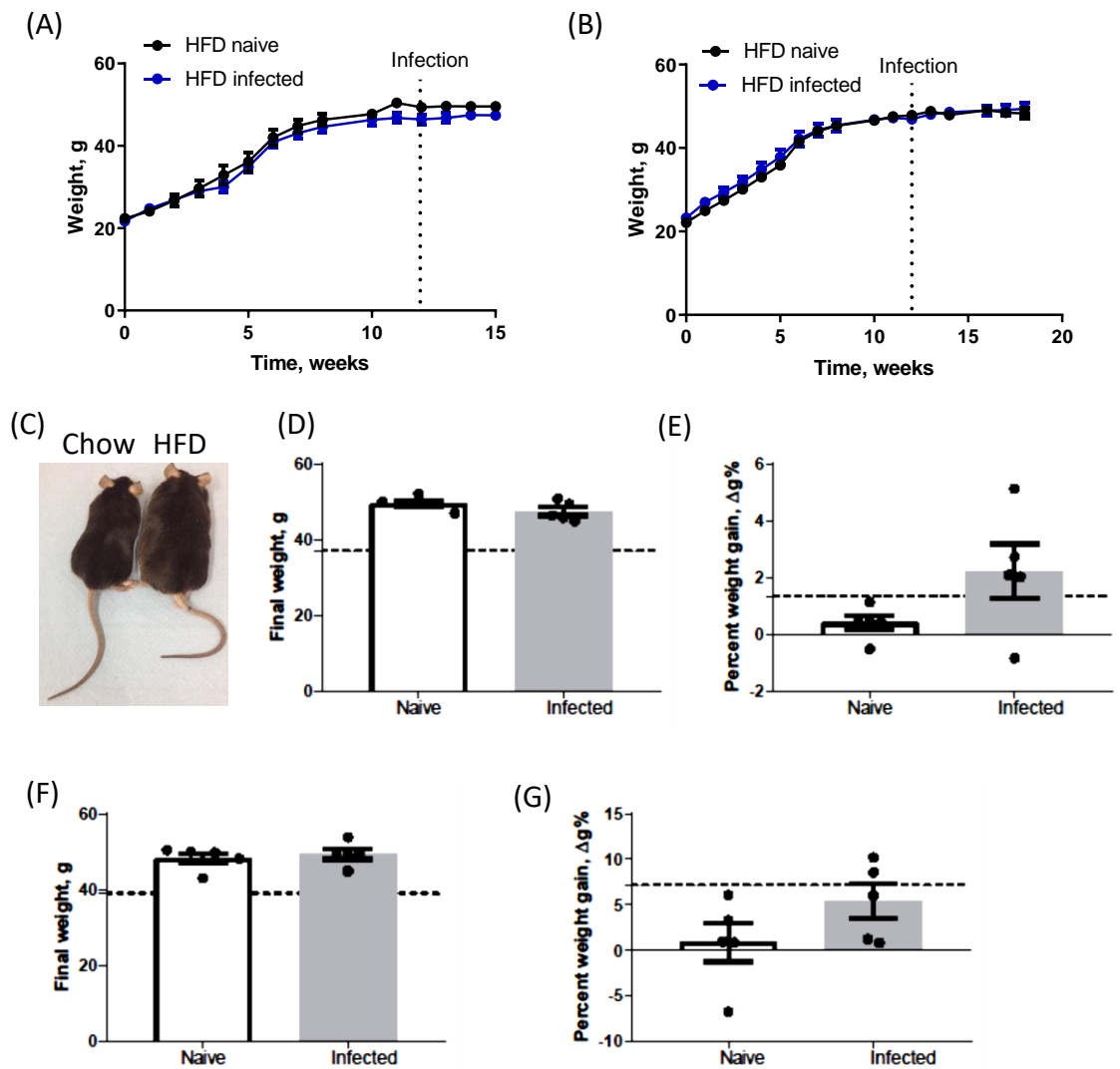


Figure 3-15: Weight change in single low dose *T. muris* infected HFDIO mice.

C57BL/6 mice were fed on a HFD for 12 weeks and then given a single low dose infection of *T. muris*. The weights of the mice were recorded weekly throughout the experiment. (A) Weekly weight record of mice (naïve and infected) until day 21 post infection. (B) Weekly weight record of mice (naïve and infected) until day 42 post infection. (C) Representative image of normal chow and HFDIO infected mice. (D) Final weight of the HFDIO mice (naïve and infected) at day 21 post infection. (E) Percentage weight gain of the HFDIO mice from the time of infection until 21 days post infection compared to naïve mice. (F) Final weight of the HFDIO mice at day 42 post infection compared to naïve mice. (G) Percentage weight gain of the HFDIO mice from the time of infection until day 42 post infection compared to naïve mice. N = 5, results show mean \pm SEM. Horizontal line represents the respective mean value of the naïve normal chow group.

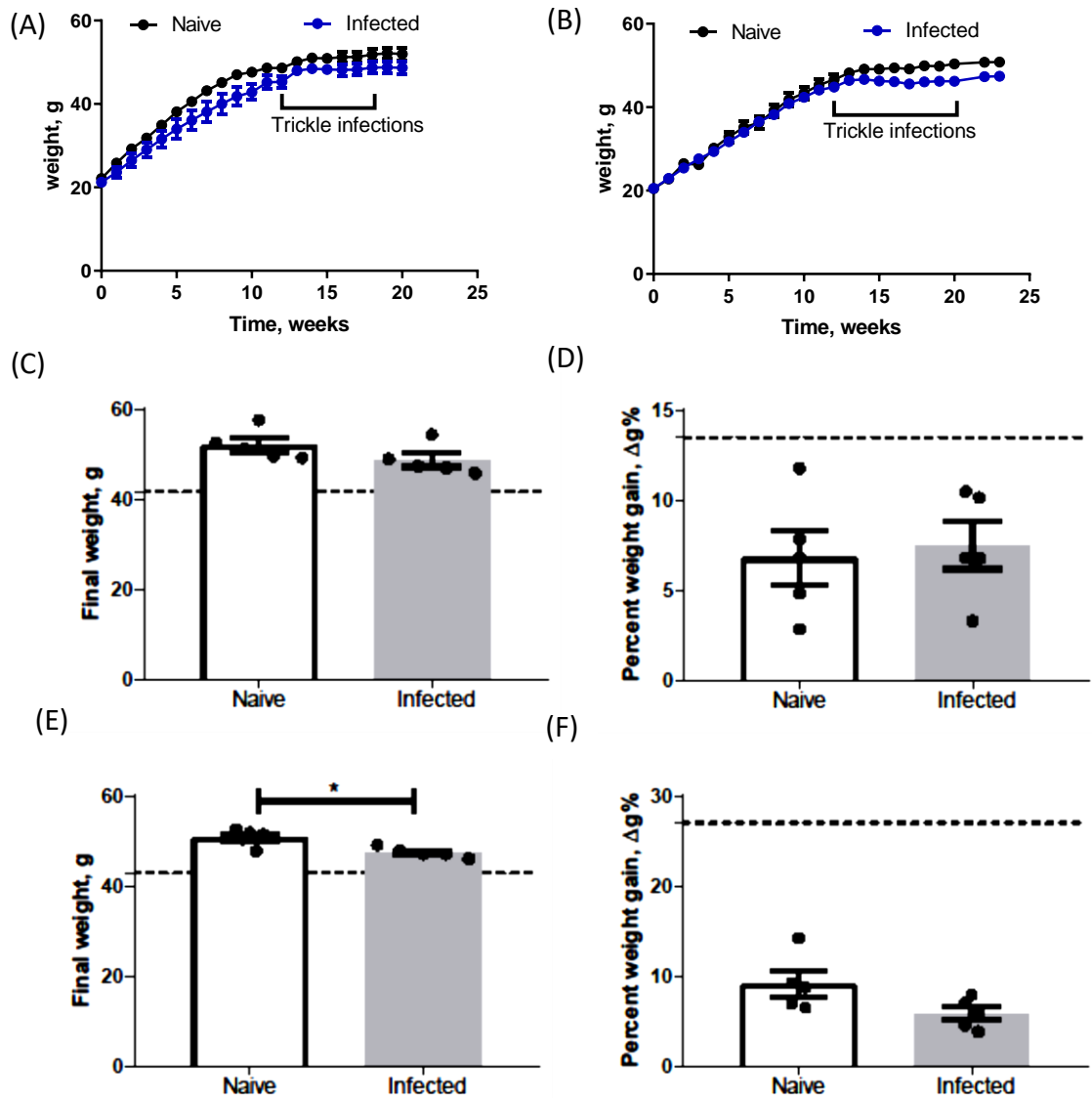


Figure 3-16: Weight change in trickle low dose *T. muris* infected HFDIO mice.

C57BL/6 mice were fed on a HFD for 12 weeks and then given trickle *T. muris* infections for 7 or 9 weeks and then observed for 2 weeks before sacrifice. The weights of the mice were recorded weekly throughout the experiment. (A) Weekly weight record of 7 week trickle HFDIO mice and naïve mice. (B) Weekly weight record of 9 week trickle HFDIO mice and naïve mice. (C) Final weight of the 7 week trickle HFDIO mice and naïve mice. (D) Percentage weight gain of the 7 week trickle HFDIO mice and naïve mice. (E) Final weight of the 9 week trickle HFDIO mice and naïve mice. (F) Percentage weight gain of the 9 week trickle HFDIO mice and naïve mice. N = 5, results show mean \pm SEM. Horizontal line represents the respective mean value of the naïve normal chow group.

II. Comparison of epididymal and subcutaneous fat pads between naïve and *T. muris* infected HFDIO mice

The mean weight of the epididymal fat pads in the naïve and infected HFDIO mice was lower than in the normal chow naïve (figure 3.17 A to D). However, the mean weight of the subcutaneous fat pads in the HFDIO mice was higher in the HFDIO mice in comparison to the normal chow mice (figure 3.17 E and F). Therefore, the weight of the subcutaneous fat pads correlated with the increased body weight observed in HFDIO mice.

In the single low dose experiments, there was no difference in the mean weight of the epididymal fat pads between naïve and infected HFDIO mice at day 21 and day 42 post infection (figure 3.17 A and B). After 7 and 9 weeks of trickle infection there was no difference in the mean weight of the epididymis fat pads between naïve and infected HFDIO mice (figure 3.17 C and D). Furthermore, no difference was observed in the mean weight of the subcutaneous fat pads between naïve and infected mice at day 42 post infection (single low dose) nor after 9 weeks of trickle infection (figure 3.17 D and E).

III. Comparison of food intake between naïve and trickle dose infected HFDIO mice

After 9 weeks of trickle infection, there was no significant difference in mean food consumption between naïve normal chow mice and the HFDIO mice. However, when converted to calories, the HFD fed mice consumed a higher amount of calories per mouse in comparison to the normal chow mice. There was no difference in food intake between naïve and infected HFDIO mice in neither week 9 nor week 10 (3.18 A). In line with this, conversion of the amount of food consumed per mouse to calories showed no difference between infected and naïve HFDIO mice (figure 3.18 B).

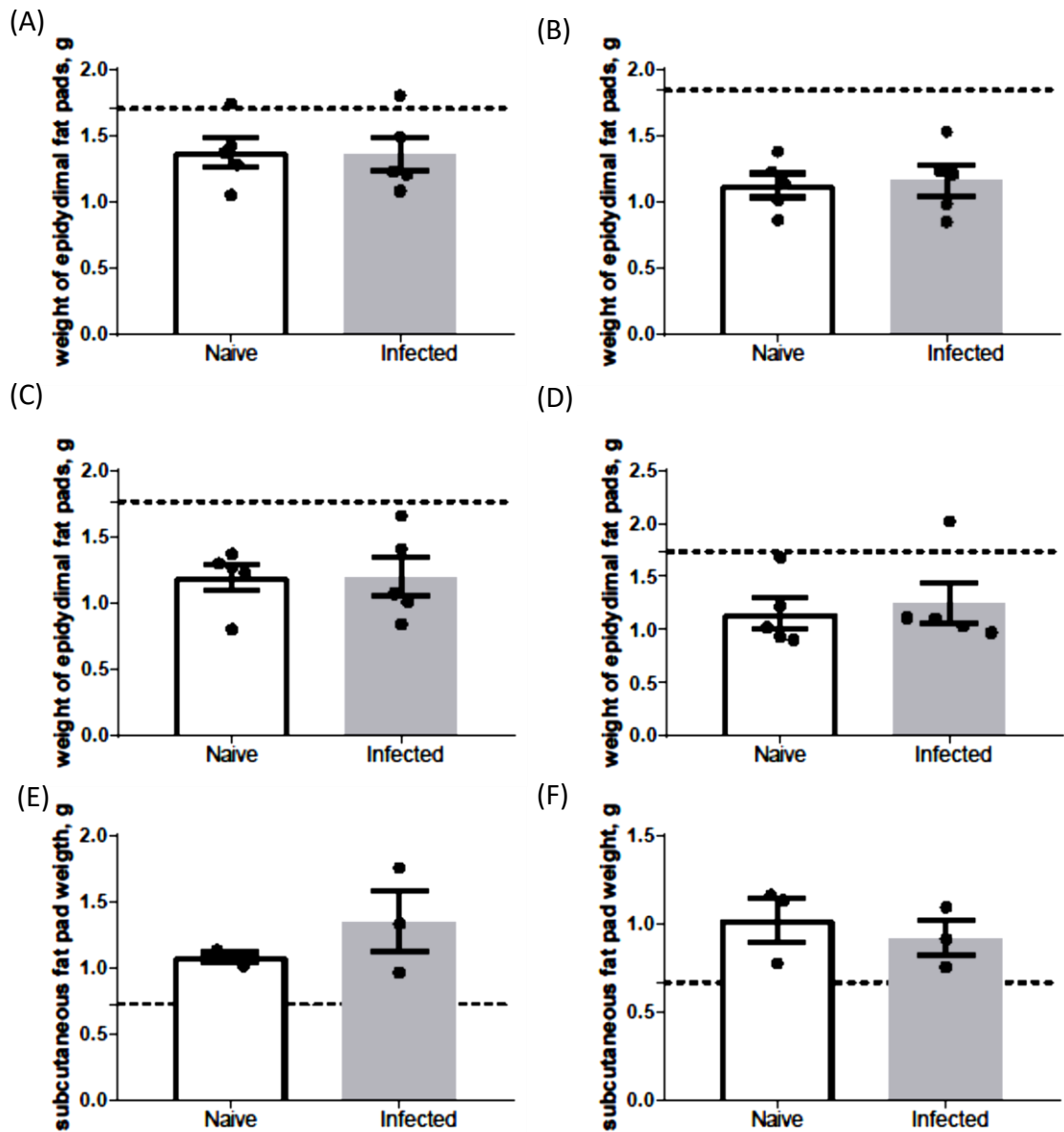


Figure 3-17: Comparison of epididymal and subcutaneous fat pads in single low dose and trickle infected HFDIO mice.

C57BL/6 mice were fed on a HFD for 12 weeks and then given either a single low dose or trickle *T. muris* infection. At the time of sacrifice we collected and weighed the epididymal and subcutaneous fat pads. (A) Weight of epididymal fat pads of single low dose infected HFDIO mice at day 21 post infection and naïve mice. (B) Weight of epididymal fat pads of single low dose infected HFDIO mice at day 42 post infection and naïve mice. (C) Weight of epididymal fat pads of 7 week trickle infected HFDIO mice at week 9 and naïve mice. (D) Weight of epididymal fat pads of 9 week trickle infected HFDIO mice at week 11 and naïve mice. (E) Weight of subcutaneous fat pads of single low dose infected HFDIO mice at day 42 post infection and naïve mice. (F) Weight of subcutaneous fat pads of 9 week trickle infected HFDIO mice at week 11 and naïve mice. N = 3 to 5, results show mean \pm SEM. Horizontal line represents the respective mean value of the naïve normal chow group.

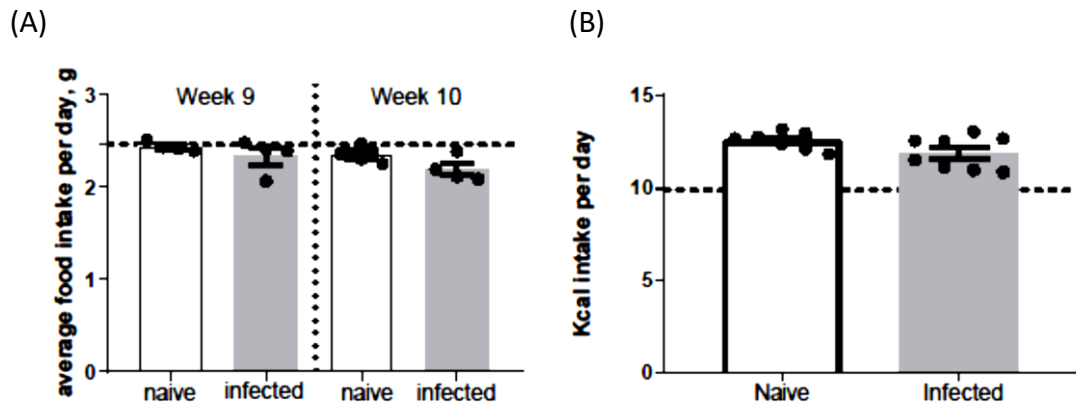


Figure 3-18: Comparison of food consumption between naïve and trickle dose infected HFDIO mice.

C57BL/6 mice were fed on a HFD for 12 weeks and then given trickle *T. muris* infections for 9 weeks. The mice were observed for 2 weeks after the last dose of infection. The amount of food consumed was recorded daily. (A) Average daily food per mouse during week 9. (B) Average daily food intake per mouse during week 10. N = 5 to 10, results show mean \pm SEM. Horizontal line represents the respective mean value of the naïve normal chow group.

IV. Comparison of serum leptin levels and adipocyte area between naïve and *T. muris* infected HFDIO mice

Serum leptin was measured in naïve mice and in mice at day 21 or day 42 post a single low dose infection. The mean serum leptin levels in the HFDIO mice were elevated in comparison the naïve normal chow mice.

At both day 21 and day 42 post infection there was a significant increase in serum leptin in the infected HFDIO mice as compared to the HFDIO naïve mice (figure 3.19 A). In contrast, the serum leptin levels were more variable in the 7 week trickle infected HFDIO mice and there was no difference in the mean concentration of serum leptin between naïve and infected HFDIO mice (figure 3.19 B).

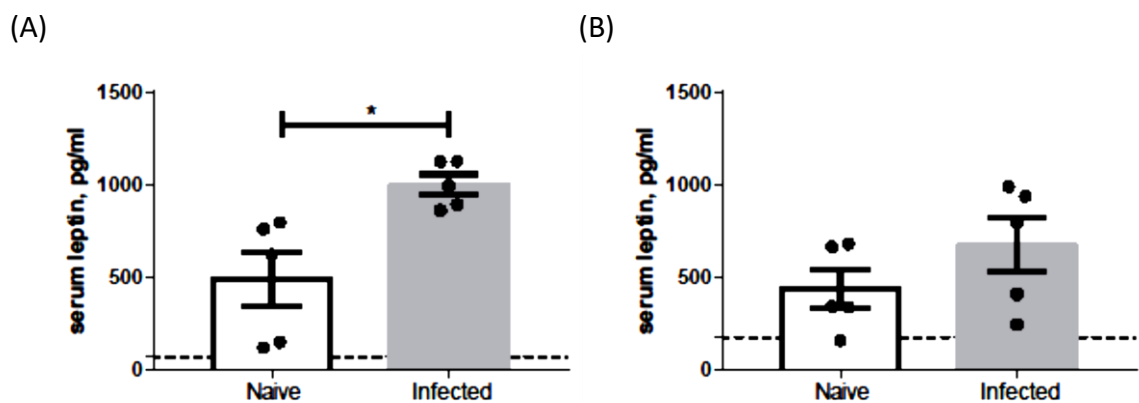


Figure 3-19: Comparison of serum leptin between naïve and *T. muris* infected HFDIO mice.

C57BL/6 mice were fed on a HFD for 12 weeks and then given either a single low dose or trickle *T. muris* infection. At the time of sacrifice blood was collected from the mice and centrifuged at 13000 x g to collect serum. Serum leptin was measured using a commercially available kit from Abcam. (A) Serum leptin levels of single low dose infected HFDIO mice at day 21 post infection and in naïve mice. (B) Serum leptin levels of 7 week trickle infected HFDIO mice at week 9 and in naïve mice. N = 5, results show mean \pm SEM. Horizontal line represents the respective mean value of the naïve normal chow group.

Representative images of sections collected from mesenteric fat on naïve and infected HFDIO mice are shown in figure 3.20 A and B. Obesity is associated with the formation of crown-like structures which form when resident macrophages surround dying adipocytes (Murano et al., 2008). Crown-like structures were observed in both naïve and infected HFDIO mice (indicated in the figure). There was a trend towards increased area of adipocytes in the HFDIO mice in comparison to the naïve normal chow mice. At days 21 and 42 post infection, there was no difference in the mean area of adipocytes between naïve and infected HFDIO mice (figure 3.20 C). Similarly, after 7 and 9 weeks of trickle infection there was no significant difference in the adipocyte area compared to naïve mice (figure 3.20 D).

V. Comparison of macrophages, eosinophils and dendritic cells in mesenteric fat between naïve and *T. muris* infected mice

Representative plots showing the gating on macrophages, eosinophils and dendritic cells from mesenteric fat collected from HFDIO mice are shown in figure 3.21. There was a trend towards increased number of macrophages, eosinophils and dendritic cells in the HFDIO mice in comparison to the normal chow mice however no clear trend was observed in the percentage number of cells (figure 3.22).

There was no significant difference in the mean percentage macrophages and dendritic cells between naïve and infected HFDIO mice whereas there was a significant increase in the percentage of eosinophils in the HFDIO mice (figure 3.22 A, C and E). However, there was no difference in the mean number of macrophages, eosinophils and dendritic cells in the infected HFDIO mice in comparison to the naïve HFDIO mice (figure 3.22 B, D and F).

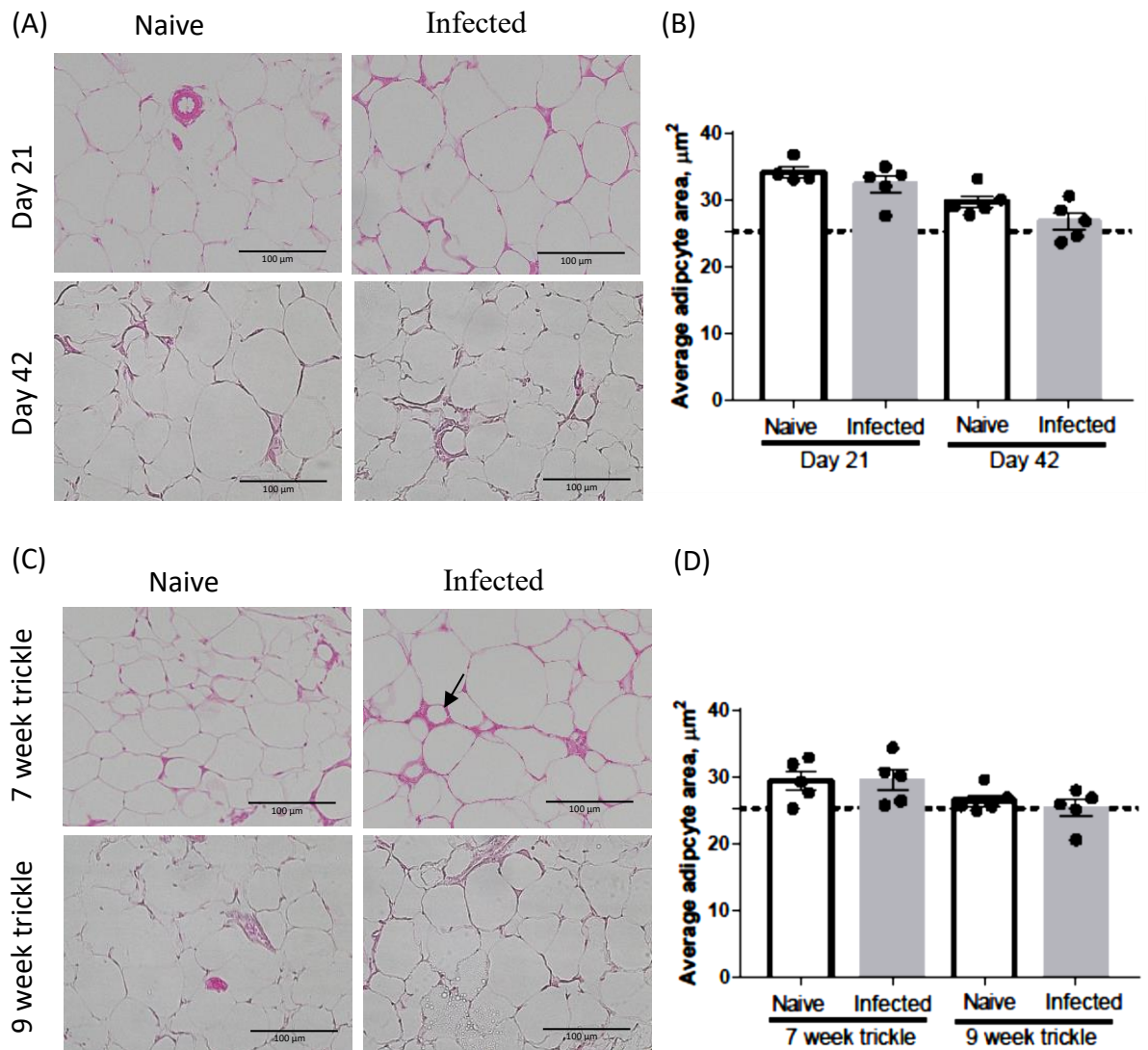


Figure 3-20: Comparison of adipocyte area between naïve and infected HFDIO mice.

C57BL/6 mice were fed on a HFD for 12 weeks and then given either a single low dose or trickle *T. muris* infection. At the time of sacrifice the mesenteric fat was collected and fixed in NBF before embedding in wax. (A) Representative images of H&E stained sections of the mesenteric fat at day 21 and day 42 post infection in single low dose infected HFDIO mice and naïve mice. (B) Representative images of H&E stained sections of the mesenteric fat after 7 and 9 weeks of trickle infection. (C) Average area of adipocytes at day 21 and day 42 post infection in single dose infected HFDIO mice and in naïve mice. (D) Average area of adipocytes in 7 and 9 week trickle HFDIO mice and naïve mice. $\times 20$ magnification, bars = $100 \mu\text{m}$. $N = 5$, results show mean \pm SEM. The black arrow shows an example of a crown like structure. Horizontal line represents the respective mean value of the naïve normal chow group (mean values of adipocyte area at day 21 post infection (single dose group) and 7 week trickle group are shown).

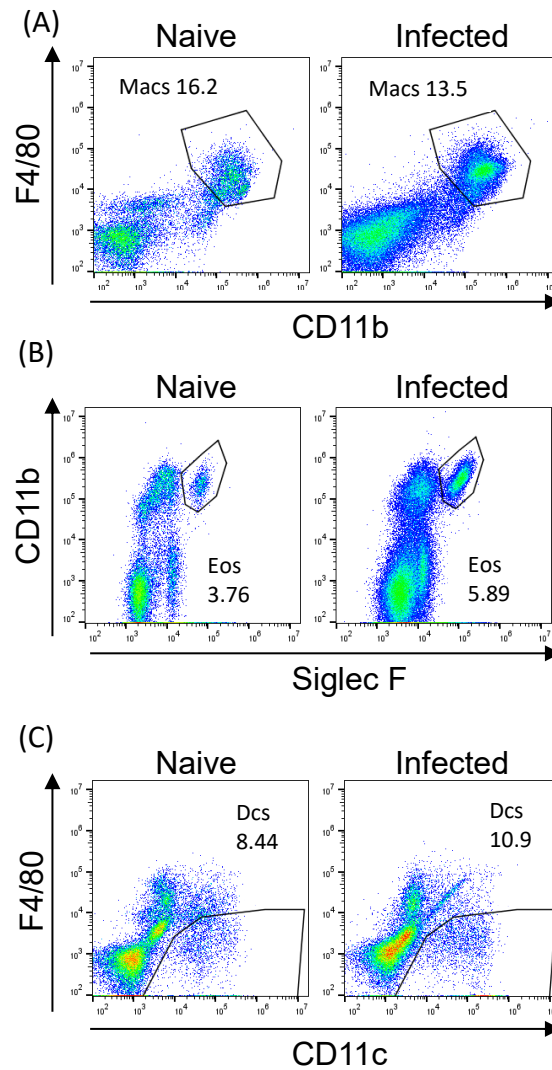


Figure 3-21: Flow gating strategy for macrophages, eosinophils and dendritic cells in naive and *T. muris* infected HFDO mice.

C57BL/6 mice were fed on a HFD for 12 weeks and then given a single low dose *T. muris* infection. Mesenteric fat was collected at day 21 post infection and digested enzymatically in order to extract immune cells. The collected cells were analysed by flow cytometry. Representative plots show the gating on: (A) F4/80⁺CD11b⁺ macrophages; (B) SiglecF⁺CD11b⁺ eosinophils; (C) CD11c⁺F4/80⁻ dendritic cells. Macrophages (Macs), Eosinophils (Eos), Dendritic cells (Dcs).

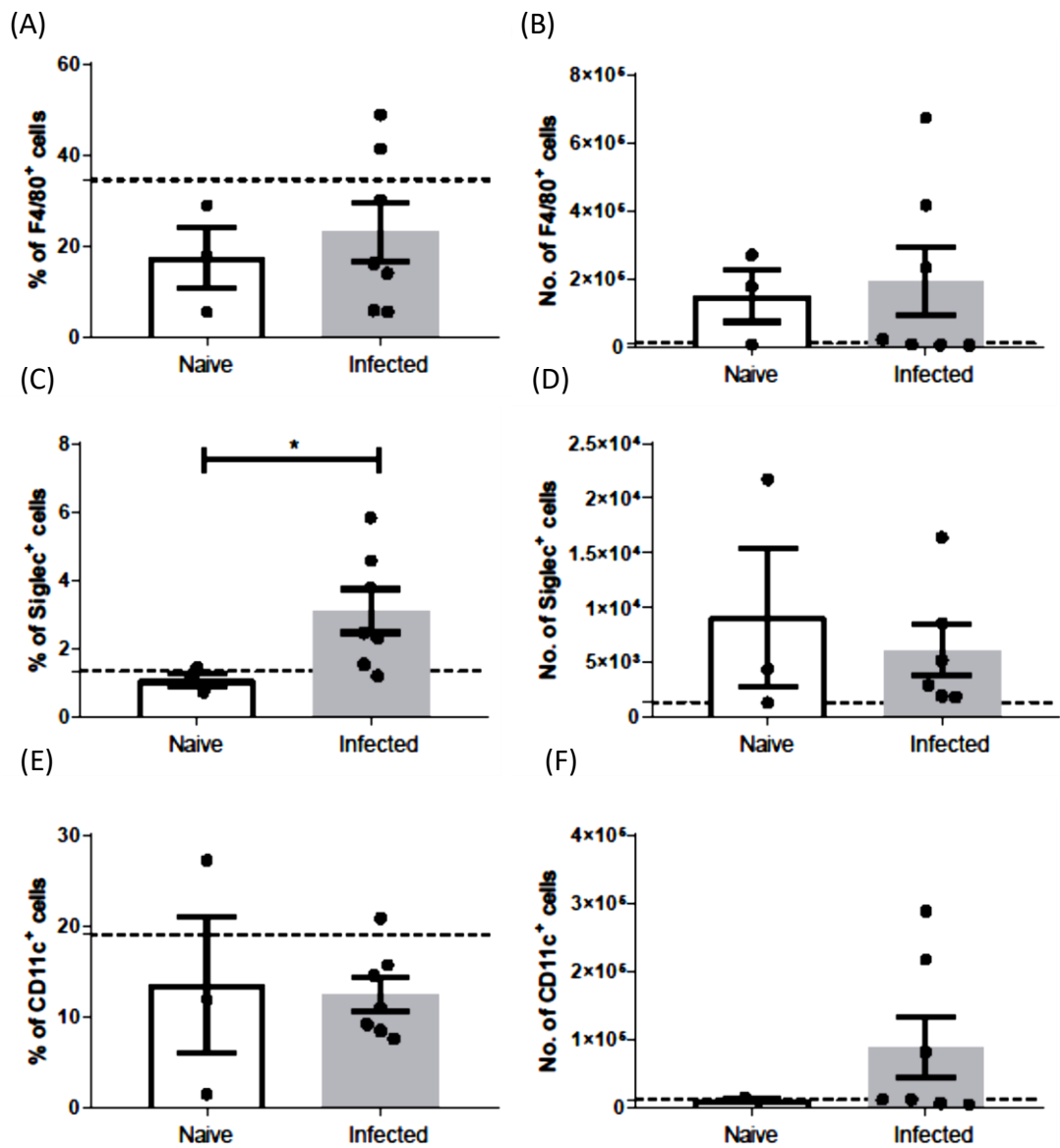


Figure 3-22: Comparison of macrophages, eosinophils and dendritic cell populations in mesenteric fat from naive and *T. muris* infected HFDIO mice.

C57BL/6 mice were fed on a HFD for 12 weeks and then given a single low dose *T. muris* infection. Mesenteric fat was collected at day 21 post infection and digested enzymatically in order to extract immune cells. The collected cells were analysed by flow cytometry. (A) Percentage of F4/80⁺CD11b⁺ macrophages. (B) Number of F4/80⁺CD11b⁺ macrophages. (C) Percentage of Siglec⁺CD11b⁺ eosinophils. (D) Number of Siglec⁺CD11b⁺ eosinophils. (E) Percentage of CD11c⁺CD11b⁻ dendritic cells. (F) Number of CD11c⁺CD11b⁻ dendritic cells. N = 3 to 7, results show mean ± SEM. Horizontal line represents the respective mean value of the naïve normal chow group.

3.2.4 The effect of low dose *T. muris* on the pancreas, liver and lung in HFDIO mice

I. Comparison of blood glucose levels and area of pancreatic islet of Langerhans between naïve and *T. muris* infected HFDIO mice

The mean blood glucose concentration in the HFDIO mice was measured at day 30 and day 37 after a single low dose infection. Overall there was a trend towards increased blood glucose levels in the HFDIO mice in comparison to the naïve normal chow mice.

At day 30, no difference in the mean concentration of blood glucose was observed between naïve and infected HFDIO mice. However, at day 37 there was a reduction in blood glucose in the infected HFDIO mice compared to naïve HFDIO mice (figure 3.23 A). No difference in the mean blood glucose was observed in the 9 week trickle infected HFDIO mice in comparison to the naïve HFDIO mice (figure 3.23 B).

Representative images of pancreas tissue sections from naïve and single low dose infected HFDIO mice are shown in figure 3.24 A and B. The islet area in the HFDIO mice was increased in comparison to the normal chow mice. At day 21 and day 42 there was no difference in the mean area of the islet of Langerhans between naïve and infected HFDIO mice (figure 3.24 C). In addition, no difference was observed in the mean area of the islets of Langerhans in the 7 and 9 week trickle infected HFDIO mice in comparison to their naïve counterparts (figure 3.24 D).

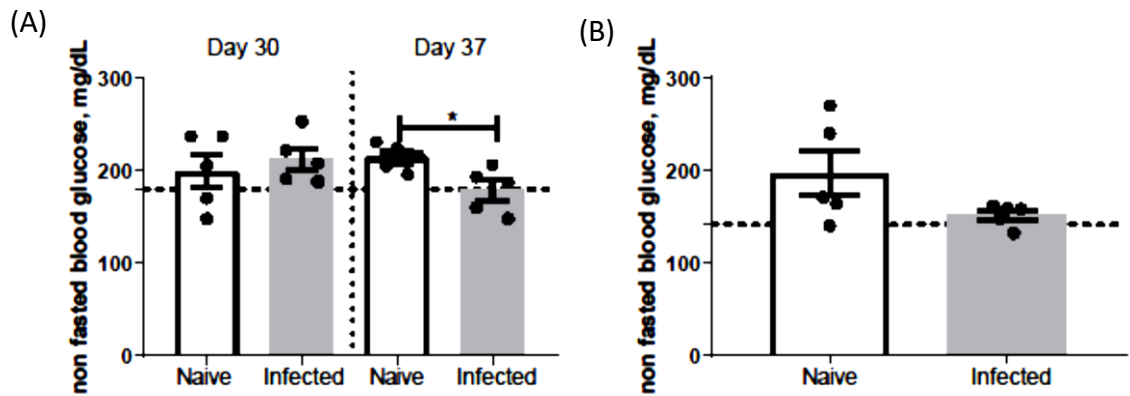


Figure 3-23: Comparison of blood glucose between naïve and *T. muris* infected HFDIO mice.

C57BL/6 mice were fed on a HFD for 12 weeks and then given either a single low dose or trickle *T. muris* infection. A drop of blood was collected from the tail of unfasted mice and blood glucose was measured using an Accu-chek Aviva glucometer. (A) Blood glucose levels in mg/dL measured at day 30 and day 37 post infection after a single low dose infection and in naïve mice. (B) Blood glucose levels in mg/dL measured in week 10 after 9 weeks of trickle infections and in naïve mice. N = 5, results show mean \pm SEM. Horizontal line represents the respective mean value of the naïve normal chow group (mean values of blood glucose taken at 30 post infection (single dose group) and in week 10 (trickle dose group) are shown).

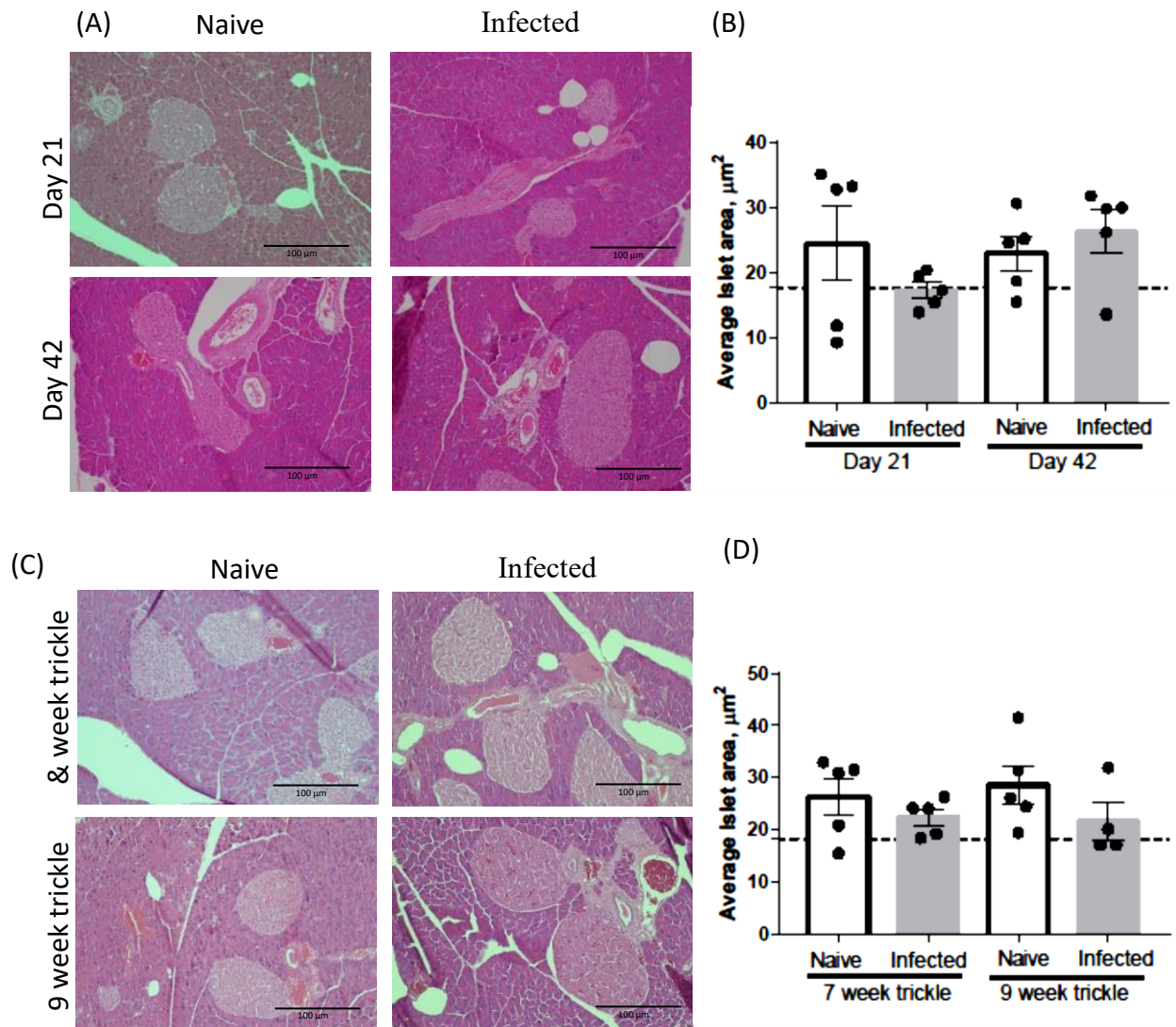


Figure 3-24: Comparison of the islet of Langerhans area between naïve and infected HFDIO mice.

C57BL/6 mice were fed on a HFD for 12 weeks and then given either a single low dose or trickle *T. muris* infection. At the time of sacrifice the pancreas was collected and fixed in NBF before embedding in wax. (A) Representative images of H&E stained sections of the pancreas at day 21 and day 42 post infection in single low dose infected HFDIO mice and naïve mice. (B) Average area of islets at day 21 and day 42 post infection in single low dose infected HFDIO mice and in naïve mice. (C) Representative images of H&E stained sections of the pancreas at after 7 and 9 weeks of trickle infection and naïve mice. (D) Average area of islets in 7 and 9 week trickle HFDIO mice and in naïve mice. x20 magnification, bars, 100 μm N = 5, results show mean \pm SEM. Horizontal line represents the respective mean value of the naïve normal chow group (mean values of islet area at day 21 post infection (single dose group) and 7 week trickle group are shown).

II. Assessment of liver function in *T. muris* infected HFDIO mice

Representative images of liver sections from naïve and infected HFDIO mice (21 days after a single low dose infection) shows that the mice had developed fatty livers and hepatic steatosis (figure 3.25 A). Analysis of liver function makers showed that there was no difference in serum albumin, ALP and total protein between naïve normal chow mice and the HFDIO mice. However the HFDIO mice had elevated levels of serum ALT in comparison to the naïve normal chow mice (figure 3.25 and 3.26).

At day 21 and day 42 post infection, there was no difference in serum albumin, ALP, ALT and total protein between naïve and infected HFDIO mice (figure 3.25 B and C). Similarly, after 7 weeks of trickle infection no difference was observed in serum albumin, ALP, ALT and total protein between naïve and infected mice (figure 3.26)

III. Comparison of PAS/AB stained sections of lung tissue from HFDIO mice

Representative images of PAS/AB stained lung sections from mice with HFDIO are shown in figure 3.27 A and C. There was no difference in the PAS/AB stained sections between naïve normal chow mice and HFDIO mice. There was also no difference in the PAS/AB stained sections of lung tissue collected from naïve and infected HFDIO mice at day 21 and day 42 post infection. No difference in staining was also observed between naïve and trickle dose infected HFDIO mice (figure 3.27 B and D).

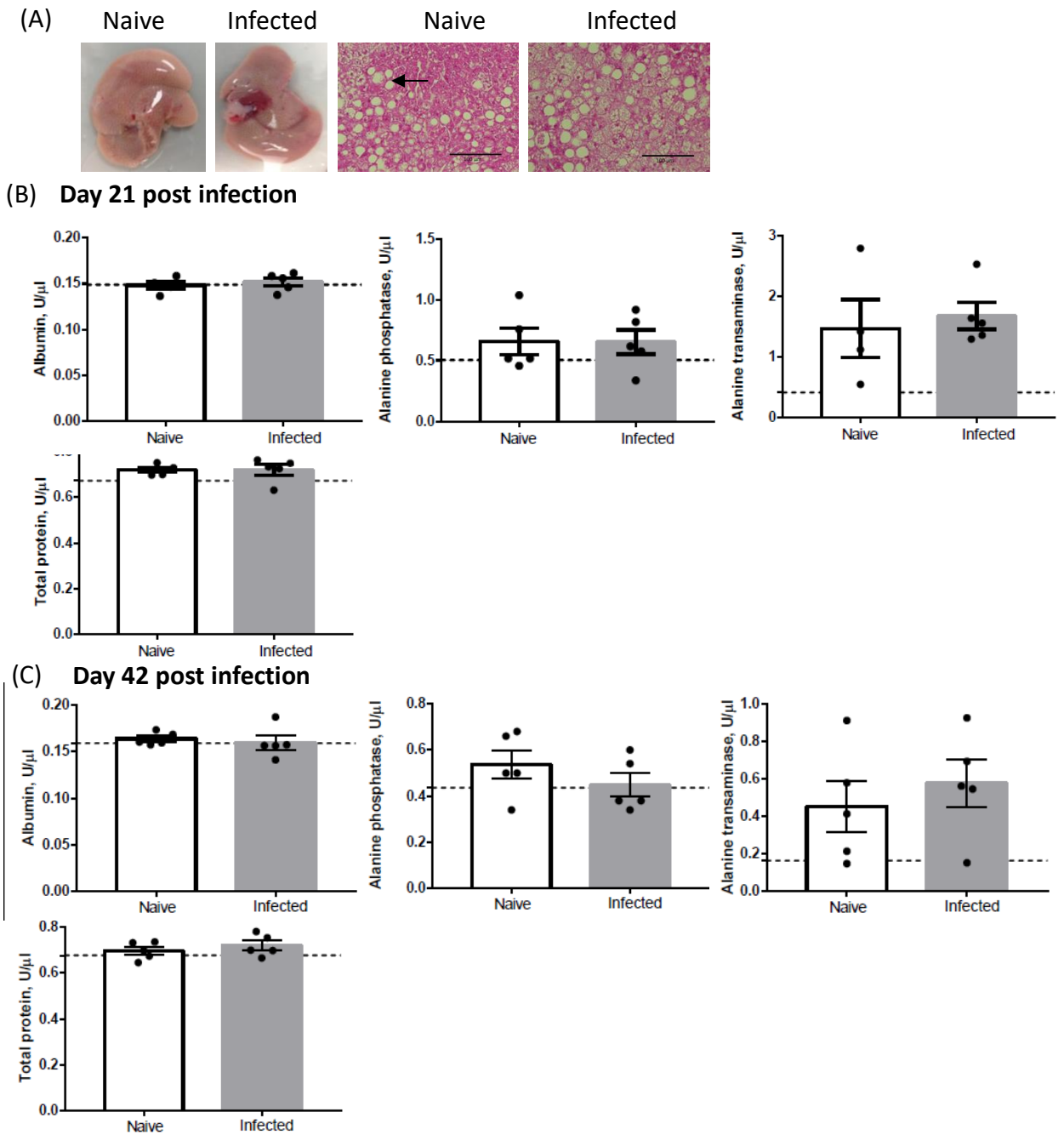


Figure 3-25: Serum liver function tests in single dose infected HFDIO mice.

C57BL/6 mice were fed on a HFD for 12 week and then given a single low dose infection of *T. muris*. Blood was collected from mice at day 21 post infection to collect serum used for the liver function tests. (A) Representative images of fresh liver and H&E stained liver sections from HFDIO mice at 21 days post infection and in naive mice. (B) Results of liver function tests performed on serum collected at day 21 post infection (infected and naive mice). (C) Results of liver function tests performed on serum collected at day 42 post infection (infected and naive mice). x20 magnification, bars = 100 μ m. N = 5, results show mean \pm SEM. Black arrow shows areas of hepatic steatosis. Horizontal line represents the respective mean value of the naive normal chow group.

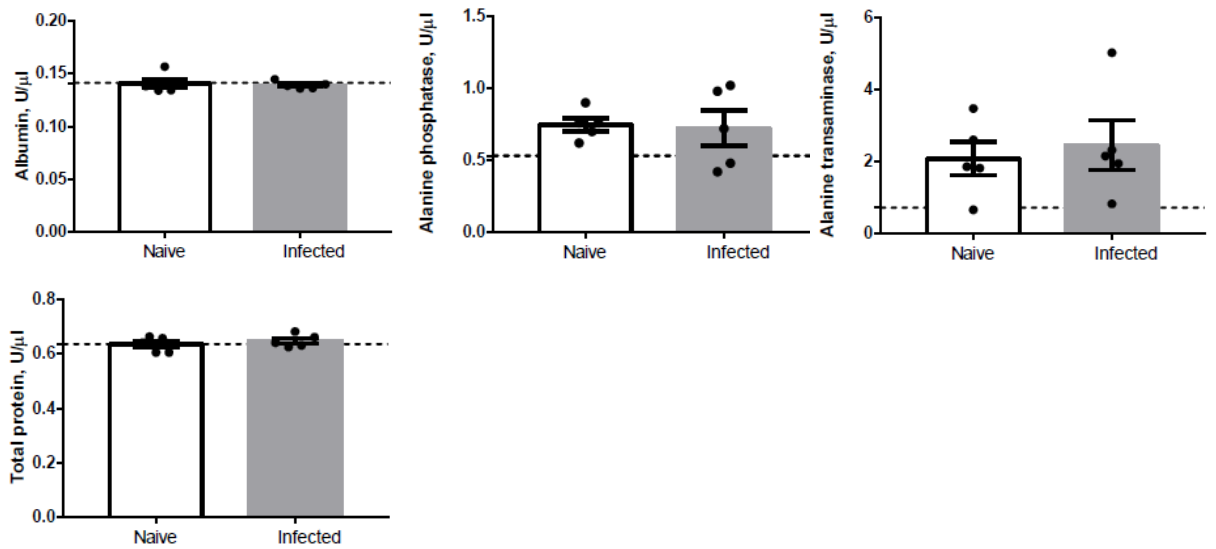


Figure 3-26: Serum liver function tests in naïve and trickle dose infected HFDIO mice.

C57BL/6 mice were fed on a HFD for 12 weeks and then given a trickle low dose infection of *T. muris* for 7 weeks. Blood was collected from mice in week 9 to collect serum used for the liver function tests. Liver function tests compared levels of serum albumin, alanine phosphatase, alanine transaminase and total protein between naïve and infected mice. N = 5, results show mean \pm SEM. Horizontal line represents the respective mean value of the naïve normal chow group.

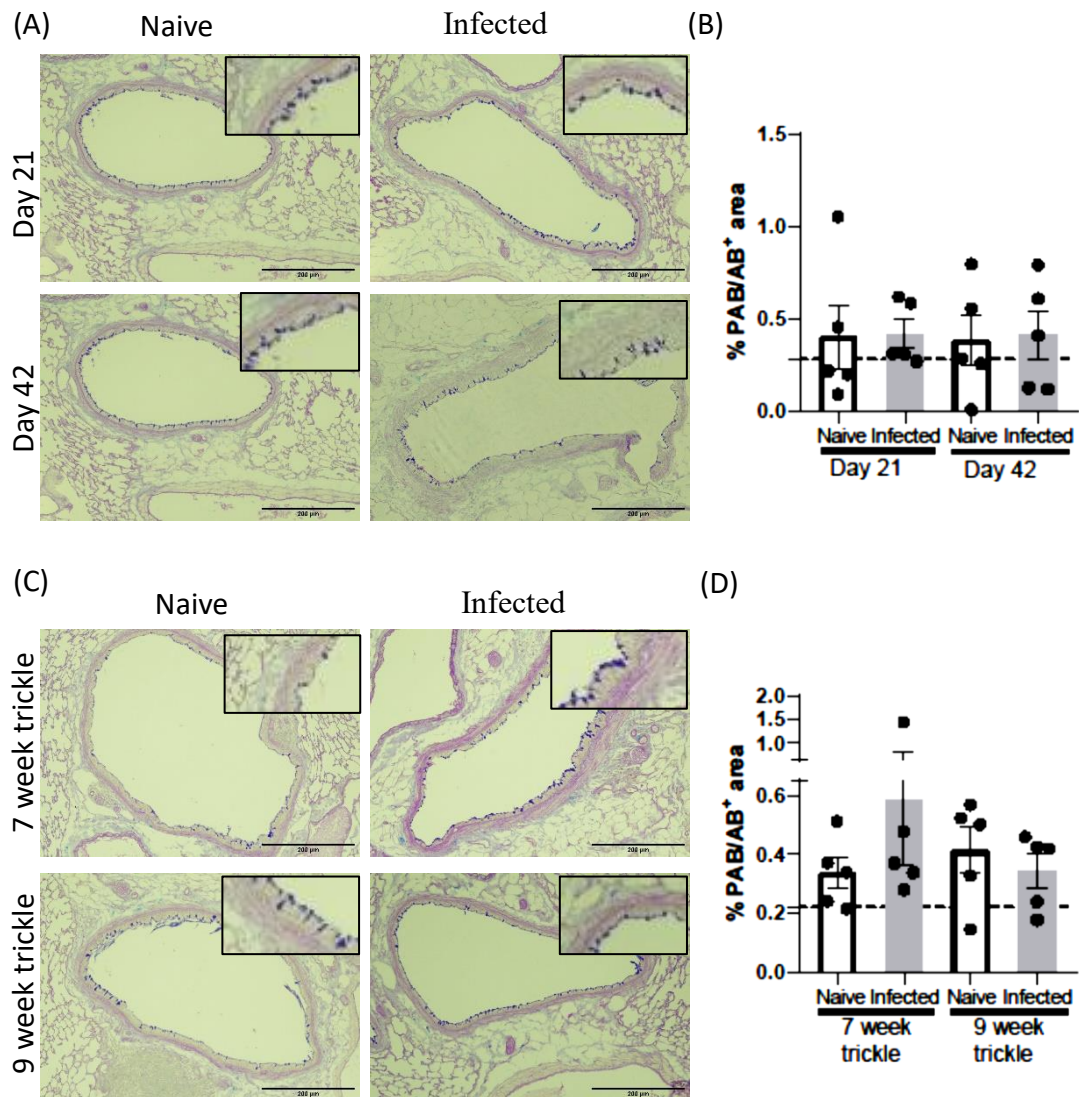


Figure 3-27: Comparison of PAS/AB stained lung sections from naïve and *T. muris* infected HFDIO mice.

C57BL/6 mice were fed on a HFD for 12 weeks and then given either a single low dose or trickle *T. muris* infection. At the time of sacrifice the single left lung lobe was fixed in Carnoy's reagent before embedding in wax. (A) Representative images of PAS/AB stained lung sections at day 21 and day 42 post infection in single dose infected mice (B) Mean percentage of total area per field of view that is PAS/AB+ at day 21 and day 42 post infection (C) Representative images of PAS/AB stained lung sections from 7 and 9 week trickle mice and naïve mice. (D) Mean percentage of total area per field of view that is PAS/AB+ from 7 and 9 week trickle mice. x10 magnification, bars, 200 µm. Insert shows x500 magnification of the lung section. N = 5, results show mean ± SEM. Horizontal line represents the respective mean value of the naïve normal chow group (mean values of PAS/AB+ area at day 21 post infection (single dose group) and 7 week trickle group are shown).

3.3 Discussion

In this chapter, the effect of *T. muris* infection on the physiology of normal mice as well as HFDIO mice was studied. The different parameters measured have provided baseline data on the general effects of low dose *T. muris* infection as well as HFD in C57BL/6 mice.

3.3.1 A low dose of *T. muris* infection did not have an effect on body weight

Body weight changes were monitored in single and trickle dose infected mice. The appearance of the mice was asymptomatic throughout the study period. No weight loss was observed in the single dose infected mice. A trend in reduced weight gain and food intake was observed in the trickle infected mice. However, there was no significant difference in the overall body weight and in the weight of fat pads. Similar to these observations, Kopper and colleagues reported that infection with a high dose of 75 *T. muris* eggs in C57BL/6 mice was asymptomatic, whereas severe disease was only observed in IL-10 deficient mice (Kopper et al., 2015).

The results also showed that a single low dose of *T. muris* in HFDIO mice did not result in overall body weight changes or changes to the size of fat pads in comparison to naïve mice. Previous studies have shown that Infection of HFDIO mice with *N. brasiliensis*, *H. polygyrus* and *S. mansoni* resulted in significant reduction in body weight (Hussaarts et al., 2015; Su et al., 2018; Yang et al., 2013). However, in these studies, the mice were shown to develop strong Th2 immune responses. Th2 immune responses are associated with increased infiltration of eosinophils and M2 macrophages in white adipose tissue which increase the rate of metabolism by up-regulating UCP1 (Hussaarts et al., 2015; Su et al., 2018). A low dose *T. muris* infection does not induce a strong Th2 immune response and no significant changes in macrophages as well as eosinophils were observed in the mesenteric fat. However, in the HFDIO mice, there was a significant increase in the percentage of eosinophils in the *T. muris* infected mice although no differences in the macrophage population were observed. Further work can be carried out to investigate changes in the ratio of M2/M1 in the mesenteric fat in the HFDIO *T. muris* mice. This

would provide more insight into the inflammatory and metabolic state of the mesenteric fat.

3.3.2 Serum *leptin* levels were increased in infected HFDIO mice but not in normal mice after single and trickle low dose of *T. muris* infection

Previous work has shown that mice that are resistant to the nematode *Trichinella spiralis* have reduced levels of leptin. Additionally, the *Trichinella*-infected mice also lost weight and underwent phases of reduced food intake (hypophagia) (Worthington et al., 2013b). Furthermore, intraperitoneal administration of recombinant leptin to restore leptin levels in these mice resulted in delayed worm expulsion (Worthington et al., 2013b). No difference was observed in serum leptin levels or adipocyte area between naïve and *T. muris* infected normal mice. In the work carried out by Worthington and colleagues, *T. spiralis* infection was used as the infection model and the mice were resistant to the infection. The mice were able to mount a Th2 immune response resulting in worm expulsion and this correlated with reduced level of serum leptin. In the current study there was no clear difference in serum leptin between naïve and infected normal chow fed mice. The difference in observations between the current study and the study conducted by Worthington and colleagues could be due to that differences in the infection model used. In the current study the mice were given a low dose of *T. muris* infection which typically results in a Th1 immune response and chronic infection (Bancroft et al., 2001). Therefore, as the mice do not establish a Th2 immune response they fail to clear the *T. muris* parasite and this could provide an explanation for the observation that the serum leptin levels remained unchanged in the infected mice.

In contrast when serum levels between naïve and infected HFDIO were compared, an increase in serum leptin was observed in the *T. muris* infected HFDIO mice. In contrast, *H. polygyrus* infection was shown to down-regulate the expression of leptin in gonadal fat from HFDIO mice. However, no changes in food intake were observed between naïve and *H. polygyrus* infected HFDIO mice (Su et al., 2018). Similarly, no changes in food intake were found in the *T. muris* infected HFDIO mice in spite of the increased leptin levels.

Therefore, leptin responses in obese mice maybe more complex maybe partly be due to the increased leptin insensitivity observed in obesity (Koch et al., 2013).

3.3.3 A low dose of *T. muris* infection did not have a significant effect on blood glucose levels or pancreas pathology

HFDIO mice had elevated levels of blood glucose ranging between 150 to 250 mg/dL, whereas the majority of the normal chow mice had blood glucose reading ranging between 100 to 200 mg/dL. Hyperglycaemia in HFD fed male C57BL/6 mice has been shown to be associated with a corresponding increase in the size of the islets of Langerhans in order to increase the β -cell mass (Pettersson et al., 2012). Helminth driven Th2 immune responses have been shown to reduce levels of blood glucose in HFDIO mice and improve insulin sensitivity (Hussaarts et al., 2015). The present results showed no difference in blood glucose or islet area between naïve and infected in HFDIO mice. This suggests that low dose *T. muris* infection which drives pro-inflammatory immune responses does not improve glucose homeostasis in HFDIO mice. Similarly, no significant changes in blood glucose and islet area were observed between naïve and infected normal mice. However chronic inflammation has been associated with increased insulin insensitivity and destruction of pancreatic β -cells (Suk et al., 2001; Wu et al., 2013). Therefore, more work needs to be carried out to determine if persistent chronic *T. muris* infection may also result in dysregulated glucose metabolism.

As previously stated, the average blood glucose levels of the HFD mice were higher than that of the normal chow which would signify elevated blood glucose associated with obesity. However, within groups there was a degree of variability in the glucose readings of the mice. In this study the blood glucose was measured from unfasted mice. One main disadvantage is the high variability in the blood glucose measurement. This could have been caused by differences in the time that each mouse last consumed food before the measurements were taken. An alternate approach would be to measure the blood glucose after a period of overnight fasting which would reduce the variability. However, mice consume most of their calories at night and it has been suggested overnight feeding in mice may induce a state that resembles starvation (Andrikopoulos et al., 2008). Shorter day time fasting of approximately 6 hours has been suggested to present a better fasting

strategy and this can be coupled with tests such as glucose tolerance test (GTT) or insulin tolerance test (ITT) (Andrikopoulos et al., 2008). In both cases the blood glucose is recorded before the administration of a fixed amount of either glucose or insulin. The blood glucose is then measured periodically over a chosen period and the changes in blood glucose provide a good indication of how the mice are able to regulate the blood glucose.

3.3.4 A low dose of *T. muris* did not result in liver pathology or improve symptoms of fatty liver disease

Helminths such as *S. mansoni* have also been associated with liver injury (Jacobs et al., 1999). Mice infected with *S. japonicum* develop granulomas in the liver around trapped eggs. The formation of granulomas results in liver injury and obstruction of circulatory vessels which would affect liver function (Chen et al., 2014). A range of tests were carried out on the serum collected from naïve and infected mice in order to assess if *T. muris* infection would also have any effect on liver function. Alanine transaminase (ALT) is a marker of hepatocyte damage, whereas alanine phosphatase is a marker of bile duct obstruction. Chronic liver disease is also associated with reduced albumin which plays an important role as a carrier for various substances in the blood (Gowda et al., 2009). Both single and trickle low dose infection did not cause significant changes in any of the parameters tested in the normal mice suggesting that chronic *T. muris* infection did not have an effect on liver function. One reason for this could be that unlike bloodstream dwelling schistosomes where highly metabolic eggs are trapped in the liver during infection, *T. muris* eggs are secreted into the intestinal lumen and excreted out of the host, with no trapping in the liver.

Elevated levels of ALT were observed in the HFDIO mice ranging between 1.5 to 2 U/ μ l in comparison to the normal mice which had ALT levels ranging between 0.2 to 0.8 U/ μ l. Elevated ALT and hepatic steatosis are associated with early stages of non-alcoholic fatty liver disease (NAFLD) with HFD induced fibrosis and inflammation only becoming apparent after long-term feeding (Asgharpour et al., 2016). *T. muris* infected HFDIO mice had fatty liver with hepatic steatosis and no reduction in serum ALT even after trickle infections. In contrast, *N. brasiliensis* infection in obese mice which induced a strong Th2

immune response was shown to improve the symptoms of hepatic steatosis (Yang et al., 2013). However, a recent study by Hart and colleagues has shown that Th1 responses are protective against NAFLD while Th2 immune responses enhance the symptoms NAFLD. They showed that obese IL-10 KO mice were protected against non-alcoholic steatohepatitis which was associated with increased levels of hepatic IFN- γ (Hart et al., 2017). Furthermore, IFN- γ deficient obese mice had exacerbated liver disease with increased steatosis and serum ALT. The mice also displayed early signs of fibrosis at 15 weeks which was not observed in the wild type mice (Hart et al., 2017). Therefore, it is possible that persistent chronic *T. muris* infection would improve the symptoms of NAFLD.

3.3.5 A low dose of *T. muris* infection did not increase lung PAS/AB staining in normal and HFDIO mice

N. brasiliensis has a migratory stage through the host's lung where it causes damage to the lung tissue as well as inducing protective CD4⁺ T-cell responses (Harvie et al., 2010; Marsland et al., 2008). Single and trickle low dose *T. muris* infection did not result in significant changes to the PAS/AB staining in both normal and HFDIO mice suggesting no increase in mucus production. Similar to the current observations a study carried out by Chenery and co-workers reported that even though chronic *T. muris* infection resulted in increased production of IFN- γ and IL-10 in the lung, no airway pathology was observed (Chenery et al., 2016). In addition a HFD has been associated with increased hyper-responsiveness in the lung airways however no changes in goblet cells were observed in HFD fed mice (Singh et al., 2015). Therefore, even though both *T. muris* and HFD affect the lung microenvironment they do not result in severe pathology.

3.4 Conclusion

The results in this chapter indicate that:

- I. Single and trickle low dose *T. muris* infections did not result in significant reduction in body weight in normal and HFDIO mice

- II. Single and trickle low dose *T. muris* infections did not alter serum leptin levels in normal mice but were increased in HFDIO mice
- III. Single and trickle low dose *T. muris* infections did not induce pathology in the liver, lung nor pancreas of normal mice
- IV. Single and trickle low dose *T. muris* infections did not reverse the symptoms of HFD induced pathology in the liver and pancreas of HFDIO mice

The worm burden and immune response of the mice described in this chapter are discussed in chapter 4. Overall there was a tendency for the mice fed on a HFD to expel worms much earlier than the mice fed on the normal chow diet. However, the ability of HFD fed mice to expel worms at an earlier stage might have influenced the outcome of the observed and it is possible that more significant changes in the pathology of obesity might have been observed if the HFD fed obese mice had developed chronic infections.

Chapter 4 : Results II

Does HFD alter the outcome of chronic *T. muris* infection in mice?

4.1 Introduction

In the preceding chapter it was shown that mice given low dose *T. muris* infection mice remained asymptomatic. Furthermore, it was shown that low dose *T. muris* infection was not able to reverse the pathology associated with obesity. An alternative hypothesis was that HFD altered the susceptibility to chronic *T. muris* infection.

Chronic *T. muris* infections develop in susceptible strains of mouse, such as AKR which fail to expel high dose infections (Else et al., 1992). In addition, susceptibility can be induced in normally resistant BALB/K or C57BL/6 mice by administering a low dose of approximately 20 to 40 eggs resulting in mice developing chronic infections (Bancroft et al., 1994a).

Resistance is associated with the development of a Th2 immune response characterised by increased production of IL-4, IL-13 and IL-9. These cytokines are involved in the development of resistance mechanisms such as increased epithelial turnover, increased mucus production and contraction of the intestinal wall which ultimately result in worm expulsion (Cliffe et al., 2005; Faulkner et al., 1998; Hasnain et al., 2011b). However, susceptible mice develop a Th1 immune response characterised by increased production of pro-inflammatory cytokines IFN- γ , IL-6 and IL-17A (Artis et al., 1999b; Bancroft et al., 1994a; Else et al., 1992). The mice fail to expel worms thereby developing chronic infections. The worm expulsion kinetics have been shown to correlate very well with worm specific serum antibody responses. Resistance is associated with elevated levels of worm specific IgG1. On the other hand, susceptibility is associated with elevated levels of worm specific IgG2a and reduced levels of IgG1 (Blackwell and Else, 2002).

The use of single dose infections has been very useful in gaining insight into the immunity in resistant and susceptible mice. However, in nature the infection pattern is more variable, and most individuals face high risk of repeated infections. Therefore, trickle infections were designed to model naturally occurring infections. Trickle infection in C57BL/6 mice results in a build-up in worm burden to a threshold at which the mice start to generate resistance and expel worms (Bancroft et al., 2001; Glover, 2017). Work using *H. polygyrus* and *N. brasiliensis* also showed that resistance could be induced during trickle infections (Brailsford and Behnke, 1992; Jenkins and Phillipson, 1971). However,

additional factors such as nutrition and host physiology may also affect the outcome of helminth infection (Bundy, 1988). In recent years, the rise in global obesity has led to increased attention to the importance of proper nutrition. Furthermore, people in developing countries who are already at high risk of STH are also now facing the challenges of lifestyle associated diseases including obesity due to consumption of sugary and fatty food (Popkin, 2012).

To gain a greater insight into what effect HFD consumption may have on chronic *T. muris* infection, the outcome of single or trickle *T. muris* infection in C57BL/6 mice that had been fed on either HFD before or after infection was observed.

The main objectives presented in this chapter are:

- I. To investigate the effect of HFDIO on the outcome of a single low dose of *T. muris* infection.
- II. To investigate the effect of short term HFD feeding on the outcome of a single low dose of *T. muris* infection.
- III. To investigate the effect of HFDIO on the outcome of trickle low dose of *T. muris* infection.
- IV. To investigate the effect of HFD feeding on the outcome of pre-infected *T. muris* mice.

4.2 Results

The results presented in this chapter were collected from mice in groups A, B, C and D which have introduced in chapter 3 as well additional groups E, F, G and H which are described in table 2.2.

4.2.1 How does HFDIO affect the outcome of a single low dose of *T. muris* infection?

To investigate how HFDIO affects the outcome of a chronic *T. muris* infection, C57BL/6 were pre-fed either a normal diet or HFD for 12 weeks before administering a single low dose infection of approximately 20 embryonated *T. muris* eggs. The mice were observed for either 21 or 42 days before sacrifice. In the preceding chapter, it was already shown that at the end of the experimental period the final weight of the mice fed on a HFD was more than the final weight of the mice fed on a normal chow diet (figure 3.15 C, D and F).

I. Worm burden of single dose *T. muris* infected mice

To assess worm burden at day 21 post infection, L4 larvae present in the caecum-proximal colon of infected mice were counted. Interestingly, the average number of larvae recovered from HFDIO mice was less than half of the mean number of larvae recovered from normal chow fed mice (figure 4.1 A). Comparison of the two groups by Mann-Whitney analysis indicated that the difference in the worm burden was not significant.

At day 42 post infection, adult worms were recovered from the guts of chow fed mice as would be expected in a chronic infection but strikingly there was a significant reduction in the number of worms recovered from HFDIO mice with a significance value $p < 0.001$ and worms completely absent in 8/11 animals (figure 4.1 B).

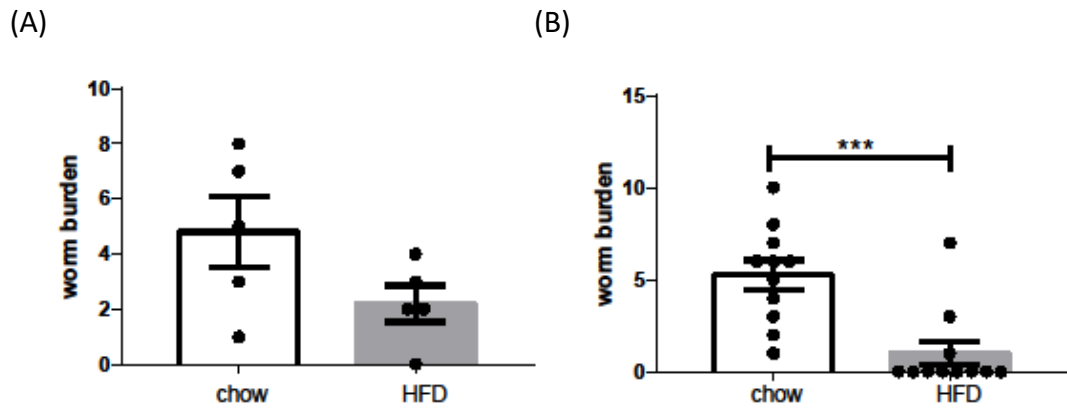


Figure 4-1: Worm burden of single low dose mice pre-fed for 12 weeks.

Mice were fed on either normal chow or HFD for 12 weeks and then they were given a single low dose (20 eggs) *T. muris* infection via oral gavage. Mice were sacrificed 21- or 42-days post infection. Worms were counted from the caecum and proximal colon collected from infected mice. (A) Worm count at day 21 post infection. (B) Worm count at day 42 post infection (representative of 2 independent experiments). N = 5 to 11, results show mean \pm SEM.

II. Serum antibody responses of single dose *T. muris* infected mice

It was then determined if the serum *T. muris* specific IgG1 and IgG2a/c profile would correlate with the observed worm expulsion kinetics. The *T. muris* specific antibody responses between the normal chow fed mice and the HFDIO mice were compared by antibody ELISA. As a control, the serum collected from naïve mice fed on each respective diet was analysed, these naïve mice had negligible amounts of *T. muris* specific IgG1 and IgG2a/c (figure 4.2 A and B).

At 21 days post infection, there was a similar increase in IgG1 in both normal chow and HFDIO mice. By day 42 post infection, the difference in the antibody responses is more pronounced between the groups. There were higher levels of parasite specific IgG1 in the HFDIO mice in comparison to the normal chow fed mice (figure 4.2 A).

There was no increase in parasite specific IgG2a/c in the infected mice at day 21 post infection. At day 42 post infection there were higher levels of parasite specific IgG2a/c in the normal chow mice as compared to the HFDIO mice, with the HFDIO mice having a weaker parasite specific IgG2a/c response (figure 4.2 B).

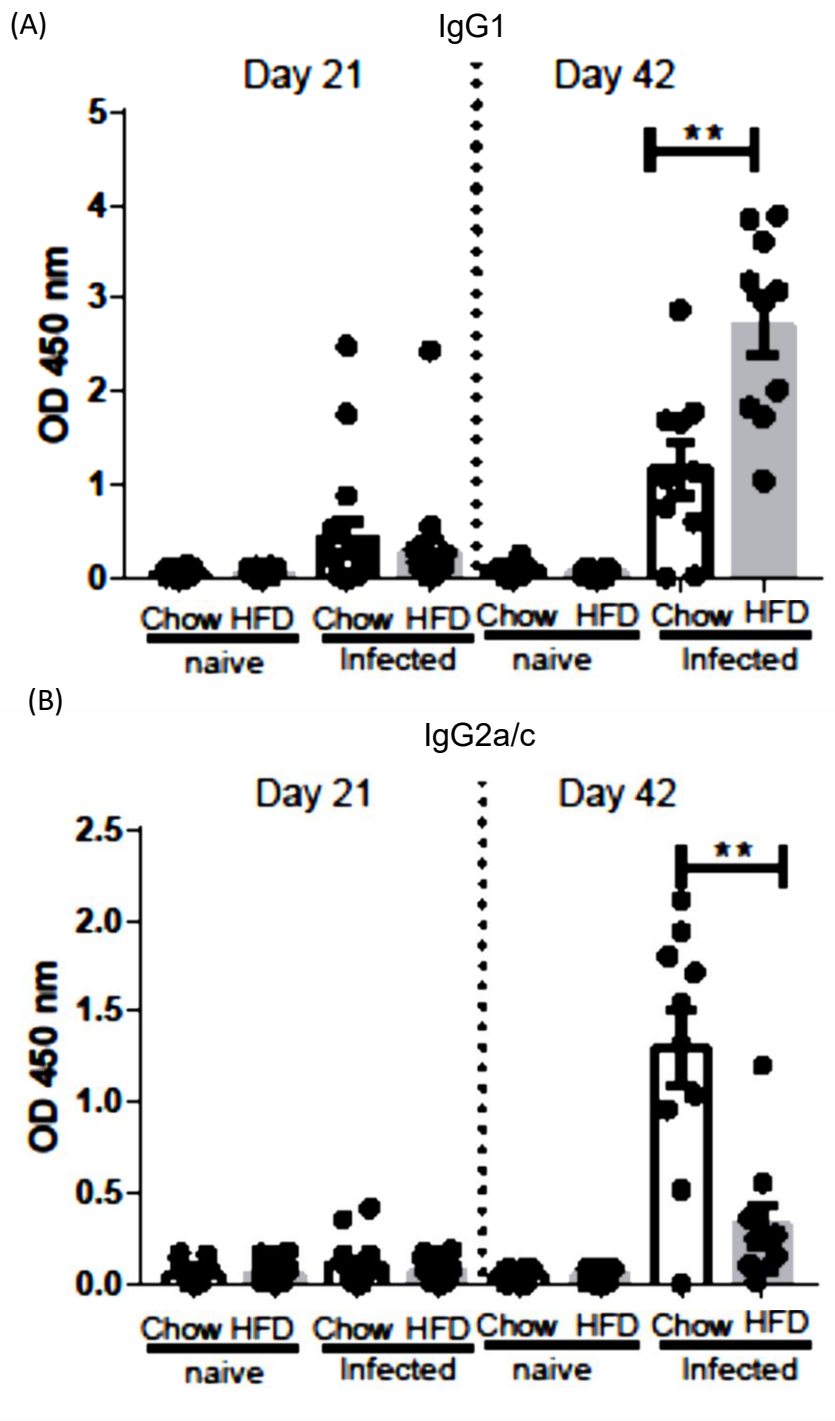


Figure 4-2: Parasite specific IgG1 and IgG2a/c antibody ELISA of single dose infected mice after 12 weeks of feeding.

Mice were fed on either normal chow or HFD for 12 weeks and they were given a single low dose *T. muris* infection. Mice were sacrificed 21- or 42-days post infection. Parasite specific antibodies were analysed by ELISA using serum from blood collected from mice. Absorbance readings at a serum dilution of 1 in 40 are shown. (A) Parasite specific IgG1 response at day 21 and day 42 post infection (B) Parasite specific IgG2a/c response at day 21 and day 42 post infection. N = 10, results show mean \pm SEM. Representative of 2 independent experiments.

III. Cytokine responses of re-stimulated immune cells collected from single dose *T. muris* infected mice

In order to compare the cytokine response, cells were collected from the mesenteric lymph nodes and re-stimulated the cells for 48 hours using *T. muris* derived E/S. Cytokine production was assessed by collecting the supernatant and analysing by CBA. The production of Th2 associated cytokines was compared between the normal chow and HFDIO mice at day 21 post infection, which is the around the peak time of the cytokine response (Else and Grecis, 1991). There was a significant increase in the levels of IL-5, IL-9 and IL-13 (figure 4.3 A, B and C) in HFDIO mice. There was a similar increase in IL-10 in both infected groups. We also compared pro-inflammatory cytokines. The normal chow mice had higher levels of IFN- γ , and IL-6 compared to the HFDIO mice (figure 4.3 E and F). In addition, there was a trend towards increased levels of IL-17A in normal chow mice compared to the HFDIO mice (figure 4.3 G). TNF- α was also significantly higher in the normal chow fed mice in comparison to the HFDIO mice with $p < 0.01$ (figure 4.3 H).

4.2.2 How does short-term HFD feeding affect the outcome of a single low dose of *T. muris* infection?

Given this exciting demonstration that HFD allows expulsion of a chronic infection, it was then investigated if the altered response to *T. muris* could be observed after only a short period of HFD feeding before the mice develop HFDIO. Therefore, mice were pre-fed on either normal chow or HFD for only 3 weeks before administering a single low dose of *T. muris*. The mice were observed for 21 or 42 days post infection before sacrifice.

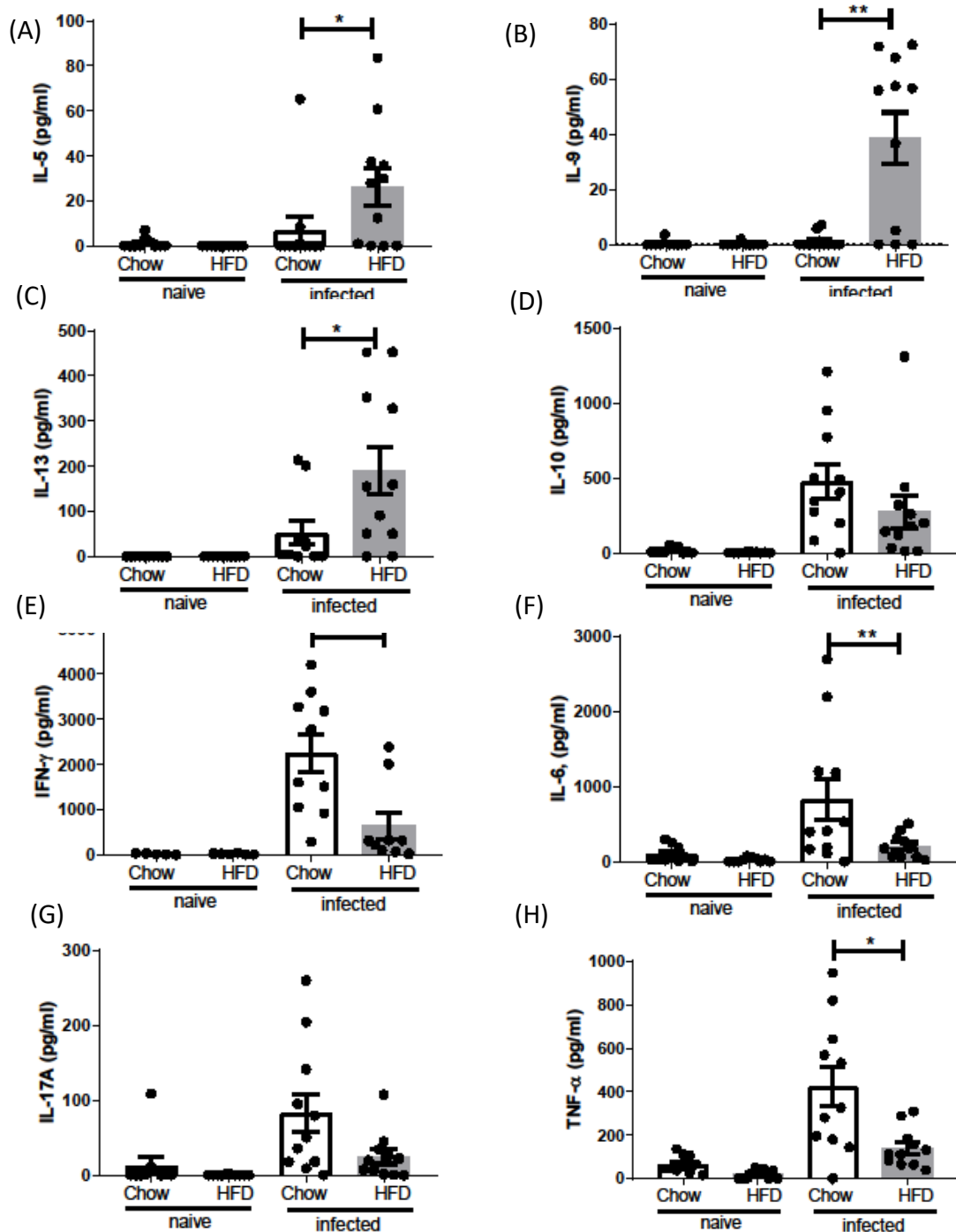


Figure 4-3: Re-stimulation of mesenteric lymph node derived cells from single low dose infected mice after 12 weeks of pre-feeding.

Mice were fed on either normal chow or HFD for 12 weeks and they were given a single low dose *T. muris* infection. Mice were sacrificed 21 post infection. Immune cells were extracted from mesenteric lymph nodes and re-stimulated for 48 hours using *T. muris* derived E/S after which the supernatant was collected and analysed for cytokines using the cytometric bead array. (A) IL-5 (B) IL-9 (C) IL-13 (D) IL-10 (E) IFN- γ (F) IL-6 (G) IL-17A. (H) TNF- α . N = 6 to 11, Results show mean \pm SEM. Representative of 2 independent experiments.

I. Worm burden of single dose *T. muris* infected 3-week pre-fed mice

There was no significant difference in the average weight gain between naïve and infected mice fed on the same diet (figure 4.4 A and B). At day 21 fewer worms were recovered from the HFD mice but there was no significant difference in the mean number of worms recovered between the HFD mice and the normal chow mice (figure 4.4 C). By day 42 post infection, the HFD fed had all expelled the worms, whereas adult worms were recovered from some of the normal chow fed mice (figure 4.4 D).

II. Serum antibody responses of single dose *T. muris* infected mice after 3 weeks of HFD feeding

The serum *T. muris* specific IgG1 and IgG2a/c were also compared. Similar to the 12-week pre-fed mice, there was a higher level of parasite specific IgG1 in HFD fed mice at day 21 HFD fed infected mice whereas the parasite specific IgG2a/c was relatively the same in both groups after infection. At day 42 after infection, there was a significantly higher level of parasite specific IgG1 in the HFD fed mice (figure 4.5 A). Furthermore, it was observed that the normal chow fed mice had significantly higher levels of parasite specific IgG2a/c, as compared to the HFDIO mice (figure 4.5 B).

III. Cytokine responses of re-stimulated immune cells collected from single dose *T. muris* infected mice after 3 weeks of HFD feeding

The levels of Th2 associated cytokines IL-5, IL-9 and IL-13 were increased upon infection in both groups of mice, but there was a high variability within each group (figure 4.6 A, B and C). IL-10 production was also increased in both normal chow and HFD mice with no difference between the groups (figure 4.6 D). High levels of the IFN- γ were observed in both normal chow and HFD mice (4.6 E). There was a trend in relatively lower levels of IL-6, IL-17A and TNF- α in the HFD fed mice compared to the normal chow mice, although the differences were not significant (figure 4.6 C, G and H).

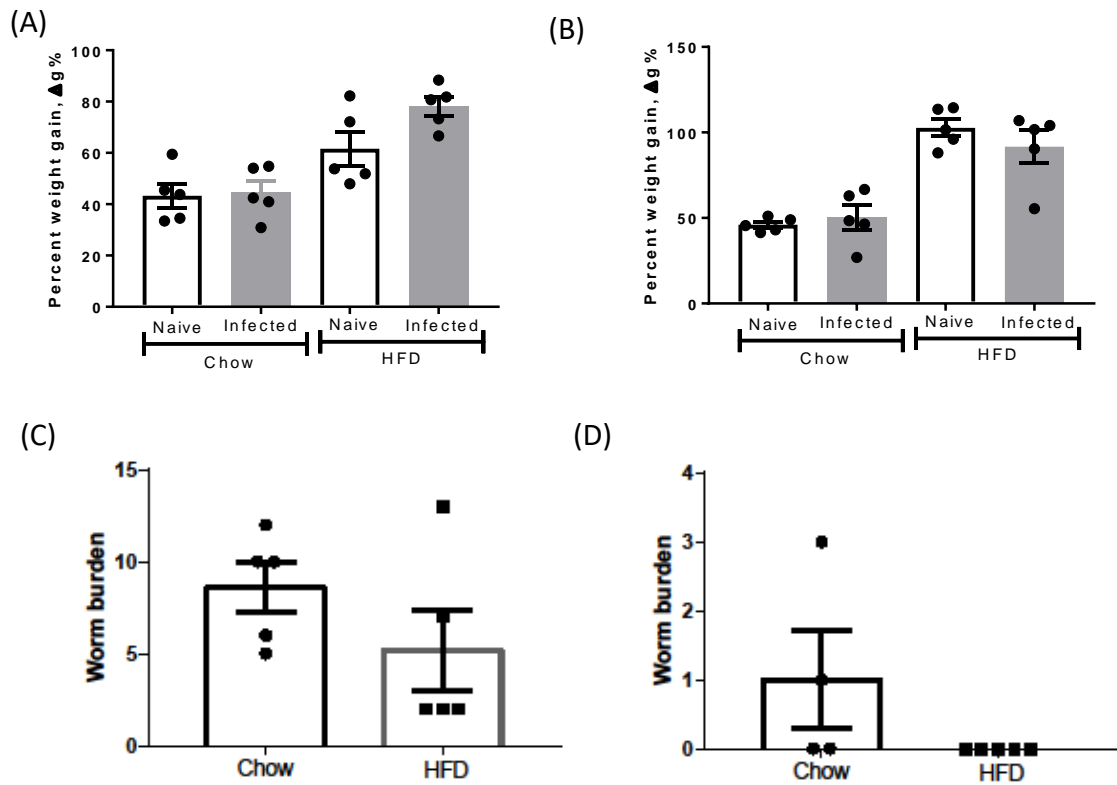


Figure 4-4: Worm burden of single low dose mice pre-fed for 3 weeks.

Mice were fed on either normal chow or HFD for 3 weeks and then they were given a single low dose (20 eggs) *T. muris* infection. Mice were sacrificed 21- or 42-days post infection. Worms were counted from the caecum and proximal colon collected from infected mice. (A) Percentage increase in body weight at day 21 post infection. (B) Percentage increase in body weight at day 42 post infection (C) Worm count at day 21 post infection. (D) Worm count at day 42 post infection. N = 5, results show mean \pm SEM.

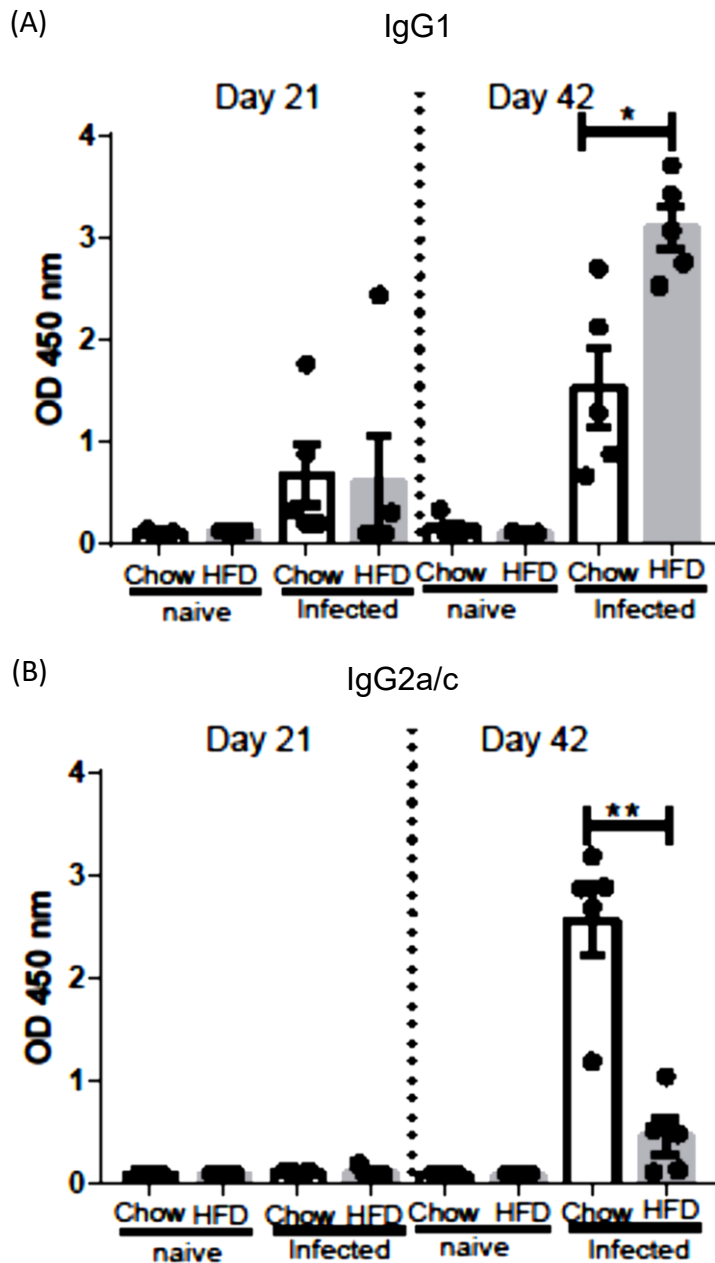


Figure 4-5: IgG1 and IgG2a/c antibody ELISA of single dose infected mice after 3 weeks of pre-feeding.

Mice were fed on either normal chow or HFD 3 for weeks and they were given a single low dose *T. muris* infection. Mice were sacrificed 21- or 42-days post infection. Parasite specific antibodies were analysed by ELISA using serum from blood collected from mice. Absorbance readings at a serum dilution of 1 in 40 are shown. (A) Parasite specific IgG1 response at day 21 and day 42 post infection (B) Parasite specific IgG2a/c response at day 21 and day 42 post infection. N = 5, results show mean \pm SEM.

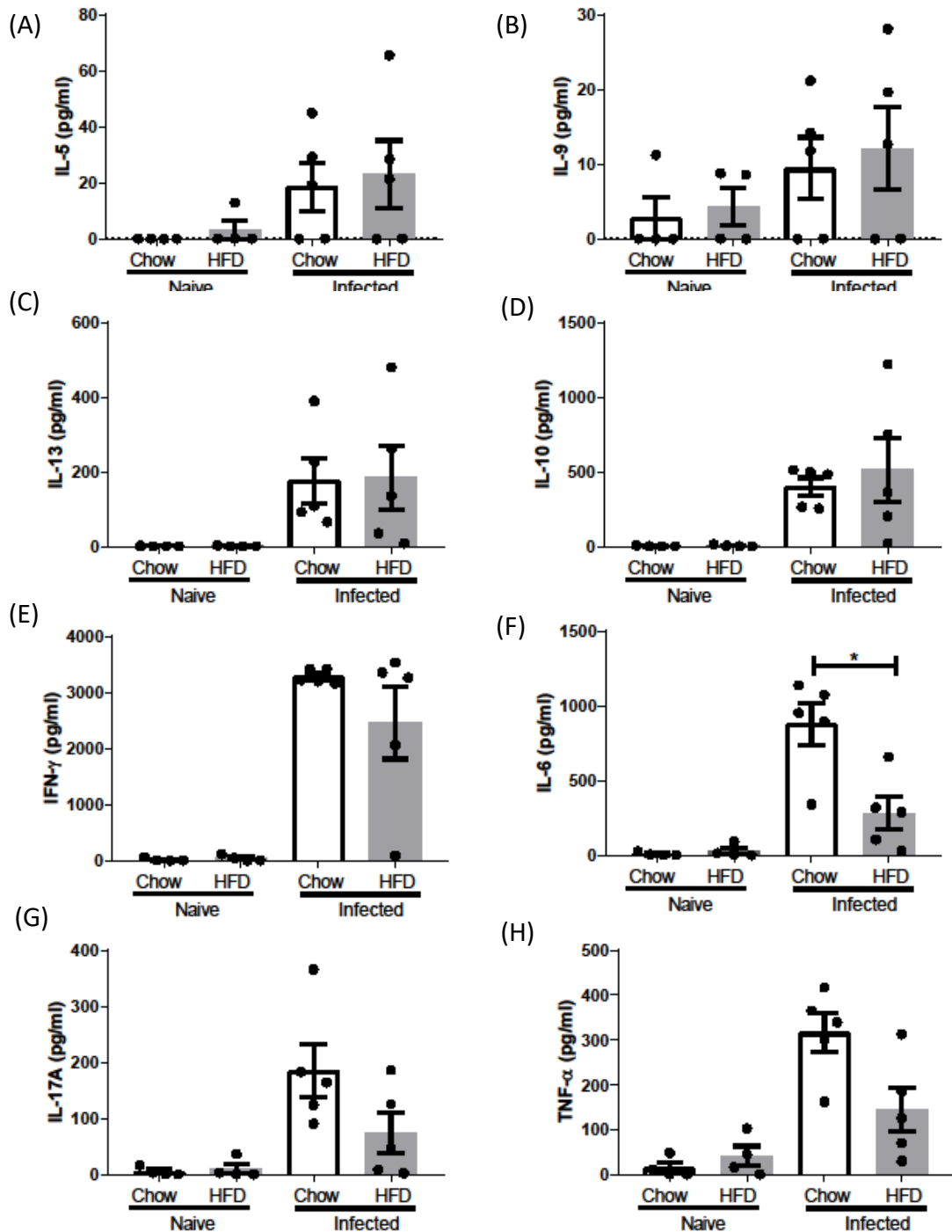


Figure 4-6: Re-stimulation of mesenteric lymph node derived cells from single low dose infected mice after 3 weeks of pre-feeding.

Mice were fed on either normal chow or HFD for 12 weeks and they were given a single low dose *T. muris* infection. Mice were sacrificed 21 post infection. Immune cells were extracted from mesenteric lymph nodes collected and re-stimulated for 48 hours using *T. muris* derived E/S after which the supernatant was collected and analysed for cytokines using the cytometric bead array. (A) IL-5 (B) IL-9 (C) IL-13 (D) IL-10 (E) IFN- γ (F) IL-6 (G) IL-17A (H) TNF- α . N = 5. Results show mean \pm SEM.

4.2.3 How does HFDIO affect the outcome of a low dose trickle infection with *T. muris*?

Trickle infections were used to investigate how HFDIO would influence the outcome of repeated *T. muris* infection which is more representative of natural infections. Mice were pre-fed either on a HFD or normal chow for 12 weeks before giving the mice low dose infections with approximately 20 *T. muris* eggs once every week for 7 or 9 weeks. The mice were sacrificed two weeks after the last dose of infection.

I. Worm burden of trickle dose *T. muris* infected mice after 12 weeks of HFD feeding

The presence of *T. muris* eggs was checked in faecal pellets collected at week 8, 9 and 11 weeks of infection. Whereas faecal pellets from the normal chow mice had *T. muris* eggs at week 8 and 9, few eggs were found in the faecal pellets collected from the HFDIO mice at these time points. By week 11, no eggs were detected in either group of mice (figure 4.7 A). During a trickle infection mice are expected to initially develop chronic infections with resistance developing after 7 trickle infections ((Glover, 2017). The worm burdens were assessed two weeks after 7 or 9 weeks of trickle infection. After 7 weeks of trickle infection, worms were recovered from the normal chow fed mice. No worms were recovered from the HFDIO mice (figure 4.7 B). After 11 weeks of trickle infection, some mice on normal chow had completely expelled worms and again the HFDIO mice had expelled all the worms (figure 4.7 C).

II. Serum antibody responses of trickle dose *T. muris* infected mice after 12 weeks of HFD feeding

Serum antibody responses against *T. muris* were compared between the different groups. Strong antibody responses were observed in both infected groups in comparison to the naïve mice as shown in figure 4.8.

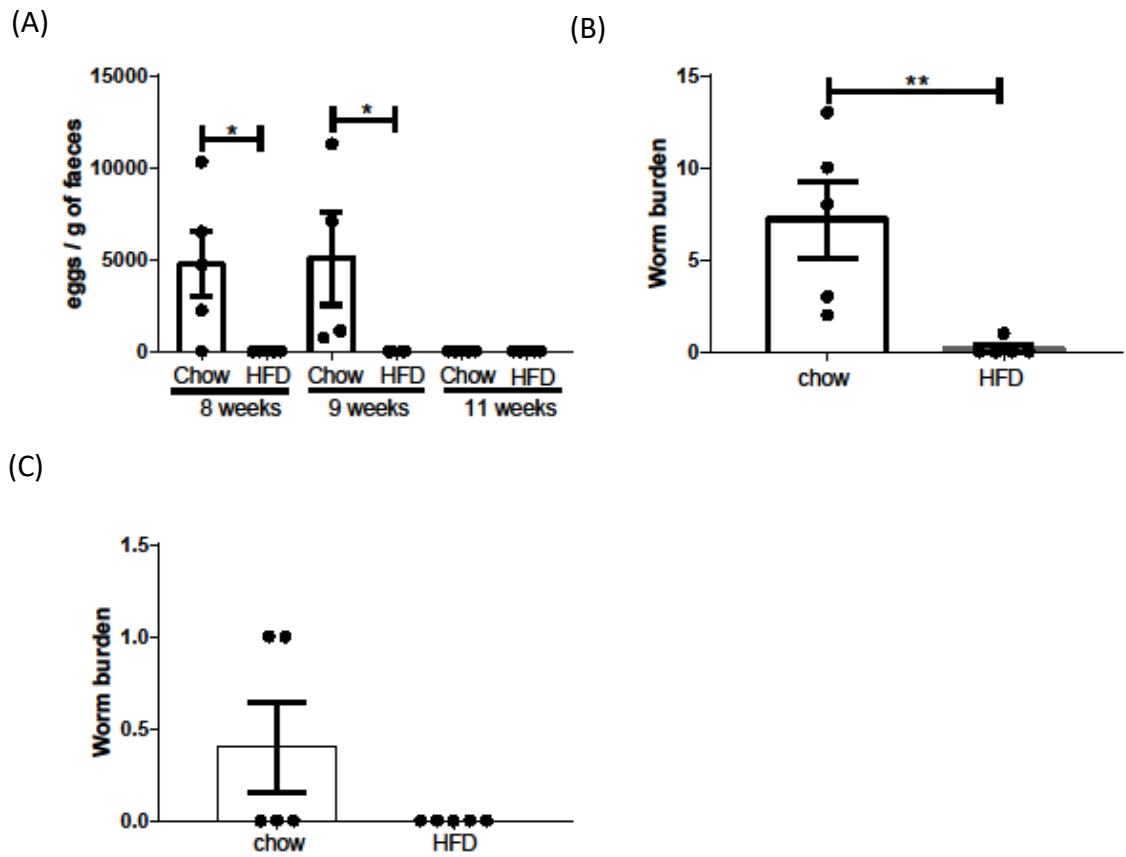


Figure 4-7: Worm burden and faecal egg count of mice given a trickle low dose of *T. muris* after 12 weeks of feeding.

Mice were fed on either normal chow or HFD for 12 weeks and then they were given trickle low dose *T. muris* infection for 7 or 9 weeks. Mice were observed for 2 weeks after the last infection before they were sacrificed. Worms were counted from the caecum and proximal colon collected from infected mice. (A) Faecal egg counts at week 8, 9 and 11 in the 9 week trickle group (B) Worm count after 7 week trickle infections (C) Worm count after 9 week trickle infections. N = 5, results show mean \pm SEM.

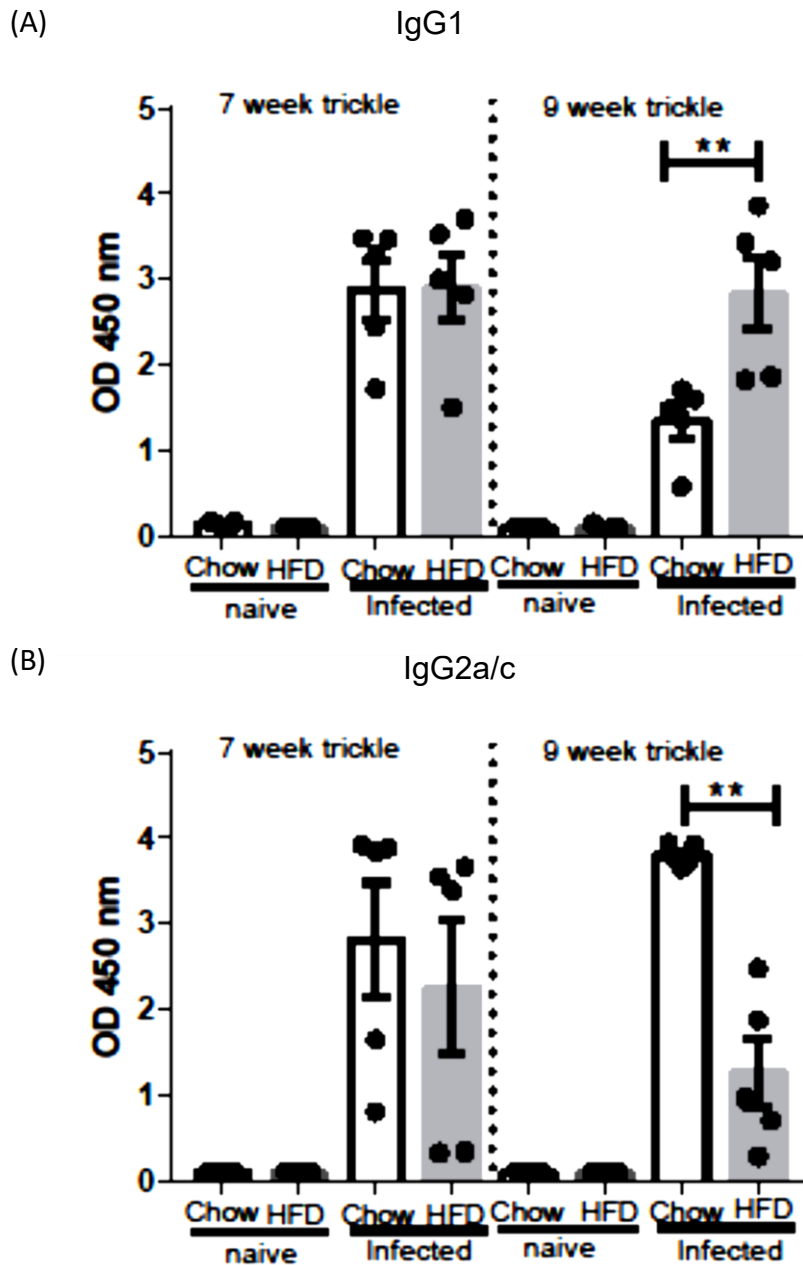


Figure 4-8: Parasite specific IgG1 and IgG2a/c antibody ELISA of trickle low dose infected mice after 12 weeks of pre-feeding.

Mice were fed on either normal chow or HFD for 12 weeks and they were given a single low dose *T. muris* infection. Mice were sacrificed 21- or 42-days post infection. Parasite specific antibodies were analysed by ELISA using serum from blood collected from mice. Absorbance readings at a serum dilution of 1 in 40 are shown. (A) Parasite specific IgG1 response after 7 and 9 weeks of trickle infections. (B) Parasite specific IgG2a/c response after 7 and 9 weeks of trickle infections. N = 5, results show mean \pm SEM.

After 7 weeks of trickle infection, both HFDIO and normal chow fed mice had high levels of parasite specific IgG1. After 9 weeks of trickle infection, there was a significantly lower parasite specific IgG1 response in the normal chow fed mice as compared to the HFDIO mice (figure 4.8 A). Even though there was an increase in parasite specific IgG2a/c in both normal chow and HFD mice after infection, the response was variable within each group after 7 weeks of trickle infection. However, after 9 weeks of trickle infection there is a significantly higher amount of parasite specific IgG2a/c in the normal chow mice as compared to the HFDIO mice (figure 4.8 B).

III. Cytokine responses of re-stimulated immune cells collected from trickle dose *T. muris* infected mice after 12 weeks of HFD feeding

The cytokine production of immune cells extracted from the mesenteric lymph nodes was compared. The cytokine production was variable within the groups. However, there was a trend towards increased average concentration of IL-5, IL-9 and IL-13 in the HFDIO mice after 7 weeks of trickle infection. After 9 weeks of trickle infection, there was a lower concentration of the Th2 cytokines in both HFDIO and normal chow fed mice and no differences in the mean concentrations (figure 4.9 A, B and C). IL-10 responses were variable within all the groups (figure 4.9 D). The IFN- γ was similar after 7 weeks of trickle infection, however after 9 weeks of trickle infection there was a weaker IFN- γ response in the HFDIO mice as compared to the normal chow mice. There was no difference in the IL-6, IL-17A and TNF- α response between the normal chow and HFDIO mice (figure 4.9 E to H).

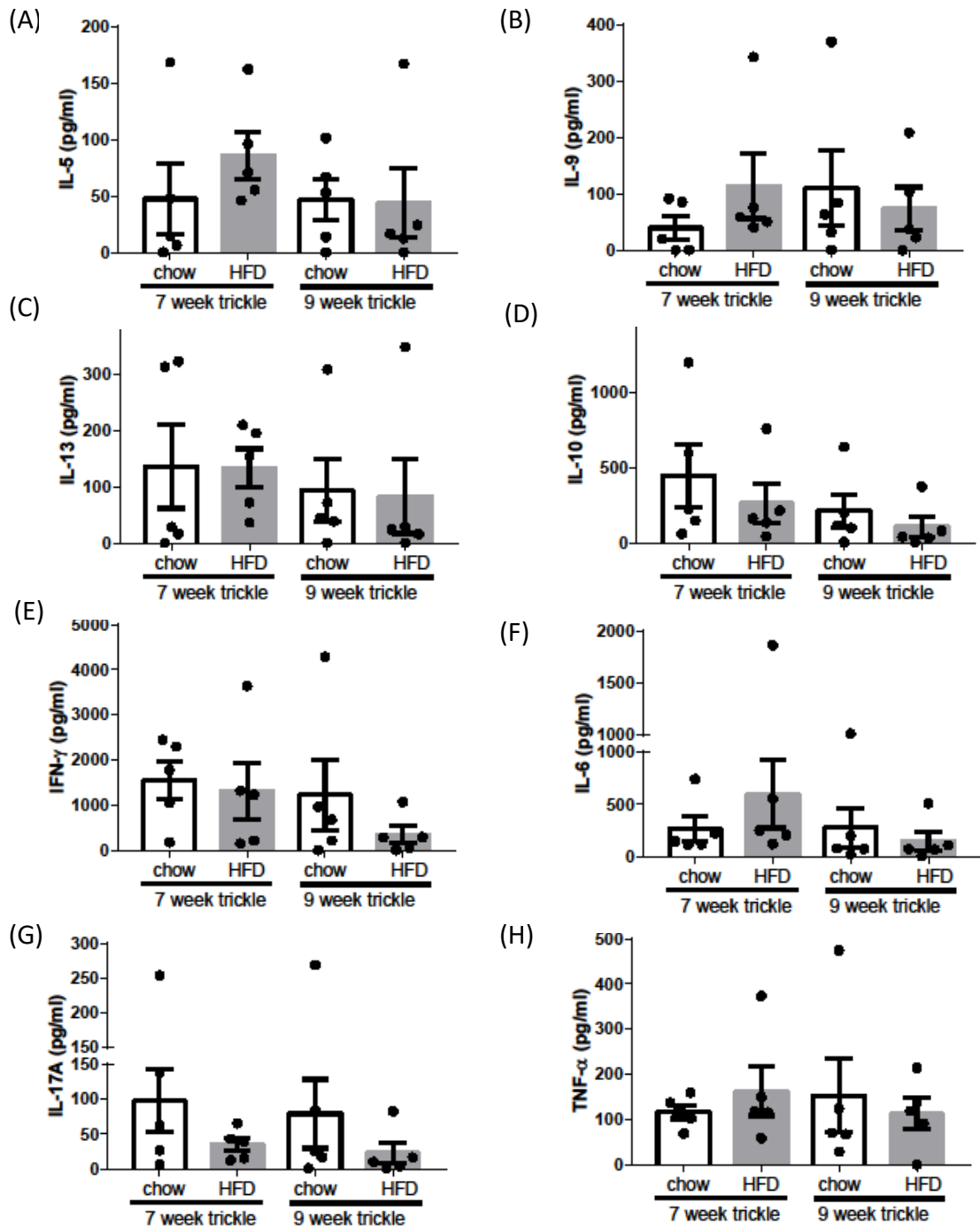


Figure 4-9: Re-stimulation of mesenteric lymph node derived cells from mice given trickle low dose infection after 12 weeks of feeding.

Mice were fed on either normal chow or HFD for 12 weeks and then they were given trickle low dose *T. muris* infection for 7 or 9 weeks. Mice were observed for 2 weeks after the last infection before they were sacrificed. Immune cells were extracted from mesenteric lymph nodes collected and re-stimulated for 48 hours using *T. muris* derived E/S after which the supernatant was collected and analysed for cytokines using the cytometric bead array. (A) IL-5 (B) IL-9 (C) IL-13 (D) IL-10 (E) INF- γ (F) IL-6 (G) IL-17A (H) TNF- α . N = 5. Results show mean \pm SEM.

4.2.4 How does HFD feeding affect the outcome of pre-infected *T. muris* mice?

Lastly, it was investigated if HFD consumption in already infected mice would have any effect on the development of a chronic infection. Mice were started on a HFD feeding either 13 days post infection or 32 days post infection. The mice were sacrificed approximately 3 weeks after starting on normal chow or HFD. Therefore, samples were collected from the mice at day 31 and day 52 post infection as indicated in figure 4.10.

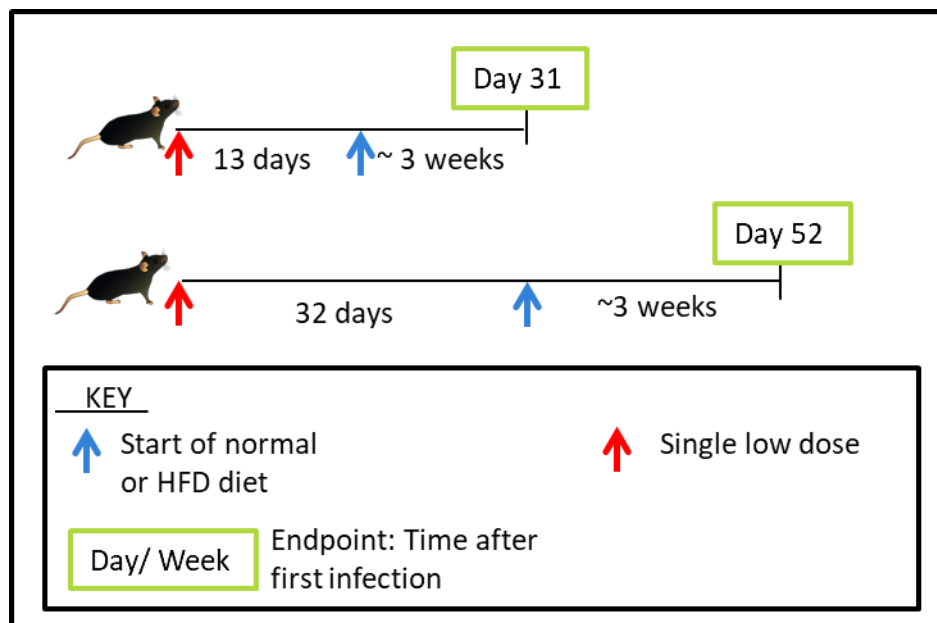


Figure 4-10: Experimental design.

C57BL/6 mice were given a single low dose of *T. muris* infection. 13 days post infection, the first group of mice were started on normal chow or HFD and sacrificed at day 31 post infection. The second group of mice were started on normal chow or HFD at day 32 post infection and sacrificed at day 52 post infection.

I. Worm burden of *T. muris* infected mice started on a HFD at either day 13 or day 32 post infection.

At day 31, the mean increase in weight was the same in the normal chow and HFD fed mice (figure 4.11 A). At day 52, there was considerable variation in the weight change although there was a trend showing that the weight increase was greater in the HFD mice as compared to the normal chow mice (figure 4.11 B). At day 31, worms were recovered

from mice on both HFD and normal chow (figure 4.11 C). At day 52 both normal chow and HFD mice had developed chronic infection and the mean number of recovered worms was the same in both groups (figure 4.11 D). The faecal egg load in the HFD mice was very variable within the groups with one mouse having a particularly high egg burden. However, on average there was no statistical difference in the mean faecal egg load between the two groups (figure 4.11 E).

II. Serum antibody responses of post-fed *T. muris* infected mice

At day 31, the parasite specific IgG1 response in both normal chow and HFD mice was low. By day 52 there was an increase in serum parasite specific IgG1 in both normal chow and HFD with the normal chow mice having significantly higher levels (4.12 A). At day 31, the parasite specific IgG2a/c response was similar in both normal chow and HFD fed mice. At day 52, both groups had strong parasite specific IgG2a/c responses with the normal chow mice having a significantly higher response (figure 4.12 B).

III. Cytokine responses of re-stimulated immune cells collected from post-fed *T. muris* infected mice

Cytokine responses were compared between the normal chow and HFD mice. IL-5 production was variable within the groups both at day 31 and day 52 (figure 3.9 A). Very low levels of IL-9 and IL-13 were observed (Non-detected for IL-13) (figure 3.9 B and D). The IL-10 responses were similar between both normal chow and HFD mice at day 31. At day 52, the IL-10 response was weak in both normal chow and HFD mice (figure 4.13 C). The average IFN- γ responses at day 31 were high in both normal chow and HFD. In addition, at day 52 the IFN- γ response was very weak in both groups of mice with no statistical difference between the two groups (figure 4.13 E). There was no difference in IL-6 and IL-17A responses between the normal chow and HFD mice (figure 4.13 F and G).

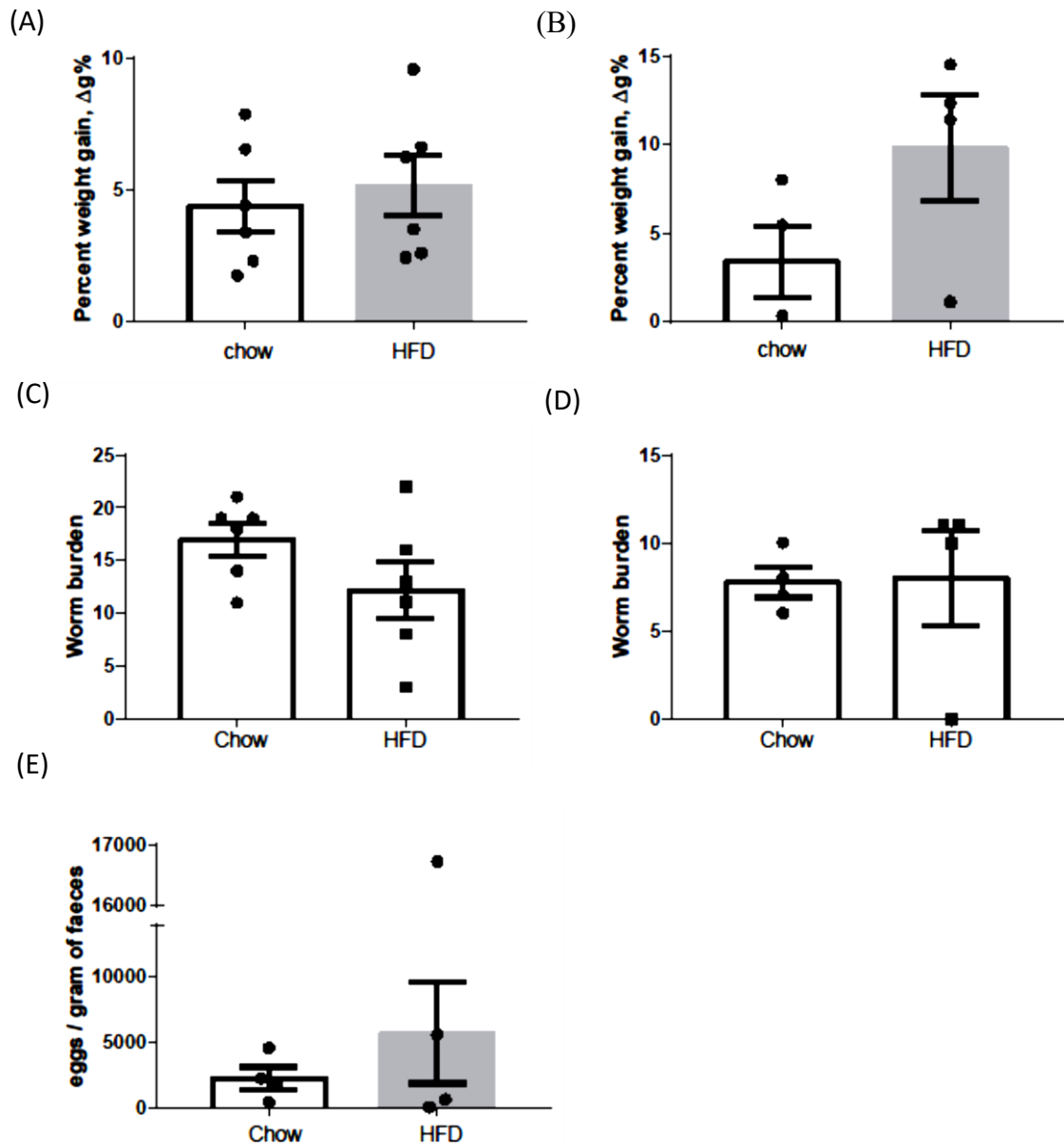


Figure 4-11: Weight gain and worm burden of mice started on a HFD after *T. muris* infection.

Mice were given an oral infection with a low dose of *T. muris* eggs. Mice were started on normal chow or HFD at either day 13 or day 32 post infection and sacrificed at day 31 or day 52 respectively. (A) Percentage increase in body weight at day 31 post infection (B) Percentage increase in body weight at day 52 post infection (C) worm burden at day 31 post infection (D) Worm counts at day 52 post infection (E) Faecal egg count at day 52 post infection. N = 4-6, results show mean \pm SEM.

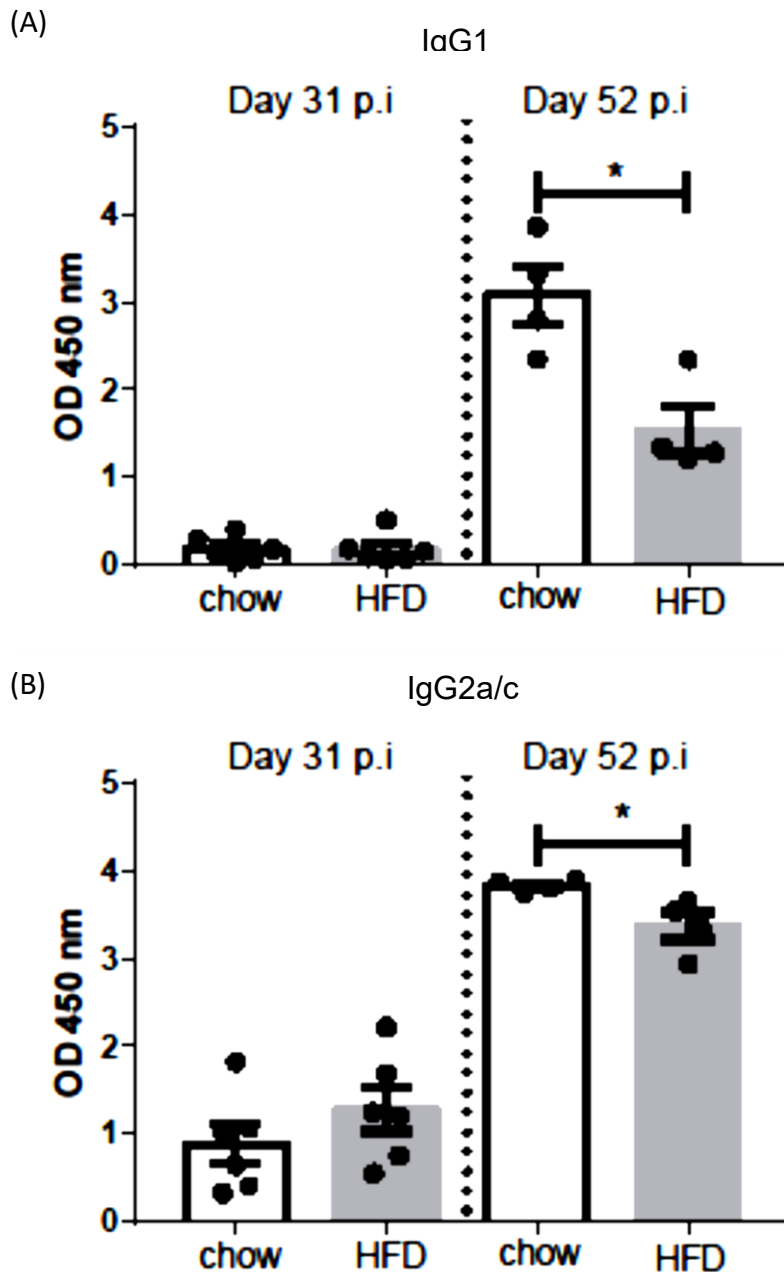


Figure 4-12: *T. muris* specific antibody responses of mice started on a HFD after *T. muris* infection.

Mice were given a low dose of *T. muris* and then started on a HFD or normal chow at different time points. Mice were started on diet either at day 13 or day 32 post infection and observed for 3 weeks before being sacrificed at day 31 or day 52 post infection respectively. Parasite specific antibodies were analysed by ELISA using serum from blood collected from mice. Absorbance readings at a serum dilution of 1 in 40 are shown. (A) Parasite specific IgG1 response at day 31 and day 52 post infection. (B) Parasite specific IgG2a/c response at day 31 and day 52 post infection. N = 4-6, results show mean \pm SEM.

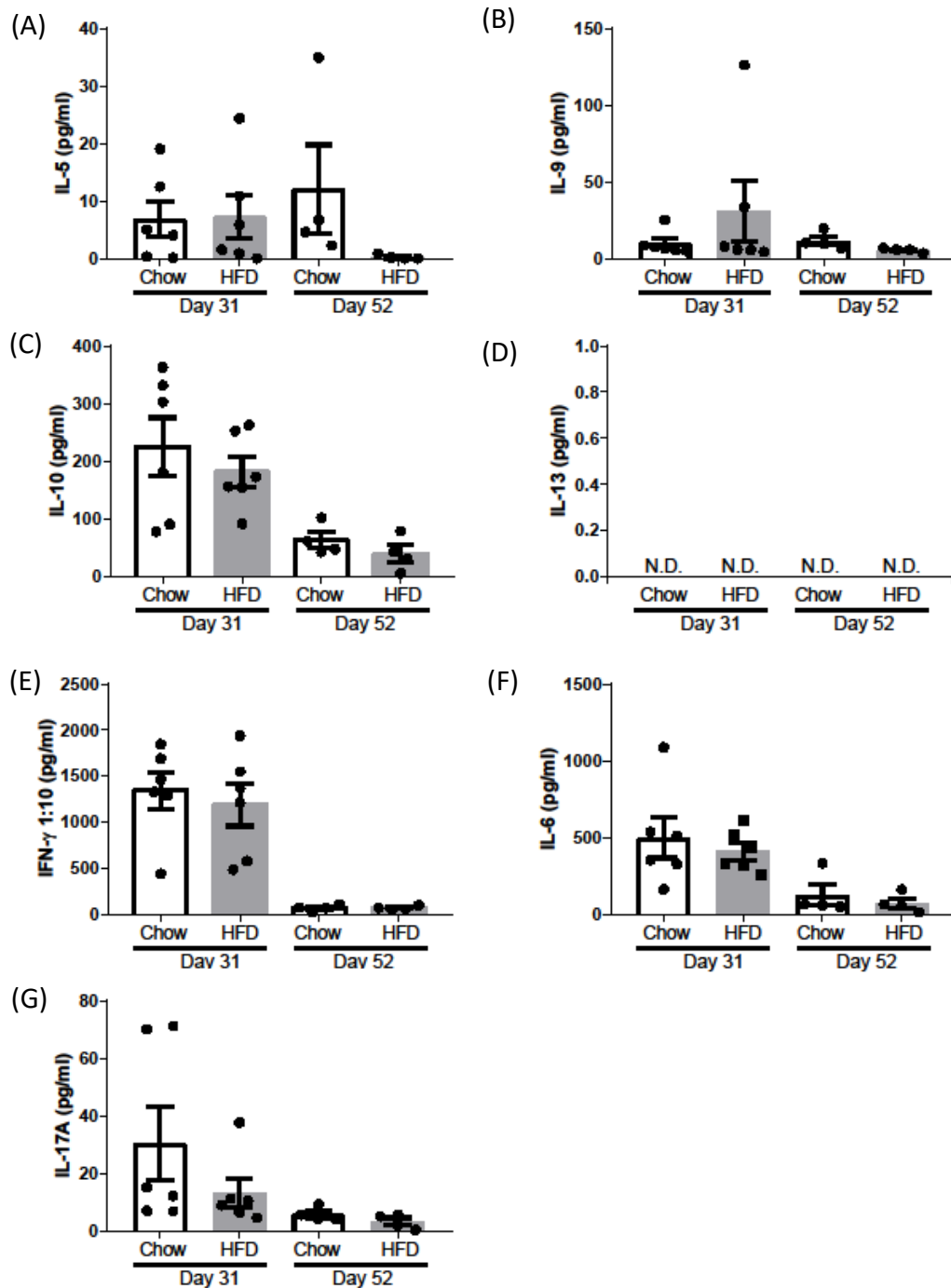


Figure 4-13: Re-stimulation of mesenteric lymph node derived cells from post-fed mice given a single low dose infection.

Mice were given a low dose of *T. muris* and then started on a HFD or normal chow at different time points. Mice were started on diet either at day 13 or day 32 post infection and observed for 3 weeks before being sacrificed at day 31 or day 52 post infection respectively. Immune cells were extracted from mesenteric lymph nodes collected and re-stimulated for 48 hours using *T. muris* derived E/S after which the supernatant was collected and analysed for cytokines using the cytometric bead array. (A) IL-5 (B) IL-8 (C) IL-10 (D) IL-13 (E) IFN- γ (F) IL-6 (G) IL-17A. N = 4 -6. Results show mean \pm SEM.

4.3 Discussion

4.3.1 HFD induces early worm expulsion during chronic *T. muris* infection

Given that *T. muris* infection had no effect on metabolic disease, it was postulated if HFD was able to influence the worm expulsion kinetics from mice infected with a single low dose of *T. muris*. Previous experiments have shown that mice given a low dose of *T. muris* are expected to develop chronic infection (Bancroft et al., 1994a; Bancroft et al., 2001). After 12 weeks of HFD feeding and the induction of obesity, C57BL/6 mice were infected with a single low dose of approximately 20 eggs. Based on the infectivity of the eggs, at least 5 to 15 worms were expected to fully embed in the epithelium. Figure 4.1 shows the worm burdens at day 21 and day 42 post infection. The normal chow fed mice developed a chronic infection as would be expected. Surprisingly, there was a reduction in the number of worms in the HFD mice by day 21 and this became significantly lower by day 42 post infection. To know if this early worm expulsion could be induced even after a shorter term of HFD feeding, mice were infected with a single low dose after 3 weeks of pre-feeding with HFD. Like the HFDIO mice, there was a reduction in worm burden at day 21 post infection in the HFD fed mice and by day 42 all the HFD fed mice had cleared the worms (figure 4.4). In both experiments, worms were recovered from the normal chow fed mice and they developed a chronic infection as would be expected. Therefore, the data suggests that HFD induced early worm expulsion after a single low dose of infection.

To test the model further, trickle infections were given to mice which had been fed on a HFD for 12 weeks. Previous work in C57BL/6 mice given trickle *T. muris* infections showed that there was a build of worms during the course of the trickle infection which was not observed in the more resistant BALB/c mice (Bancroft et al., 2001). Further work showed that after 7 weeks of trickle infections, C57BL/6 mice remained susceptible. However, previous work has shown that resistance starts to build up and after 9 weeks of trickle infections, the total number of recovered worms is much lower (Glover, 2017). Figure 4.7 shows that after 7 and 9 weeks of trickle infection the normal chow fed mice developed chronic infections, although the recovered number of worms was lower than expected. On the other hand, no worms were recovered from the HFD mice after 7 or 9 weeks of trickle infections. This was a remarkable outcome as it suggests that when mice are fed

on a HFD the threshold for resistance to *T. muris* infection is achieved earlier than when mice are fed on a normal diet. In addition, the early expulsion of worms could explain why no *T. muris* eggs were recovered from faecal pellets collected from the HFD mice at the selected time points during the experiment (figure 4.7 A).

4.3.2 HFD changes the worm specific antibody profile after a low dose *T. muris* infection

Worm expulsion kinetics correlate with the type of antibody responses generated upon infection. Worm expulsion is associated with increased production of parasite specific IgG1 and the failure to expel the parasites results in increased parasite specific IgG2a (Blackwell and Else, 2002). Analysis of the serum *T. muris* specific antibody responses highlighted increased parasite specific IgG1 production in the HFDIO and HFD pre-fed mice as compared to the normal chow fed mice after single low dose infections. Increased parasite specific IgG1 production is associated with resistant Th2 responses and this is in line with our observation that the HFDIO and HFD fed mice were better at worm expulsion. The normal chow pre-fed mice had higher serum parasite specific IgG2a/c production after a single or trickle dose infection as would be expected of chronic infections. The HFDIO and HFD pre-fed mice had a lower parasite specific IgG2a/c level which again was consistent with the worm burden data as they had expelled worms and did not develop chronic infections.

After 7 weeks of trickle infections both the normal chow and HFDIO mice had enhanced parasite specific IgG1 and IgG2a/c responses. This is consistent with previous work which showed that when C57BL/6 are given trickle low dose infections, they had a mixed parasite specific IgG1 and IgG2a/c response (Bancroft et al., 2001). However, after 9 weeks of trickle infections, there was a change in the antibody profile between the two groups with the HFDIO having significantly more parasite specific IgG1, whereas the normal chow produced more parasite specific IgG2a/c. This antibody response correlates with the worm expulsion kinetics in the trickle mice with the HFDIO mice expelling much earlier as compared to the normal chow mice. Overall, a strong relationship between the antibody responses and worm expulsion kinetics was observed.

4.3.3 HFD enhances a Th2 immune response

HFD is associated with the development of low-grade inflammation. This has been attributed to increased intestinal permeability resulting in the translocation of bacterial products such as LPS which trigger the immune response (Cani et al., 2008). Adaptive T-cell responses play an immune role in the development of immunological responses. Naïve T-cells collected from the spleen of HFD fed mice have been shown to have a strong inflammatory profile and this has been suggested to play a role in the inflammatory responses associated with obesity (Verwaerde et al., 2006). On the other hand, T-cells collected from the spleen of ovalbumin immunized HFD mice had impaired antigen dependent proliferation in comparison to T-cells from control mice and exhibited a trend towards a Th2 responses (Verwaerde et al., 2006). Overall this suggests that whereas naïve T-cells from HFD mice have a proinflammatory response, antigen experienced T-cells from HFD fed mice have impaired responses with a trend towards anti-inflammatory Th2 immune responses.

In this current study, the effect of HFD on T-cell responses was studied by comparing cytokine production by cells extracted from the mesenteric lymph node and re-stimulated by exposure to *T. muris* antigen. The cytokine production between the HFD fed mice and normal chow mice was compared. After 12 weeks of feeding and a single dose infection there was an increase in the Th2 associated cytokines IL-5, IL-9 and IL-13 in the HFDIO mice in comparison to the normal chow fed mice at day 21 post infection. Resistance is associated with increased production of Th2 cytokines (Else et al., 1992). IL-13 has been shown to be a critical factor involved in the resistance against *T. muris* (Bancroft et al., 2000; McKenzie et al., 1998). So far, the data suggests that HFDIO was favouring the development of the Th2 immune response and this would explain why the HFDIO mice were better at expelling the worms compared to the normal chow mice.

Previous work has shown increased production of Th2 cytokines after 9 weeks of trickle infection which is the period when mice start to develop resistance and show a reduction in worm burden (Glover, 2017). There was a trend in increased IL-5 and IL-9. IL-13 responses which seemed mixed in both groups both after 7 and 9 weeks of trickle

infection. It is possible that the peak of cytokine production may have occurred at a much earlier time point especially in the HFDIO mice which had already expelled worms by the time of analysis.

There was a lot of variation with the IL-10 response. IL-10 is a regulatory cytokine which enhances Th2 response (Schopf et al., 2002b). On average there is no significant change in the production of IL-10 changes between the normal and HFD mice given single or trickle infection. Therefore, more work needs to be done to understand the regulatory mechanism involved in the HFD mice after infection.

4.3.4 HFD dampened the Th1 immune response

One of the main cytokines produced during a chronic infection is IFN- γ (Artis et al., 1999b; Else et al., 1994). The normal chow fed mice developed chronic infections and had increased levels of IFN- γ as expected. What was particularly interesting was the reduction in IFN- γ production by the single low dose infected HFDIO mice. Although not significant, there was a trend in reduced IFN- γ in the 3-week pre-fed HFD mice and in the HFDIO mice after 9 weeks of week of trickle infections.

IL-6 has been associated with mucosal inflammation during *T. muris* infection (Hurst et al., 2013). HFD which causes a low-grade inflammation in the host is often associated with increased IL-6 production. Increased level of IL-6 were observed in C57BL/6 mice after 8 weeks of feeding on a HFD (Kim et al., 2012). Therefore, it was very striking to see that there was a consistent reduction in IL-6 production by the HFD infected mice after a single low dose infection both after 12 weeks or 3 weeks of HFD pre-feeding.

IL-17A has been shown to be associated with increased pathology during *N. brasiliensis* infection (Sutherland et al., 2014). The normal chow infected mice produced higher levels of IL-17A in comparison to the HFD infected mice in both single and trickle infected mice. Furthermore, there was a significant reduction in TNF- α production in the HFD mice after single dose infection. TNF- α is increased in HFD mice and also plays a regulatory role during *T. muris* (Hayes et al., 2007; Kim et al., 2012). Hence the results suggest that HFD

led to reduced production of pro-inflammatory cytokines thereby dampening the Th1 immune response.

The early stages of infection play a critical role in driving the immune response. In the development of an immune response upon exposure to antigen, the priming of CD4⁺ T-cells is important in determining development of either Th1 or Th2 immunity. Dendritic cells have been shown to play a role in priming the T helper cell response. An increase in dendritic cells has been reported following *T. muris* infection (Cruikshank et al., 2009). In addition, it has been previously shown that specific dendritic cell subsets play a role in the induction of either Th1 or Th2 immune responses to *T. muris* infection (Demiri et al., 2017). Mice lacking IRF4-dependent classical dendritic cells were unable to expel a high dose of infection implying increased susceptibility to infection. On the other hand, mice lacking IRF8-dependent classical dendritic cells were able to expel a low dose infection of *T. muris* implying they had enhanced resistance (Demiri et al., 2017). This suggests that IRF4-dependent classical dendritic cells are involved in the development of Th2 immunity while IRF8-dependent classical dendritic cells are involved in the development of Th1 immunity. Based on these observations further work can be carried out to investigate changes in dendritic cell subsets during the early stages of infection in the HFD mice to determine how these subsets may be contributing to the enhanced resistance observed in HFD mice. Investigating changes in the IRF4-dependent classical dendritic cells in the HFD mice in comparison to normal chow mice during *T. muris* infection can be done. This can be carried out at early stages of infection such as day 7 to day 13, as well as at the peak of the cytokine response, day 18 in order to understand changes in the IRF4-dependent classical dendritic cells during the course of infection in the HFD mice.

4.3.5 HFD feeding does not induce resistance in *T. muris* infected mice started on a HFD at either day 13 or day 32 post infection

Lastly, mice were infected and then commenced on a HFD at different time points through the infection period. *T. muris* undergoes development through different larval stages in the host. By day 13 post infection, the parasite would have developed into L3 larvae found embedded within the epithelium whereas by day 32, adult worms would

have matured from L4 larvae (Cliffe and Grencis, 2004). One group of infected mice was started on a HFD at day 13 post infection and the second group was started on a HFD at day 32 post infection. The mice were fed on the HFD for 3 weeks as previous data indicated that mice fed on a HFD for 3 weeks before infection had lower worm burden in comparison to control at day 21 and day 42 post infection (figure 4.4 C and D). Therefore, in order to examine if the same observation would be true if the 3 weeks of feeding was started post infection, mice were started on a HFD at different time point post infection and the outcome the infection was studied.

There was no difference in worm burden of mice from both groups and delayed antibody responses in both normal chow and HFD mice. In addition, the Th2 cytokine response was very weak in both normal chow and HFD mice however there was a strong IFN- γ response at day 31 which would be expected of a chronic infection. Taken all together the results show that the development of the larvae stages was not affected by HFD feeding once they were already established. Furthermore, HFD consumption could not induce expulsion of adult worms within the time period studied. Indicating that the properties associated with HFD induced resistance must be already set in the host before infection. It is possible that if the mice were maintained on HFD for longer periods of time, a reduction in worm burden in the HFD fed mice might have been observed in comparison to the normal chow mice as the HFD would start to induce changes in the mice. In order to investigate this, an additional experiment can be carried out where the mice started on the HFD at the different time points after infection and left for longer periods of time on the diet before comparing the worm burden and immune response.

4.4 Conclusion

The results in this chapter indicate that:

- I. Pre-feeding mice with HFD induces early worm expulsion after a single and trickle infection with *T. muris*.
- II. HFD fed mice produce more parasite specific IgG1 and reduced parasite specific IgG2a/c which correlates with the worm expulsion kinetics.

- III. HFD enhances the production of Th2 associated cytokines after a single dose of *T. muris* infection
- IV. HFD dampens down the pro-inflammatory response in both single and trickle low dose infected mice
- V. The HFD induced resistance is not observed when mice are fed on a HFD after *T. muris* infection.

Based on these conclusions it was next investigated if the enhanced Th2 cytokines were accompanied by classical helminth expulsion mechanisms that would lead to increased resistance in the HFD fed mice after *T. muris* infection.

Chapter 5 : Results III

Investigating the mechanism of HFD induced resistance against *T. muris*

5.1 Introduction

The results from the previous chapter show that HFDIO mice were able to expel a chronic infection as compared to normal chow fed mice during single and trickle low dose *T. muris* infections. Furthermore, HFD feeding after infection did not result in resistance. This suggests that the enhanced resistance which led to worm expulsion in the HFDIO mice was because of HFD induced changes in the host that occurred before infection.

HFD changes the composition of the intestinal host microbial population with an increase in *Firmicutes* and reduction in *Bacteroidetes* (Turnbaugh et al., 2006a, b). In addition, HFD is associated with a reduction in the expression of epithelial tight junction proteins which results in increased gut permeability (Benoit et al., 2015; Lam et al., 2012). As a result of this increased permeability there is an increase in the translocation of bacterial products into the systemic circulation causing low grade inflammation that is associated with the development of metabolic syndrome (Cani et al., 2008; Lam et al., 2012). Furthermore, HFD has been associated with an increase in the number of colonic goblet cells and increased sialo/sulphomucin ratio of goblet cell mucins (Mastrodonato et al., 2014).

A number of studies have also investigated the association between HFD and the immune system. Obesity is associated with increased production of leptin from adipocytes. Studies have shown that leptin modulates T-cell responses and promotes Th1 immune responses (Lord et al., 2002). *In vitro* studies have shown that cells collected from HFD fed obese mice have impaired T-cell responses suggesting that obesity is linked to immunosuppression which may increase susceptibility to infection (Katagiri et al., 2007; Sato Mito et al., 2009).

The balance between anti- and pro-inflammatory cytokines plays an important role in determining the outcome of the immune response to *T. muris* (Else et al., 1992). The production of Th2 associated cytokines IL-4, IL-9 and IL-13 by Th2 CD4⁺ T-cells increases the rate of epithelial turn over, muscle contractions and mucus production which result in worm expulsion (Cliffe et al., 2005; Faulkner et al., 1998; Hasnain et al., 2011b). In susceptible mice, there is an enhanced production of the pro-inflammatory cytokine INF- γ

which has been associated with reduced epithelial turnover (Artis et al., 1999b; Cliffe et al., 2007)

No previous study has investigated the effect of HFD on the establishment of *T. muris* in the host and how HFD may influence the development of protective immune responses against *T. muris*.

The aims of this chapter were to:

- I. Investigate if HFD-induced changes in host microbiota have an effect on the establishment of *T. muris* infection.
- II. Investigate the effect of *T. muris* infection on the faecal microbial population of HFDIO mice.
- III. Investigate the effect of HFDIO on T-cell responses in *T. muris* infected mice.
- IV. Investigate the effect of HFDIO on caecal goblet cell numbers and RELM β expression in response to *T. muris* infection.
- V. Investigate the effect of HFDIO on the outcome of a low dose *T. muris* infection in C57BL/6 RAG^{-/-} mice.
- VI. Investigate the effect of HFDIO on tuft cell responses in *T. muris* infected mice.
- VII. Investigate the relationship between worm burden and mouse weight.

5.2 Results

The results presented in this chapter were collected from mice in groups I, J and K which are described in table 2.2. Goblet cell analysis was performed on samples collected from mice in groups A and B.

5.2.1 The effect of HFDIO on the establishment of *T. muris*

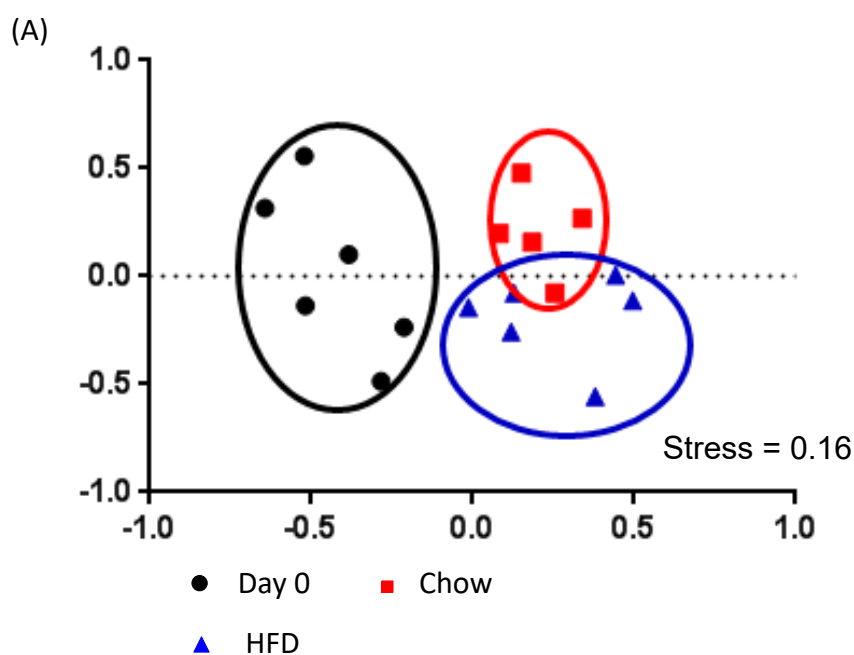
The first set of experiments aimed to determine if the reduced worm burden in the HFDIO mice may have been due to failure of the parasite to establish in the host as previous studies has shown that hatching of *T. muris* requires interaction with the host microflora which is altered by HFD (Cani et al., 2008; Hayes et al., 2010; Turnbaugh et al., 2006b).

The faecal microbial composition of mice after 12 weeks of feeding on normal chow or HFD was compared using DGGE. Non-parametric multidimensional scaling (NMDS) analysis was used to determine differences between the groups. The NMDS plots show the spatial distribution of the samples and gives an indication of how similar they are in terms of microbial population based on the binary matrix generated from the DGGE gel. In the NMDS plots mice belonging to the same group are given a unique colour and this differentiates between the different treatment groups. Furthermore, multiple comparison analysis is carried out to determine if there is any statistical difference between the groups.

Faecal pellets were collected from 7 week old mice (day 0) and then collected after 12 weeks of feeding with either normal chow or HFD. NMDS analysis of the DGGE data revealed that after 12 weeks of feeding the mice on normal chow or HFD there was a significant shift in the cluster of the microbial population relative to the microbial population of the mice at the start of the experiment. In addition, the microbial population of the normal chow mice also differed from that of the HFDIO mice although based on the calculated Bonferoni value which takes into account multiple comparisons, the difference between the two populations was not significant (figure 5.1 A). The stress value indicates how well the data fit in the computed NMDS plots. The lower the stress

value the better the fit and with a value greater than 0.2 is considered as a good fit (Clarke and Ainsworth, 1993; Cliffe and Grencis, 2004).

After 12 weeks of feeding on normal chow or HFD, the mice were given a high dose of *T. muris* infection. A high dose infection was used to allow for larval counts to be conducted at day 13 post infection in order to determine if the *T. muris* parasites were able to establish in the host. There was no difference in the mean number of larvae recovered between the normal chow and HFDIO mice (figure 5.2).



(B)

Pairwise comparisons	P value	Bonferoni value
Day 0 vs Chow	0.0024	0.0008
Day 0 vs HFD	0.0023	0.0008
Chow vs HFD	0.0070	0.0023

Figure 5-1: DGGE analysis of faecal microbiota after 12 weeks of feeding.

C57BL/6 mice were placed on either normal chow or HFD for 12 weeks. DNA was extracted from faecal pellets that were collected from the mice at the start of feeding (day 0) and after 12 of feeding on each diet. The DNA was analysed by denaturing gradient gel electrophoresis after amplification of the 16S rRNA. (A) NMDS analysis of bacterial communities, the axis represents the scale for the Euclidian distance between samples. Stress indicates the quality of fit of data (> 0.2 is a good fit). (B) Statistical analysis of the NMDS plots calculated by permutational ANOVA. N = 5 to 6. The Bonferoni value (p value/ number of pairwise comparisons) was considered significant when less than 0.001.

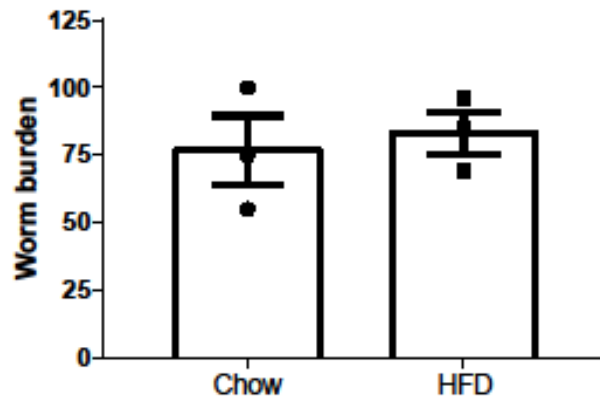


Figure 5-2: Worm burdens at day 13 post infection in normal chow and HFDIO mice.

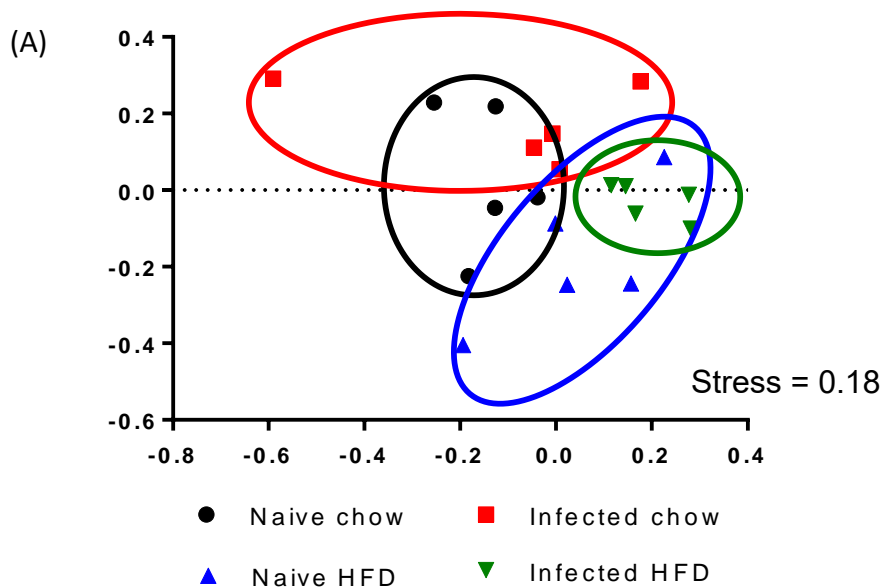
C57BL/6 mice were placed on either normal chow or HFD for 12 weeks. Mice were then given a high dose of *T. muris* infection and sacrificed at day 13 post infection. The whole caecum was collected from each mouse and frozen. Once frozen, the faecal contents were removed, and the tissue was sheared using forceps in order to release larvae from the epithelium. The larvae were counted under a microscope. N = 3, results show mean \pm SEM.

5.2.2 Faecal microbial population at day 21 post infection in normal chow and HFDIO mice

The faecal microbial population was also compared between normal chow and HFDIO mice at day 21 post infection in order to determine if HFD would have any effect on the ability of *T. muris* to alter the host microbiota. The faecal microbial composition was compared using DGGE. There was a shift in the microbial population in naive normal chow compared to HFDIO mice. In addition, there was only a slight shift in the microbial between naïve and infected population (figure 5.3 A). Based on the calculated Bonferroni values, there was no significant difference between all the groups (figure 5.3 B).

5.2.3 The effect of HFDIO on T-cell responses in *T. muris* infected mice

Having confirmed the ability of *T. muris* to establish in the HFDIO mice, the role of T-cells in enhancing the resistance to *T. muris* in the HFDIO mice was investigated. C57BL/6 mice were fed on either normal chow or HFD for 12 weeks. The mice were then given a single low dose of *T. muris* eggs. In chapter 4, it was reported that by day 21 post infection, there was a trend towards reduced worm burden in the HFDIO mice. Therefore, for this chapter, the main focus was on comparing the immune response at day 21 post infection.



(B)

Pair wise comparison	p-value	Bonferoni value
Naïve chow vs Naïve HFD	0.1098	0.0183
Naïve chow vs Infected chow	0.1115	0.0186
Naïve chow vs infected HFD	0.0079	0.0013
Naïve HFD vs Infected chow	0.0079	0.0013
Naïve HFD vs Infected HFD	0.0081	0.0013
Infected chow vs Infected HFD	0.0450	0.0075

Figure 5-3: DGGE analysis of faecal microbiota at day 21 post infection.

C57BL/6 mice were placed on either normal chow or HFD for 12 weeks. The mice were then given a single low dose *T. muris* infection mice and faecal pellets were collected from naïve and infected mice at day 21 post infection. DNA was extracted from faecal pellets and analysed by denaturing gradient gel electrophoresis after amplification of the 16S rRNA. (A) NMDS analysis of bacterial communities, the axis represents the scale for the Euclidian distance between samples. Stress indicates the quality of fit of data (> 0.2 is a good fit). (B) Statistical analysis of the NMDS plots calculated by permutational ANOVA, N = 5 to 6. The Bonferoni value (p value/ number of pairwise comparisons) was considered significant when less than 0.001.

I. Cytokine production of CD3/CD28 activated T-cells from the mesenteric lymph nodes

Cells collected from the mesenteric lymph nodes of *T. muris* infected normal chow and HFDIO mice were re-stimulated with *T. muris* derived E/S or activated with antiCD3/CD28 antibodies. Similar to the results reported in chapter 4, section 4.2.1 (part III), re-stimulation of cells with E/S resulted in a trend towards increased production of Th2 associated cytokines, IL-5, IL-9, IL10 and IL-13, by cells from HFDIO mice (figure 5.4 A to D) and dampened production of proinflammatory cytokines IFN- γ , IL-6, IL-17A and TNF- α in comparison to cells collected from normal chow mice (figure 5.5 A to D).

To investigate T-cell specific responses, the cells were activated by stimulation with immobilised anti-CD3. The co-stimulatory signal was provided by anti-CD28 which enhances proliferation and the production of cytokines (Riddell and Greenberg, 1990; Thompson et al., 1989).

The cytokine production of CD3/CD28 activated T-cells collected from either normal or HFDIO *T. muris* infected mice were compared. CD3/CD28 activation enhanced the production of IL-5, IL-9 and IL-13 from T-cells collected from HFDIO mice in comparison to the T-cells from normal chow mice. However, the difference in the mean concentration of the cytokines between the two groups was not significant (figure 5.4 A to D). Furthermore, CD3/CD28 activated T-cells from HFDIO mice produced lower levels of IL-6, IL-17A and TNF- α in comparison to CD3/CD28 activation T-cells from normal chow mice (figure 5.5 B to D). There was no difference in IFN- γ production between the two groups upon activation (figure 5.5 A). Therefore, T-cells from *T. muris* infected HFDIO mice showed enhanced ability to produce Th2 type cytokines and dampened pro-inflammatory responses.

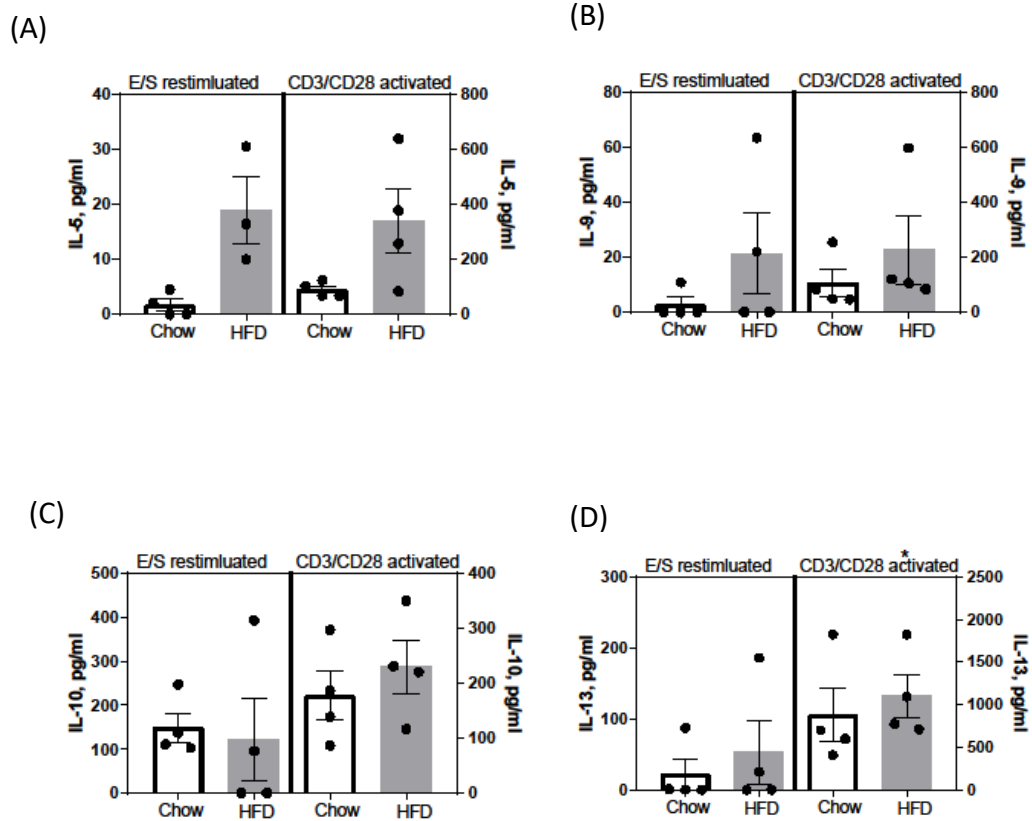


Figure 5-4: Comparison of Th2 associated cytokine production of cells re-stimulated with *T. muris* E/S or activated via CD3/CD28 stimulation.

C57BL/6 mice were fed on normal chow or HFD for 12 weeks. The mice were then given a single low dose of *T. muris* infection and scarified at day 21 post infection. Cells were extracted from the mesenteric lymph node and re-stimulated with *T. muris* derived E/S or activated by incubating with immobilised anti-CD3 followed by co-stimulation with anti-CD28. Supernatants were collected after 48 hours and analysed for cytokines by CBA. (A) IL-5. (B) IL-9. (C) IL-10. (D) IL-13. N= 4, results show mean \pm SEM.

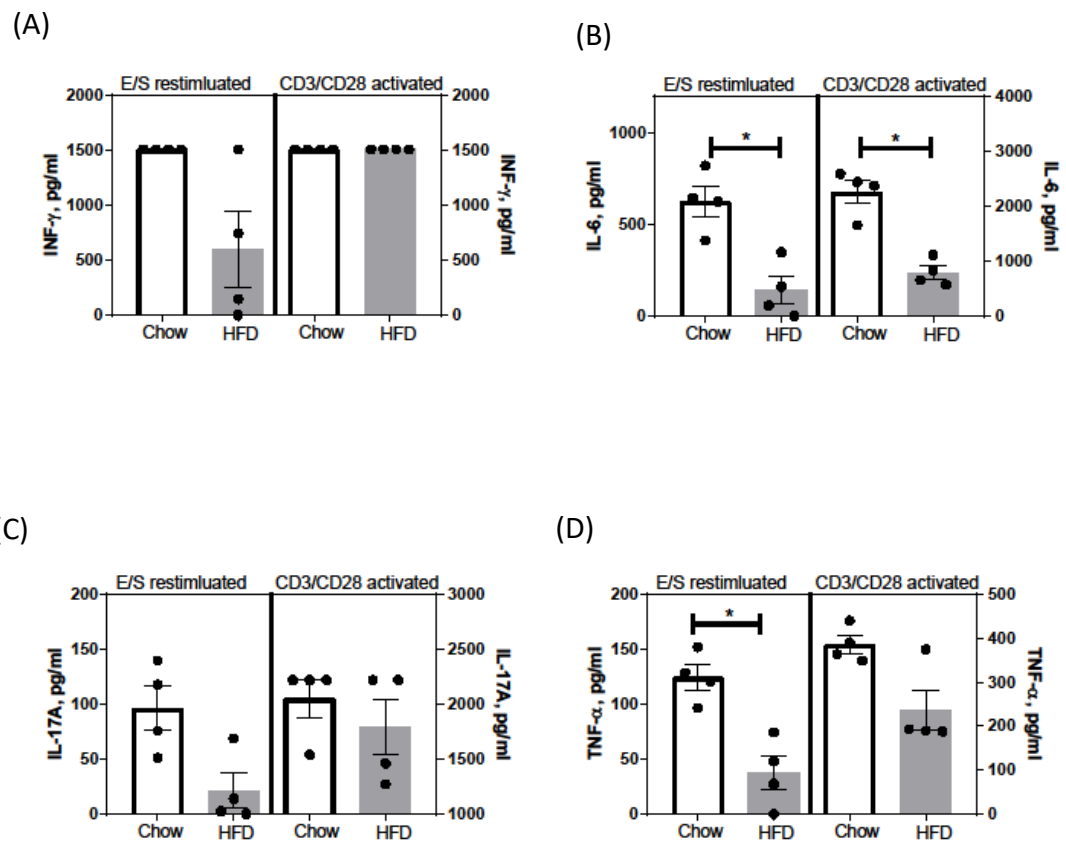


Figure 5-5: Comparison of proinflammatory cytokine production of cells re-stimulated with *T. muris* E/S or activated via CD3/CD28 stimulation.

C57BL/6 mice were fed on normal chow or HFD for 12 weeks. The mice were then given a single low dose of *T. muris* infection and scarified at day 21 post infection. Cells were extracted from the mesenteric lymph node and re-stimulated with *T. muris* derived E/S or activated by incubating with immobilised anti-CD3 followed by co-stimulation with anti-CD28. Supernatants were collected after 48 hours and analysed for cytokines. (A) IFN- γ . (B) IL-6. (C) IL-17A. (D) TNF- α . N= 4, results show mean \pm SEM.

II. CD4⁺IFN- γ ⁺ T-cell population in the mesenteric lymph nodes and lamina propria at day 21 post infection

IFN- γ is one of the predominant cytokines produced by CD4⁺ T-cells during chronic infections (Else and Grecis, 1991; Else et al., 1992). After E/S re-stimulation lower levels of IFN- γ were produced by cells collected from HFDIO mice in comparison to cells collected from normal chow mice. To further confirm if HFD was having an effect on IFN- γ production of CD4⁺ T-cells, cells collected from the mesenteric lymph node and lamina propria of normal chow and HFDIO mice were activated using the PMA/Ionomycin cell stimulation cocktail. Intracellular levels of IFN- γ in CD4⁺ T-cells were then analysed by flow cytometry. Representative gating on CD4⁺IFN- γ ⁺ T-cells is shown in figures 5.6 A and 5.7 A.

In the mesenteric lymph node there was no difference in the percentage and number of CD4⁺IFN- γ ⁺ T-cells between naïve normal chow and HFDIO mice. However, there was a higher percentage and number of CD4⁺IFN- γ ⁺ T-cells in the infected normal chow mice as compared to the HFDIO mice (figure 5.6 B and C). Similarly, in the lamina propria there was no difference in the CD4⁺IFN- γ ⁺ T-cells between naïve normal chow and HFDIO mice. Upon infection there was a trend towards increased percentage and number of CD4⁺IFN- γ ⁺ T-cells in the normal chow mice in comparison to the HFDIO although the difference was not significant (figure 5.7 B and C).

The detection of intracellular IL-13 was very weak hence no analysis could be carried out on the production of IL-13 by CD4⁺ T-cells.

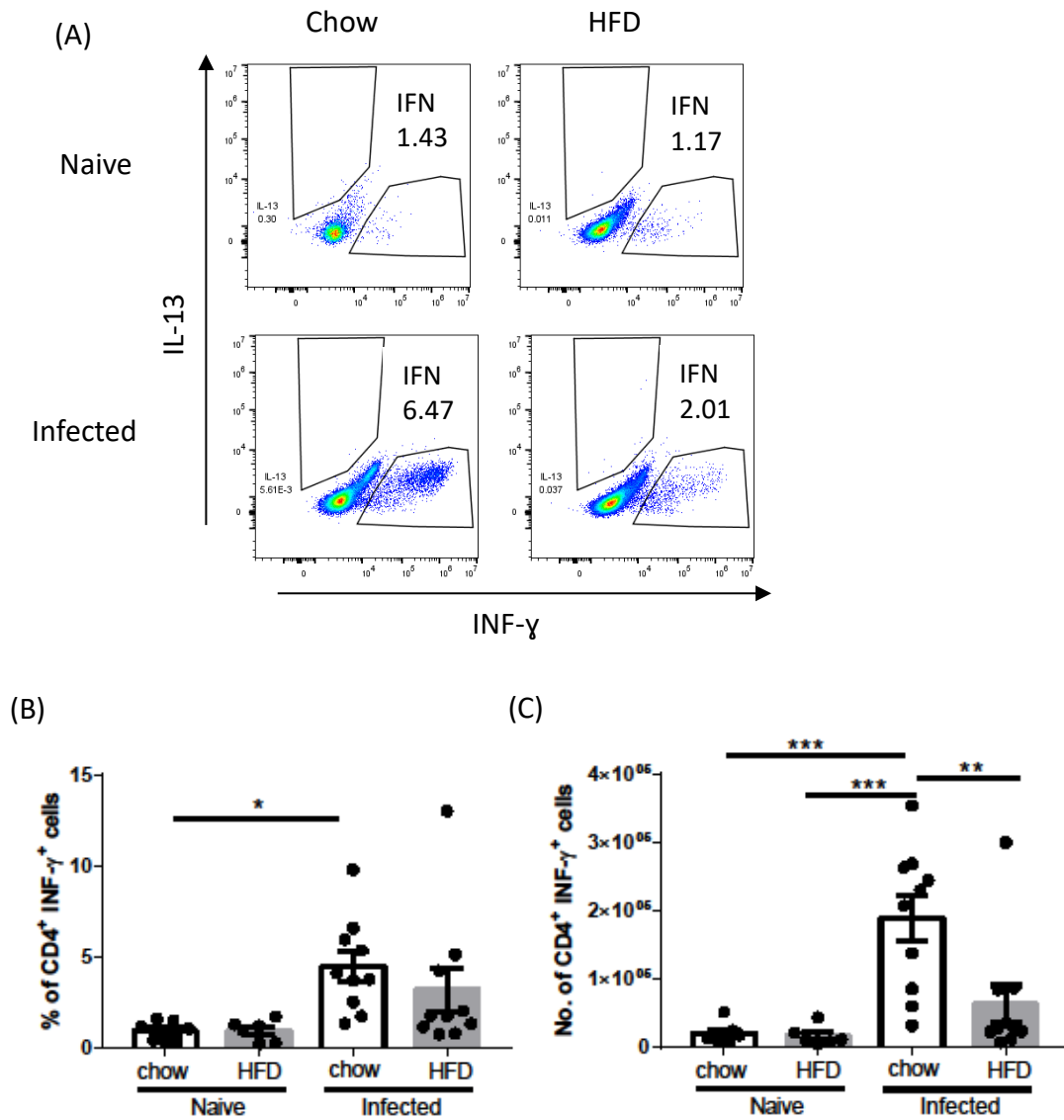


Figure 5-6: Analysis of Interferon- γ producing CD4⁺T cells in the mesenteric lymph nodes.

C57BL/6 mice were fed on normal chow or HFD for 12 weeks. The mice were then given a single low dose of *T. muris* infection and sacrificed at day 21 post infection. Cells were extracted from the mesenteric lymph node and stimulated overnight using the PMA/Ionomycin cell stimulation cocktail. Cytokine release was blocked by adding Brefeldin A. Cells were collected by centrifuging at 500 x g and analysed by flow cytometry. Gating strategy: CD45, TCR β , CD4, IFN- γ . (A) Representative gating of CD4⁺IFN- γ ⁺ T-cells. (B) Percentage of CD4⁺IFN- γ ⁺ T-cells. (C) Number of CD4⁺IFN- γ ⁺ T-cells. N= 7 to 10, results show mean \pm SEM. Data shown was collected from 3 independent experiments.

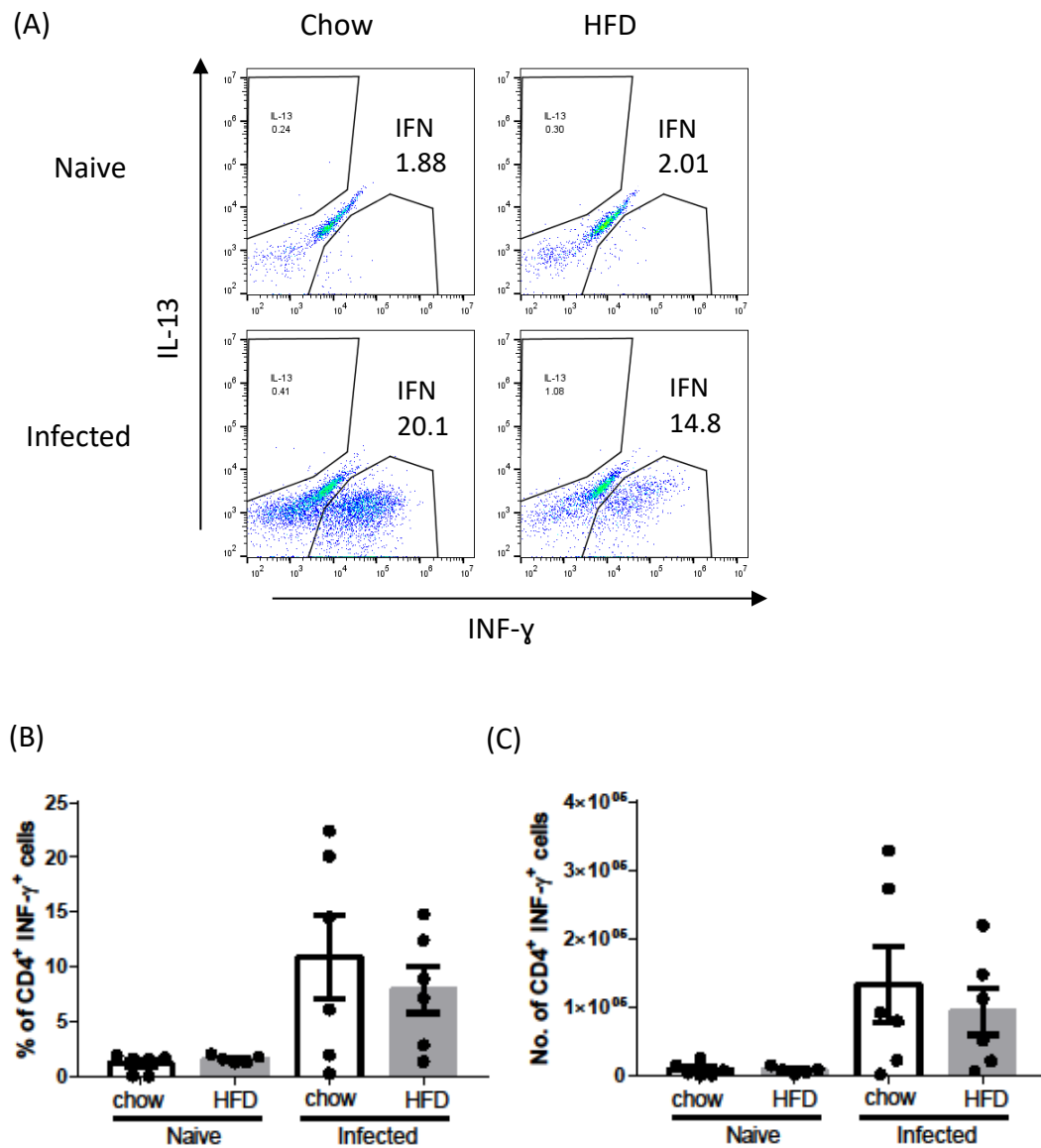


Figure 5-7: Analysis of Interferon- γ producing CD4⁺ T cells in the lamina propria.

C57BL/6 mice were fed on normal chow or HFD for 12 weeks. The mice were then given a single low dose of *T. muris* infection and sacrificed at day 21 post infection. Cells were extracted from the lamina propria and stimulated overnight using the PMA/Ionomycin cell stimulation cocktail. Cytokine release was blocked by adding Brefeldin A. Cells were collected by centrifuging at 500 x g and analysed by flow cytometry. Gating strategy: CD45, TCR β , CD4, IFN- γ . (A) Representative gating of CD4⁺IFN- γ ⁺ T-cells. (B) Percentage of CD4⁺IFN- γ ⁺ T-cells. (C) Number of CD4⁺IFN- γ ⁺ T-cells. N= 5 to 6, results show mean \pm SEM. Data shown was collected from 2 independent experiments.

III. CD4⁺FoxP3⁺ T-cells (Tregs) and CD4⁺Tbet⁺ T-cells in the mesenteric lymph nodes at day 21 post infection

CD4⁺FoxP3⁺ Tregs are associated with susceptibility to *T. muris* infection and have been shown to limit the induction of protective immune responses against specific strains of *T. muris* (D'Elia et al., 2009a). HFD has been linked to a reduction in the number of Tregs in obese mice (Pettersson et al., 2012; Wang et al., 2014). The CD4⁺FoxP3⁺ Treg population between the normal chow and HFDIO mice was compared. Representative gating on CD4⁺FoxP3⁺ is shown in figure 5.8 A. There was no difference in the mean percentage of CD4⁺FoxP3⁺ Tregs between the normal chow and HFDIO mice. However, the mean number of CD4⁺FoxP3⁺ Tregs was lower in the HFDIO in comparison to the normal chow mice (figure 5.8 C and D).

In addition, the expression of the transcription factor T-bet (T-box expressed in T-cells) by CD4⁺ T-cells was also compared. T-bet reinforces Th1 immune responses in CD4⁺ T-cells and promotes transcription of pro-inflammatory cytokines (Szabo et al., 2002). Representative gating on CD4⁺Tbet⁺ is shown in figure 5.8 B. There was no difference in the mean percentage of CD4⁺Tbet⁺ T-cells between normal chow and HFDIO infected mice. However, there was trend towards reduced number of CD4⁺Tbet⁺ T-cells in the HFDIO mice in comparison to the normal chow mice (figure 5.8 E and F).

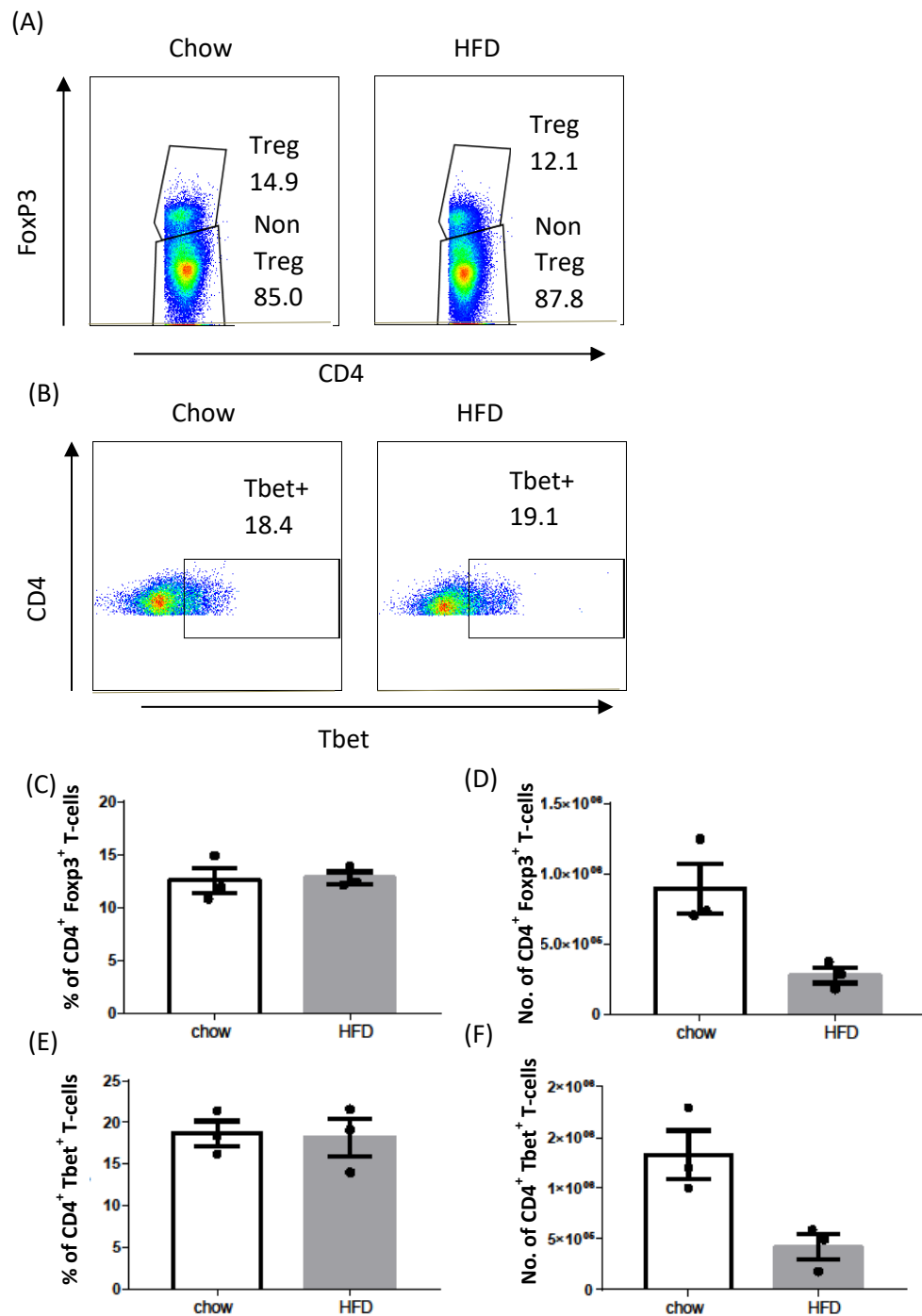


Figure 5-8: Analysis of CD4⁺FoxP3⁺ Tregs and CD4⁺Tbet⁺ T-cells in the mesenteric lymph nodes.

C57BL/6 mice were fed on normal chow or HFD for 12 weeks. The mice were then given a single low dose *T. muris* infection and sacrificed at day 21 post infection. Cells were extracted from the mesenteric lymph node and analysed by flow cytometry. Gating strategy: CD45, TCR β , CD4, FoxP3, Tbet. (A) Representative gating of CD4⁺FoxP3⁺ T-cells. (B) Representative gating of CD4⁺FoxP3⁺ T-cells. (C) Percentage of CD4⁺FoxP3⁺ T-cells. (D) Number of CD4⁺FoxP3⁺ T-cells. (E) Percentage of CD4⁺Tbet⁺ T-cells. (F) Number of CD4⁺Tbet⁺ T-cells. N= 3, results show mean \pm SEM.

5.2.4 TSLP gene expression in the caecum at day 21 post infection

Resistance in mice is associated with increased expression of TSLP and its receptor TSLPR. TSLP is involved in the early stages of the generation of protective Th2 immune responses against *T. muris* (Humphreys et al., 2008). The gene expression of TSLP in the caecum at day 21 post infection was compared between normal chow and HFDIO mice. A trend towards increased gene expression of TSLP was observed in both the normal chow and HFDIO infected mice in comparison to the naïve mice. However, there was no significant difference in the gene expression of TSLP between the groups (figure 5.9).

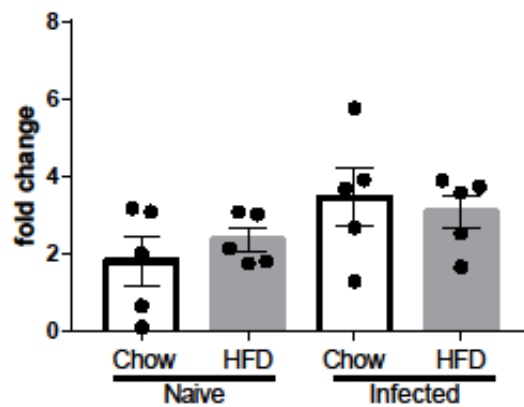


Figure 5-9: Comparison of TSLP expression in the caecum of between naïve and single dose infected mice.

C57BL/6 mice were fed on normal chow or HFD for 12 weeks. The mice were then given a single low dose of *T. muris* infection and sacrificed at day 21 post infection. Caecal tips were collected and frozen on dry ice. RNA was collected using the phenol-chloroform protocol. cDNA was prepared from the RNA and the expression of TSLP relative to the control gene, β -actin, was compared using qPCR. N= 5, results show mean \pm SEM.

5.2.5 Goblet cell responses and crypt depth measurements in the caecum

Resistance to *T. muris* is associated with goblet cell hyperplasia resulting in increased mucus production which facilitates worm expulsion (Hasnain et al., 2011b). The goblet cell response was compared between normal chow and HFDIO mice in order to investigate the effect of HFD on goblet cell response to *T. muris* infection.

Freshly collected caecal sections were fixed in Carnoy's solution before embedding in wax. Representative images of PAS/AB and Muc2 stained caecal sections collected at day 21 post infection are shown in figure 5.10 A. At 21 days post infection there were no detectable changes in the number of goblet cells and in the crypt depth measurements between naïve HFD or normal chow mice. In addition, *T. muris* infection did not result in an increase in the number of goblet cells or changes in crypt depth in both normal chow and HFDIO mice (figure 5.10 B and C).

Representative images of PAS/AB and Muc2 stained caecal sections collected at day 42 post infection are shown in figure 5.11 A. At day 42 post infection there was no difference in the number of goblet cells between naïve normal chow and HFDIO mice. However, there was an increase in the number of goblet cells in the infected mice. In particular, the HFDIO infected mice had significantly more goblet cells than their naïve counterparts. However, there is no difference in the mean number of goblet cells between infected normal chow and HFDIO mice (figure 5.11 B). Furthermore, there was no difference in the crypt depth measurements between all groups (figure 5.11 C).

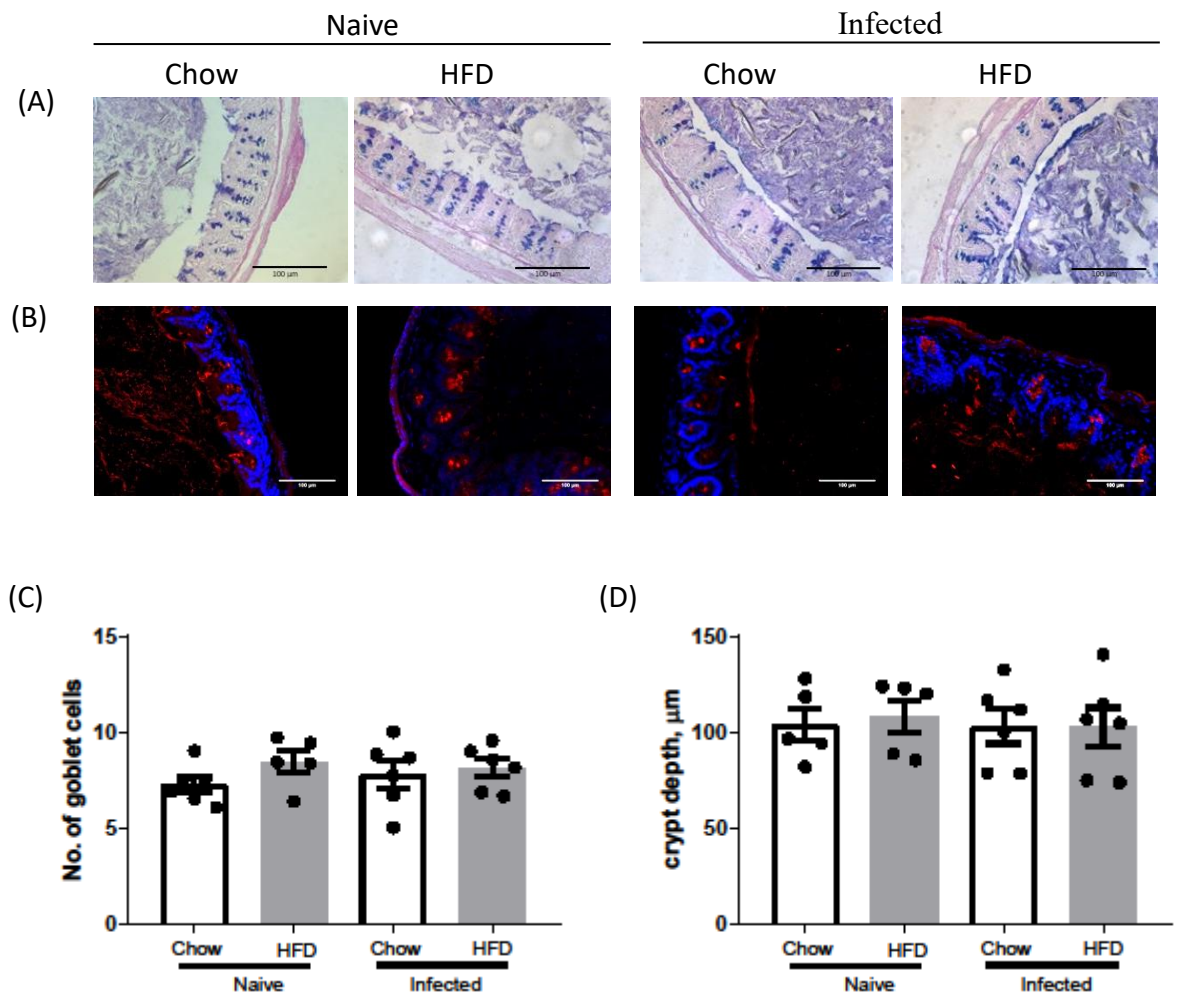


Figure 5-10: PAS/AB and Muc2 stained caecum sections from naïve and *T. muris* infected mice at day 21 post infection.

C57BL/6 mice were fed on normal chow or HFD for 12 weeks. The mice were then given a single low dose of *T. muris* infection and sacrificed at day 21. Freshly collected caecum sections were fixed in Carnoy's solution. Paraffin wax embedded sections were co-stained with periodic acid Schiff reagent (PAS) and alcian blue (AB). A separate set of sections were used for Muc2 immunofluorescence staining. (A) Representative images of PAS/AB stained caecum sections. (B) Representative images of Muc2 (red) and DAPI (blue) stained caecum sections. (C) Number of goblet cells per crypt at day 21 post infection. (D) Average crypt depth at day 21 post infection. x20 magnification, Bars = 100 μm . N= 5 to 6, results show mean \pm SEM.

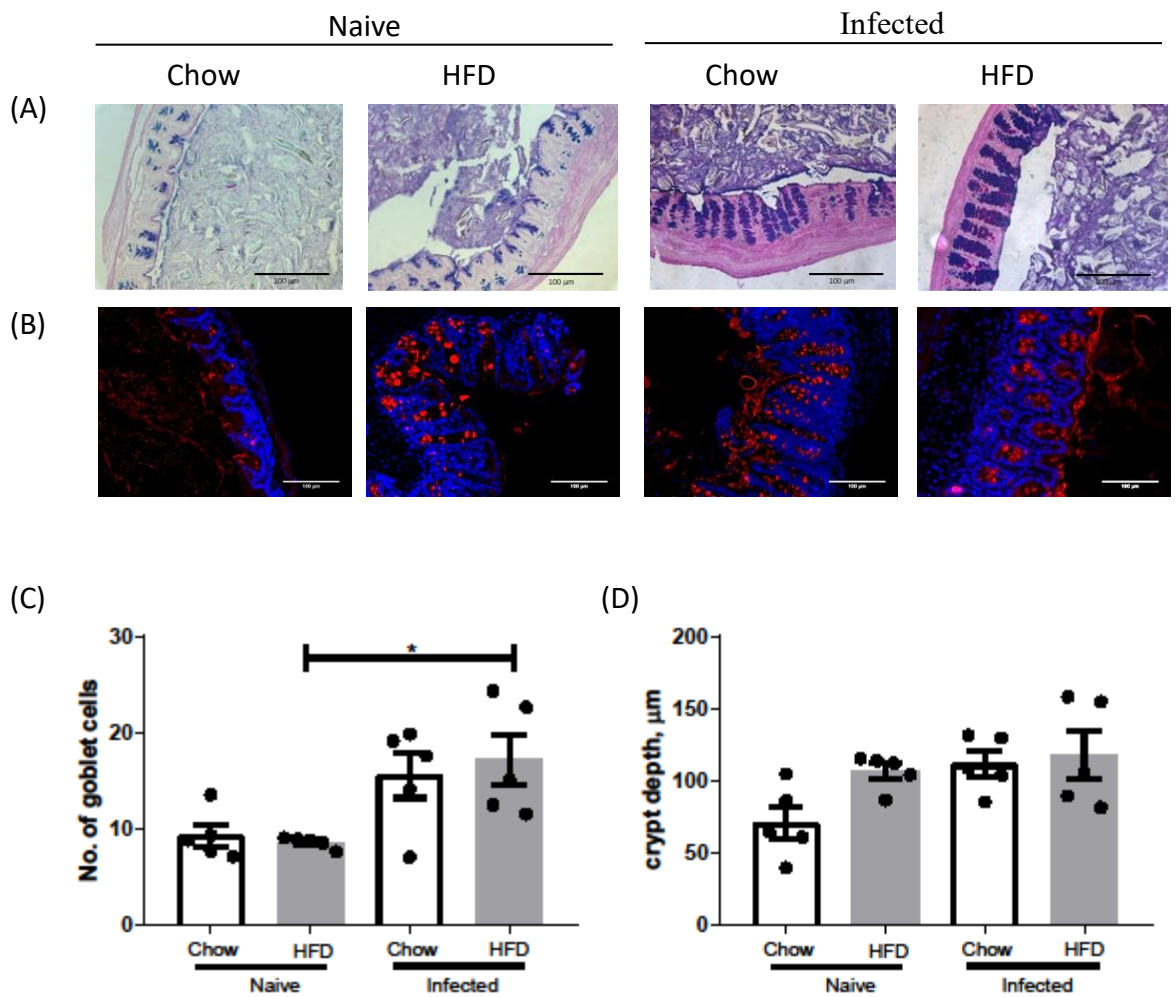


Figure 5-11: PAS/AB and Muc2 stained caecum sections from naïve and *T. muris* infected mice at day 42 post infection.

C57BL/6 mice were fed on normal chow or HFD for 12 weeks. The mice were then given a single low dose of *T. muris* infection and sacrificed at day 42. Freshly collected caecum sections were fixed in Carnoy's solution. Paraffin wax embedded sections were stained with periodic acid-Schiff and alcian blue. A separate set of sections were used for Muc2 immunofluorescence staining. (A) Representative images of PAS/AB stained caecum sections. (B) Representative images of Muc2 (red) and DAPI (blue) stained caecum sections. (C) Number of goblet cells per crypt at day 42 post infection. (D) Average crypt depth at day 42 post infection. x20 magnification, Bars = 100 μ m. N= 5, results show mean \pm SEM.

5.2.6 RELM β gene expression in the caecum at day 21 post infection

T. muris infection is associated with increased production of the antimicrobial protein RELM β which affects the chemotaxis of nematodes thus possibly facilitating worm expulsion (Artis et al., 2004). The expression of RELM β at day 21 post infection was compared between normal chow and HFDIO mice. There was a trend toward increased gene expression of RELM β in the naïve HFDIO in comparison to the normal chow mice, however, the difference in expression was not significant. In addition, there was no significant difference in the gene expression of RELM β between the infected normal chow and HFDIO mice (figure 5.12).

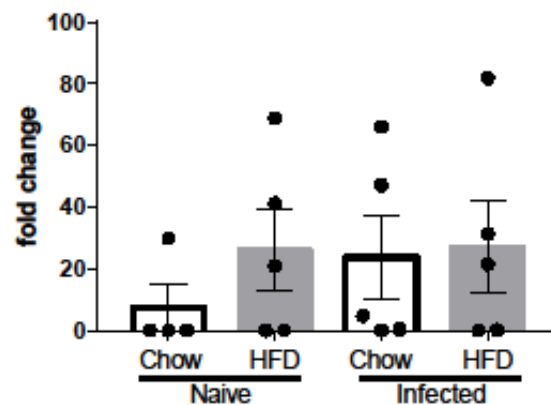


Figure 5-12: Comparison of RELM β expression in the caecum of between naïve and single dose infected mice.

C57BL/6 mice were fed on normal chow or HFD for 12 weeks. The mice were then given a single low dose of *T. muris* infection and sacrificed at day 21 post infection. Caecum tips were collected and frozen on dry ice. RNA was collected using the phenol-chloroform protocol. cDNA was prepared from the RNA and the expression of RELM β relative to the control gene, β -actin, was compared using qPCR. N= 5, results show mean \pm SEM.

5.2.7 The outcome of a low dose *T. muris* infection in normal chow and HFDIO C57BL/6 RAG^{-/-} mice

To investigate if the innate immune response played a role in the resistance observed in HFDIO mice, C57BL/6 RAG^{-/-} mice were used as they do not have mature T and B lymphocytes. C57BL/6 RAG^{-/-} mice were fed on either normal chow or HFD for 12 weeks. The mice were then given a low dose of *T. muris* and sacrificed at day 42 post infection.

I. Body weight and blood glucose levels of C57BL/6 RAG^{-/-} mice

RAG^{-/-} mice fed on a HFD gained weight faster than the RAG^{-/-} mice fed on normal chow and by day 42 post-infection, there was a trend towards increased body weight in the HFDIO RAG^{-/-} mice in comparison to the normal chow RAG^{-/-} mice (figure 5.13 A and B). There was also a trend towards increased weight of epididymal and subcutaneous fat pads in the HFDIO RAG^{-/-} mice in comparison to the normal chow RAG^{-/-} mice (figure 5.13 C and D). Blood glucose was significantly higher in the HFDIO RAG mice as compared to the normal chow RAG^{-/-} mice (figure 5.13 E).

II. Outcome of infection in normal chow and HFDIO RAG^{-/-} mice

The worm burden at day 42 post infection was compared between the normal chow and HFDIO RAG^{-/-} mice. Adult worms were recovered from normal chow and HFDIO RAG^{-/-} mice. However, there was a significant reduction in the mean number of worms recovered from the HFDIO RAG^{-/-} mice in comparison the normal chow RAG^{-/-} mice (figure 5.14).

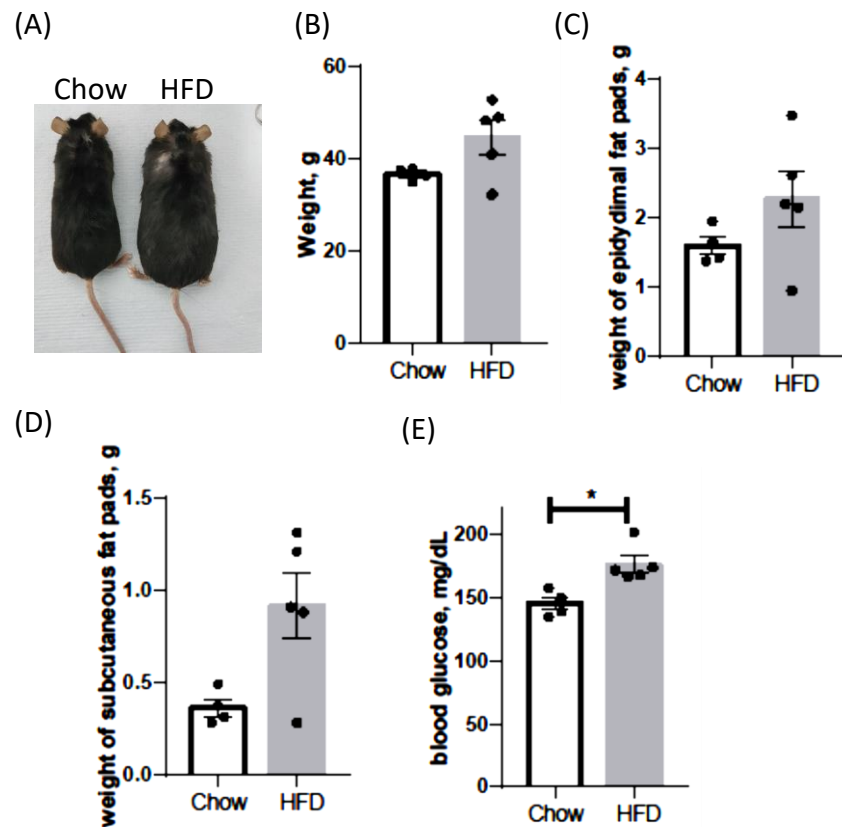


Figure 5-13: Body weight, fat pad weight and blood glucose measurements of C56BL/6 $RAG^{-/-}$ mice infected with a single low dose of *T. muris*.

C57BL/6 $RAG^{-/-}$ mice were fed on normal chow or HFD for 12 weeks. The mice were then given a single low dose of *T. muris* infection and sacrificed at day 42 post infection. (A) Representative images of normal chow mouse and HFDIO mice. (B) Final weight of mice. (C) Weight of epididymal fat pads. (D) Weight of subcutaneous fat pads. (E) Blood glucose in mg/dL measured immediately at the time of sacrifice. N= 5, results show mean \pm SEM.

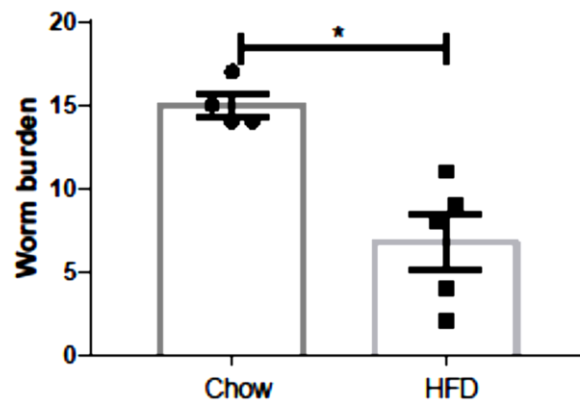


Figure 5-14: Outcome of a single low dose of *T. muris* infection in C57BL/6 RAG^{-/-} mice.

C57BL/6 RAG^{-/-} were fed on normal chow or HFD for 12 weeks. The mice were then given a single low dose of *T. muris* infection. Worm burden between normal chow and HFDIO mice was compared at day 42 post infection. N= 5, results show mean \pm SEM.

III. Caecal goblet cell responses and crypt depth measures in *T. muris* infected normal chow and HFDIO RAG^{-/-} mice

The number of goblet cells in the caecum and crypt depth was compared between the two groups. Representative images of PAS/AB stained sections are shown in figure 5.15 A. The mean number of goblet cells per crypt was significantly greater in the HFDIO RAG^{-/-} mice in comparison to the normal chow RAG^{-/-} mice (figure 5.15 B). In addition, there was a significant reduction in crypt depth in the HFDIO RAG^{-/-} mice in comparison to the normal chow RAG^{-/-} mice (figure 5.15 C).

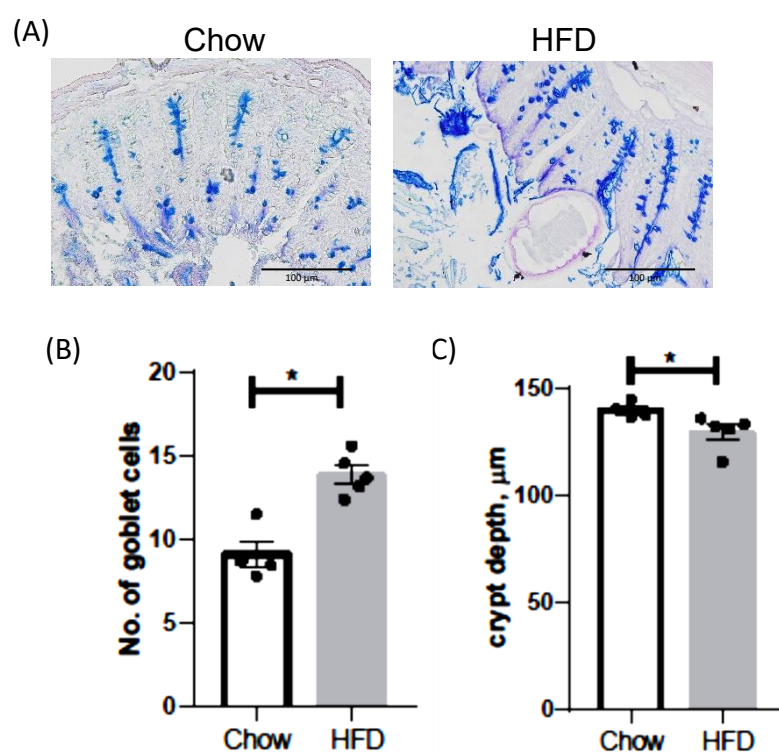


Figure 5-15: Comparison of PAS/AB stained caecum sections from normal chow and HFDIO C57BL/6 RAG^{-/-} mice.

C57BL/6 RAG^{-/-} were fed on normal chow or HFD for 12 weeks. The mice were then given a single low dose of *T. muris* infection and sacrificed at day 42 post infection. Freshly collected caecum sections were fixed in Carnoy's solution. Paraffin wax embedded sections were co-stained with periodic acid Schiff reagent and alcian blue. (A) Representative images of caecum sections collected from mice at day 42 post infection. (B) Number of goblet cells per crypt at day 42 post infection. (C) Average crypt depth at day 42 post infection. x20 magnification, Bars = 100 µm. N= 5, results show mean ± SEM.

5.2.8 Tuft cell responses at day 21 post infection in normal chow and HFDIO C57BL/6 mice

To further investigate the role of the innate immune response in the enhanced resistance against *T. muris* the number of tuft cells in normal chow and HFDIO mice was compared. Tuft cells produce the cytokine IL-25 which increases the number of ILC2s (von Moltke et al., 2016). Previous studies have shown that infection with helminths such as *N. brasiliensis* and *H. polygyrus* is associated with an increase in tuft cells (Gerbe et al., 2016; von Moltke et al., 2016)

To investigate if HFD was influencing tuft cell responses, the number of tuft cells in the jejunum, caecum as well as the colon of normal chow and HFDIO mice was compared at day 21 post infection. Tuft cells were identified as DCAMKL1⁺ cells and representative images are shown in figure 5.16. There was no difference in the number of tuft cells in the jejunum between naive and infected mice fed on either normal chow or HFD. There was also no difference in the tuft cell response in infected normal chow and HFDIO mice (figure 5.17 A). Similarly, in the caecum, there was no difference in the number of tuft cells between all the groups (figure 5.17 B). There was also no difference in the number of tuft cells in the proximal colon between normal chow and HFDIO naïve or infected mice (figure 5.17 C).

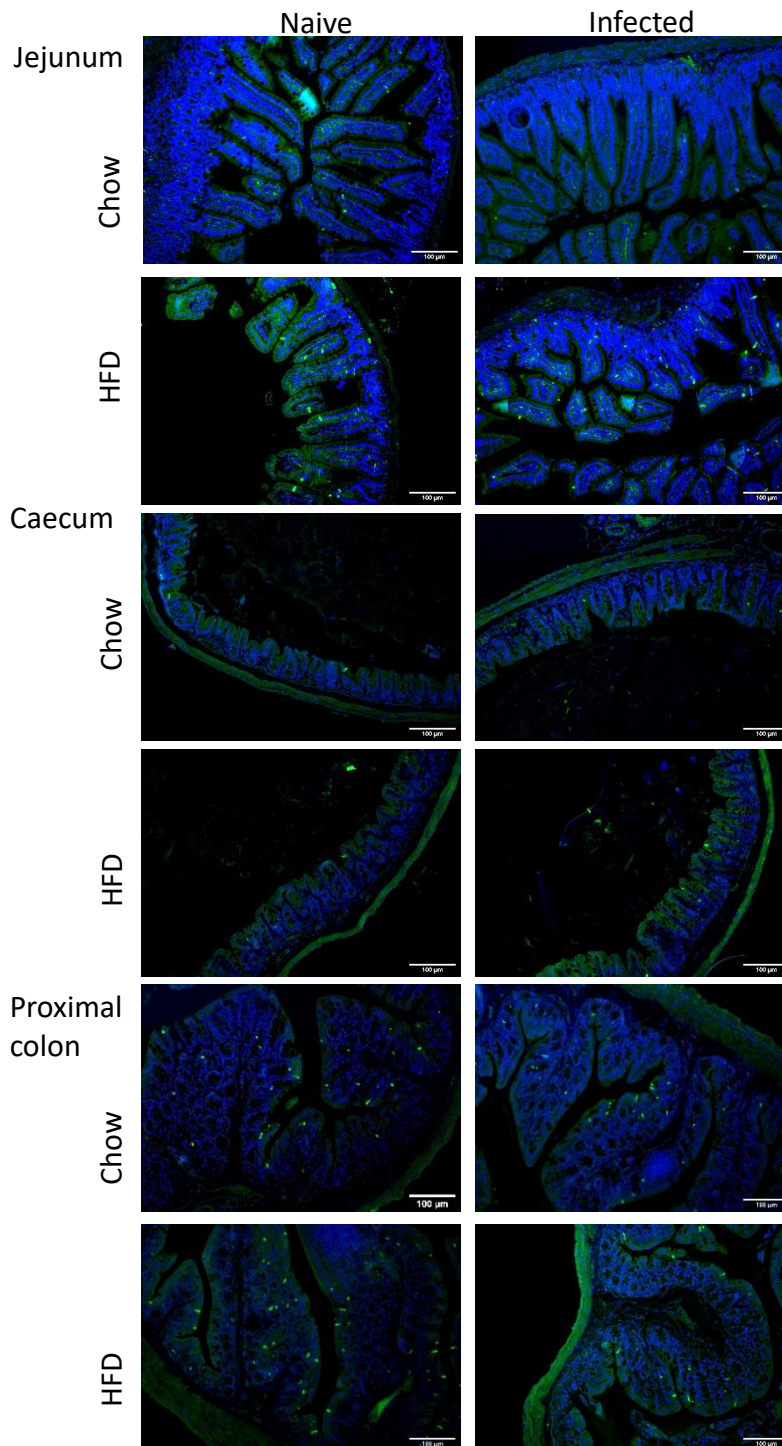


Figure 5-16: Representative images of tuft cell staining in the jejunum, caecum and colon.

C57BL/6 mice were fed on normal chow or HFD for 12 weeks. The mice were infected with *T. muris* and sacrificed 21 days post infection. Freshly collected jejunum, caecum and colon tissue were fixed NBF (caecum and colon sections were fixed in Carnoy's solution) and embedded in paraffin. 5 micron thick Sections were stained for Tuft cells using DCAMKL1 antibody (green) and nuclei were stained using DAPI to visualise the crypts (blue). Tuft cells were identified as DCAMKL1⁺ cells. X10 magnification, Bars = 100 μm.

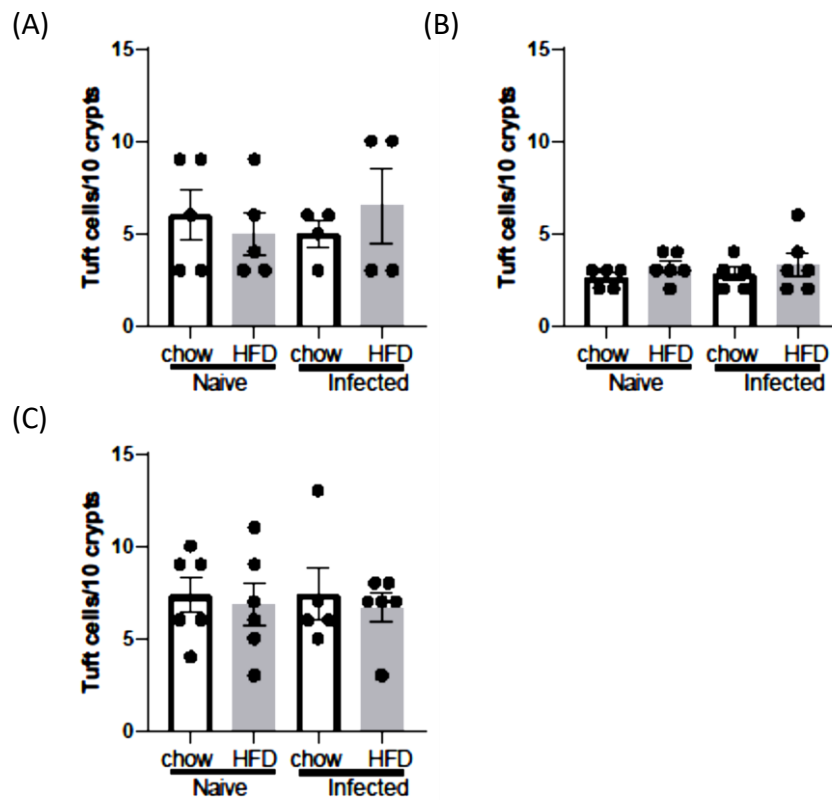


Figure 5-17: Comparison of the number of tuft cells in normal chow and HFDIO mice.

C57BL/6 mice were fed on normal chow or HFD for 12 weeks. The mice were infected with *T. muris* and sacrificed 21 days post infection. Freshly collected jejunum, caecum and colon tissue were fixed NBF (caecum and colon sections were fixed in Carnoy's solution) and embedded in paraffin. 5 micron thick Sections were stained for Tuft cells using DCAMKL1 antibody (green) and nuclei were stained using DAPI to visualise the crypts (blue). Tuft cells were identified as DCAMKL1⁺ cells. The number of tuft cells in 10 adjacent villi (jejunum) or crypts (caecum and proximal colon) was compared between the groups. (A) Jejunum. (B) Caecum. (C) Proximal colon. N = 4 to 6. Results shown as mean SEM.

5.2.9 Correlation between worm burden and weight of *T. muris* infected mice

In order to determine if adiposity had an influence on worm burden the relationship between worm burden and mouse weight was described using linear regression and correlation analysis.

At day 21 post infection, there was no correlation between worm burden and weight in the normal chow mice (figure 5.18 A). There was a negative trend in the relationship between worm burden and weight in the normal chow mice suggesting that as weight increases, the worm burden reduced. However, the correlation was not significant (figure 5.18 B). Similarly, at day 42 post infection, there was a negative trend in the relationship between worm burden and weight in both normal chow and HFDIO mice. However, the correlation in both groups was not significant (figure 5.19 A and B).

The relationship between worm burden and weight was also compared in the RAG^{-/-} mice. In both normal chow and HFDIO RAG^{-/-} mice there was a negative correlation between worm burden and weight. In the HFDIO RAG^{-/-} mice, the correlation was not significant whereas in the normal chow RAG^{-/-} mice the correlation was significant (figure 5.20 A and B).

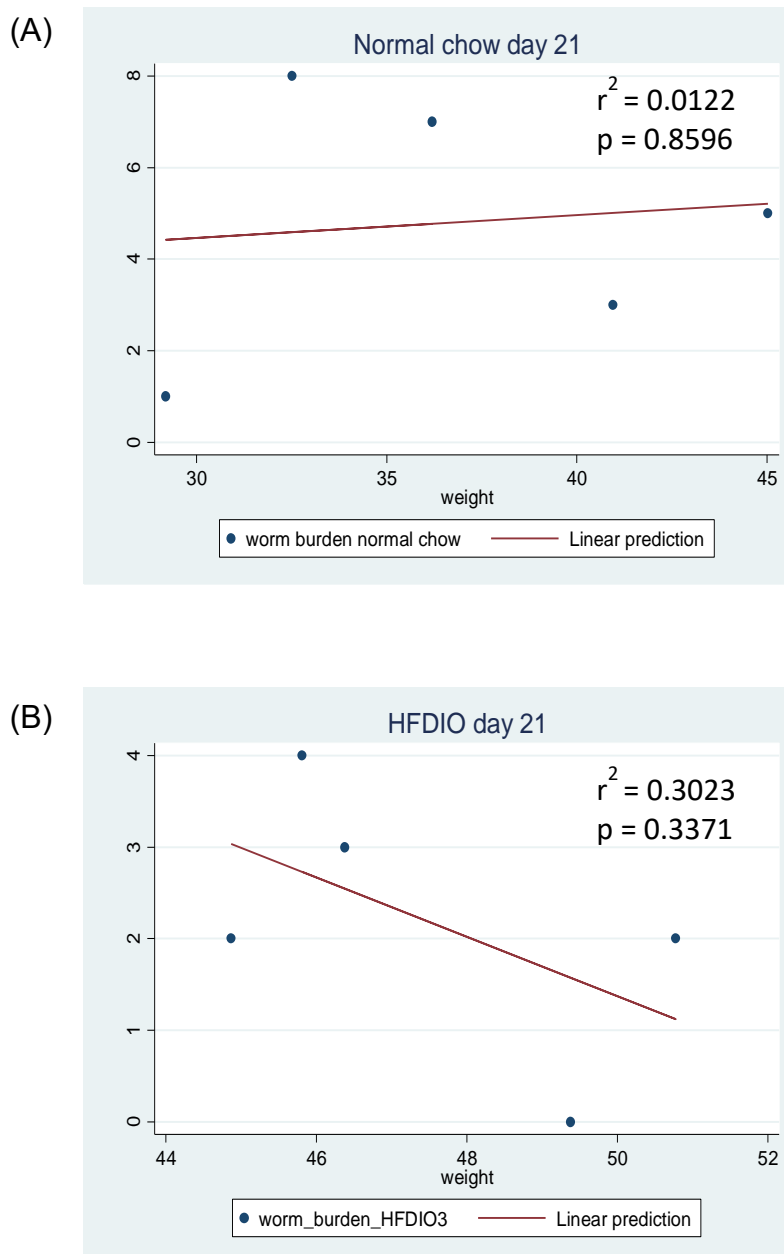


Figure 5-18: Regression analysis between the number of *T. muris* worms and mouse weight at day 21 post infection.

C57BL/6 mice were placed on either normal chow or HFD for 12 weeks. The mice were then given a single low dose *T. muris* infection mice and sacrificed at day 21 post infection. Regression analysis between worm burden and mouse weight: (A) Normal chow mice (B) HFDIO mice.

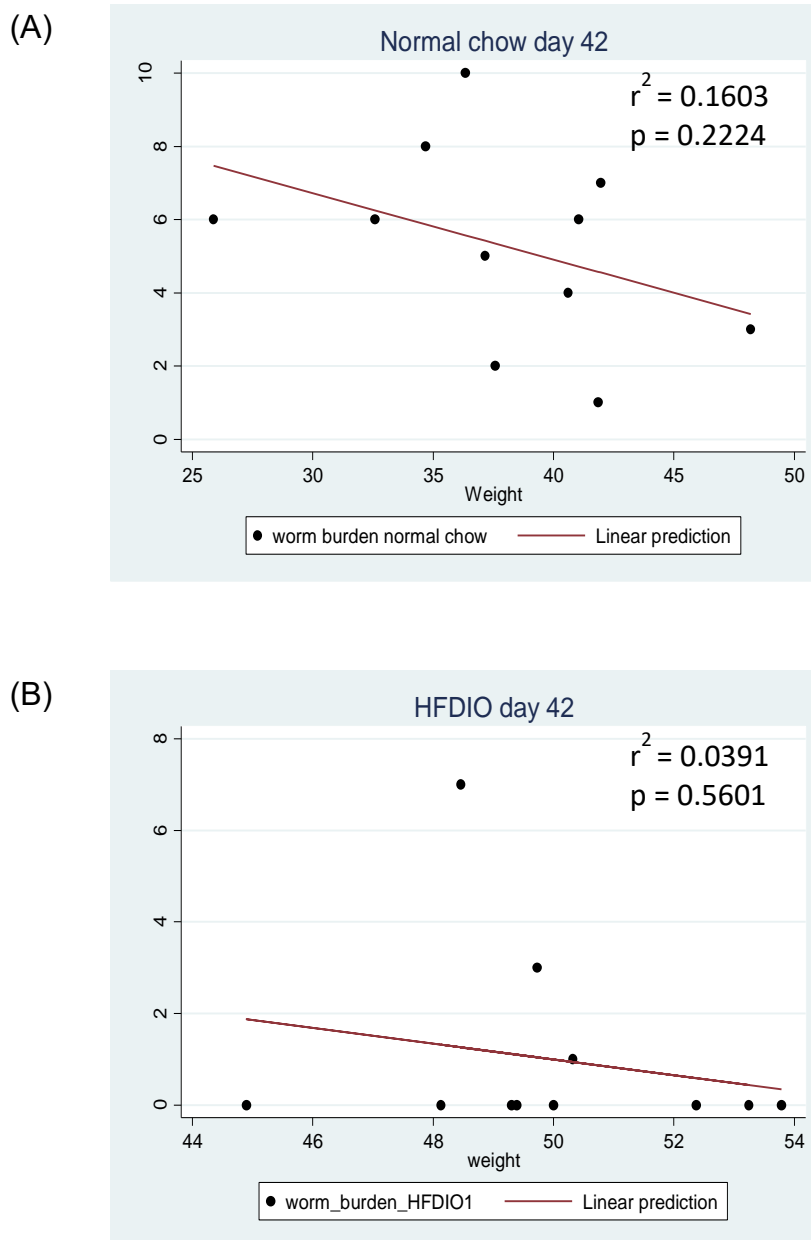


Figure 5-19: Regression analysis between the number of *T. muris* worms and mouse weight at day 42 post infection.

C57BL/6 mice were placed on either normal chow or HFD for 12 weeks. The mice were then given a single low dose *T. muris* infection mice and sacrificed at day 42 post infection. Regression analysis between worm burden and mouse weight: (A) Normal chow mice (B) HFDIO mice.

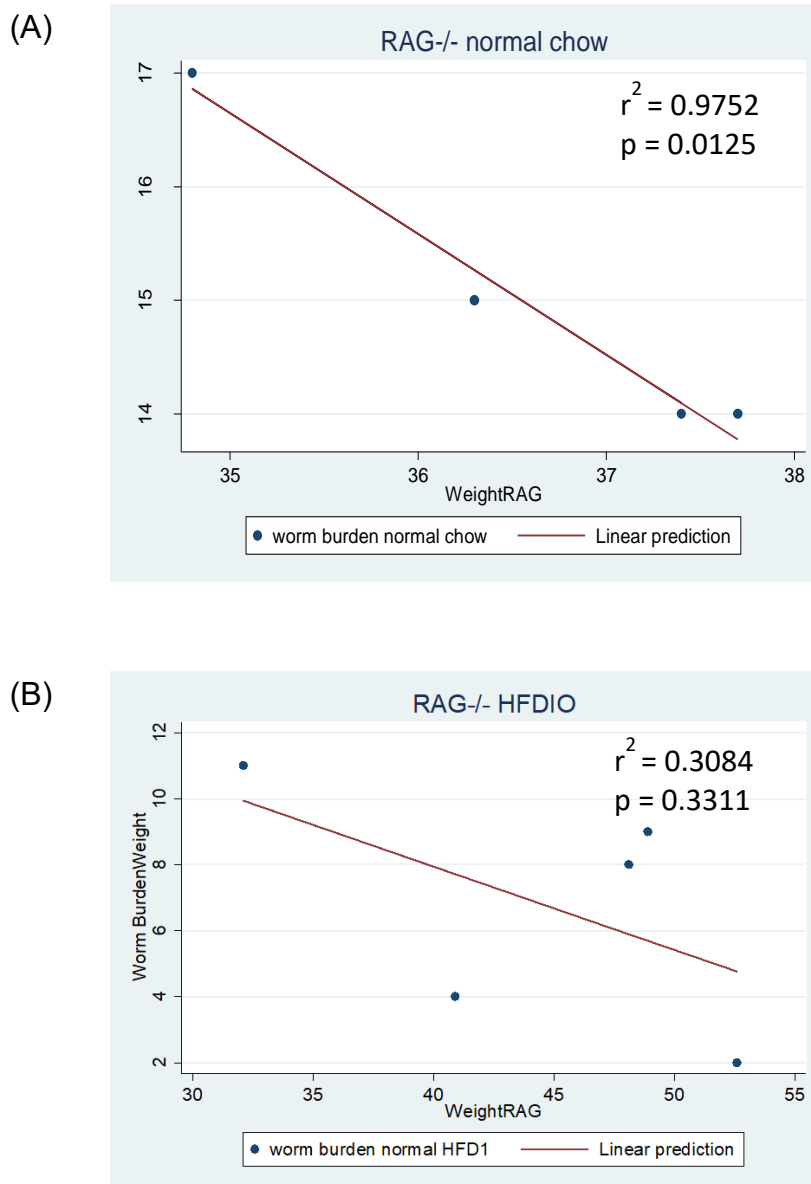


Figure 5-20: Regression analysis between the number of *T. muris* worms and mouse weight at day 42 post infection for normal chow and HFDIO C57BL/6 RAG^{-/-} mice.

C57BL/6 RAG^{-/-} mice were placed on either normal chow or HFD for 12 weeks. The mice were then given a single low dose *T. muris* infection mice and sacrificed at day 42 post infection. Regression analysis between worm burden and mouse weight: (A) Normal chow mice (B) HFDIO mice.

5.3 Discussion

In this chapter the mechanisms involved in the resistance to *T. muris* were investigated in order to determine what factors may be contributing to the reduced worm burden observed in the HFDIO mice. The reduced worm burden observed in the HFDIO mice could have been due to either failure of the worms to establish in the host or enhanced resistance of the host to infection.

5.3.1 HFD induced changes to the intestinal microbiota did not affect the ability of *T. muris* to establish in the host

HFD has been reported to induce changes in the host microbiota resulting in an increased ratio of *Firmicutes* to *Bacteroidetes* (Cani et al., 2008; Turnbaugh et al., 2006a). The work presented in this thesis showed that after 12 weeks of feeding there was a change in the bacterial composition of the HFDIO mice in comparison to the normal chow mice. Previous work has shown that interactions between *T. muris* eggs and the bacterial microbiota are important for the induction of parasite hatching resulting in the release of L1 larvae (Hayes et al., 2010). Eggs hatch to release L1 larvae in the caecum approximately 90 minutes post infection and by day 13 post infection L2 larvae which are embedded in the epithelium would be maturing into L3 larvae (Cliffe and Grecis, 2004; Wakelin, 1967).

In order to determine if the change in microbiota maybe influencing hatching of the *T. muris* eggs, the number of larvae recovered from normal chow and HFDIO mice given a high dose of *T. muris* infection were compared at day 13. There was no difference in the mean number of larvae recovered at day 13 from HFDIO in comparison to the normal chow mice. This suggests that the *T. muris* eggs were able to hatch and embed successfully in the HFDIO mice despite the shift in the microbiota. Hence, the difference in worm burden observed between HFDIO and normal chow mice was more likely due to enhanced resistance HFDIO mice to infection with the parasite.

5.3.2 HFD did not cause a significant shift in the faecal microbial population of *T. muris* infected mice at day 21 post infection

At day 21 post infection, there was a shift in the faecal microbial population in the infected normal chow mice in comparison to the naïve normal chow mice. However, the change was not significant. Previous studies have shown that *T. muris* can induce changes in the host microbiota between day 14 and 28 post infection, however the changes only become apparent at day 41 post infection (Holm et al., 2015; Houlden et al., 2015). At phylum level, chronic *T. muris* infection was associated with a reduction in *Bacteroidetes* and increase in *Firmicutes* (Houlden et al., 2015). Furthermore, *T. muris* infection was associated with an increase in lactobacilli which is suggested to play a role in modulating the host immune response thus favouring the survival of *T. muris* in the host (Holm et al., 2015).

A number of studies have shown that HFD induces changes to the microbial population in mice (Kim et al., 2012; Turnbaugh et al., 2006a; Zhou et al., 2017). At day 21 post infection, there was a shift in the microbial population between naïve normal chow and HFDIO mice. Similar to the normal chow mice, upon infection there was no significant change in the microbial population of the HFDIO mice. Furthermore, there was no significant difference in the microbial population between the infected normal chow and infected HFDIO mice. A recent study by Pace and co-workers investigated the changes in the microbiota of control and HFD fed mice which had been infected with the nematode *S. venezuelensis*. They reported that both control and HFD infected mice had an increased proportion of *Firmicutes* in comparison to their naïve counterparts. Furthermore, *S. venezuelensis* infection was associated with an increase in lactobacilli in both control and HFD fed mice (Pace et al., 2018). Taken together this suggests that diet does not limit the ability of helminths to modulate host microbiota.

One main limitation of DGGE analysis is that it does not provide details of the bacterial species therefore specific changes in the microbiota cannot be determined. 16 S sequencing of the DNA extracted from the faecal pellets is a more advanced technique which can identify different species and provides a more in-depth analysis of the microbiota. 16 S sequencing has been previously used to study in microbial changes in

T. muris infected mice (Holm et al., 2015; Houlden et al., 2015). Therefore, further work can be carried out using 16 S sequencing to determine microbial changes in the HFD induced obese mice at different time point after *T. muris* infection. DNA from faecal pellets collected at various time points such as day 14, day 28, day 42 and day 50 can be analysed to compare how microbiota changes with infection and after worm expulsion. This would provide more insight into the ability of *T. muris* to regulate host microbiome in obesity.

5.3.2 HFD influences T-cell specific responses which alters the balance of Th1/Th2 responses

T-cells are required for the generation of adaptive immune response and produce cytokines in response to different to the signals they receive. Cells from the mesenteric lymph nodes of infected HFDIO mice showed a trend toward increased production of Th2 cytokines upon re-stimulation with *T. muris* derived E/S. Antibody mediated T-cell receptor stimulation via CD3 and co-stimulation with anti-CD28 was used to further investigate T-cell specific responses. Katagiri and co-workers investigated the effect of HFD on T-cell responses to different stimulants. They reported that re-stimulated T-cells from HFD fed mice treated with the irritant TNCB produced lower levels of both IFN- γ and IL-4 (Katagiri et al., 2007). However, when they compared the cytokine responses of cells collected from HFD or control mice challenged with ovalbumin they observed no difference in IFN- γ production (Katagiri et al., 2007). This suggests that the effect of HFD on T-cell responses is dependent on the antigen or stimulant. In the current study, T-cells from *T. muris* infected HFDIO mice produced higher levels of Th2 associated cytokines in comparison to T-cells from normal chow mice. On the other hand, the T-cells from HFDIO mice generally produced less inflammatory cytokines as compared to the normal chow mice. This reinforces the notion that HFD has an effect on T-cell responses which in turn alters the balance of the Th1/Th2 immune response upon exposure to antigen.

TSLP is a cytokine that promotes Th2 immune responses and is constitutively expressed in the skin, lungs and gut (He and Geha, 2010). In addition, Turcot and colleagues showed that TSLP was expressed in visceral adipose tissue and that the expression of TSLP is significantly reduced in severely obese individuals (Turcot et al., 2012). The association

between TSLP and HFD induced obesity has also been shown by studies in mice. Silva and colleagues reported that obesity did not alter the levels of TSLP in the lung although obese mice produced lower levels of TSLP in response to ovalbumin challenge as compared to control mice (Silva et al., 2017). In another study, Wu and colleagues reported that HFD feeding increased serum levels of TSLP in apolipoprotein knockout mice on a C57BL/6 background which are used to model atherosclerosis (Wu et al., 2014). The effect of HFD on the production of TSLP in the intestine has not been described. The data presented in this chapter show that there was no significant difference in the gene expression of TSLP between normal chow and HFDIO mice. At day 21 post infection, there was a slight increase in TSLP expression in the infected mice, however there was no difference between normal chow and HFD mice. Previous work has shown that by TSLP gene expression was elevated in response to *T. muris* infection in resistant mice by day 7 post infection whereas TSLP expression was unchanged in susceptible mice (Humphreys et al., 2008). Therefore, in order to fully appreciate the effect of HFD on TSLP expression in *T. muris* infected mice additional time points early in infection would need to be investigated. Alternatively, the cytokine response and worm burden at day 21 can be investigated in TSLPR KO mice which have been fed on a HFD, or neutralising TSLP in HFD fed mice, and then administering a low dose of *T. muris* infection so as to determine if TSLP plays a critical role in enhancing the TH2 response in HFD fed mice.

The population of CD4⁺FoxP3⁺ Tregs was also compared between normal chow and HFDIO mice. There was no difference in the percentage of Treg between the normal chow and HFDIO mice. However, there was a trend towards a reduction in the number of Tregs in the HFDIO mice. Previous work has shown that Treg depletion early in infection resulted in increased worm expulsion and improved histopathology in the intestine (D'Elia et al., 2009a). In a separate study, the depletion of Tregs by the injection of diphtheria toxin into DERE mice on C57BL/6 background did not result in enhanced *T. muris* worm expulsion (Worthington et al., 2013a). In addition, the adoptive transfer of Tregs into resistant mice did not result in increased susceptibility to *T. muris* (Worthington et al., 2013a). Therefore, the role of Tregs in the protection against *T. muris* is not yet fully understood.

Furthermore, there was no difference in the percentage of CD4⁺Tbet⁺ T-cells between normal chow and HFDIO mice. Similar to CD4⁺FoxP3⁺ T-cells there was also a trend

towards reduced number of CD4⁺Tbet⁺ T-cells in the HFDIO mice. CD4⁺ T-cells that lack in the transcription factor Tbet have reduced ability to produce IFN- γ which is one of the predominant cytokines produced in Th1 immune responses (Szabo et al., 2002). Long term *T. muris* infection is associated with a reduction in the population of FoxP3⁺ Tregs in the lamina propria and Tbet⁺ Th1 cells in the epithelium (Holm et al., 2015; Houlden et al., 2015). Therefore, more works needs to be carried out to study the role of FoxP3⁺ Tregs and Tbet⁺ Th1 cells in the regulation of *T. muris* infection, and if HFD induced changes in FoxP3⁺ Tregs and Tbet⁺ Th1 cell population would contribute to the enhanced resistance observed in the HFDIO mice.

5.3.3 HFDIO alters CD4 T-cell responses which are important in driving mechanisms of resistance against *T. muris* infection

HFD affects the balance of Th1 and Th2 immune responses which define the immune responses to *T. muris* infection (Else et al., 1992). A key maker of chronic *T. muris* infection is the elevated production of INF- γ by Th1 CD4 T-cells which is associated with increased inflammation and hyper proliferation of epithelial cells (Artis et al., 1999b). Increased turnover of the epithelium under the control of IL-13 is required for dislodging worms embedded in the epithelium thus facilitating worm expulsion (Cliffe et al., 2005). IFN- γ is associated with reduced epithelial turnover (Cliffe et al., 2007). The number of IFN- γ producing CD4 T-cells was significantly less in HFDIO mice in comparison to normal chow mice. Further investigations need to be carried out to determine if this would be associated with increased levels of epithelial turnover in the HFDIO mice which might be facilitating worm expulsion.

The production of IL-13 by T-cells was also compared because IL-13 is a critical cytokine required for resistance to *T. muris* (Bancroft et al., 1998). Flow cytometry analysis of intracellular IL-13 was not successful; however, there was a trend towards increased IL-13 production upon re-stimulation with E/S or CD3/CD28 activation from cells collected from the mesenteric lymph nodes of HFDIO mice. The increased production of IL-13 is associated with the increase in the number of caecal goblet cells which results in increased mucus production in resistant mice (Hasnain et al., 2011b; McKenzie et al.,

1998). In spite of the elevated IL-13 production, there was no observed increase in the number of goblet cells at day 21 post infection in the HFDIO mice. A previous study by Hayes and co-workers reported that C57BL/6 treated with recombinant TNF- α had increased production of IL-13 but no observed increase in the number of goblet cells. They suggested that one reason for this could be that the mice also produced increased levels of IFN- γ which might have affected the immune response (Hayes et al., 2007). The HFDIO mice produced IFN- γ although it was less than the normal chow mice. However, this might have still affected the development of protective immune responses.

HFD alone has been shown to increase the number of goblet cells in the colon (Mastrodonato et al., 2014). In contrast, Gulhane and colleagues reported no difference in colonic PAS/AB and Muc2 staining of HFD fed mice (Gulhane et al., 2016; Mastrodonato et al., 2014). In addition, other studies have shown that HFD is associated with a reduction in goblet cells in the small intestine and caecum (Hamilton et al., 2015; Lee et al., 2017). No difference in the number of goblet cells was observed between normal chow and HFDIO naïve mice. At day 42 post infection there was an increase in the number of goblet cells in the infected mice which was observed in both normal chow and HFDIO mice. Overall this suggests that HFD may not be significantly affecting the goblet cell responses in *T. muris* mice.

RELM β is an antimicrobial protein also derived from intestinal goblet cells. HFD has been associated with increased levels of RELM β in the serum which was attributed to increased expression in the colon and is believed to contribute to hepatic insulin resistance (Rajala et al., 2003; Shojima et al., 2005). There was a trend towards increased RELM β in the naïve HFDIO mice although the difference was not significant. In line with this, a study by Fujio and colleagues also reported a trend towards increased colonic RELM β in HFD mice whereas mice fed on protein or carbohydrate rich diets had significant reduction in colonic RELM β . Therefore, host nutrition has an effect on RELM β expression (Fujio et al., 2008). Upon infection there was no significant increase in RELM β expression at day 21 post infection in both normal chow and HFDIO mice. Previous work has also shown that there is no significant increase in RELM β expression in mice that are susceptible to *T. muris* infection whereas resistant mice had elevated RELM β expression by day 16 post infection (Artis et al., 2004). However, RELM β is not a critical factor in the resistance against *T. muris* as RELM β deficient mice are still capable of expelling worms (Nair et al.,

2008). Taken together this suggests that RELM β did not play a significant role in the resistance to *T. muris* infection observed in the HFDIO mice.

5.3.4 Resistance to a low dose of *T. muris* in HFDIO mice is also observed in the absence of the adaptive immune response

To study if other factors apart from the adaptive immune response also contributed to the resistance observed in the HFDIO mice, obesity was induced in RAG^{-/-} mice which were then given a single low dose of *T. muris* infection. RAG^{-/-} mice do not have mature T and B lymphocytes and are susceptible to *T. muris* infection (Owyang et al., 2006). The data presented in this chapter showed that the mean number of worms recovered from the HFDIO RAG^{-/-} mice was significantly lower in comparison to normal chow fed RAG^{-/-} mice. This suggests that innate immune responses are contributing to the resistance observed in the HFDIO mice. Furthermore, an increase in the number of goblet cells was observed in the HFDIO RAG^{-/-} mice as compared to the normal chow RAG^{-/-} mice. As previously mentioned, IL-13 regulates goblet cell responses, therefore apart from CD4 T-cells, HFDIO RAG^{-/-} mice must have another source of IL-13 that is inducing the increase in the number of goblet cells. Group 2 innate lymphoid cells (ILC2s) are involved in immunity against gastrointestinal nematodes and have been shown to play important roles in the protection against *N. brasiliensis* as well as *H. polygyrus* (Gerbe et al., 2016; von Moltke et al., 2016). In contrast, the number of ILCs does not increase in *T. muris* infected mice and the depletion of ILC2s does not impair the immunity to *T. muris* indicating that ILC2s do not play a significant role in the protection against *T. muris* (Glover, 2017). However, Spencer and co-workers reported that in Vitamin A deficient mice, an increase in the number of ILC2s mediated immunity to *T. muris* in RAG^{-/-} mice (Spencer et al., 2014). In addition, upon activation ILC2s take up more fatty acids and preferentially utilise fatty acid oxidation to meet their metabolic requirements (Wilhelm et al., 2016). These studies highlight the dynamic adaptation of ILC2s under nutritional stress in order to maintain host immunity. Therefore, it is possible that in response to the HFD, there might be an increase in the number of ILC2 in the HFDIO mice which enhance the resistance to *T. muris*.

5.3.5 HFD had no effect on the number of intestinal tuft cells

Recent studies have shown that an increase in ILC2s during helminth infection is due to increased number of tuft cells (Gerbe et al., 2016; von Moltke et al., 2016). The regulation of tuft cells by HFD has not been well defined. A recent study by Aladegbami and colleagues reported that mice fed on a liquid diet which consisted of 35 % fat, 47 % carbohydrate and 17.3 % protein expelled the protozoa, *Tritrichomonas muris* (Tm), which resides in the small intestine (Aladegbami et al., 2017). Tuft cells drive type 2 immune responses against Tm infection. However, in the study it was reported that even after the mice had undergone small bowel resection which led to a reduction in the number of tuft cells, the mice which had to be fed on the liquid diet after the operation cleared the Tm infection (Aladegbami et al., 2017). In this study there was no difference in the number of tuft cells between normal chow and HFDIO naïve mice in jejunum, caecum and proximal colon. Furthermore, *T. muris* infection did not result in an increase in tuft cells in neither normal chow nor HFDIO mice in the jejunum, caecum and proximal colon. This agrees with previous work which showed that there was no difference in the number of tuft cells in the jejunum and caecum between naïve and *T. muris* infected mice (Glover, 2017). Overall these results show that both HFD and *T. muris* infection do not increase the number of tuft cells in the intestine suggesting that tuft cells may not be playing an important role in the resistance against *T. muris*.

5.3.6 There was no clear correlation between worm burden and mouse weight

In chapter 3 the body weight and fat mass of the mice after long-term HFD feeding was variable which is consistent with results from previous studies (Koza et al., 2006; Yang et al., 2014). In addition, the variability in body weight and fat mass was also observed in the normal chow mice. In line with this observation Koza and colleagues reported that variations in body weight occur even in mice fed on low fat diet due to differences in epigenetic mechanisms which also make some mice more susceptible to diet induced obesity (Koza et al., 2006).

In order to determine if the degree of adiposity had an effect on the outcome of infection regression and linear correlation between worm burden and weight was calculated. There was no significant correlation between worm burden and weight in normal chow and HFDIO mice. There was also no significant correlation between worm burden and weight in the RAG^{-/-} HFDIO mice. However, there was a significant correlation between worm burden and weight in the RAG^{-/-} normal chow. Altogether even though the regression analysis indicated there was a negative relationship between worm burden and weight, no clear correlation was evident for most of the groups. This suggests that adiposity alone cannot account for the difference in worm burden. The negative correlation between worm burden and weight seems to be more apparent in the normal chow mice in comparison to the HFDIO mice. However, this could be because at the selected time points, most of the HFDIO mice had already expelled worms or had very low worm burdens which would result in a weak correlation.

5.4 Conclusion

The results in this chapter indicate that:

1. HFDIO did not affect the ability of *T. muris* to establish in the host.
2. *T. muris* infection did not result in significant changes in the host microbiota in both normal chow and HFDIO mice at day 21 post infection.
3. T-cells from HFDIO *T. muris* infected mice showed a trend towards increased production of Th2 cytokines and reduced production of Th1 cytokines in comparison to T-cells from normal chow *T. muris* infected mice.
4. There was no difference in the number of goblet cells and RELM β expression between normal chow and HFDIO *T. muris* infected mice.
5. The innate immune response contributes to the enhanced resistance to *T. muris* infection that is observed in HFDIO mice
6. There was no difference in the number of tuft cell between normal chow and HFDIO *T. muris* infected mice.
7. There was no clear correlation between worm burden and weight in the normal chow and HFDIO mice.

Chapter 6 : General Discussion

It is estimated that at least 464 million people worldwide are infected with *T. trichuria* (Pullan et al., 2014). Infections are prevalent in Sub-Saharan Africa and Asia due to the warm and moist environment, where the lack of adequate sanitary facilities and poor hygiene practises increases the risk of infection especially in rural and peri-urban communities. People in developing countries now have additional burden of diet related diseases due to the adoption of new diets that contain high levels of refined sugar and fat (Popkin, 2006). Lifestyle habits such as lack of exercise and cultural beliefs that weight is a status symbol has led to an increase the prevalence of obesity.

T. muris infection in mice provides a good model to study the immune response to *T. trichuria* (Foth et al., 2014; Roach et al., 1988). Previous work has shown that the outcome of *T. muris* infection in mice can be altered by changing the dose of infection. When C57BL/6 mice are given a high dose infection, they develop a resistant Th2 immune response. On the other hand, when given a low dose infection the mice develop a Th1 immune response which results in the development of chronic infection (Bancroft et al., 1994b; Bancroft et al., 2001). Naturally the risk of repeated exposure to infection is very high. Therefore in order to reflect natural infections, repeated low dose infections are administered to mice and these are referred to as trickle infections (Wakelin, 1973). During the course of trickle infection, the parasitic burden increases in C57BL/6 mice until a threshold level of infection is reached. Above this threshold expulsion is induced as immunity occurs (Bancroft et al., 2001; Glover, 2017).

C57BL/6 mice have also provided a good model to study the development and progression of HFD induced obesity. When fed on a HFD, C57BL/6 mice become overweight, have elevated blood glucose levels and develop fatty liver disease as a result of increased deposition of fat in the liver (Rebuffé-Scrive et al., 1993; Surwit et al., 1995). These characteristics of HFD mice are features of metabolic syndrome which increase the risk of cardiovascular disease and type II diabetes (Lee and Pratley, 2005).

In this study the progression of single and trickle low dose *T. muris* infection in C57BL/6 mice was investigated in normal chow and HFDIO mice. Furthermore, the effect of HFD on the outcome of *T. muris* infection was investigated.

6.1 HFD induced obesity induces early expulsion of *T. muris* worms

The most significant finding to emerge from this study was that HFDIO mice had enhanced resistance to a single and trickle low dose of *T. muris* infection in comparison to normal chow mice. Low dose *T. muris* infections normally result in chronic infections (Bancroft et al., 1994b; Bancroft et al., 2001). Surprisingly, the HFDIO mice showed a trend in worm expulsion by day 21 post infection after a single low dose infection. By day 42 post infection most of the HFDIO mice had completely expelled the worms unlike the normal chow mice which developed chronic infections. The ability to expel worms earlier was observed even after the mice were pre-fed on a HFD for only 3 weeks. In addition, when the HFDIO mice were given trickle infections, the mice had expelled all the worms by week 9 following 7 weeks of trickle infections. Previous work has shown that the number of worms builds up during the course of infection. However after 7 weeks of trickle infection, the mice start to expel worms as they develop resistance and after 9 weeks of trickle infection, the mice have a much lower worm burden (Glover, 2017). Therefore, the HFDIO expelled much earlier than would have been expected which further supports the idea of the HFDIO mice having enhanced resistance against *T. muris*. Furthermore, correlation of body weight to worm burden at days 21 and 42 post infection indicated that the degree of obesity did not influence the outcome of infection.

The production of parasite specific antibodies has been shown to correlate with worm expulsion kinetics (Koyama and Ito, 1996; Koyama et al., 1999). Assessment of the levels of parasite specific antibodies indicated that the single dose infected HFDIO mice had elevated parasite specific IgG1 which is associated with resistance, whereas the normal chow fed mice had elevated levels of IgG2a/c. Trickle infected mice had elevated IgG1 and IgG2a/c which has been previously described as mixed antibody response (Bancroft et al., 2001). However, there was a significant reduction in IgG2a/c in the HFDIO mice in comparison to the normal chow mice which correlates with the observation that the mice had expelled the worms. These findings indicate that HFDIO is protective against *T. muris* infection.

How these findings relate to human whipworm infection is not known. However, in communities where helminth infections are endemic, people are at high risk of infection with other types of gastrointestinal pathogens. Preliminary investigations indicated that

the HFDIO had no effect on the outcome of *H. polygyrus* infection in mice (Personal communications, Colombo 2018). In contrast, *S. mansoni* parasites thrived in the cholesterol-rich environment induced by HFD ensuring reproductive success of the adult worms. Furthermore, the intestinal, liver and faecal egg counts were significantly higher in the HFD mice in comparison to the standard chow mice (Alencar et al., 2009; Neves et al., 2007). Taken together these studies suggest that the effect of HFD has different effects on the outcome of infection for different parasites. One main thing to note is that these studies were carried out in controlled environments where mice only faced the challenge of a single parasite species. Therefore, this raises important questions on how obesity may influence the dynamics of infection when more than one type of parasite is present which is a common occurrence for people living in endemic areas.

In chapter 4, it is shown that even a 3 week HFD pre-treatment pushed the HFD fed mice towards resistance. Further investigations were carried out to determine if 3 weeks of HFD feeding could induce resistance in mice if the mice were started on diet at different time points after infection. Interestingly when mice already infected with *T. muris* were started on a HFD at day 13 post infection there was no difference in worm burden at day 31 post infection in comparison the normal chow mice. Similarly, when mice were started on a HFD at day 31 post infection, they developed chronic infection and there was no difference in the number of worms recovered at day 52 post infection between normal chow and HFD mice. This implies that HFD feeding before infection induces changes in the host which are protective against *T. muris*. Hence it is possible that if the infected mice were left on a HFD for a longer period beyond day 52, there could be a significant reduction in worm burden in the HFD fed mice in comparison to the normal chow mice as they start to develop features of obesity.

In this study the effect of HFD on the growth and fertility of *T. muris* parasites was not investigated in detail. The faecal egg count in normal chow and HFDIO mice was checked in weeks 8, 9 and 11 in the trickle infected mice at which point the mice would have been expected to have mature adult worms. Whereas eggs were recovered in the normal chow mice, there were no eggs recovered from the HFDIO mice therefore the effect of HFD on egg production of *T. muris* parasites could not be assessed. However, other studies have shown that HFD can directly affect the growth and fertility of worms. *S. mansoni* infected mice fed on a HFD had an increased egg load which was attributed to elevated serum

cholesterol which induces egg production during embryogenesis among female *S. mansoni* parasites (Neves et al., 2007). On the other hand, *S. mansoni* worms in under-nourished mice had stunted development and the mice had milder chronic lesions in contrast to well fed mice (Coutinho et al., 2003; Oliveira et al., 2003). HFD has also been shown to affect the dry weight of the intestinal fluke *E. caproni* and lower uterine egg numbers were observed in HFD fed mice in comparison to the control diet mice (Sudati et al., 1996). Therefore, further research should be done to compare egg counts between normal chow and HFDIO *T. muris* infected mice. This can be done between days 32 and 42 so as to ensure the egg production can be compared just as the worms start to mature until they are expelled in the HFDIO mice. In addition, more work can be done to explore if HFD directly affects the growth of *T. muris* parasites by carrying out morphometric analysis of worms recovered from HFD mice.

Taken together, these findings showed that HFD enhanced host resistance to *T. muris* infection. The resistance was only observed in mice that have been fed on a HFD before infection, whereas mice that were already infected before starting on a HFD did not show enhanced resistance, at least at over the time-course studied.

6.2 HFD induced obesity skews T-cells towards a Th2 immune response

Low dose *T. muris* infection results in chronic infection which is characterised by increased production of Th1 cytokines. On the other hand, resistance is associated with increased production of Th2 cytokines IL-4, IL-9 and IL-13 (Else et al., 1994). In the current study, E/S re-stimulated cells from the mesenteric lymph nodes collected from HFDIO mice showed a trend towards increased production of Th2 cytokines and lower levels of pro-inflammatory cytokines such as IFN- γ , IL-6 and IL17A. The same pattern in cytokine production was observed in the T-cell specific activation assay after CD3/CD28 stimulation to enhance cytokine production. Furthermore, there was a significant reduction in the number of INF- γ ⁺CD4⁺ T-cells in the mesenteric lymph nodes. In the lamina propria there was a reduction in the number of INF- γ ⁺CD4⁺ T-cells, although this was not significant.

Further work was carried to investigate what could be driving the Th2 response in the HFDIO mice. TSLP is a cytokine that promotes the Th2 immune response and is elevated in early stages of *T. muris* infection in resistant mice (Humphreys et al., 2008). HFD has also been associated with elevated levels of TSLP in the serum (Wu et al., 2014). In this study there was no difference in TSLP gene expression in the caecum between HFDIO and normal chow infected mice at day 21 post infection. The expression of T-bet in CD4⁺ T-cells was also compared as T-bet expression promotes Th1 immune responses and the production of IFN- γ (Szabo et al., 2002). There was no difference in the percentage of CD4⁺T-bet⁺ T-cells between HFDIO and normal chow mice although there was a reduction in number of CD4⁺T-bet⁺ T-cells in the HFDIO mice. A similar trend was also observed in the percentage and number of CD4⁺ FoxP3⁺ Tregs between HFDIO and normal chow mice. Based on these finding alone, it is not possible to determine which factor is playing a critical role in promoting Th2 immune responses in the HFDIO infected mice. Differences in TSLP gene expression as well as changes in the population of CD4⁺T-bet⁺ T-cells and FoxP3⁺ Tregs might be more evident at early stages of infection as the immune responses are being established in the normal chow and HFDIO mice.

It is argued that investigations carried out in mice do not always correlate with observations in humans. However, in a study carried out using peripheral blood mononuclear cells (PBMCs) derived from obese and lean human volunteers, Van der Weerd and co-workers reported that was more IL-4 producing CD4⁺ T-cells (Th2) in obese individuals in comparison to lean individuals. Although in this study they did not observe significant changes in INF- γ (Th1) and IL-17A T-cells (Th17) (van der Weerd et al., 2012). In a separate study, CD4⁺ and CD8⁺ T-cells from overweight and obese individuals were shown to have reduced expression of activation markers. In addition, the number of CD4⁺ and CD8⁺ T-cells producing INF- γ in response to stimulation with live influenza pH1N1 virus was significantly lower in overweight and obese individuals as compared to lean individuals (Paich et al., 2013). Furthermore, the levels of IL-5 were increased in the supernatant collected after re-stimulation of PBMCs with pH1N1 from obese individuals with a trend in reduced levels of IFN- γ . The reduced pro-inflammatory response is believed to be the reason why obese individuals are more susceptible to influenza virus infection (Paich et al., 2013).

Taken altogether these studies support the hypothesis that obesity skews T-cell responses towards a Th2 phenotype not only in mice but in humans as well. This alters the balance of the Th1/Th2 immune responses. Th2 cytokines have been shown to play important roles in generating protective mechanisms against *T. muris* infection. IL-13 is a critical cytokine required for protection against *T. muris* (Bancroft et al., 1998). IL-13 promotes goblet cell responses which are associated with resistance (Bancroft et al., 1998; Hasnain et al., 2011b; McKenzie et al., 1998). In this study, no difference in the number of goblet cells or RELM β expression was observed between normal chow and HFDIO mice at day 21 post infection. By day 42 the increase in goblet cells was evident in both normal chow and HFDIO mice. On the other hand, INF- γ is the predominant cytokine produced in chronic infection which increases host inflammation and reduces the rate of epithelial turnover (Artis et al., 1999b; Cliffe et al., 2007). Therefore, the reduction in INF- γ production in the HFDIO mice might result in increased epithelial turnover which would facilitate worm expulsion. Additional work can be carried out to compare the rate of epithelial turnover between normal chow and HFDIO *T. muris* infected mice. This can be done by immunohistochemical staining for bromodeoxyuridine (BrdU) in caecal sections collected from mice that have been given a single injection of BrdU before sacrifice. Epithelial turnover can be assessed by comparing the distance proliferating cells move up the crypt axis over a given time period for example a 12 hour period.

Much of what is known about immune responses to helminth infection has been derived from studies using mouse models. Usually the experimental mice are approximately 7 to 11 weeks in age. However, it is now appreciated that ageing influences the immune response as it is with remodelling of the immune system. Previous work has shown that age has an effect on the amount of circulating CD4⁺ T-cells in C57BL/6 mice (Pinchuk and Filipov, 2008). The amount of circulating CD4⁺ T-cell was reduced in 18-month-old mice in comparison to 3 and 5-month-old. Interestingly even though BALB/c mice also showed a reduction in the amount of CD4⁺ T-cells with age, the effect was pronounced in the C57BL/6 mice indicating that genetics were also influencing the age-related changes in the immune cell populations (Pinchuk and Filipov, 2008). Furthermore 19-month-old C57BL/6 mice were shown to be more vulnerability to gastrointestinal diseases as compared to 10-week-old C57BL/6 mice (Sovran et al., 2019). Transcriptomics showed that the older mice had reduced expression immunity associated genes including genes

that encode cytokines, T-cell markers such as CD3 ϵ and CD4 suggesting a reduction in the abundance of T-cells. There was also a reduction in the thickness of the colonic mucus layer in the older mice as a result of increased apoptosis of goblet cells (Sovran et al., 2019). Therefore, age related changes in the host immune system may influence the development of immune responses to infection. Follow up experiments can be conducted in mice to investigate if age would influence the ability of HFD induced obesity to enhance Th2 immunity in response to helminth infection. This can be done by carrying out experiments on mice which have been fed on either normal chow or HFD for prolonged periods of time, such as 5 months, 10 months and 18 months before administration of low dose *T. muris* infection. This would provide insight into the effect of age on the immune response to chronic *T. muris* infection and if HFD is able to enhance Th2 immunity in older mice.

In humans the expression of Th2 cytokines was shown to have a curvilinear relationship with age and the peak of expression was approximately at 18 years after which the expression gradually reduced (Jackson et al., 2004). Similar to these findings, Turner and colleagues reported that there was an inverse relationship between Th2 responses and intensity of *T. trichuria* infection which were only evident in individuals older than 11-years which indicates an age dependent immunity against infection (Turner et al., 2003). In developing countries, the burden of obesity is mostly observed in adults (Deleuze Ntandou Bouzitou et al., 2005; Freire et al., 2018). Therefore, it would be worthwhile to carry out studies to assess the relationship between adult obesity and Th2 cytokine expression in response to *T. trichuria* antigen. In addition, work could be done to investigate the burden of infection in overweight/obese individuals, who have higher body mass index (BMI), in comparison to people with a lower BMI. This would determine if the observation that HFD fed obese mice were more resistant to *T. muris* infection would also translate to human helminth infection.

6.3 Innate immune responses contribute to enhanced protection against *T. muris* in HFDIO mice

CD4⁺ T-cells have been shown to important roles in driving Th2 immune responses that are required for resistance against *T. muris* infection. ILC2s are also capable of driving Th2

immune responses. ILC2s have been shown to play important roles in the protection against *H. polygyrus* and *N. brasiliensis* (Gerbe et al., 2016; von Moltke et al., 2016). In contrast, studies have indicated that ILC2s do not play an important role in the protection against *T. muris* infection and depletion of ILC2s did not have a significant effect on the outcome of *T. muris* infection (Glover, 2017). Furthermore *T. muris* infection was not associated with an increase in intestinal tuft cells (Glover, 2017). In line with these observations, there was no difference in the number of tuft cells between naïve and infected normal chow or HFDIO mice. Interestingly HFDIO RAG^{-/-} mice given a single low dose of *T. muris* infection had significantly lower worm burden in comparison to normal chow RAG^{-/-} mice. This indicates even in the absence of the adaptive immune response, HFD is able to induce worm expulsion. The HFDIO RAG^{-/-} mice also had an increase in caecal goblet cells in comparison to the normal chow mice at day 42 post infection. It is possible that ILC2s in the HFDIO *T. muris* mice produced IL-13 which resulted in an increased number of goblet cells. An increase in ILC2s and enhanced IL-13 production was reported in Vitamin A deficient mice which had enhanced resistance against *T. muris* infection (Spencer et al., 2014). The work carried out by Spencer and colleagues highlight the important role that ILC2s play in host resistance when host nutrition is limited. Therefore, ILC2s must have a mechanism to generate sufficient energy for expansion and cytokine production in comparison to cells of the adaptive immune response. Further investigations into the metabolism of ILC2s showed that ILC2s constructively take up high amounts of fatty acids which are used to generate energy through the efficient fatty acid oxidation (Wilhelm et al., 2016). In contrast to ILC2s, naïve T-cells utilise oxidative phosphorylation and upon activation, T-cells switch to aerobic glycolysis in order to meet energy demand required for proliferation and production of cytokines (Frauwirth et al., 2002; Roos and Loos, 1973; van der Windt and Pearce, 2012). Aerobic glycolysis presents a faster way of generating energy however, it produces fewer ATP molecules. Therefore, in a nutrient deficient host, aerobic glycolysis to support T-cell function during infection would be unfavourable. ILC2s which are mainly driven by fatty acid oxidation present a strategy to generate energy in glucose deprived environments and drive Th2 responses to maintain barrier integrity (Wilhelm et al., 2016). Therefore, ILC2s are more adaptable to dynamic changes in host nutrition and it could be possible that HFD favours the activity of ILC2s in *T. muris* infected mice.

Taken together the results of this study strengthen the idea of the innate immune response maintaining barrier protection against pathogenic infection when host nutrition is not well balanced. Nutritional deficiencies are prevalent in developing countries therefore more work should be done to investigate if the innate immune response and ILC2s in particular are playing an important role in host protection against helminth infection in endemic areas.

6.4 Single and trickle low dose *T. muris* infections do not cause significant pathology in normal chow mice

The majority of helminth infections are not fatal and in chronic infections symptoms such as general malaise, impaired growth, poor appetite and abdominal pain develop gradually. Symptoms of infection vary depending on the parasite and the site of infection (Jourdan et al., 2018). *T. muris* parasites have neither systemic nor migratory phases in the host and they are restricted to the intestine. In chapter 3 it was shown that normal chow mice given a single low dose *T. muris* infection had no significant loss in body weight and on average, they gained the same weight as naïve mice. In addition, no changes were observed in the mean weight of epididymal and subcutaneous fat pads. These results are consistent with what was previously reported by Kopper and colleagues who also showed that *T. muris* infection did not cause significant weight loss in mice (Kopper et al., 2015). However, when the mice were given trickle low dose *T. muris* infections, there was a trend towards reduced body weight in the infected mice in comparison to the naïve mice. By the end of the 9 week trickle infection regime, the mice gained significantly less weight in comparison to the naïve mice. However, no difference in the mean weight of epididymal and subcutaneous fat pads was observed. Ashley and co-workers reported that long-term *T. muris* infection resulted in reduced weight gain although they observed no overt signs of distress such as poor body skin or fur condition in the infected mice (Houlden et al., 2015). Therefore, even though long-term *T. muris* infection may result in reduced weight gain the infection remains asymptomatic.

In addition, no differences in the mean levels of blood glucose and serum leptin were observed between normal chow fed naïve and infected mice. There was also no pathology observed in the pancreas, liver and lung of single and trickle dose infected

mice. Previous studies have shown that chronic *T. muris* infection does influence cytokine production at sites distant from the caecum (the site of infection) such as the lung which was shown to cause suppressed allergic airway inflammation (Chenery et al., 2016). However in a study carried out in Ethiopia, there is no evidence to show that that *T. trichuria* protects against allergic diseases and protection against allergy disease was mostly associated with parasites that have a systemic phase in the host (Dagoye et al., 2003). Therefore, more work needs to be carried to fully understand how *T. muris* induced changes in cytokine environment at different tissues would affect their function.

Taken together the results confirm that chronic *T. muris* infection is asymptomatic and does not cause severe pathology in the host. Similarly, in humans even though infected individuals may at times report abdominal pain the infected individual normally remains asymptomatic (Jourdan et al., 2018; Kelly et al., 2009). Helminths are believed to regulate the host immune response so as to cause minimal pathology while also creating a conducive environment for them to survive (Turner et al., 2003). As a result, most people will not realise they are infected and will not seek treatment. This allows the parasites to persist in the communities. Community based campaigns to encourage regular deworming and to teach methods of hygiene can be used in combination with school deworming programs to reduce the burden of infection in endemic areas (Clarke et al., 2018).

6.5 Single and trickle low dose *T. muris* infection did not reverse the pathology of HFD induced obesity

Over recent years, research into therapeutic use of helminths for treating obesity and related diseases has been gaining more interest based on observations from experimental mice studies. Obese mice infected with *S. mansoni*, *H. polygyrus* or *N. brasiliensis* had reduced weight and improved insulin sensitivity (Hussaarts et al., 2015; Su et al., 2018; Yang et al., 2013). In the current study, C57BL/6 mice were fed on a HFD for 12 weeks in order to induce obesity. Consistent with literature the C57BL/6 became overweight and showed signs of obesity such as elevated blood glucose, fatty liver and increased serum leptin (Rebuffé-Scrive et al., 1993; Surwit et al., 1995). It was shown that when the HFDIO mice were infected with single or trickle low dose *T. muris* infection there was no

significant loss of body weight or difference in mean weight gain in comparison to the naïve HFDIO mice. Furthermore *T. muris* infection did not have an effect on a HFD induced liver inflammation.

The HFDIO had enlarged islets of Langerhans with irregular shapes as previously described in literature (Pettersson et al., 2012). There was no difference in the islet size between infected and naïve HFDIO mice. Furthermore, *T. muris* infection did not cause a reduction in non-fasted blood glucose levels. Further work can be carried using glucose tolerance tests and insulin tolerance tests to determine if *T. muris* infection would improve insulin sensitivity in the HFDIO mice.

One unanticipated finding was the increased levels of serum leptin in the infected HFDIO mice in comparison to the naïve HFDIO mice. Leptin is produced by adipocytes and plays an important role in regulating food intake (Friedman and Halaas, 1998; Halaas et al., 1995). Recently leptin regulation has been associated with protection against helminth infections (Worthington et al., 2013b). Resistance to *T. spiralis* was associated with reduced levels of serum leptin which causes the mice to eat less (Worthington et al., 2013b). Leptin acts as a proinflammatory cytokine and the reduction in serum leptin was believed to be part of a complex mechanism that favours the generation of Th2 immune response ((Lord et al., 2002; Worthington et al., 2013b). In this study, there was no difference in serum leptin between naïve and infected normal chow mice. However, in chapter 4, it was shown that the normal chow mice developed chronic infections with the production of inflammatory cytokines IFN- γ , IL-6 and IL-17A. Therefore the leptin levels in susceptible mice would be likely to remain unchanged. *H. polygyrus* infected obese mice which had strong Th2 immune response had reduced leptin expression although they did not show any difference in their food consumption (Su et al., 2018). Therefore, it could be that leptin response to helminth infection in obese mice is more complex which could be due to leptin insensitivity that is associated with obesity.

Overall these results suggest that single or trickle low dose *T. muris* did not seem to have a significant influence on the pathology of obesity. One explanation for this could be that a low dose *T. muris* infection did not generate a strong Th2 immune response. Th2 immune responses result in increased number of eosinophils in the adipose tissue which plays an important role in metabolic homeostasis. The eosinophils recruit M2

macrophages which increase thermogenesis by inducing the expression of UCP1 (Hussaarts et al., 2015; Su et al., 2018). There was a trend in increased percentage and number of eosinophils in the mesenteric fat of *T. muris* infected HFDIO mice at day 21 post infection but no changes in the macrophage population were observed. However, more work can be done to investigate changes in the ratio of M2 to M1 macrophages which could provide more insight into the state of inflammation in the adipose tissue.

A second reason why no changes in the pathology of obesity were observed between naïve and infected HFDIO mice could have been that the HFDIO mice expelled worms earlier than the normal chow mice as shown in chapter 4. Therefore, it could be possible that if the HFDIO mice had developed persistent infections the effect on metabolism would have become more apparent.

Studies have now shown that the administration of helminth derived products can promote anti-inflammatory responses in obese mice. The administration of either *S. mansoni* soluble egg antigen (SEA) or *S. mansoni* immunomodulatory glycan lacto-N-fucopentaose III (LNFPIII) in HFD fed mice at the onset of obesity reduced inflammation in the adipose tissue. The treated mice also had reduced liver inflammation and increased in insulin sensitivity in comparison to untreated mice (Bhargava et al., 2012; Hussaarts et al., 2015). Additional work could be carried out to investigate if the administration of *T. muris* derived E/S to HFDIO mice would also improve metabolic homeostasis which could provide a useful tool in the treatment of metabolic disorders.

6.6 HFDIO induced shift in faecal microbial population has no effect on establishment of *T. muris* infection.

The intestine is home to trillions of bacteria which have developed a symbiotic relationship with their hosts (Smith, 1965). They provide protection by competing with pathogenic bacteria and breakdown complex polysaccharides resulting in the release of SCFAs as by-products of the fermentation processes which play a role in the regulation of host immunity (Rémésy et al., 1992; Sekirov et al., 2008). The highest density of bacteria is in the caecum (large intestine for humans) which is the site of establishment of *T. muris* in the host. As the parasite occupies the same niche, the interaction between commensal

bacteria and *T. muris* parasites would be an important factor that determines the host immune response to infection. It is well established that a direct interaction between bacteria and *T. muris* eggs induces hatching to release L1 larvae (Hayes et al., 2010).

Studies have shown that HFD causes changes in the composition of the intestinal bacteria with an increase in *Firmicutes* but a reduction in *Bacteroidetes* (Kim et al., 2012; Turnbaugh et al., 2006a). In chapter 5 the NMDS analysis after 12 weeks of feeding on either normal chow or HFD revealed a difference in the bacterial population between the two groups of mice. However, the difference was not statistically significant. In order to determine if the shift in bacterial composition would affect *T. muris* establishment, the number of larvae at day 13 post infection were compared between the normal chow and HFDIO mice. There was no difference in the number of larvae recovered from HFDIO in comparison to normal chow mice. This indicates that despite changes in the bacterial population, the eggs were able to hatch and the released larvae were able to establish in the host. This supports the evidence that a variety of micro-organisms are able to induce *T. muris* hatching (Hayes et al., 2010). Furthermore, this confirms that changes in worm burden that were observed at later time points were due to enhanced ability of the HFDIO mice to expel the parasites and not an inability to establish an infection.

6.7 There was no difference in faecal microbial population between normal chow and HFDIO *T. muris* infected mice at day 21 post infection

A number of studies have analysed the effect of *Trichuris* infection on host microbiota. In a study carried out in Malaysia, *Trichuris* infection was associated with increased diversity and a particular increase in Paraprevotellaceae in the infected individuals in comparison to uninfected individuals (Lee et al., 2014). In contrast, Cooper and colleagues found no association between *Trichuris* infection and faecal microbiota in school children in Ecuador (Cooper et al., 2013). A number of factors could be contributing to the differences in observations including differences in experimental design as well as factors such as host nutrition and environment. Studies in mice can be carried out under controlled environments and have been used to investigate the effect of *Trichuris* infection on host microbiota. Recent studies have shown that by day 28 post infection

there was a change in host microbiota which became more evident by day 42 post infection (Holm et al., 2015; Houlden et al., 2015).

Since HFD and *T. muris* infection both induce changes in the host microbiota, the change in microbial population in the HFDIO mice was compared to the normal chow mice at day 21 post infection. There was a similar trend towards in the shift of the bacterial population in both normal chow and HFDIO infected mice. This could indicate that infection caused a similar shift in the microbial composition of the normal chow and HFDIO mice which was independent of diet. Alternatively, it could be that more evident differences between the normal chow and HFDIO infected mice may be more apparent at later time points such as day 42. Recently it was shown that infection with *S. venezuelensis* increases the population of *Firmicutes* in both control and HFD mice (Pace et al., 2018). Furthermore, the study also showed that infection resulted in an increase in *Lactobacillus spp* in both control and HFD fed mice which was also reported during chronic *T. muris* infection (Holm et al., 2015; Pace et al., 2018). *Lactobacilli* have been shown to modulate host immune responses and oral administration of *Lactobacillus casei* increases susceptibility to *T. muris* infection (Dea-Ayuela et al., 2008).

In this study, DGGE analysis of bacteria composition could not provide sufficient detail to determine the specific changes in bacterial species. Therefore, further work using 16S rRNA can provide more insight into the different species that might be affected by *T. muris* in the HFDIO mice.

6.8 What could be driving the HFD induced resistance against a low dose *T. muris* infection?

The main results of this study are summarised in figure 6.1. The mice fed on a HFD had enhanced resistance resulting in early worm expulsion. HFD consumption resulted in a reduction in the number of CD4+ IFN- γ + T-cells in *T. muris* infected mice and enhanced production of Th2 cytokines by re-stimulated cells which suggest that HFD altered the immune response to a low dose of *T. muris* infection. However additional work needs to be carried out to investigate the mechanisms involved in the priming of the T helper response in the HFD fed mice and the downstream effect of the Th2 cytokines resulting in

worm expulsion as indicated in figure 6.1. Furthermore, additional work using 16 S sequencing needs to be carried out to study the ability of *T. muris* to alter the host microbial composition in HFD fed mice which may have an effect on the ability of *T. muris* to moderate the host environment to make it more conducive for it to occupy.

6.9 Conclusions

This study was designed to investigate the effects of the co-occurrence of obesity and helminth infection. This study has shown that HFD enhances host resistance against *T. muris* resulting in early worm expulsion. Furthermore the *T. muris* infected HFD mice showed a trend toward increased production of Th2 associated cytokines and a reduction in the production of pro-inflammatory cytokines. Preliminary investigations suggest that the innate immune responses may be also be playing a role in the protection against *T. muris* in the HFDIO mice. This study has also shown that a low dose *T. muris* infection does not cause significant pathology in normal chow mice and does not improve the symptoms of obesity. It has also been shown that HFD did not have an effect on the ability of *T. muris* to establish in the host. The findings of this study suggest several potential areas of research such as investigation of the establishment of the immune response at early stages of infection and to determine the role of ILC2s in host protection in the HFDIO mice. Lastly more work could be done to determine if the reduction in IFN- γ production in the HFDIO in comparison to the normal chow mice is having an effect on the rate of epithelial turnover which plays an important role in worm expulsion.

This study confirms the importance of nutritional status in determining the outcome of infection and the adaptability of immune responses to maintain host protection. The increasing prevalence of obesity calls for more work to be done to investigate the implications of dual burden of obesity and helminth infection.

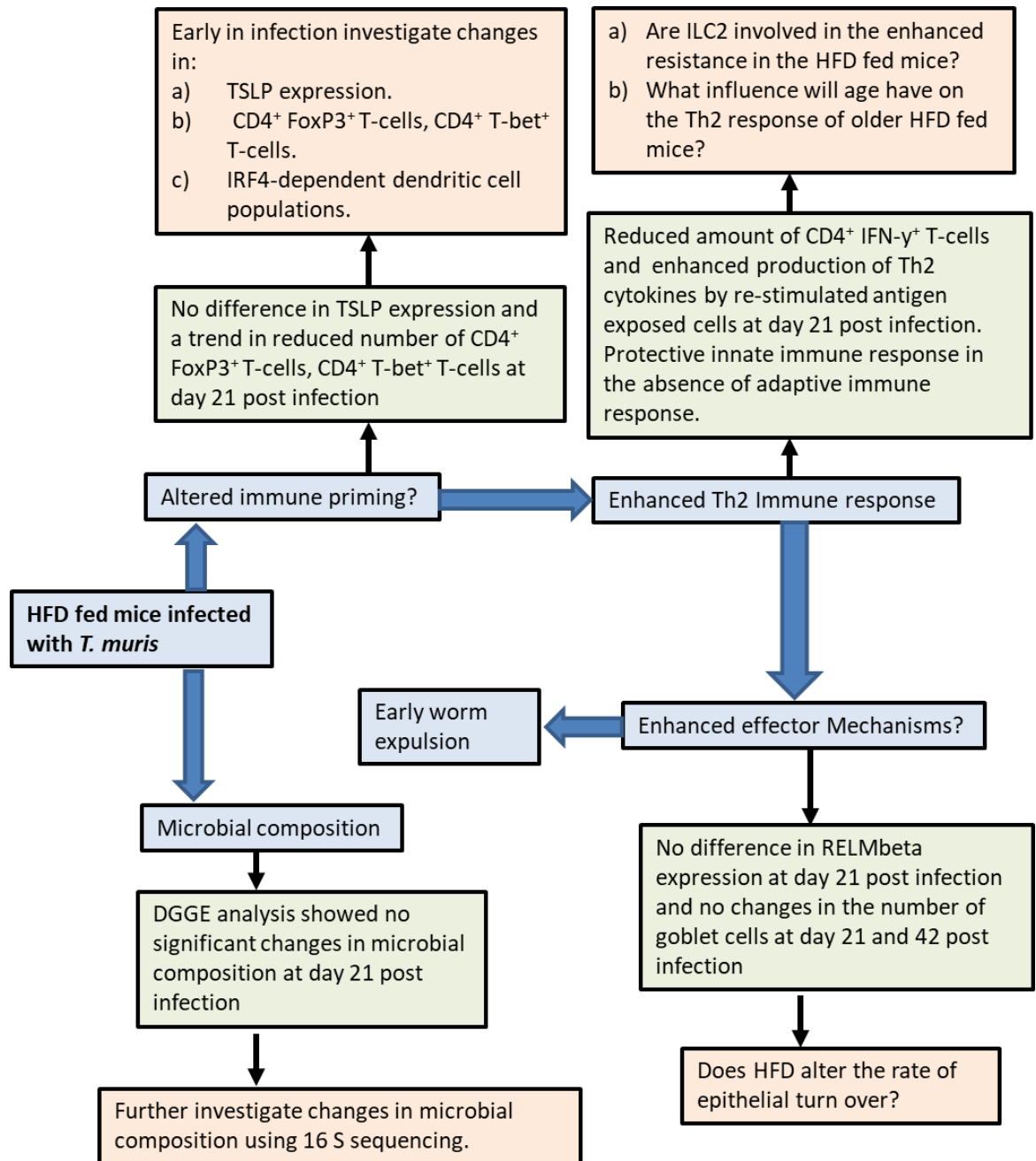


Figure 6-1: Understanding mechanism behind the enhanced resistance in HFD mice

HFD increased the resistance to *T. muris* infection resulting in early worm expulsion. The HFD fed mice had enhanced Th2 immune responses. However more work needs to be carried out to understand how HFD alters the priming of T helper cells during early days of infections, how age may influence the immune response in HFD mice and what effector mechanisms play an important role in worm expulsion. There is also need to investigate if *T. muris* is able to moderate the host microbiota in HFD fed mice so as to create a conducive environment in the host.

Chapter 7 : References

- Aladegbami, B., L. Barron, J. Bao, J. Colasanti, C. R. Erwin, B. W. Warner, and J. Guo, 2017, Epithelial cell specific Raptor is required for initiation of type 2 mucosal immunity in small intestine: *Sci Rep*, v. 7, p. 5580.
- Alencar, A. C. M. d. B., R. H. Neves, M. B. Águila, C. A. Mandarim-de-Lacerda, D. C. Gomes, and J. R. Machado-Silva, 2009, High fat diet has a prominent effect upon the course of chronic schistosomiasis mansoni in mice: *Memórias do Instituto Oswaldo Cruz*, v. 104, p. 608-613
- Amugsi, D. A., Z. T. Dimbuene, B. Mberu, S. Muthuri, and A. C. Ezeh, 2017, Prevalence and time trends in overweight and obesity among urban women: an analysis of demographic and health surveys data from 24 African countries, 1991-2014: *BMJ Open*, v. 7.
- Andrikopoulos, S., A. R. Blair, N. Deluca, B. C. Fam, and J. Proietto, 2008, Evaluating the glucose tolerance test in mice: *American Journal of Physiology-Endocrinology and Metabolism*, v. 295, p. E1323-E1332.
- Artis, D., N. E. Humphreys, A. J. Bancroft, N. J. Rothwell, C. S. Potten, and R. K. Grencis, 1999a, Tumor necrosis factor alpha is a critical component of interleukin 13-mediated protective T helper cell type 2 responses during helminth infection: *The Journal of experimental medicine*, v. 190, p. 953-962.
- Artis, D., C. S. Potten, K. J. Else, F. D. Finkelman, and R. K. Grencis, 1999b, *Trichuris muris*: Host intestinal epithelial cell hyperproliferation during chronic infection is regulated by interferon-gamma: *Experimental Parasitology*, v. 92, p. 144-153.
- Artis, D., M. L. Wang, S. A. Keilbaugh, W. He, M. Brenes, G. P. Swain, P. A. Knight, D. D. Donaldson, M. A. Lazar, H. R. P. Miller, G. A. Schad, P. Scott, and G. D. Wu, 2004, RELM β /FIZZ2 is a goblet cell-specific immune-effector molecule in the gastrointestinal tract: *Proceedings of the National Academy of Sciences of the United States of America*, v. 101, p. 13596-13600.
- Asgharpour, A., S. C. Cazanave, T. Pacana, M. Seneshaw, R. Vincent, B. A. Banini, D. P. Kumar, K. Daita, H. K. Min, F. Mirshahi, P. Bedossa, X. Sun, Y. Hoshida, S. V. Koduru, D. Contaifer, Jr., U. O. Warncke, D. S. Wijesinghe, and A. J. Sanyal, 2016, A diet-induced animal model of non-alcoholic fatty liver disease and hepatocellular cancer: *J Hepatol*, v. 65, p. 579-88.
- Backhed, F., J. K. Manchester, C. F. Semenkovich, and J. I. Gordon, 2007, Mechanisms underlying the resistance to diet-induced obesity in germ-free mice: *Proc Natl Acad Sci U S A*, v. 104, p. 979-84.
- Bancroft, A. J., D. Artis, D. D. Donaldson, J. P. Sypek, and R. K. Grencis, 2000, Gastrointestinal nematode expulsion in IL-4 knockout mice is IL-13 dependent: *European Journal of Immunology*, v. 30, p. 2083-2091.
- Bancroft, A. J., K. J. Else, and R. K. Grencis, 1994a, Low-level infection with *trichuris-muris* significantly affects the polarization of the cd4 response: *European Journal of Immunology*, v. 24, p. 3113-3118.
- Bancroft, A. J., K. J. Else, and R. K. Grencis, 1994b, Low-level infection with *Trichuris muris* significantly affects the polarization of the CD4 response: *Eur J Immunol*, v. 24, p. 3113-8.
- Bancroft, A. J., K. J. Else, N. E. Humphreys, and R. K. Grencis, 2001, The effect of challenge and trickle *Trichuris muris* infections on the polarisation of the immune response: *International Journal for Parasitology*, v. 31, p. 1627-1637.
- Bancroft, A. J., K. J. Else, J. P. Sypek, and R. K. Grencis, 1997, Interleukin-12 promotes a chronic intestinal nematode infection: *Eur J Immunol*, v. 27, p. 866-70.
- Bancroft, A. J., A. N. J. McKenzie, and R. K. Grencis, 1998, A critical role for IL-13 in resistance to intestinal nematode infection: *Journal of Immunology*, v. 160, p. 3453-3461.
- Bell, L. V., and K. J. Else, 2011, Regulation of colonic epithelial cell turnover by IDO contributes to the innate susceptibility of SCID mice to *Trichuris muris* infection: *Parasite Immunology*, v. 33, p. 244-249.

- Bellaby, T., K. Robinson, and D. Wakelin, 1996, Induction of differential T-helper-cell responses in mice infected with variants of the parasitic nematode *Trichuris muris*: *Infection and Immunity*, v. 64, p. 791-795.
- Benoit, B., F. Laugerette, P. Plaisancie, A. Geloën, J. Bodenec, M. Estienne, G. Pineau, A. Bernalier-Donadille, H. Vidal, and M.-C. Michalski, 2015, Increasing fat content from 20 to 45 wt% in a complex diet induces lower endotoxemia in parallel with an increased number of intestinal goblet cells in mice: *Nutrition Research*, v. 35, p. 346-356.
- Bercik, P., E. F. Verdu, J. A. Foster, J. Macri, M. Potter, X. Huang, P. Malinowski, W. Jackson, P. Blennerhassett, K. A. Neufeld, J. Lu, W. I. Khan, I. Corthesy-Theulaz, C. Cherbut, G. E. Bergonzelli, and S. M. Collins, 2010, Chronic gastrointestinal inflammation induces anxiety-like behavior and alters central nervous system biochemistry in mice: *Gastroenterology*, v. 139, p. 2102-2112.e1.
- Bergstrom, K. S. B., and L. Xia, 2013, Mucin-type O-glycans and their roles in intestinal homeostasis: *Glycobiology*, v. 23, p. 1026-1037.
- Bethony, J., S. Brooker, M. Albonico, S. M. Geiger, A. Loukas, D. Diemert, and P. J. Hotez, 2006, Soil-transmitted helminth infections: ascariasis, trichuriasis, and hookworm: *Lancet*, v. 367, p. 1521-1532.
- Betts, C. J., and K. J. Else, 1999, Mast cells, eosinophils and antibody-mediated cellular cytotoxicity are not critical in resistance to *Trichuris muris*: *Parasite Immunol*, v. 21, p. 45-52.
- Bhargava, P., C. Li, K. J. Stanya, D. Jacobi, L. Dai, S. Liu, M. R. Gangl, D. A. Harn, and C. H. Lee, 2012, Immunomodulatory glycan LNFPIII alleviates hepatosteatosis and insulin resistance through direct and indirect control of metabolic pathways: *Nat Med*, v. 18, p. 1665-72.
- Birchenough, G. M. H., M. E. V. Johansson, J. K. Gustafsson, J. H. Bergstrom, and G. C. Hansson, 2015, New developments in goblet cell mucus secretion and function: *Mucosal Immunology*, v. 8, p. 712-719.
- Blackwell, N. M., and K. J. Else, 2001, B cells and antibodies are required for resistance to the parasitic gastrointestinal nematode *Trichuris muris*: *Infection and immunity*, v. 69, p. 3860-3868.
- Blackwell, N. M., and K. J. Else, 2002, A comparison of local and peripheral parasite-specific antibody production in different strains of mice infected with *Trichuris muris*: *Parasite Immunol*, v. 24, p. 203-11.
- Bogiatzi, C., G. Gloor, E. Allen-Vercoe, G. Reid, R. G. Wong, B. L. Urquhart, V. Dinculescu, K. N. Ruetz, T. J. Velenosi, M. Pignanelli, and J. D. Spence, 2018, Metabolic products of the intestinal microbiome and extremes of atherosclerosis: *Atherosclerosis*, v. 273, p. 91-97.
- Brailsford, T. J., and J. M. Behnke, 1992, The dynamics of trickle infections with *Heligmosomoides polygyrus* in syngeneic strains of mice: *Int J Parasitol*, v. 22, p. 351-9.
- Brestoff, J. R., B. S. Kim, S. A. Saenz, R. R. Stine, L. A. Monticelli, G. F. Sonnenberg, J. J. Thome, D. L. Farber, K. Lutfy, P. Seale, and D. Artis, 2015, Group 2 innate lymphoid cells promote beiging of white adipose tissue and limit obesity: *Nature*, v. 519, p. 242-+.
- Bundy, D. A., 1988, Population ecology of intestinal helminth infections in human communities: *Philos Trans R Soc Lond B Biol Sci*, v. 321, p. 405-20.
- Cani, P. D., R. Bibiloni, C. Knauf, A. Waget, A. M. Neyrinck, N. M. Delzenne, and R. Burcelin, 2008, Changes in Gut Microbiota Control Metabolic Endotoxemia-Induced Inflammation in High-Fat Diet-Induced Obesity and Diabetes in Mice: *Diabetes*, v. 57, p. 1470-81.
- Chen, X., X. Yang, Y. Li, J. Zhu, S. Zhou, Z. Xu, L. He, X. Xue, W. Zhang, X. Dong, H. Wu, C. J. Li, H. T. Hsu, W. Kong, F. Liu, P. B. Tripathi, M. S. Yu, J. Chang, L. Zhou, and C. Su, 2014, Follicular helper T cells promote liver pathology in mice during *Schistosoma japonicum* infection: *PLoS Pathog*, v. 10, p. e1004097.
- Chenery, A. L., F. Antignano, K. Burrows, S. Scheer, G. Perona-Wright, and C. Zaph, 2016, Low-Dose Intestinal *Trichuris muris* Infection Alters the Lung Immune Microenvironment and Can Suppress Allergic Airway Inflammation: *Infect Immun*, v. 84, p. 491-501.

- Cheng, H., and C. P. Leblond, 1974, Origin, differentiation and renewal of the four main epithelial cell types in the mouse small intestine V. Unitarian theory of the origin of the four epithelial cell types: *American Journal of Anatomy*, v. 141, p. 537-561.
- Chidavaenzi, M., M. Bradley, M. Jere, and C. Nhandara, 2000, Pit latrine effluent infiltration into groundwater: the Epworth case study: *Schriftenr Ver Wasser Boden Lufthyg*, v. 105, p. 171-7.
- Clarke, K. R., and M. Ainsworth, 1993, A method of linking multivariate community structure to environmental variables: *Mar. Ecol. Prog. Ser.*, v. 92, p. 205-219.
- Clarke, N. E., A. C. A. Clements, S. Amaral, A. Richardson, J. S. McCarthy, J. McGown, S. Bryan, D. J. Gray, and S. V. Nery, 2018, (S)WASH-D for Worms: A pilot study investigating the differential impact of school- versus community-based integrated control programs for soil-transmitted helminths: *PLoS Negl Trop Dis*, v. 12, p. e0006389.
- Cliffe, L. J., and R. K. Grencis, 2004, The *Trichuris muris* system: a paradigm of resistance and susceptibility to intestinal nematode infection: *Advances in Parasitology*, Vol 57, v. 57, p. 255-307.
- Cliffe, L. J., N. E. Humphreys, T. E. Lane, C. S. Potten, C. Booth, and R. K. Grencis, 2005, Accelerated intestinal epithelial cell turnover: a new mechanism of parasite expulsion: *Science*, v. 308, p. 1463-5.
- Cliffe, L. J., C. S. Potten, C. E. Booth, and R. K. Grencis, 2007, An increase in epithelial cell apoptosis is associated with chronic intestinal nematode infection: *Infect Immun*, v. 75, p. 1556-64.
- Cooper, P., A. W. Walker, J. Reyes, M. Chico, S. J. Salter, M. Vaca, and J. Parkhill, 2013, Patent human infections with the whipworm, *Trichuris trichiura*, are not associated with alterations in the faecal microbiota: *PLoS One*, v. 8, p. e76573.
- Correale, J., and M. F. Farez, 2011, The impact of parasite infections on the course of multiple sclerosis: *J Neuroimmunol*, v. 233, p. 6-11.
- Coutinho, E. M., A. F. Barros, A. Barbosa, Jr., S. A. Oliveira, L. M. Silva, R. E. Araujo, and Z. A. Andrade, 2003, Host nutritional status as a contributory factor to the remodeling of schistosomal hepatic fibrosis: *Mem Inst Oswaldo Cruz*, v. 98, p. 919-25.
- Cox, L. M., and H. L. Weiner, 2018, Microbiota Signaling Pathways that Influence Neurologic Disease: *Neurotherapeutics*, v. 15, p. 135-145.
- Cressler, C. E., W. A. Nelson, T. Day, and E. McCauley, 2014, Disentangling the interaction among host resources, the immune system and pathogens: *Ecology letters*, v. 17, p. 284-293.
- Cruickshank, S. M., M. L. Deschoolmeester, M. Svensson, G. Howell, A. Bazakou, L. Logunova, M. C. Little, N. English, M. Mack, R. K. Grencis, K. J. Else, and S. R. Carding, 2009, Rapid Dendritic Cell Mobilization to the Large Intestinal Epithelium Is Associated with Resistance to *Trichuris muris* Infection: *The Journal of Immunology*, v. 182, p. 3055.
- D'Elia, R., J. M. Behnke, J. E. Bradley, and K. J. Else, 2009a, Regulatory T cells: a role in the control of helminth-driven intestinal pathology and worm survival: *Journal of immunology* (Baltimore, Md. : 1950), v. 182, p. 2340-2348.
- D'Elia, R., M. L. deSchoolmeester, L. A. H. Zeef, S. H. Wright, A. D. Pemberton, and K. J. Else, 2009b, Expulsion of *Trichuris muris* is associated with increased expression of angiogenin 4 in the gut and increased acidity of mucins within the goblet cell: *BMC Genomics*, v. 10, p. 492.
- Dagoye, D., Z. Bekele, K. Woldemichael, H. Nida, M. Yimam, A. Hall, A. J. Venn, J. R. Britton, R. Hubbard, and S. A. Lewis, 2003, Wheezing, allergy, and parasite infection in children in urban and rural Ethiopia: *Am J Respir Crit Care Med*, v. 167, p. 1369-73.
- Dailey, M. J., 2014, Nutrient-induced intestinal adaption and its effect in obesity: *Physiol Behav*, v. 136, p. 74-8.
- Daniel, B., 2018, Zambia STEPS Survey 2017: A Surveillance of Noncommunicable Disease Risk Factors.

- Datta, R., M. L. deSchoolmeester, C. Hedeler, N. W. Paton, A. M. Brass, and K. J. Else, 2005, Identification of novel genes in intestinal tissue that are regulated after infection with an intestinal nematode parasite: *Infect Immun*, v. 73, p. 4025-33.
- De Barros Alencar, A. C. M., R. H. Neves, A. V. De Oliveira, and J. R. Machado-Silva, 2012, Changes in the small intestine of *Schistosoma mansoni*-infected mice fed a high-fat diet: *Parasitology*, v. 139, p. 716-725.
- Dea-Ayuela, M. A., S. Rama-Iniguez, and F. Bolas-Fernandez, 2008, Enhanced susceptibility to *Trichuris muris* infection of B10Br mice treated with the probiotic *Lactobacillus casei*: *Int Immunopharmacol*, v. 8, p. 28-35.
- Deiuliis, J., Z. Shah, N. Shah, B. Needleman, D. Mikami, V. Narula, K. Perry, J. Hazey, T. Kampfrath, M. Kollengode, Q. Sun, A. R. Satoskar, C. Lumeng, S. Moffatt-Bruce, and S. Rajagopalan, 2011, Visceral adipose inflammation in obesity is associated with critical alterations in regulatory cell numbers: *PLoS One*, v. 6, p. e16376.
- Deleuze Ntandou Bouzitou, G., B. Fayomi, and H. Delisle, 2005, [Child malnutrition and maternal overweight in same households in poor urban areas of Benin]: *Sante*, v. 15, p. 263-70.
- Demiri, M., K. Muller-Luda, W. W. Agace, and M. Svensson-Frej, 2017, Distinct DC subsets regulate adaptive Th1 and 2 responses during *Trichuris muris* infection: *Parasite Immunol*, v. 39.
- Derrien, M., E. E. Vaughan, C. M. Plugge, and W. M. de Vos, 2004, *Akkermansia muciniphila* gen. nov., sp. nov., a human intestinal mucin-degrading bacterium: *Int J Syst Evol Microbiol*, v. 54, p. 1469-76.
- Dieli, F., G. Sireci, E. Scire, A. Salerno, and A. Bellavia, 1999, Impaired contact hypersensitivity to trinitrochlorobenzene in interleukin-4-deficient mice: *Immunology*, v. 98, p. 71-9.
- Dixon, H., C. Blanchard, M. L. deSchoolmeester, N. C. Yuill, J. W. Christie, M. E. Rothenberg, and K. J. Else, 2006, The role of Th2 cytokines, chemokines and parasite products in eosinophil recruitment to the gastrointestinal mucosa during helminth infection: *European Journal of Immunology*, v. 36, p. 1753-1763.
- Doetze, A., J. Satoguina, G. Burchard, T. Rau, C. Loliger, B. Fleischer, and A. Hoerauf, 2000, Antigen-specific cellular hyporesponsiveness in a chronic human helminth infection is mediated by T(h)3/T(r)1-type cytokines IL-10 and transforming growth factor-beta but not by a T(h)1 to T(h)2 shift: *Int Immunol*, v. 12, p. 623-30.
- Drake, L. J., A. E. Bianco, D. A. P. Bundy, and F. Ashall, 1994, Characterization of peptidases of adult *Trichuris muris*: *Parasitology*, v. 109, p. 623-630.
- Else, K., and D. Wakelin, 1988, The effects of H-2 and non-H-2 genes on the expulsion of the nematode *Trichuris muris* from inbred and congenic mice: *Parasitology*, v. 96, p. 543-550.
- Else, K. J., F. D. Finkelman, C. R. Maliszewski, and R. K. Grencis, 1994, Cytokine-mediated regulation of chronic intestinal helminth infection: *Journal of Experimental Medicine*, v. 179, p. 347-351.
- Else, K. J., and R. K. Grencis, 1991, Cellular immune-responses to the murine nematode parasite *trichuris-muris* .1. differential cytokine production during acute or chronic infection: *Immunology*, v. 72, p. 508-513.
- Else, K. J., and R. K. Grencis, 1996, Antibody-independent effector mechanisms in resistance to the intestinal nematode parasite *Trichuris muris*: *Infection and Immunity*, v. 64, p. 2950-2954.
- Else, K. J., L. Hultner, and R. K. Grencis, 1992, Cellular immune-responses to the murine nematode parasite *trichuris-muris* .2. differential induction of th-cell subsets in resistant versus susceptible mice: *Immunology*, v. 75, p. 232-237.
- Everard, A., C. Belzer, L. Geurts, J. P. Ouwerkerk, C. Druart, L. B. Bindels, Y. Guiot, M. Derrien, G. G. Muccioli, N. M. Delzenne, W. M. de Vos, and P. D. Cani, 2013, Cross-talk between *Akkermansia muciniphila* and intestinal epithelium controls diet-induced obesity: *Proceedings of the National Academy of Sciences of the United States of America*, v. 110, p. 9066-9071.
- Faulkner, H., J. C. Renauld, J. Van Snick, and R. K. Grencis, 1998, Interleukin-9 Enhances Resistance to the Intestinal Nematode *Trichuris muris*: *Infection and Immunity*, v. 66, p. 3832-3840.

- Foth, B. J., I. J. Tsai, A. J. Reid, A. J. Bancroft, S. Nichol, A. Tracey, N. Holroyd, J. A. Cotton, E. J. Stanley, M. Zarowiecki, J. Z. Liu, T. Huckvale, P. J. Cooper, R. K. Grencis, and M. Berriman, 2014, Whipworm genome and dual-species transcriptome analyses provide molecular insights into an intimate host-parasite interaction: *Nature Genetics*, v. 46, p. 693.
- Frauwirth, K. A., J. L. Riley, M. H. Harris, R. V. Parry, J. C. Rathmell, D. R. Plas, R. L. Elstrom, C. H. June, and C. B. Thompson, 2002, The CD28 signaling pathway regulates glucose metabolism: *Immunity*, v. 16, p. 769-77.
- Freire, W. B., W. F. Waters, G. Rivas-Mariño, and P. Belmont, 2018, The double burden of chronic malnutrition and overweight and obesity in Ecuadorian mothers and children, 1986–2012: *Nutrition and Health*, p. 0260106018782826.
- Friedman, J. M., and J. L. Halaas, 1998, Leptin and the regulation of body weight in mammals: *Nature*, v. 395, p. 763-70.
- Friedmann, P. S., 1989, Contact hypersensitivity: *Curr Opin Immunol*, v. 1, p. 690-3.
- Fujio, J., A. Kushiyama, H. Sakoda, M. Fujishiro, T. Ogihara, Y. Fukushima, M. Anai, N. Horike, H. Kamata, Y. Uchijima, H. Kurihara, and T. Asano, 2008, Regulation of gut-derived resistin-like molecule beta expression by nutrients: *Diabetes Res Clin Pract*, v. 79, p. 2-10.
- Gautam, S. C., J. A. Matriano, N. F. Chikkala, M. G. Edinger, and R. R. Tubbs, 1991, L3T4 (CD4+) cells that mediate contact sensitivity to trinitrochlorobenzene express I-A determinants: *Cell Immunol*, v. 135, p. 27-41.
- Gerbe, F., E. Sidot, D. J. Smyth, M. Ohmoto, I. Matsumoto, V. Dardalhon, P. Cesses, L. Garnier, M. Pouzolles, B. Brulin, M. Bruschi, Y. H Marcus, V. S. Zimmermann, N. Taylor, R. M. Maizels, and P. Jay, 2016, Intestinal epithelial tuft cells initiate type 2 mucosal immunity to helminth parasites: *Nature*, v. 529, p. 226-U260.
- Gerbe, F., J. H. van Es, L. Makrini, B. Brulin, G. Mellitzer, S. Robine, B. Romagnolo, N. F. Shroyer, J.-F. Bourgaux, C. Pignodel, H. Clevers, and P. Jay, 2011, Distinct ATOH1 and Neurog3 requirements define tuft cells as a new secretory cell type in the intestinal epithelium: *Journal of Cell Biology*, v. 192, p. 767-780.
- Glover, M., 2017, Trickle infection and immunity to *Trichuris muris* (Doctoral dissertation), University of Manchester.
- Gould, J., 2017, Nutrition: A world of insecurity: *Nature*, v. 544, p. S6.
- Gowda, S., P. B. Desai, V. V. Hull, A. A. K. Math, S. N. Vernekar, and S. S. Kulkarni, 2009, A review on laboratory liver function tests: *The Pan African medical journal*, v. 3, p. 17-17.
- Greenwood, B. M., 1968, Autoimmune disease and parasitic infections in Nigerians: *Lancet*, v. 2, p. 380-2.
- Guigas, B., and A. B. Molofsky, 2015, A worm of one's own: how helminths modulate host adipose tissue function and metabolism: *Trends in parasitology*, v. 31, p. 435-441.
- Gulhane, M., L. Murray, R. Lourie, H. Tong, Y. H. Sheng, R. Wang, A. Kang, V. Schreiber, K. Y. Wong, G. Magor, S. Denman, J. Begun, T. H. Florin, A. Perkins, P. O. Cuiv, M. A. McGuckin, and S. Z. Hasnain, 2016, High Fat Diets Induce Colonic Epithelial Cell Stress and Inflammation that is Reversed by IL-22: *Scientific reports*, v. 6, p. 28990-28990.
- Gum, J. R., J. W. Hicks, N. W. Toribara, B. Siddiki, and Y. S. Kim, 1994, Molecular-cloning of human intestinal mucin (muc2) cDNA - identification of the amino-terminus and overall sequence similarity to prepro-von-willebrand factor: *Journal of Biological Chemistry*, v. 269, p. 2440-2446.
- Guslandi, M., 2011, Rifaximin in the treatment of inflammatory bowel disease: *World J Gastroenterol*, v. 17, p. 4643-6.
- Halaas, J. L., K. S. Gajiwala, M. Maffei, S. L. Cohen, B. T. Chait, D. Rabinowitz, R. L. Lallone, S. K. Burley, and J. M. Friedman, 1995, Weight-reducing effects of the plasma protein encoded by the obese gene: *Science*, v. 269, p. 543-6.
- Hamilton, M. K., G. Boudry, D. G. Lemay, and H. E. Raybould, 2015, Changes in intestinal barrier function and gut microbiota in high-fat diet-fed rats are dynamic and region dependent: *American Journal of Physiology - Gastrointestinal and Liver Physiology*, v. 308, p. G840-G851.

- Hams, E., R. M. Locksley, A. N. J. McKenzie, and P. G. Fallon, 2013, Cutting Edge: IL-25 Elicits Innate Lymphoid Type 2 and Type II NKT Cells That Regulate Obesity in Mice: *Journal of Immunology*, v. 191, p. 5349-5353.
- Hart, K. M., T. Fabre, J. C. Sciruba, R. L. Gieseck, 3rd, L. A. Borthwick, K. M. Vannella, T. H. Acciani, R. de Queiroz Prado, R. W. Thompson, S. White, G. Soucy, M. Bilodeau, T. R. Ramalingam, J. R. Arron, N. H. Shoukry, and T. A. Wynn, 2017, Type 2 immunity is protective in metabolic disease but exacerbates NAFLD collaboratively with TGF-beta: *Sci Transl Med*, v. 9.
- Hartmann, P., C. T. Seebauer, M. Mazagova, A. Horvath, L. Wang, C. Llorente, N. M. Varki, K. Brandl, S. B. Ho, and B. Schnabl, 2016, Deficiency of intestinal mucin-2 protects mice from diet-induced fatty liver disease and obesity: *American Journal of Physiology-Gastrointestinal and Liver Physiology*, v. 310, p. G310-G322.
- Harvie, M., M. Camberis, S. C. Tang, B. Delahunt, W. Paul, and G. Le Gros, 2010, The lung is an important site for priming CD4 T-cell-mediated protective immunity against gastrointestinal helminth parasites: *Infect Immun*, v. 78, p. 3753-62.
- Hasnain, S. Z., P. A. Dawson, R. Lourie, P. Hutson, H. Tong, R. K. Grencis, M. A. McGuckin, and D. J. Thornton, 2017, Immune-driven alterations in mucin sulphation is an important mediator of *Trichuris muris* helminth expulsion: *PLOS Pathogens*, v. 13, p. e1006218.
- Hasnain, S. Z., C. M. Evans, M. Roy, A. L. Gallagher, K. N. Kindrachuk, L. Barron, B. F. Dickey, M. S. Wilson, T. A. Wynn, R. K. Grencis, and D. J. Thornton, 2011a, Muc5ac: a critical component mediating the rejection of enteric nematodes: *The Journal of Experimental Medicine*, v. 208, p. 893.
- Hasnain, S. Z., M. A. McGuckin, R. K. Grencis, and D. J. Thornton, 2012, Serine Protease(s) Secreted by the Nematode *Trichuris muris* Degrade the Mucus Barrier. : *PLoS Negl Trop Dis*, v. 6, p. e1856.
- Hasnain, S. Z., D. J. Thornton, and R. K. Grencis, 2011b, Changes in the mucosal barrier during acute and chronic *Trichuris muris* infection: *Parasite Immunology*, v. 33, p. 45-55.
- Hasnain, S. Z., H. Wang, J.-E. Ghia, N. Haq, Y. Deng, A. Velcich, R. K. Grencis, D. J. Thornton, and W. I. Khan, 2010, Mucin Gene Deficiency in Mice Impairs Host Resistance to an Enteric Parasitic Infection: *Gastroenterology*, v. 138, p. 1763-U45.
- Hayes, K. S., A. J. Bancroft, M. Goldrick, C. Portsmouth, I. S. Roberts, and R. K. Grencis, 2010, Exploitation of the Intestinal Microflora by the Parasitic Nematode *Trichuris muris*: *Science*, v. 328, p. 1391-1394.
- Hayes, K. S., A. J. Bancroft, and R. K. Grencis, 2007, The role of TNF-alpha in *Trichuris muris* infection II: global enhancement of ongoing Th1 or Th2 responses.: *Parasite Immunol*, v. 29, p. 583-94.
- Hayes, K. S., L. J. Cliffe, A. J. Bancroft, S. P. Forman, S. Thompson, C. Booth, and R. K. Grencis, 2017, Chronic *Trichuris muris* infection causes neoplastic change in the intestine and exacerbates tumour formation in APC min/+ mice: *PLoS Negl Trop Dis*, v. 11, p. e0005708.
- He, R., and R. S. Geha, 2010, Thymic stromal lymphopoietin: *Ann N Y Acad Sci*, v. 1183, p. 13-24.
- Hepworth, M. R., M. J. Hardman, and R. K. Grencis, 2010, The role of sex hormones in the development of Th2 immunity in a gender-biased model of *Trichuris muris* infection: *Eur J Immunol*, v. 40, p. 406-16.
- Holm, J. B., D. Sorobetea, P. Kiilerich, Y. Ramayo-Caldas, J. Estelle, T. Ma, L. Madsen, K. Kristiansen, and M. Svensson-Frej, 2015, Chronic *Trichuris muris* Infection Decreases Diversity of the Intestinal Microbiota and Concomitantly Increases the Abundance of Lactobacilli: *Plos One*, v. 10.
- Holt, F., S. J. Gillam, and J. M. Ngondi, 2012, Improving Access to Medicines for Neglected Tropical Diseases in Developing Countries: Lessons from Three Emerging Economies: *PLoS Neglected Tropical Diseases*, v. 6, p. e1390.
- Hooper, L. V., T. S. Stappenbeck, C. V. Hong, and J. I. Gordon, 2003, Angiogenins: a new class of microbicidal proteins involved in innate immunity: *Nature Immunology*, v. 4, p. 269.

- Hotamisligil, G. S., N. S. Shargill, and B. M. Spiegelman, 1993, Adipose expression of tumor necrosis factor- α : direct role in obesity-linked insulin resistance: *Science*, v. 259, p. 87.
- Houlden, A., K. S. Hayes, A. J. Bancroft, J. J. Worthington, P. Wang, R. K. Grencis, and I. S. Roberts, 2015, Chronic *Trichuris muris* Infection in C57BL/6 Mice Causes Significant Changes in Host Microbiota and Metabolome: Effects Reversed by Pathogen Clearance: *PLoS ONE*, v. 10, p. e0125945.
- Howard, J. K., G. M. Lord, G. Matarese, S. Vendetti, M. A. Ghatei, M. A. Ritter, R. I. Lechler, and S. R. Bloom, 1999, Leptin protects mice from starvation-induced lymphoid atrophy and increases thymic cellularity in ob/ob mice: *J Clin Invest*, v. 104, p. 1051-9.
- Hugo, G., 1983, Food for tomorrow's population: *Majalah Demografi Indones*, v. 10, p. ii-33-60.
- Hummel, K. P., D. L. Coleman, and P. W. Lane, 1972, The influence of genetic background on expression of mutations at the diabetes locus in the mouse. I. C57BL/KsJ and C57BL/6J strains: *Biochemical Genetics*, v. 7, p. 1-13.
- Humphreys, N. E., D. Xu, M. R. Hepworth, F. Y. Liew, and R. K. Grencis, 2008, IL-33, a potent inducer of adaptive immunity to intestinal nematodes: *J Immunol*, v. 180, p. 2443-9.
- Hurst, R. J., A. De Caul, M. C. Little, H. Kagechika, and K. J. Else, 2013, The retinoic acid receptor agonist Am80 increases mucosal inflammation in an IL-6 dependent manner during *Trichuris muris* infection: *J Clin Immunol*, v. 33, p. 1386-94.
- Hussaarts, L., N. Garcia-Tardon, L. van Beek, M. M. Heemskerk, S. Haerberlein, G. C. van der Zon, A. Ozir-Fazalalikhani, J. F. Berbee, K. Willems van Dijk, V. van Harmelen, M. Yazdanbakhsh, and B. Guigas, 2015, Chronic helminth infection and helminth-derived egg antigens promote adipose tissue M2 macrophages and improve insulin sensitivity in obese mice: *Faseb j*, v. 29, p. 3027-39.
- Ikemoto, S., M. Takahashi, N. Tsunoda, K. Maruyama, H. Itakura, and O. Ezaki, 1996, High-fat diet-induced hyperglycemia and obesity in mice: differential effects of dietary oils: *Metabolism*, v. 45, p. 1539-46.
- Ingalls, A. M., M. M. Dickie, and G. D. Snell, 1950, Obese, a new mutation in the house mouse: *J Hered*, v. 41, p. 317-8.
- Jackson, J. A., J. D. Turner, L. Rentoul, H. Faulkner, J. M. Behnke, M. Hoyle, R. K. Grencis, K. J. Else, J. Kamgno, M. Boussinesq, and J. E. Bradley, 2004, T helper cell type 2 responsiveness predicts future susceptibility to gastrointestinal nematodes in humans: *J Infect Dis*, v. 190, p. 1804-11.
- Jacobs, W., G. van Dam, J. Bogers, A. Deelder, and E. Van Marck, 1999, Schistosomal granuloma modulation. I. *Schistosoma mansoni* worm antigens CAA and CCA prime egg-antigen-induced hepatic granuloma formation: *Parasitol Res*, v. 85, p. 7-13.
- James, P. T., 2004, Obesity: The worldwide epidemic: *Clinics in Dermatology*, v. 22, p. 276-280.
- Jenkins, D. C., and R. F. Phillipson, 1971, The kinetics of repeated low-level infections of *Nippostrongylus brasiliensis* in the laboratory rat: *Parasitology*, v. 62, p. 457-65.
- Johansson, M. E., M. Phillipson, J. Petersson, A. Velcich, L. Holm, and G. C. Hansson, 2008, The inner of the two Muc2 mucin-dependent mucus layers in colon is devoid of bacteria: *Proc Natl Acad Sci U S A*, v. 105, p. 15064-9.
- Jourdan, P. M., P. H. L. Lamberton, A. Fenwick, and D. G. Addiss, 2018, Soil-transmitted helminth infections: *Lancet*, v. 391, p. 252-265.
- Jullien, S., D. Sinclair, and P. Garner, 2016, The impact of mass deworming programmes on schooling and economic development: an appraisal of long-term studies: *International Journal of Epidemiology*, v. 45, p. 2140-2153.
- Kaczmarek, J. L., S. M. MUSAAD, and H. D. Holscher, 2017, Time of day and eating behaviors are associated with the composition and function of the human gastrointestinal microbiota: *Am J Clin Nutr*, v. 106, p. 1220-1231.
- Katagiri, K., S. Arakawa, R. Kurahashi, and Y. Hatano, 2007, Impaired contact hypersensitivity in diet-induced obese mice: *Journal of Dermatological Science*, v. 46, p. 117-126.

- Katukiza, A. Y., M. Ronteltap, A. Oleja, C. B. Niwagaba, F. Kansiime, and P. N. Lens, 2010, Selection of sustainable sanitation technologies for urban slums--a case of Bwaise III in Kampala, Uganda: *Sci Total Environ*, v. 409, p. 52-62.
- Kelly, P., J. Todd, S. Sianongo, J. Mwansa, H. Sinsungwe, M. Katubulushi, M. J. Farthing, and R. A. Feldman, 2009, Susceptibility to intestinal infection and diarrhoea in Zambian adults in relation to HIV status and CD4 count: *BMC Gastroenterology*, v. 9, p. 7.
- Khan, W. I., P. Blennerhasset, C. Ma, K. I. Matthaehi, and S. M. Collins, 2001, Stat6 dependent goblet cell hyperplasia during intestinal nematode infection: *Parasite Immunology*, v. 23, p. 39-42.
- Khan, W. I., M. Richard, H. Akiho, P. A. Blennerhasset, N. E. Humphreys, R. K. Grecis, J. Van Snick, and S. M. Collins, 2003, Modulation of intestinal muscle contraction by interleukin-9 (IL-9) or IL-9 neutralization: Correlation with worm expulsion in murine nematode infections: *Infection and Immunity*, v. 71, p. 2430-2438.
- Kim, D.-H., Z. Xiao, S. Kwon, X. Sun, D. Ryerson, D. Tkac, P. Ma, S.-Y. Wu, C.-M. Chiang, E. Zhou, H. E. Xu, J. J. Palvimo, L.-F. Chen, B. Kemper, and J. K. Kemper, 2014, A dysregulated acetyl/SUMO switch of FXR promotes hepatic inflammation in obesity: *The EMBO Journal*, v. 34, p. 184-199.
- Kim, K.-A., W. Gu, I.-A. Lee, E.-H. Joh, and D.-H. Kim, 2012, High Fat Diet-Induced Gut Microbiota Exacerbates Inflammation and Obesity in Mice via the TLR4 Signaling Pathway: *Plos One*, v. 7.
- Kim, S., M. Prout, H. Ramshaw, A. F. Lopez, G. LeGros, and B. Min, 2010, Cutting edge: basophils are transiently recruited into the draining lymph nodes during helminth infection via IL-3, but infection-induced Th2 immunity can develop without basophil lymph node recruitment or IL-3: *J Immunol*, v. 184, p. 1143-7.
- Koch, C., R. A. Augustine, J. Steger, G. K. Ganjam, J. Benzler, C. Pracht, C. Lowe, M. W. Schwartz, P. R. Shepherd, G. M. Anderson, D. R. Grattan, and A. Tups, 2010, Leptin Rapidly Improves Glucose Homeostasis in Obese Mice by Increasing Hypothalamic Insulin Sensitivity: *The Journal of Neuroscience*, v. 30, p. 16180.
- Koch, C. E., C. Lowe, D. Pretz, J. Steger, L. M. Williams, and A. Tups, 2013, High-Fat Diet Induces Leptin Resistance in Leptin-Deficient Mice: *Journal of Neuroendocrinology*, v. 26, p. 58-67.
- Kopper, J. J., J. S. Patterson, and L. S. Mansfield, 2015, Metronidazole-but not IL-10 or prednisolone-rescues *Trichuris muris* infected C57BL/6 IL-10 deficient mice from severe disease: *Vet Parasitol*, v. 212, p. 239-52.
- Kostyla, C., R. Bain, R. Cronk, and J. Bartram, 2015, Seasonal variation of fecal contamination in drinking water sources in developing countries: a systematic review: *Sci Total Environ*, v. 514, p. 333-43.
- Koyama, K., and Y. Ito, 1996, Comparative studies on immune responses to infection in susceptible B10.BR mice infected with different strains of the murine nematode parasite *Trichuris muris*: *Parasite Immunol*, v. 18, p. 257-63.
- Koyama, K., H. Tamauchi, M. Tomita, T. Kitajima, and Y. Ito, 1999, B-cell activation in the mesenteric lymph nodes of resistant BALB/c mice infected with the murine nematode parasite *Trichuris muris*: *Parasitol Res*, v. 85, p. 194-9.
- Koza, R. A., L. Nikonova, J. Hogan, J. S. Rim, T. Mendoza, C. Faulk, J. Skaf, and L. P. Kozak, 2006, Changes in gene expression foreshadow diet-induced obesity in genetically identical mice: *PLoS Genet*, v. 2, p. e81.
- Kübeck, R., C. Bonet-Ripoll, C. Hoffmann, A. Walker, V. M. Müller, V. L. Schüppel, I. Lagkouvardos, B. Scholz, K.-H. Engel, H. Daniel, P. Schmitt-Kopplin, D. Haller, T. Clavel, and M. Klingenspor, 2016, Dietary fat and gut microbiota interactions determine diet-induced obesity in mice: *Molecular Metabolism*, v. 5, p. 1162-1174.
- Kwiringira, J., P. Atekyereza, C. Niwagaba, and I. Gunther, 2014, Descending the sanitation ladder in urban Uganda: evidence from Kampala Slums: *BMC Public Health*, v. 14, p. 624.
- Lam, Y. Y., C. W. Y. Ha, C. R. Campbell, A. J. Mitchell, A. Dinudom, J. Oscarsson, D. I. Cook, N. H. Hunt, I. D. Caterson, A. J. Holmes, and L. H. Storlien, 2012, Increased Gut Permeability and

- Microbiota Change Associate with Mesenteric Fat Inflammation and Metabolic Dysfunction in Diet-Induced Obese Mice: *Plos One*, v. 7.
- Lee, J.-C., H.-Y. Lee, T. K. Kim, M.-S. Kim, Y. M. Park, J. Kim, K. Park, M.-N. Kweon, S.-H. Kim, J.-W. Bae, K. Y. Hur, and M.-S. Lee, 2017, Obesogenic diet-induced gut barrier dysfunction and pathobiont expansion aggravate experimental colitis: *PloS one*, v. 12, p. e0187515-e0187515.
- Lee, M.-W., J. I. Odegaard, L. Mukundan, Y. Qiu, A. B. Molofsky, J. C. Nussbaum, K. Yun, R. M. Locksley, and A. Chawla, 2015, Activated Type 2 Innate Lymphoid Cells Regulate Beige Fat Biogenesis: *Cell*, v. 160, p. 74-87.
- Lee, S. C., M. S. Tang, Y. A. Lim, S. H. Choy, Z. D. Kurtz, L. M. Cox, U. M. Gundra, I. Cho, R. Bonneau, M. J. Blaser, K. H. Chua, and P. Loke, 2014, Helminth colonization is associated with increased diversity of the gut microbiota: *PLoS Negl Trop Dis*, v. 8, p. e2880.
- Lee, S. H., D. Y. Cho, K. S. Han, S. W. Yang, J. H. Kim, S. M. Kim, and K. N. Kim, 2018, A Randomized Clinical Trial of Synbiotics in Irritable Bowel Syndrome: Dose-Dependent Effects on Gastrointestinal Symptoms and Fatigue: *Korean J Fam Med*.
- Lee, Y. H., and R. E. Pratley, 2005, The evolving role of inflammation in obesity and the metabolic syndrome: *Curr Diab Rep*, v. 5, p. 70-5.
- Levison, S. E., J. T. McLaughlin, L. A. Zeef, P. Fisher, R. K. Grencis, and J. L. Pennock, 2010, Colonic transcriptional profiling in resistance and susceptibility to trichuriasis: phenotyping a chronic colitis and lessons for iatrogenic helminthosis: *Inflamm Bowel Dis*, v. 16, p. 2065-79.
- Ley, R. E., P. J. Turnbaugh, S. Klein, and J. I. Gordon, 2006, Microbial ecology: human gut microbes associated with obesity: *Nature*, v. 444, p. 1022-3.
- Lindstrom, P., 2007, The physiology of obese-hyperglycemic mice [ob/ob mice]: *ScientificWorldJournal*, v. 7, p. 666-85.
- Little, M. C., L. V. Bell, L. J. Cliffe, and K. J. Else, 2005, The characterization of intraepithelial lymphocytes, lamina propria leukocytes, and isolated lymphoid follicles in the large intestine of mice infected with the intestinal nematode parasite *Trichuris muris*: *J Immunol*, v. 175, p. 6713-22.
- Liu, Y., C. Meyer, C. Xu, H. Weng, C. Hellerbrand, P. ten Dijke, and S. Dooley, 2012, Animal models of chronic liver diseases: *American Journal of Physiology-Gastrointestinal and Liver Physiology*, v. 304, p. G449-G468.
- Lord, G. M., G. Matarese, J. K. Howard, S. R. Bloom, and R. I. Lechler, 2002, Leptin inhibits the anti-CD3-driven proliferation of peripheral blood T cells but enhances the production of proinflammatory cytokines: *Journal of Leukocyte Biology*, v. 72, p. 330-338.
- Mah, A. T., L. Van Landeghem, H. E. Gavin, S. T. Magness, and P. K. Lund, 2014, Impact of diet-induced obesity on intestinal stem cells: hyperproliferation but impaired intrinsic function that requires insulin/IGF1: *Endocrinology*, v. 155, p. 3302-14.
- Mann, A., A. Thompson, N. Robbins, and A. L. Blomkalns, 2014, Localization, identification, and excision of murine adipose depots: *Journal of visualized experiments : JoVE*, p. 52174.
- Mao, J., X. Hu, Y. Xiao, C. Yang, Y. Ding, N. Hou, J. Wang, H. Cheng, and X. Zhang, 2013, Overnutrition stimulates intestinal epithelium proliferation through beta-catenin signaling in obese mice: *Diabetes*, v. 62, p. 3736-46.
- Marsland, B. J., M. Kurrer, R. Reissmann, N. L. Harris, and M. Kopf, 2008, *Nippostrongylus brasiliensis* infection leads to the development of emphysema associated with the induction of alternatively activated macrophages: *Eur J Immunol*, v. 38, p. 479-88.
- Martinez-Medina, M., J. Denizot, N. Dreux, F. Robin, E. Billard, R. Bonnet, A. Darfeuille-Michaud, and N. Barnich, 2014, Western diet induces dysbiosis with increased *E coli* in CEABAC10 mice, alters host barrier function favouring AIEC colonisation: *Gut*, v. 63, p. 116-124.
- Mastrodonato, M., D. Mentino, P. Portincasa, G. Calamita, G. E. Liquori, and D. Ferri, 2014, High-fat diet alters the oligosaccharide chains of colon mucins in mice: *Histochemistry and Cell Biology*, v. 142, p. 449-459.

- McGuckin, M. A., S. K. Linden, P. Sutton, and T. H. Florin, 2011, Mucin dynamics and enteric pathogens: *Nature Reviews Microbiology*, v. 9, p. 265-278.
- McKenzie, G. J., A. Bancroft, R. K. Grencis, and A. N. J. McKenzie, 1998, A distinct role for interleukin-13 in Th2-cell-mediated immune responses: *Current Biology*, v. 8, p. 339-342.
- Miguel, E., and M. Kremer, 2003, Worms: Identifying Impacts on Education and Health in the Presence of Treatment Externalities: *Econometrica*, v. 72, p. 159-217.
- Moe, C. L., and R. D. Rheingans, 2006, Global challenges in water, sanitation and health: *J Water Health*, v. 4 Suppl 1, p. 41-57.
- Mohamed, S. M. A., T. Saber, A. A. Taha, H. S. Roshdy, and N. E. Shahien, 2017, Relation between schistosome past infection and metabolic syndrome: *J Egypt Soc Parasitol*, v. 47, p. 137-143.
- Monteiro, C. A., E. C. Moura, W. L. Conde, and B. M. Popkin, 2004, Socioeconomic status and obesity in adult populations of developing countries: a review: *Bulletin of the World Health Organization*, v. 82, p. 940-946.
- Murano, I., G. Barbatelli, V. Parisani, C. Latini, G. Muzzonigro, M. Castellucci, and S. Cinti, 2008, Dead adipocytes, detected as crown-like structures, are prevalent in visceral fat depots of genetically obese mice: *J Lipid Res*, v. 49, p. 1562-8.
- Musso, G., R. Gambino, and M. Cassader, 2011, Interactions Between Gut Microbiota and Host Metabolism Predisposing to Obesity and Diabetes: *Annual Review of Medicine*, Vol 62, 2011, v. 62, p. 361-380.
- Nair, M. G., K. J. Guild, Y. Du, C. Zaph, G. D. Yancopoulos, D. M. Valenzuela, A. Murphy, S. Stevens, M. Karow, and D. Artis, 2008, Goblet cell-derived resistin-like molecule beta augments CD4+ T cell production of IFN-gamma and infection-induced intestinal inflammation: *J Immunol*, v. 181, p. 4709-15.
- Neves, R. H., A. C. Miranda de Barros Alencar, M. Costa-Silva, M. B. Águila, C. A. Mandarim-de-Lacerda, J. R. Machado-Silva, and D. C. Gomes, 2007, Long-term feeding a high-fat diet causes histological and parasitological effects on murine schistosomiasis mansoni outcome: *Experimental Parasitology*, v. 115, p. 324-332.
- Oldenhove, G., E. Boucquoy, A. Taquin, V. Acolty, L. Bonetti, B. Ryffel, M. Le Bert, K. Englebert, L. Boon, and M. Moser, 2018, PD-1 Is Involved in the Dysregulation of Type 2 Innate Lymphoid Cells in a Murine Model of Obesity: *Cell Rep*, v. 25, p. 2053-2060.e4.
- Oliveira, S. A., A. A. Barbosa, Jr., D. C. Gomes, J. R. Machado-Silva, A. F. Barros, R. H. Neves, and E. M. Coutinho, 2003, Morphometric study of *Schistosoma mansoni* adult worms recovered from Undernourished infected mice: *Mem Inst Oswaldo Cruz*, v. 98, p. 623-7.
- Ottman, N., J. Reunanen, M. Meijerink, T. E. Pietilä, V. Kainulainen, J. Klievink, L. Huuskonen, S. Aalvink, M. Skurnik, S. Boeren, R. Satokari, A. Mercenier, A. Palva, H. Smidt, W. M. de Vos, and C. Belzer, 2017, Pili-like proteins of *Akkermansia muciniphila* modulate host immune responses and gut barrier function: *PLoS ONE*, v. 12, p. e0173004.
- Owyang, A. M., C. Zaph, E. H. Wilson, K. J. Guild, T. McClanahan, H. R. Miller, D. J. Cua, M. Goldschmidt, C. A. Hunter, R. A. Kastelein, and D. Artis, 2006, Interleukin 25 regulates type 2 cytokine-dependent immunity and limits chronic inflammation in the gastrointestinal tract: *J Exp Med*, v. 203, p. 843-9.
- Pace, F., B. M. Carvalho, T. M. Zanotto, A. Santos, D. Guadagnini, K. L. C. Silva, M. C. S. Mendes, G. Z. Rocha, S. M. Alegretti, G. A. Santos, R. R. Catharino, R. Paroni, F. Folli, and M. J. A. Saad, 2018, Helminth infection in mice improves insulin sensitivity via modulation of gut microbiota and fatty acid metabolism: *Pharmacological Research*, v. 132, p. 33-46.
- Paich, H. A., P. A. Sheridan, J. Handy, E. A. Karlsson, S. Schultz-Cherry, M. G. Hudgens, T. L. Noah, S. S. Weir, and M. A. Beck, 2013, Overweight and obese adult humans have a defective cellular immune response to pandemic H1N1 influenza A virus: *Obesity (Silver Spring)*, v. 21, p. 2377-86.
- Park, J. S., E. J. Lee, J. C. Lee, W. K. Kim, and H. S. Kim, 2007, Anti-inflammatory effects of short chain fatty acids in IFN-gamma-stimulated RAW 264.7 murine macrophage cells:

- involvement of NF-kappaB and ERK signaling pathways: *Int Immunopharmacol*, v. 7, p. 70-7.
- Peng, W., and E. M. Berry, 2018, Global nutrition 1990–2015: A shrinking hungry, and expanding fat world: *PLoS ONE*, v. 13, p. e0194821.
- Perez-Vilar, J., and R. L. Hill, 1999, The structure and assembly of secreted mucins: *Journal of Biological Chemistry*, v. 274, p. 31751-31754.
- Perrigoue, J. G., S. A. Saenz, M. C. Siracusa, E. J. Allenspach, B. C. Taylor, P. R. Giacomin, M. G. Nair, Y. Du, C. Zaph, N. van Rooijen, M. R. Comeau, E. J. Pearce, T. M. Laufer, and D. Artis, 2009, MHC class II-dependent basophil-CD4+ T cell interactions promote T(H)2 cytokine-dependent immunity: *Nat Immunol*, v. 10, p. 697-705.
- Pettersson, U. S., T. B. Walden, P. O. Carlsson, L. Jansson, and M. Phillipson, 2012, Female mice are protected against high-fat diet induced metabolic syndrome and increase the regulatory T cell population in adipose tissue: *PLoS One*, v. 7, p. e46057.
- Pinchuk, L. M., and N. M. Filipov, 2008, Differential effects of age on circulating and splenic leukocyte populations in C57BL/6 and BALB/c male mice: *Immunity & ageing : I & A*, v. 5, p. 1-1.
- Popkin, B. M., 1994, The nutrition transition in low-income countries: an emerging crisis: *Nutr Rev*, v. 52, p. 285-98.
- Popkin, B. M., 2006, Global nutrition dynamics: the world is shifting rapidly toward a diet linked with noncommunicable diseases: *The American Journal of Clinical Nutrition*, v. 84, p. 289-298.
- Popkin, B. M., 2012, Global nutrition transition and the pandemic of obesity in developing countries (vol 70, pg 3, 2012): *Nutrition Reviews*, v. 70, p. 256-256.
- Pradhan, A. D., J. E. Manson, N. Rifai, J. E. Buring, and P. M. Ridker, 2001, C-reactive protein, interleukin 6, and risk of developing type 2 diabetes mellitus: *Jama*, v. 286, p. 327-34.
- Pullan, R. L., J. L. Smith, R. Jasrasaria, and S. J. Brooker, 2014, Global numbers of infection and disease burden of soil transmitted helminth infections in 2010: *Parasit Vectors*, v. 7, p. 37.
- Qiu, Y., K. D. Nguyen, J. I. Odegaard, X. Cui, X. Tian, R. M. Locksley, R. D. Palmiter, and A. Chawla, 2014, Eosinophils and Type 2 Cytokine Signaling in Macrophages Orchestrate Development of Functional Beige Fat: *Cell*, v. 157, p. 1292-1308.
- Rajala, M. W., S. Obici, P. E. Scherer, and L. Rossetti, 2003, Adipose-derived resistin and gut-derived resistin-like molecule-beta selectively impair insulin action on glucose production: *J Clin Invest*, v. 111, p. 225-30.
- Rebuffé-Scrive, M., R. Surwit, M. Feinglos, C. Kuhn, and J. Rodin, 1993, Regional fat distribution and metabolism in a new mouse model (C57BL 6J) of non-insulin-dependent diabetes mellitus: *Metabolism - Clinical and Experimental*, v. 42, p. 1405-1409.
- Rémésy, C., C. Demigné, and C. Morand, 1992, Metabolism and Utilisation of Short Chain Fatty Acids Produced by Colonic Fermentation, *in* T. F. Schweizer, and C. A. Edwards, eds., *Dietary Fibre — A Component of Food: Nutritional Function in Health and Disease*: London, Springer London, p. 137-150.
- Riddell, S. R., and P. D. Greenberg, 1990, The use of anti-CD3 and anti-CD28 monoclonal antibodies to clone and expand human antigen-specific T cells: *J Immunol Methods*, v. 128, p. 189-201.
- Roach, T., D. Wakelin, K. J. Else, and D. A. P. Bundy, 1988, Antigenic cross-reactivity between the human whipworm, *Trichuris trichiura*, and the mouse trichuroids *Trichuris muris* and *Trichinella spiralis*: *Parasite Immunology*, v. 10, p. 279-291.
- Roos, D., and J. A. Loos, 1973, Changes in the carbohydrate metabolism of mitogenically stimulated human peripheral lymphocytes. II. Relative importance of glycolysis and oxidative phosphorylation on phytohaemagglutinin stimulation: *Exp Cell Res*, v. 77, p. 127-35.
- Rosenbloom, J. I., D. N. Kaluski, and E. M. Berry, 2008, A Global Nutritional Index: *Food and Nutrition Bulletin*, v. 29, p. 266-277.

- Rudatsikira, E., A. Muula, D. Mulenga, and S. Siziya, 2012, Prevalence and correlates of obesity among Lusaka residents, Zambia: A population-based survey, v. 5, 14 p.
- Saenz, S. A., M. C. Siracusa, L. A. Monticelli, C. G. Ziegler, B. S. Kim, J. R. Brestoff, L. W. Peterson, E. J. Wherry, A. W. Goldrath, A. Bhandoola, and D. Artis, 2013, IL-25 simultaneously elicits distinct populations of innate lymphoid cells and multipotent progenitor type 2 (MPPtype2) cells: *J Exp Med*, v. 210, p. 1823-37.
- Saenz, S. A., M. C. Siracusa, J. G. Perrigoue, S. P. Spencer, J. F. Urban, Jr., J. E. Tocker, A. L. Budelsky, M. A. Kleinschek, R. A. Kastelein, T. Kambayashi, A. Bhandoola, and D. Artis, 2010, IL25 elicits a multipotent progenitor cell population that promotes T(H)2 cytokine responses: *Nature*, v. 464, p. 1362-6.
- Sato Mito, N., M. Suzui, H. Yoshino, T. Kaburagi, and K. Sato, 2009, Long term effects of high fat and sucrose diets on obesity and lymphocyte proliferation in mice: *J Nutr Health Aging*, v. 13, p. 602-6.
- Schopf, L. R., K. F. Hoffmann, A. W. Cheever, J. F. Urban, Jr., and T. A. Wynn, 2002a, IL-10 is critical for host resistance and survival during gastrointestinal helminth infection: *J Immunol*, v. 168, p. 2383-92.
- Schopf, L. R., K. F. Hoffmann, A. W. Cheever, J. F. Urban, and T. A. Wynn, 2002b, IL-10 Is Critical for Host Resistance and Survival During Gastrointestinal Helminth Infection: *The Journal of Immunology*, v. 168, p. 2383.
- Schwartz, M. W., E. Peskind, M. Raskind, E. J. Boyko, and D. Porte, Jr., 1996, Cerebrospinal fluid leptin levels: relationship to plasma levels and to adiposity in humans: *Nat Med*, v. 2, p. 589-93.
- Sekirov, I., N. M. Tam, M. Jogova, M. L. Robertson, Y. Li, C. Lupp, and B. B. Finlay, 2008, Antibiotic-induced perturbations of the intestinal microbiota alter host susceptibility to enteric infection: *Infect Immun*, v. 76, p. 4726-36.
- Sheehan, J. K., and D. J. Thornton, 2000, Heterogeneity and size distribution of gel-forming mucins: *Glycoprotein Methods and Protocols*, v. 125, p. 87-96.
- Sheehan, J. K., D. J. Thornton, M. Howard, I. Carlstedt, A. P. Corfield, and C. Paraskeva, 1996, Biosynthesis of the MUC2 mucin: Evidence for a slow assembly of fully glycosylated units: *Biochemical Journal*, v. 315, p. 1055-1060.
- Shen, S. W., Y. Lu, F. Li, Z. H. Shen, M. Xu, W. F. Yao, Y. B. Feng, J. T. Yun, Y. P. Wang, W. Ling, H. J. Qi, and D. X. Tong, 2015, The potential long-term effect of previous schistosome infection reduces the risk of metabolic syndrome among Chinese men: *Parasite Immunol*, v. 37, p. 333-9.
- Shojima, N., T. Ogihara, K. Inukai, M. Fujishiro, H. Sakoda, A. Kushiyama, H. Katagiri, M. Anai, H. Ono, Y. Fukushima, N. Horike, A. Y. Viana, Y. Uchijima, H. Kurihara, and T. Asano, 2005, Serum concentrations of resistin-like molecules beta and gamma are elevated in high-fat-fed and obese db/db mice, with increased production in the intestinal tract and bone marrow: *Diabetologia*, v. 48, p. 984-92.
- Silva, F. M. C., E. E. Oliveira, A. C. C. Gouveia, A. S. S. Brugiolo, C. C. Alves, J. O. A. Correa, J. Gameiro, J. Mattes, H. C. Teixeira, and A. P. Ferreira, 2017, Obesity promotes prolonged ovalbumin-induced airway inflammation modulating T helper type 1 (Th1), Th2 and Th17 immune responses in BALB/c mice: *Clin Exp Immunol*, v. 189, p. 47-59.
- Singh, V. P., R. Aggarwal, S. Singh, A. Banik, T. Ahmad, B. R. Patnaik, G. Nappanveetil, K. P. Singh, M. L. Aggarwal, B. Ghosh, and A. Agrawal, 2015, Metabolic Syndrome Is Associated with Increased Oxo-Nitrative Stress and Asthma-Like Changes in Lungs: *PloS one*, v. 10, p. e0129850-e0129850.
- Sinyange, N., J. Brunkard, and N. Kapata, 2018, Cholera Epidemic — Lusaka, Zambia, October 2017–May 2018: *MMWR Morb Mortal Wkly Rep*, v. 67, p. 556–559.
- Siwila, Joyce, and A. Olsen, 2015, Risk Factors for Infection with Soil Transmitted Helminths, *Cryptosporidium* spp., and *Giardia duodenalis* in Children Enrolled in Preschools in Kafue District, Zambia: *Epidemiology Research International*.

- Smith, H. W., 1965, Observations on the flora of the alimentary tract of animals and factors affecting its composition: *J Pathol Bacteriol*, v. 89, p. 95-122.
- Sovran, B., F. Hugenholtz, M. Elderman, A. A. Van Beek, K. Graversen, M. Huijskes, M. V. Boekschoten, H. F. J. Savelkoul, P. De Vos, J. Dekker, and J. M. Wells, 2019, Age-associated Impairment of the Mucus Barrier Function is Associated with Profound Changes in Microbiota and Immunity: *Scientific reports*, v. 9, p. 1437-1437.
- Spencer, S. P., C. Wilhelm, Q. Yang, J. A. Hall, N. Bouladoux, A. Boyd, T. B. Nutman, J. F. Urban, Jr., J. Wang, T. R. Ramalingam, A. Bhandoola, T. A. Wynn, and Y. Belkaid, 2014, Adaptation of innate lymphoid cells to a micronutrient deficiency promotes type 2 barrier immunity: *Science*, v. 343, p. 432-7.
- Spychala, M. S., V. R. Venna, M. Jandzinski, S. J. Doran, D. J. Durgan, B. P. Ganesh, N. J. Ajami, N. Putluri, J. Graf, R. M. Bryan, and L. D. McCullough, 2018, Age-related changes in the gut microbiota influence systemic inflammation and stroke outcome: *Ann Neurol*, v. 84, p. 23-36.
- Stephenson, L. S., C. V. Holland, and E. S. Cooper, 2000, The public health significance of *Trichuris trichiura*: *Parasitology*, v. 121, p. S73-S95.
- Su, C. W., C.-Y. Chen, Y. Li, S. R. Long, W. Massey, D. V. Kumar, W. A. Walker, and H. N. Shi, 2018, Helminth infection protects against high fat diet-induced obesity via induction of alternatively activated macrophages: *Scientific Reports*, v. 8.
- Sudati, J. E., A. Reddy, and B. Fried, 1996, Effects of high fat diets on worm recovery, growth and distribution of *Echinostoma caproni* in ICR mice: *J Helminthol*, v. 70, p. 351-4.
- Suk, K., S. Kim, Y. H. Kim, K. A. Kim, I. Chang, H. Yagita, M. Shong, and M. S. Lee, 2001, IFN-gamma/TNF-alpha synergism as the final effector in autoimmune diabetes: a key role for STAT1/IFN regulatory factor-1 pathway in pancreatic beta cell death: *J Immunol*, v. 166, p. 4481-9.
- Surwit, R. S., M. N. Feinglos, J. Rodin, A. Sutherland, A. E. Petro, E. C. Opara, C. M. Kuhn, and M. Rebuffe-Scrive, 1995, Differential effects of fat and sucrose on the development of obesity and diabetes in C57BL/6J and A/J mice: *Metabolism*, v. 44, p. 645-51.
- Sutherland, T. E., N. Logan, D. Rückerl, A. A. Humbles, S. M. Allan, V. Papayannopoulos, B. Stockinger, R. M. Maizels, and J. E. Allen, 2014, Chitinase-like proteins promote IL-17-mediated neutrophilia in a tradeoff between nematode killing and host damage: *Nature Immunology*, v. 15, p. 1116.
- Svensson, M., L. Bell, M. C. Little, M. DeSchoolmeester, R. M. Locksley, and K. J. Else, 2011, Accumulation of eosinophils in intestine-draining mesenteric lymph nodes occurs after *Trichuris muris* infection: *Parasite Immunology*, v. 33, p. 1-11.
- Szabo, S. J., B. M. Sullivan, C. Stemann, A. R. Satoskar, B. P. Sleckman, and L. H. Glimcher, 2002, Distinct effects of T-bet in TH1 lineage commitment and IFN-gamma production in CD4 and CD8 T cells: *Science*, v. 295, p. 338-42.
- Taylor-Robinson, D. C., N. Maayan, K. Soares-Weiser, S. Donegan, and P. Garner, 2015, Deworming drugs for soil-transmitted intestinal worms in children: effects on nutritional indicators, haemoglobin, and school performance: *Cochrane Database Syst Rev*, p. Cd000371.
- Taylor, B. C., C. Zaph, A. E. Troy, Y. Du, K. J. Guild, M. R. Comeau, and D. Artis, 2009, TSLP regulates intestinal immunity and inflammation in mouse models of helminth infection and colitis: *The Journal of Experimental Medicine*, v. 206, p. 655-667.
- Thaiss, C. A., M. Levy, I. Grosheva, D. Zheng, E. Soffer, E. Blacher, S. Braverman, A. C. Tengeler, O. Barak, M. Elazar, R. Ben-Zeev, D. Lehavi-Regev, M. N. Katz, M. Pevsner-Fischer, A. Gertler, Z. Halpern, A. Harmelin, S. Amar, P. Serradas, A. Grosfeld, H. Shapiro, B. Geiger, and E. Elinav, 2018, Hyperglycemia drives intestinal barrier dysfunction and risk for enteric infection: *Science*.
- Thi Loan Anh, N., S. Vieira-Silva, A. Liston, and J. Raes, 2015, How informative is the mouse for human gut microbiota research?: *Disease Models & Mechanisms*, v. 8, p. 1-16.

- Thompson, C. B., T. Lindsten, J. A. Ledbetter, S. L. Kunkel, H. A. Young, S. G. Emerson, J. M. Leiden, and C. H. June, 1989, CD28 activation pathway regulates the production of multiple T-cell-derived lymphokines/cytokines: *Proc Natl Acad Sci U S A*, v. 86, p. 1333-7.
- Thornton, D. J., K. Rousseau, and M. A. McGuckin, 2008, Structure and function of the polymeric mucins in airways mucus: *Annual Review of Physiology*, v. 70, p. 459-486.
- Tilney, L. G., P. S. Connelly, G. M. Guild, K. A. Vranich, and D. Artis, 2005, Adaptation of a nematode parasite to living within the mammalian epithelium: *J Exp Zool A Comp Exp Biol*, v. 303, p. 927-45.
- Tomas, J., C. Mulet, A. Saffarian, J.-B. Cavin, R. Ducroc, B. Regnault, C. Kun Tan, K. Duszka, R. Burcelin, W. Wahli, P. J. Sansonetti, and T. Pédrón, 2016, High-fat diet modifies the PPAR- γ pathway leading to disruption of microbial and physiological ecosystem in murine small intestine: *Proceedings of the National Academy of Sciences of the United States of America*, v. 113, p. E5934-E5943.
- Trembleau, S., G. Penna, S. Gregori, N. Giarratana, and L. Adorini, 2003, IL-12 administration accelerates autoimmune diabetes in both wild-type and IFN-gamma-deficient nonobese diabetic mice, revealing pathogenic and protective effects of IL-12-induced IFN-gamma: *J Immunol*, v. 170, p. 5491-501.
- Turcot, V., L. Bouchard, G. Faucher, V. Garneau, A. Tchernof, Y. Deshaies, L. Perusse, S. Marceau, S. Biron, O. Lescelleur, L. Biertho, and M. C. Vohl, 2012, Thymic stromal lymphopoietin: an immune cytokine gene associated with the metabolic syndrome and blood pressure in severe obesity: *Clin Sci (Lond)*, v. 123, p. 99-109.
- Turnbaugh, P. J., F. Backhed, L. Fulton, and J. I. Gordon, 2008, Marked alterations in the distal gut microbiome linked to diet-induced obesity: *Cell host & microbe*, v. 3, p. 213-223.
- Turnbaugh, P. J., R. E. Ley, M. A. Mahowald, V. Magrini, E. R. Mardis, and J. I. Gordon, 2006a, An obesity-associated gut microbiome with increased capacity for energy harvest: *Nature*, v. 444, p. 1027-1031.
- Turnbaugh, P. J., R. E. Ley, M. A. Mahowald, V. Magrini, E. R. Mardis, and J. I. Gordon, 2006b, An obesity-associated gut microbiome with increased capacity for energy harvest: *Nature*, v. 444, p. 1027.
- Turner, J. D., H. Faulkner, J. Kamgno, F. Cormont, J. Van Snick, K. J. Else, R. K. Grencis, J. M. Behnke, M. Boussinesq, and J. E. Bradley, 2003, Th2 cytokines are associated with reduced worm burdens in a human intestinal helminth infection: *J Infect Dis*, v. 188, p. 1768-75.
- van der Weerd, K., W. A. Dik, B. Schrijver, D. H. Schweitzer, A. W. Langerak, H. A. Drexhage, R. M. Kiewiet, M. O. van Aken, A. van Huisstede, J. J. M. van Dongen, A.-J. van der Lelij, F. J. T. Staal, and P. M. van Hagen, 2012, Morbidly obese human subjects have increased peripheral blood CD4⁺ T cells with skewing toward a Treg- and Th2-dominated phenotype: *Diabetes*, v. 61, p. 401-408.
- van der Windt, G. J., and E. L. Pearce, 2012, Metabolic switching and fuel choice during T-cell differentiation and memory development: *Immunol Rev*, v. 249, p. 27-42.
- Verwaerde, C., A. Delanoye, L. Macia, A. Tailleux, and I. Wolowczuk, 2006, Influence of high-fat feeding on both naive and antigen-experienced T-cell immune response in DO10.11 mice: *Scand J Immunol*, v. 64, p. 457-66.
- von Moltke, J., M. Ji, H.-E. Liang, and R. M. Locksley, 2016, Tuft-cell-derived IL-25 regulates an intestinal ILC2-epithelial response circuit: *Nature*, v. 529, p. 221-U243.
- Wakelin, D., 1967, Acquired immunity to *Trichuris muris* in the albino laboratory mouse *Parasitology*, v. 57, p. 515-24.
- Wakelin, D., 1973, The stimulation of immunity to *Trichuris muris* in mice exposed to low-level infections: *Parasitology*, v. 66, p. 181-9.
- Wang, B., J. Sun, Y. Ma, G. Wu, Y. Shi, and G. Le, 2014, Increased oxidative stress and the apoptosis of regulatory T cells in obese mice but not resistant mice in response to a high-fat diet: *Cell Immunol*, v. 288, p. 39-46.

- Wegener Parfrey, L., M. Jirků, R. Šíma, M. Jalovecká, B. Sak, K. Grigore, and K. Jirků Pomajbíková, 2017, A benign helminth alters the host immune system and the gut microbiota in a rat model system: *PLOS ONE*, v. 12, p. e0182205.
- WFP, 2017, WFP strategic plan (2017 - 2021).
- Whitman, W. B., D. C. Coleman, and W. J. Wiebe, 1998, Prokaryotes: the unseen majority: *Proc Natl Acad Sci U S A*, v. 95, p. 6578-83.
- WHO, 2012, Soil-transmitted helminthiasis: eliminating as public health problem soil-transmitted helminthiasis in children: progress report 2001–2010 and strategic plan 2011–2020, Geneva: World Health Organization.
- Wilhelm, C., O. J. Harrison, V. Schmitt, M. Pelletier, S. P. Spencer, J. F. Urban, Jr., M. Ploch, T. R. Ramalingam, R. M. Siegel, and Y. Belkaid, 2016, Critical role of fatty acid metabolism in ILC2-mediated barrier protection during malnutrition and helminth infection: *J Exp Med*, v. 213, p. 1409-18.
- Wiria, A. E., E. Sartono, T. Supali, and M. Yazdanbakhsh, 2014, Helminth Infections, Type-2 Immune Response, and Metabolic Syndrome: *Plos Pathogens*, v. 10.
- Withers, S. B., R. Forman, S. Meza-Perez, D. Sorobetea, K. Sitnik, T. Hopwood, C. B. Lawrence, W. W. Agace, K. J. Else, A. M. Heagerty, M. Svensson-Frej, and S. M. Cruickshank, 2017, Eosinophils are key regulators of perivascular adipose tissue and vascular functionality: *Scientific Reports*, v. 7.
- Worthington, J. J., J. E. Klementowicz, S. Rahman, B. I. Czajkowska, C. Smedley, H. Waldmann, T. Sparwasser, R. K. Grencis, and M. A. Travis, 2013a, Loss of the TGFbeta-activating integrin alphaVbeta8 on dendritic cells protects mice from chronic intestinal parasitic infection via control of type 2 immunity: *PLoS Pathog*, v. 9, p. e1003675.
- Worthington, J. J., L. C. Samuelson, R. K. Grencis, and J. T. McLaughlin, 2013b, Adaptive immunity alters distinct host feeding pathways during nematode induced inflammation, a novel mechanism in parasite expulsion: *PLoS Pathog*, v. 9, p. e1003122.
- Wu, C., S. He, Y. Peng, K. K. Kushwaha, J. Lin, J. Dong, B. Wang, S. Shan, J. Liu, K. Huang, and D. Li, 2014, TSLPR deficiency attenuates atherosclerotic lesion development associated with the inhibition of TH17 cells and the promotion of regulator T cells in ApoE-deficient mice: *J Mol Cell Cardiol*, v. 76, p. 33-45.
- Wu, Y., T. Wu, J. Wu, L. Zhao, Q. Li, Z. Varghese, J. F. Moorhead, S. H. Powis, Y. Chen, and X. Z. Ruan, 2013, Chronic inflammation exacerbates glucose metabolism disorders in C57BL/6J mice fed with high-fat diet: *J Endocrinol*, v. 219, p. 195-204.
- Yan, L. D., C. Chirwa, B. H. Chi, S. Bosomprah, N. Sindano, M. Mwanza, D. Musatwe, M. Mulenga, and R. Chilengi, 2017, Hypertension management in rural primary care facilities in Zambia: a mixed methods study: *BMC Health Services Research*, v. 17, p. 111.
- Yang, K., K. H. Fan, H. Newmark, D. Leung, M. Lipkin, V. E. Steele, and G. J. Kelloff, 1996, Cytokeratin, lectin, and acidic mucin modulation in differentiating colonic epithelial cells of mice after feeding western-style diets: *Cancer Research*, v. 56, p. 4644-4648.
- Yang, Y., D. L. Smith, Jr., K. D. Keating, D. B. Allison, and T. R. Nagy, 2014, Variations in body weight, food intake and body composition after long-term high-fat diet feeding in C57BL/6J mice: *Obesity (Silver Spring, Md.)*, v. 22, p. 2147-2155.
- Yang, Z., V. Grinchuk, A. Smith, B. Qin, J. A. Bohl, R. Sun, L. Notari, Z. Zhang, H. Sesaki, J. F. Urban, Jr., T. Shea-Donohue, and A. Zhao, 2013, Parasitic nematode-induced modulation of body weight and associated metabolic dysfunction in mouse models of obesity: *Infection and immunity*, v. 81, p. 1905-1914.
- Yoichi, I., 1991, The absence of resistance in congenitally athymic nude mice toward infection with the intestinal nematode, *Trichuris muris*: Resistance restored by lymphoid cell transfer: *International Journal for Parasitology*, v. 21, p. 65-69.
- Zhang, Y., K.-Y. Guo, P. A. Diaz, M. Heo, and R. L. Leibel, 2002, Determinants of leptin gene expression in fat depots of lean mice: *American Journal of Physiology-Regulatory, Integrative and Comparative Physiology*, v. 282, p. R226-R234.

- Zhou, D., Q. Pan, F.-Z. Xin, R.-N. Zhang, C.-X. He, G.-Y. Chen, C. Liu, Y.-W. Chen, and J.-G. Fan, 2017, Sodium butyrate attenuates high-fat diet-induced steatohepatitis in mice by improving gut microbiota and gastrointestinal barrier: *World Journal of Gastroenterology*, v. 23, p. 60-75.
- Zhou, W., E. A. Davis, and M. J. Dailey, 2018, Obesity, independent of diet, drives lasting effects on intestinal epithelial stem cell proliferation in mice: *Experimental Biology and Medicine*, v. 243, p. 826-835.